

A UNIFIED APPROACH TO THE IDENTIFICATION OF
DYNAMIC BEHAVIOUR USING THE THEORY
OF VECTOR SPACES

by

T.A. BROWN

A dissertation submitted for the Degree of
Doctor of Philosophy in Engineering at
the University of Bristol

August 1985

"If you're not confused,
you really don't **understand**
the problem"

graffitti
Northern Ireland

MEMORANDUM

The accompanying dissertation entitled 'A Unified Approach to the Identification of Dynamic Behaviour Using the Theory of Vector Spaces' is submitted for the Degree of Doctor of Philosophy in the Faculty of Engineering at the University of Bristol.

The dissertation is based entirely on the independent work carried out by the author in the University of Bristol between October 1982 and August 1985, under the supervision of Professor R.D. Milne of the Department of Engineering Mathematics.

All the work and ideas recorded are original, except where acknowledged in the text or by reference.

The work contained in this dissertation has not previously been submitted for a degree or diploma of this, or any other, university or examining body. However, the following paper, presented at the 3rd International Modal Analysis Conference, and based on part of the work described in this thesis, has been published:

BROWN, T.A., MILNE, R.D: Strategies for the Verification of a Finite Element Model. **Proc. IMAC III, 1985, p.1031.**

Signed

T.A. Brown

Date

29/8/85

ACKNOWLEDGEMENTS

I would like to express **my thanks** to my supervisor, Professor R.D. Milne, for his continuous guidance and encouragement throughout the duration of this research, and for his help and advice in the preparation of the manuscript. Thanks are also due to the members (past and present) of the Earthquake Engineering Research Group, in particular Professor R.T. Severn and Dr. C.A. Taylor, for their constant interest and constructive comments.

I would like to thank the Science and Engineering Research Council for providing the financial support during this research.

Finally, I would like to thank Eleanor Gibbins **for** typing the final version of this work.

ABSTRACT

Two contrasting approaches to dynamic analysis exist. They are the finite-element method, which is an analytical technique that models the structure under investigation with a finite degree-of-freedom model - and modal analysis, where the structure is actually excited in order to assess its dynamic characteristics.

This thesis contains an investigation into both methods using specific examples in order to assess their contrasting nature. Often the dynamic performance predicted by these methods does not coincide. Attempts to reconcile the differences that emerge are reviewed initially, and the problem is then rethought in the context of vector space theory. The analysis is built up in stages, commencing with a simple (3x3) matrix example, and gradually adding in more detail as the problem becomes understood. The introduction of vector space theory permits a reassessment of the techniques mentioned in order to unify the entire process of identification, thereby clarifying the objectives and expectations of research in this area and allowing it to be extended to the case of viscous damping. A simple beam is used to illustrate the analysis throughout.

CONTENTS

| | <u>Page No.</u> |
|---|-----------------|
| MEMORANDUM | (ii) |
| ACKNOWLEDGEMENTS | (iii) |
| ABSTRACT | (iv) |
| NOTATION | |
| CHAPTER 1: INTRODUCTION AND REVIEW | 1 |
| 1.1 Preliminaries | 1 |
| 1.2 Dynamic Equations | 4 |
| 1.3 The Finite-Element Method | 7 |
| 1.4 Modal Testing | 9 |
| 1.5 Correlation of Experiment and Theory | 16 |
| 1.6 Expansion of Measured Data | 33 |
| 1.7 Overview | 36 |
| CHAPTER 2: PRELIMINARY WORK | 38 |
| 2.1 Preliminaries | 38 |
| 2.2 Setting up an FE Model | 38 |
| Example 1 - Uniform Cantilever | 40 |
| Example 2 - Uniform Simply-Supported Beam | 42 |
| Example 3 - Simply-Supported Beam with Non-Proportional Damping | 43 |
| 2.3 Experimental Modal Analysis | 44 |
| 2.3(a) Multiple Input Testing | 44 |
| 2.3(b) Single Input Testing | 47 |
| 2.4 Development of Curvefitting Program | 49 |
| 2.5 Experimental Impact Testing | 55 |
| 2.6 Comparison of FE Method and Modal Analysis | 60 |
| 2.7 Some Uses of the Mathematical Model | 62 |
| 2.8 Sensitivity Analysis | 64 |
| 2.9 Overview | 65 |
| Diagrams | 66 |
| Tables | 70 |
| Figures | 83 |
| CHAPTER 3: THEORETICAL DEVELOPMENT | 104 |
| 3.1 Preliminaries | 104 |

| | <u>Page No.</u> |
|--|-----------------|
| 3.2 Fundamentals | 105 |
| 3.3 Change of Basis | 112 |
| 3.4 Approximating the Single Symmetric Operator | 114 |
| 3.5 The Approximation and Its Uses | 119 |
| 3.6 The Unsymmetric Operator | 122 |
| 3.7 Overview | 127 |
| CHAPTER 4: THE UNDAMPED PROBLEM | 129 |
| 4.1 Preliminaries | 129 |
| 4.2 Inverse Mass and Stiffness Expressions | 131 |
| 4.3 Projection of Measured Matrices | 135 |
| 4.4 Projection of Analytical Matrices | 139 |
| 4.5 Improvement/Correction of Mass and Stiffness | 143 |
| 4.6 The Continuous Structure | 150 |
| 4.7 Hybrid Matrices | 155 |
| 4.8 Overview | 156 |
| Figures and Tables | 157 |
| CHAPTER 5: THE DAMPED PROBLEM | 174 |
| 5.1 Preliminaries | 174 |
| 5.2 Symmetric Formulation Paradox | 177 |
| 5.3 Normalisation | 178 |
| 5.4 Projection of Inverse S and T Matrices | 180 |
| 5.5 Incomplete M, C and K | 183 |
| 5.6 Comparison with Undamped Problem | 188 |
| 5.7 Error Expressions | 191 |
| 5.8 Numerical Experiments | 194 |
| 5.9 Discussion of Error Expressions | 195 |
| 5.10 Hybrid Matrices | 197 |
| 5.11 Origins of Transfer Function Expression | 199 |
| 5.12 Overview | 201 |
| Tables | 204 |
| Figures | 208 |
| CHAPTER 6: INTERPOLATION OF MEASURED MODES | 220 |
| 6.1 Preliminaries | 220 |
| 6.2 Interpolation Using Splines | 221 |
| 6.3 Interpolation Using an Analytical Model | 223 |
| 6.4 Overview | 229 |
| Tables | 231 |

| | <u>Page No.</u> |
|--|-----------------|
| CHAPTER 7: CONCLUSIONS | 241 |
| Tables | 247 |
| REFERENCES | 249 |
| APPENDIX 1: Perturbation Analysis for a Beam | 257 |
| APPENDIX 2: MAMA-2 Users Manual | 259 |
| APPENDIX 3: SDOF and MDOF Users Manual | 271 |
| APPENDIX 4: SDOF Listing | 280 |
| APPENDIX 5: MDOF Listing | 285 |

NOTATION

The following is a list of the principal notation used in each chapter of this thesis. Notation that does not appear here is defined in the text.

Chapter 1

| | |
|-------------------------------|--------------------------------------|
| $B(\lambda)$ | : system matrix |
| C | : damping matrix |
| $F(t)$ | : force |
| $F(t) \rightarrow f(\lambda)$ | : Laplace pair |
| $H(\lambda)$ | : transfer function matrix |
| I | : identity matrix |
| K | : stiffness matrix |
| K_{INC} | : incomplete stiffness matrix |
| K_a | : analytical stiffness matrix |
| K_{FULL} | : full stiffness matrix |
| K_{RED} | : reduced stiffness matrix |
| M | : mass matrix |
| M_a | : analytical mass matrix |
| M_{FULL} | : full mass matrix |
| M_{RED} | : reduced mass matrix |
| $X(t)$ | : displacement |
| $X(t) \rightarrow x(\lambda)$ | : Laplace pair |
| a_i | : i th residue |
| c | : viscous damping coefficient |
| g | : hysteretic damping coefficient |
| i | : complex variable ($= \sqrt{-1}$) |
| k | : stiffness |

| | |
|--------------|--|
| m | : mass |
| x_i | : i th eigenvector |
| x_i^R | : i th rigid body mode |
| Φ | : matrix of eigenvectors |
| Λ | : diagonal matrix of eigenvalues |
| Φ_a | : matrix of analytical eigenvectors |
| Λ_a | : diagonal matrix of analytical eigenvalues |
| λ_i | : i th eigenvalue |
| λ | : Laplace variable |
| ω_i | : i th undamped natural frequency |
| ω | : measurement frequency |
| μ_i | : percentage critical damping of i th mode |
| Ω_j | : j th measurement frequency |
| θ | : zero vector |
| δ_j^i | : 1 if $i = j$ 0 if $i \neq j$ |

Chapter 2

| | |
|--------------|----------------------------|
| D | : partial derivative |
| E | : dynamic Young's modulus |
| $F(t)$ | : force |
| $H(\lambda)$ | : transfer function |
| I | : identity matrix |
| \bar{I} | : second moment of area |
| K | : stiffness matrix |
| K^e | : element stiffness matrix |
| M | : mass matrix |
| M^e | : element mass matrix |
| $X(t)$ | : displacement |

| | |
|-------------|---------------------------------------|
| c | : damping coefficient |
| f_{ij} | : element (i,j) of flexibility matrix |
| k | : stiffness |
| k_{ij} | : element (i,j) of stiffness matrix |
| ℓ | : element length |
| m | : mass |
| m_{ij} | : element (i,j) of mass matrix |
| M | : number of measurement frequencies |
| x | : complex conjugate of x |
| x_j | : jth eigenvector |
| y | : distance along beam |
| λ_i | : ith eigenvalue |
| λ | : Laplace variable |
| w_i | : ith natural frequency |
| μ_i | : percent critical damping of mode i |
| Ω_j | : jth measurement frequency |
| $\psi_i(y)$ | : ith shape function |
| Φ | : matrix of x_i |
| θ | : zero vector |

Chapter 3

| | |
|-------------------|--|
| I | : identity matrix |
| P_i | : basis vector for $\mathcal{L}(v_n, v_n)$ |
| \underline{P}_i | : matrix representation of P_i |
| T | : linear transformation |
| \underline{T} | : matrix representation of T |
| \underline{T}^H | : hybrid matrix |
| T' | : dual of T |

| | |
|---|--|
| e_i | : standard basis $\{(1,0,\dots,0),(0,1,\dots,0)\dots(0,0,\dots,1)\}$ |
| x, y | : vectors |
| x_i | : eigenvector (of T) |
| $\underline{x}_i, (\xi_i^1, \xi_i^2, \dots, \xi_i^n)$ | : coordinate n -tuple representing x_i relative to e_i basis |
| \underline{x}_i^T | : transpose of \underline{x}_i |
| \bar{x} | : complex conjugate of x |
| λ_i | : i th eigenvalue |
| Λ | : diagonal matrix of eigenvalues |
| Φ | : matrix of x_i |
| Φ^T | : transpose of Φ |
| Π | : matrix of y_i |
| $\text{Proj}(T)_{\mathcal{V}_m}$ | : projection of T onto subspace \mathcal{V}_m |
| $\text{Proj}(T)_{\mathcal{V}_m^\perp}$ | : projection of T onto subspace \mathcal{V}_m^\perp |
| e | : zero vector |
| $\mathcal{N}(T)$ | : null space of T |
| $\mathcal{R}(T)$ | : range space of T |
| \mathcal{V} | : vector space |
| \mathcal{V}_n | : n -dimensional vector space |
| \mathcal{V}_m | : m -dimensional vector space |
| \mathcal{V}_m^\perp | : orthogonal complement of \mathcal{V}_m |
| \mathcal{V}_n^* | : algebraic dual space of \mathcal{V}_n |
| \mathcal{W} | : subspace (of \mathcal{V}) |
| $\mathcal{L}(\mathcal{V}_n, \mathcal{V}_n)$ | : space of operators $T : \mathcal{V}_n \rightarrow \mathcal{V}_n$ |
| \mathcal{R}_n | : space of real n -tuples |
| \mathcal{C}_n | : space of complex n -tuples |
| $[x_i]$ | : space spanned by vectors x_i |
| $\langle \dots \rangle$ | : inner product |
| $\ \cdot \ $ | : norm |
| $[\dots]$ | : linear functional |

Chapter 4

| | |
|---------------------------|---|
| A, B | : matrices or linear transformations |
| I | : identity matrix |
| K | : stiffness matrix |
| K_a | : analytical stiffness matrix |
| M | : mass matrix |
| M_a | : analytical mass matrix |
| x_i | : i th eigenvector (mode) |
| x_{ai} | : i th analytical eigenvector |
| $\lambda_i = \omega_i^2$ | : i th eigenvalue |
| w_i | : i th natural frequency |
| λ_{ai} | : i th analytical eigenvalue |
| Λ | : diagonal matrix of λ_i |
| Λ_a | : diagonal matrix of λ_{ai} |
| Φ | : matrix of x_i |
| Φ_a | : matrix of x_{ai} |
| θ | : zero vector |
| $\mathcal{R}(\)$ | : range space |
| $\mathcal{N}(\)$ | : null space |
| \mathcal{V}_n | : space spanned by x_i $i = 1, \dots, n$ |
| \mathcal{V}_n^A | : space spanned by x_{ai} $i = 1, \dots, n$ |
| $\langle \dots \rangle_A$ | : weighted inner product |

Chapter 5

| | |
|-----|--------------------|
| C | : damping matrix |
| I | : identity matrix |
| K | : stiffness matrix |
| M | : mass matrix |

| | |
|---|---|
| $X = \begin{bmatrix} \Phi \\ \Phi \Lambda \end{bmatrix}$ | : mass matrix of x^1 |
| Y | : matrix of y_i |
| $x^i = \begin{bmatrix} x_1 \\ \vdots \\ x_i \\ \vdots \\ x_n \end{bmatrix}$ | : i th eigenvector of $(2n \times 2n)$ problem |
| x_i | : i th eigenvector |
| $\overline{x_i}$ | : complex conjugate of x_i |
| y_j | : j th eigenvector of dual $(2n \times 2n)$ problem |
| λ_i | : i th eigenvalue |
| h | : matrix of λ_i |
| ω_i | : i th undamped natural frequency |
| Ω_j | : j th measurement frequency |
| Ω | : diagonal matrix of ω_i |
| Φ | : matrix of x_i |
| k_i | : i th normalisation constant |
| \mathcal{V}_{2n} | : vector space spanned by $[x^i]_{i=1, \dots, 2n}$ |
| \mathcal{V}_{2n}^A | : vector space spanned by $[x_a^i]_{i=1, \dots, 2n}$ |
| θ | : zero vector |
| $\langle a$ | : analytical equivalent of . |
| $[...]$ | : linear functional |
| $\langle ..., \rangle$ | : inner product |

Chapter 6

| | |
|-----------|---|
| E | : Young's modulus |
| \bar{I} | : second moment of area |
| N | : number of degrees-of-freedom of FE model |
| M, K | : FE $(N \times N)$ mass and stiffness matrices |
| $S(y)$ | : cubic spline |
| $S'(y)$ | : first derivative of $S(y)$ |

| | |
|-------------|-----------------------------------|
| $S''(y)$ | : second derivative of $S(y)$ |
| x_i | : measured mode |
| x_{1i} | : known values of measured mode |
| x_{2i} | : unknown values of measured mode |
| y_i | : i th position along beam |
| m | : mass per unit length |
| λ_i | : i th measured eigenvalue |
| θ | : zero vector |
| $\cdot 1$ | : measurement position |
| $\cdot 2$ | : non-measurement position |
| $\cdot a$ | : analytical equivalent |

INTRODUCTION AND REVIEW1.1 Preliminaries

An understanding of the dynamic behaviour of structures has been sought for many years. This search has been greatly enhanced by the onset of computer technology, which has allowed an ever-increasing degree of sophisticated analysis in order to gain a fuller comprehension of how structures exhibit vibrational characteristics. The sorts of structure that provoke interest in terms of their dynamic behaviour are extremely varied and far too numerous to mention here. However, to cite but a few examples: civil engineering structures such as **bridges**, dams and **multi-storey frames** have been investigated^(5,30,34,41,100), with **particular** attention being paid to how the structure would behave in an earthquake environment; aircraft dynamics is another area where a good understanding is required in order to provide the optimum **design**⁽⁴³⁾; other structures of interest include offshore **structures**⁽⁴⁸⁾, space vehicles⁽²³⁾, motor cars⁽⁴⁰⁾, and so on, in a seemingly endless list. In order to assess the dynamic properties of these structures, two methods have emerged in recent years with which to analyse the problem. The first of these methods is the finite-element method, which has been logically expanded from its use in static analysis to incorporate dynamic behaviour. This technique has now firmly established itself as an extremely **powerful** numerical method. A brief review of how it **is** adapted for use in dynamic work is given in Section 1.3. The second technique is modal testing, in which the structure (or a scale model of it) is

actually excited and measurements of the structure's response are made in order to assess its dynamic characteristics. Equipment capable of these measurements is relatively new and the interest and amount of activity in the field of modal testing continues to expand at an increasing rate. This fact is demonstrated by the existence of the International Modal Analysis Conferences, which began in 1982 and continue to grow in terms of support and the quality and quantity of papers submitted. However, modal analysis techniques are not being developed with the objective of replacing the long-standing theoretical, finite-element dominated type of analysis - the two are designed to enhance one another. If both methods indicate the same type of response patterns, then an even greater confidence that this would be the true **response** of the structure may be asserted. With greater control and demands being put on the design of modern structures, the time **when an FE** analysis alone would suffice to indicate the vibrational characteristics of that structure is rapidly drawing to a close. The modern **dynamicist** needs to be both a good analytical engineer and also a proficient experimental engineer. This dual role implies that two sets of data will emerge. The ideal situation would be if these two sets agreed with each other so that the modal test and the **FE** analysis may co-exist and complement one another in mutual harmony. However, both methods have errors attached to them. The FE method is an approximation to the real continuous structure with a finite **degree-**of-freedom model and consequently can never be a perfect representation of that structure. In addition to this, modal testing also has its associated errors. These are concerned with the way in which data are collected and subsequently analysed. However, there

exist two insurmountable limitations with test methods. The first of these is the fact that it is generally not possible to measure at all the nodes or degrees-of-freedom required. This is especially true when one considers rotational motion. The second limitation is that in all but the most trivial example an incomplete set of data is obtained. That is, the number of degrees of freedom exceeds the number of measured modes. Despite this, it cannot be overlooked that the test measurements do offer the most accurate representation of the structure. So, experimentation provides the best source of information, which is nearly always incomplete, whereas the analysis provides a complete picture but is often inaccurate. It is prudent, therefore, to try to extract the most salient features of both types of approach. The way forward, thinking in general terms, would perhaps be to somehow combine the two in an effort to provide a third and optimum set of information which includes data from the modal tests and retains the additional data available only from an **FE** analysis. The theme of this thesis is concerned with problems of this nature.

Attempts to reconcile the contrasting sets of information that exist between experiment and analysis in the literature are firstly reviewed towards the end of this chapter. Chapters 3 to 6 set out to reanalyse the problem in the context of vector space theory, starting initially from an idealistic, oversimplified example and gradually introducing more factors as each previous stage is explained and understood. Vector space theory is a mathematical tool which is an extension of simple geometric concepts, so at each stage of the analysis a vivid picture of the meaning of the work will **be** readily available. All the expressions previously

presented, using a wide range of alternative mathematical techniques, appear in the analysis contained herein - along with other expressions, previously unseen. The advantage and motivation for the use of vector space theory is that it simplifies the problem into simple geometric terms, provides a unification for the whole, and therefore permits an extension to more complicated cases where other techniques might possibly be buried in their own algebra. **As** a direct result of the use of this method, cautionary notes may be injected outlining the limitations and expectations that will exist, no matter what type of approach is adopted, because of the very nature of the problem.

Chapter 2 presents a limited investigation into experimental and analytical methods, using as a test-piece a simple uniform beam. Some description of how the beam was analysed using experimental modal analysis and how a mathematical model was formulated using the FE method is given. This serves as an introduction to both methods and allows the problem to be set in context with an appreciation of the two contrasting approaches.

The principal results and conclusions that are drawn from the entire analysis are reviewed and discussed in the final chapter, and the thesis draws to a close with a brief discussion of how the entire line of research stands at present - and where it is likely to move, as a greater understanding is attained, in the foreseeable future.

1.2 Dynamic Equations

For the analysis, we assume that we are dealing with a linear system, so the usual way in which the equations of motion are

introduced is via the one degree-of-freedom mass-spring-damper set-up^(25,52,63). The equation of motion is considered in terms of forces acting on the body, and written as

$$m\ddot{X}(t) + c\dot{X}(t) + kX(t) = F(t)$$

where $F(t)$ represents the external force, $X(t)$ the response and its derivatives with respect to time, and m , c and k represent the mass, viscous damping and stiffness of the system. For multi-degree-of-freedom systems with n degrees of freedom, the motion is said to be adequately described (assuming small motion, elastic materials etc.) by n linear differential equations with constant coefficients, written as

$$M\ddot{X}(t) + C\dot{X}(t) + KX(t) = F(t).$$

Now, $X(t)$ and $F(t)$ are displacement and force n -vectors respectively and M , C and K are $(n \times n)$ mass, viscous damping and stiffness matrices. The text of this thesis is concerned with the viscous damping model. This model has the advantage that it is mathematically plausible, as opposed to hysteretic damping where the equations of motion differ and cause difficulties at zero frequency, with a finite dissipation of energy. Hysteretic damping is often introduced in the light of the observation that damping is independent of frequency. However, no entirely satisfactory model, in the form of a differential equation, exists to incorporate this and for light damping the equivalent viscously damped system is practically justifiable⁽⁶⁵⁾.

We may take the Laplace transform of the model to obtain

$$(M\lambda^2 + C\lambda + K)x(\lambda) = f(\lambda)$$

that is

$$B(\lambda)x(\lambda) = f(\lambda)$$

where $B(X) = M\lambda^2 + C\lambda + K$

$B(X)$ is known as the $(n \times n)$ system matrix and its inverse $H(X)$ is the transfer function matrix. So, assuming $\det|B(\lambda)| \neq 0$, and that all the poles lie in the left-hand half-plane (stability condition), we have

$$H(\lambda) = [B(\lambda)]^{-1}$$

so that

$$x(\lambda) = H(\lambda)f(\lambda)$$

If we assume that there are no repeated roots, then $H(X)$ may be written in partial fraction form as

$$H(\lambda) = \sum_{i=1}^{2n} \frac{a_i}{\lambda - \lambda_i}$$

where a_i = i th residue of the system

λ_i = i th pole of the system (eigenvalue)

and $\lambda_i = -\mu_i \omega_i \pm i\omega_i \sqrt{1 - \mu_i^2}$

for the dissipative system. Here, ω_i is the undamped natural frequency of mode i , which is the square root of the i th pole of B with $C = 0$. μ_i is the percent critical damping for mode i , where a critically damped system returns to a state of equilibrium without oscillation. The frequency response function, rather than the transfer function, is obtained by substituting $\lambda = i\omega$, thus,

$$H(i\omega) = \sum_{k=1}^{2n} \frac{a_k}{i\omega - \lambda_k}$$

These expressions are derived by Lancaster⁽⁵⁸⁾ and again at the end of Chapter 5, in the context of vector space theory. For free vibration, $f(A)$ is put equal to zero so that

$$(M\lambda^2 + C\lambda + K)x(\lambda) = \theta.$$

For consistency, A must adopt the $2n$ values satisfying the charac-

teristic equation

$$|M\lambda_i^2 + C\lambda_i + K| = 0 \quad i = 1, \dots, 2n$$

The associated eigenvector x_i which-satisfies the equation

$$(M\lambda_i^2 + C\lambda_i + K)x_i = 0$$

is, in matrix form, for $i = 1, \dots, 2n$, equivalent to

$$M\Phi\Lambda^2 + C\Phi\Lambda + K\Phi = 0$$

where Λ = diagonal matrix of eigenvalues

Φ = matrix of eigenvectors.

If $c = 0$, then we have

$$M\Phi\Lambda = K\Phi.$$

This is the undamped free vibration equation and when this is solved, gives the undamped normal modes x_i and the undamped natural frequencies ω_i^2 . Orthogonality conditions emerge from the analysis which must be satisfied. These are given by

$$\Phi^T M \Phi = I$$

and $\Phi^T K \Phi = A$

for an undamped system. Further developments of this type of analysis are to be found in References (79) and (80).

1.3 The Finite-Element Method

The onset of the rapid development of computer technology permitted the development of the FE method so that it now represents a powerful numerical tool in the analysis of, amongst others, dynamic structures. To complement this, several texts have appeared in the literature describing the FE method from first principles. A selection of these appear as References (11), (18), (29), (31), (71), (85) and (110). It is not the objective here to analyse or

criticise the basic principles of the FE method as it is a tool of proven worth that is now well established.

To be brief, the FE method is a way of replacing the ^{partial} differential equations describing the structure by a (possibly large) set of matrix equations. The matrices are finite-dimensional analogues of the differential (stiffness) operator and the mass. The matrices are obtained by discretising the structure into much smaller, simpler elements, whose mass and stiffness properties may be estimated with the use of **localised** shape functions of a simple polynomial nature, in order to derive element mass and stiffness matrices. These elemental matrices may then be combined to form the global mass and stiffness matrices. If the numbering of the nodes of the elements is done in a sensible fashion, these global matrices will be banded in nature. Elements are assembled by ensuring continuity of displacement and slope (rotation) at a finite number of points on contiguous groups of elements. The resulting finite-dimensional model thus satisfies compatibility throughout the structure in this sense, while equilibrium is satisfied only in a variational or weak sense. The procedure, for this reason, is often referred to as the displacement method. Boundary conditions which occur are incorporated at the assembly stage. Accurate assessment of the boundary conditions is a **crucial, but** difficult, task and caution needs to be exercised to ensure that what is being **modelled** reflects the real situation accurately.

In general, two types of mass matrix may appear. The first is a consistent mass matrix, so called because its derivation is arrived at in a similar fashion to that of the stiffness matrix. The second is a lumped mass matrix, which may be interpreted almost

literally. All the mass of the structure is assumed to be concentrated at the node points and so this matrix will be *usually* diagonal and hence will require less computer storage space. The solution of the equation

$$M\Phi\Lambda = K\Phi$$

is then sought for the first several eigenvectors (starting with the lowest eigenvalue). The eigenvectors will correspond to the normal modes of the structure and the eigenvalues will correspond to the square of the undamped natural frequencies. It is usual for the damping matrix to be assumed to be negligible when conducting this type of analysis, so normally only the conservative behaviour of the structure will be predicted.

1.4 Modal Testing

The amount of interest and activity that surrounds the field of modal analysis continues to swell. This is hardly surprising, considering the potential rewards such a method offers. Modal testing has been in existence much *longer* than its name, and dates back to the early days of vibration measurement. Its appeal lies in the fact that it is an experimental technique as opposed to an analytical one. A far more confident appraisal of the dynamic characteristics of the structure under consideration may be presented if it has been directly tested rather than artificially modelled, and the derived model subsequently analysed. Of course, the price for dealing with the real world is having to cope with all the real phenomena that exist, such as damping, non-linearities etc. However, far from dissipating interest as a result of these unattractive features, the subject continues to expand because of the new and exciting

challenges these problems provide for both the experimental and analytical engineer. The amount of literature that has appeared in the field of experimental modal analysis is vast, and there is far too much for it all to be cited here. The interested reader is referred to References (3), (67) and (68) for good bibliographies on the current literature covering all aspects of testing, including results obtained on specific test-pieces. The purpose of this section is to provide a general overview of the field and highlight some of the more significant contributions which are of a more general nature.

The motivation for conducting a modal test is to extract a mathematical model of the behaviour of that structure. Ewins^(35,37) suggests that the model will be of three possible forms:

1. Response - containing the forced response characteristics of the structure, usually as functions of time or frequency.
2. Modal - a knowledge of the principal modes of vibration, natural frequencies and damping estimates.
3. Spatial - a description of the distribution in space of the structure's mass, stiffness and damping characteristics.

The ease with which each of these models may be formulated varies. Model 1 is rapidly established if good measurements are made and the subsequent analysis of the data is conducted sensibly. Model 2 may be extracted from model 1, but some mathematical constraints and limitations must be imposed. The evaluation of model 3 from experimental data alone presents severe difficulties and is usually conducted with the aid of other information (analytical). Model 3 is clearly of most benefit to the **practising** engineer, since it

tells him something about the physical characteristics of the structure under investigation, permits a prediction of its response due to given loading conditions, and models 2 and 1 can be derived directly from it. Hence the derivation of model 3 will be a principal concern of this thesis, and for purposes of review at this stage the various techniques available for the formulation of models 1 and 2 only will be considered.

In essence, experimental modal analysis consists of three stages:

1. Acquisition of Data.
2. Analysis of Data - formulation of model 1.
3. Curvefit of Data - formulation of model 2.

Each of these steps requires careful thought and preparation if the time spent on a modal test is to be advantageous. The experimenter needs to be aware of his objectives and goals at the beginning of the investigation, and not halfway through, in the light of unforeseen assumptions and avoidable errors. For example, for the test engineer, one hour spent calibrating a single accelerometer correctly will be, in the long term, infinitely more advantageous than two weeks spent analysing data that is inherently wrong in the first place. Stein^(95,96) observes that the analysis of data is a 'right' that has to be 'earned' by successfully obtaining valid data at the outset. He remarks that the actual collection of data in the first place is an extremely important stage, since all further analysis - if it is to be valid - depends on the accuracy of the data first acquired. He adds that in a test situation the equipment must be assumed to be 'guilty' of generating unwanted

types of noise and it is for the engineer to convince himself that these unwanted measurements are sufficiently controlled either by removing them completely or by limiting their significance.

Ewins⁽³⁶⁾ also injected a few words of warning with the results of his round-robin tests, where many engineers were asked to analyse and test a simple structure, and then demonstrated the spread of opinion in the results obtained by displaying them all simultaneously in graphical form.

The type of test that is conducted depends largely on the type of structure under investigation and the quality of information sought. Many authors^(37,55,82) have listed techniques used in order to extract the data. Among the methods are sine-sweep testing, random input, pseudo-random input, multiple shaker sine dwell technique, impact testing, and so on. These techniques require the use of electromagnetic exciters, force transducers, accelerometers and other associated pieces of equipment now generally available. A brief investigation into two of these techniques (multiple shaker sine dwell and impact testing) is given in Chapter 2.

Once the data have been collected they need to be processed. The first stage is usually analogue-to-digital conversion. The onset of computer technology and the development of the Fast Fourier Transform (FFT), first developed by Cooley and Tukey⁽²⁷⁾ in 1965, has meant that the data can be processed at high speed and presented in either a time or frequency domain in one of the many forms of presentation available. Again, these techniques and the associated considerations required for their effective implementation are becoming well established, and discussion here will be limited to

that of equipment available at Bristol University and the **experiences** gained from it, as described in Chapter 2. Having obtained the data in this form, model 1 is said to have been established. This usually consists of a knowledge of the frequency response function between excitation location, i , and response measurement location, j . The assumption of linearity throughout the structure infers that if one row or column of the frequency response matrix is known, then the whole matrix can be evaluated. Two software packages exist at Bristol University for the analysis of data using this approach.

Once the data is in this form, the next stage is the interesting problem of curvefitting the measured data so that a mathematical function with disposable parameters approximates it as closely as possible. Much effort has been devoted to this problem, in recent years, with analyses being conducted in either the time or frequency domains. In the time domain, perhaps the two most significant methods of parameter estimation are the Ibrahim time domain technique⁽⁵³⁾ and the poly-reference complex exponential method^(4,105). Both methods use the free decay response of the structure to determine the system's eigensolutions and fit a model of the form

$$X(t) = \sum_{i=1}^{2n} x_i e^{\lambda_i t} + \{\eta(t)\}$$

where $\eta(t)$ represents the noise. The poly-reference technique obtains the free decay responses by an inverse **FFT** on the obtained transfer functions. It has also been developed for use in the frequency domain⁽²⁸⁾.

More commonly in the frequency domain, however, the approach is again to fit the mathematical expression to the data. The analytical expression used here is **as before**

$$H(i\omega) = \sum_{k=1}^{2n} \frac{a_k}{i\omega - \lambda_k}.$$

To reiterate, the a_k 's are known as the residues and contain information concerning the mode shapes of the structure. However, the function here is non-linear, with respect to the λ_k 's, and this problem may lead to difficulties. Much discussion upon how this function may be fitted to the experimental data may be found in the literature^(19,45,111), and consideration of this problem is given in Chapter 2 with details concerning how the curvefitter was coded on the PDP 11/34 at Bristol University. Some authors acknowledge the fact that the fitting of an analytical model requires that certain parameters (i.e. natural frequency and damping) need to be global properties of the structure, but curvefitting does not entirely confirm this (especially with damping), so that global curvefitting procedures are introduced whereby all the frequency response functions are fitted simultaneously so that only one **frequency** and one damping estimate is extracted for each mode.

Other curvefitting techniques include a circle-fit, which is a single-degree-of-freedom method first introduced by Kennedy and Pancu⁽⁵⁷⁾, and fits a circle to the experimentally-obtained data plotted on a real vs imaginary diagram of the frequency response function. The method is relatively simple to implement and hence its attraction to many analysts. However, its use is limited to well-separated peaks.

Richardson and Formenti⁽⁸³⁾ have utilised orthogonal polynomials in order to remove some of the ill-conditioning of the non-linear least squares **curvefit** and have used these polynomials to **curvefit** an expression of the form

$$H(i\omega) = \frac{\sum_{k=0}^m a_k \lambda^k}{\sum_{k=0}^n b_k \lambda^k} \Big|_{\lambda = i\omega}$$

where n is set as the number of identified roots and m may be specified by the analyst. Having solved this problem, the residues are then found by using the usual expression. Other factors that are considered are the contribution of modes outside the frequency range of interest and how additional terms may be included to account for **this**^(19,111).

Once completed, a successful **curvefit** will yield estimates of the mode shapes of the structure and the natural frequency and damping estimates. This is the modal model (model 2). The mode shapes will be, depending upon the complexity and distribution of natural frequencies, either real or complex. Since the function used to **curvefit** the data is complex, in general complex modes will be generated. If damping is small and the natural frequencies are well spaced, the complex modes are often replaced by their real part, making the assumption that the imaginary contribution is negligible. The modal model may then be used for comparison against the eigensolutions of the analytical model.

Another area of research in this field which is of significance is the use of the Hilbert transform for the detection of non-linear systems. If

$$\bar{Z}(\omega) = \int_{-\infty}^{\infty} z(t)e^{i\omega t} dt = \bar{X}(\omega) + i\bar{Y}(\omega)$$

$$\text{then } \bar{X}(\omega) = \frac{1}{\pi} \int_{-\infty}^{\infty} \frac{Y(\Omega)}{\omega - \Omega} d\Omega$$

$$\text{and } \bar{Y}(\omega) = \frac{1}{\pi} \int_{-\infty}^{\infty} \frac{X(\Omega)}{\omega - \Omega} d\Omega$$

So here the fact that the imaginary part of a frequency response function may be generated from the real part via the Hilbert transform and vice versa is utilised in order to determine areas of **non-linearity**^(50,93,102,104). Some work on taking into account non-linearities in the curvefitting procedure has also been conducted⁽³⁹⁾. Other work has also been undertaken on the determination of structural defects using modal test techniques and a knowledge of the mass and stiffness distribution of the structure^(1,21).

Overall, modal analysis is a current area of intense research and as methods, equipment and techniques improve, so does the confidence in the natural frequencies, damping factors and mode shapes that are extracted using this method. Clearly, if this is the case, some harmony between the test and the FE analysis must prevail. Correlation of the two is reviewed in the next section.

1.5 Correlation of Experiment and Theory

One of the key objectives of activity in the area of dynamic analysis in recent years has been to derive measured mass and stiffness matrices from the modes and frequencies that will have been obtained from a modal test, or in other words, to generate model 3.

Richardson and Potter⁽⁸¹⁾, in an early paper, offered an immediate solution to this problem for the damped case. This analysis started from the expression for the transfer function matrix

$$H(\lambda) = \sum_{i=1}^{2n} \frac{a_i}{\lambda - \lambda_i} = (M\lambda^2 + C\lambda + K)^{-1}.$$

If λ is put equal to 0, then

$$H(0) = - \sum_{i=1}^{2n} \frac{a_i}{\lambda_i} = K^{-1}$$

hence $K = \{H(0)\}^{-1}$.

Then differentiating with respect to λ we have

$$H'(\lambda)[M\lambda^2 + C\lambda + K] + H(\lambda)[2M\lambda + C] = 0$$

and again putting $\lambda = 0$ gives

$$H'(0)K + H(0)C = 0$$

$$H(0)^{-1}H'(0)K + C = 0$$

$$C = -KH'(0)K$$

and again differentiating w.r.t. λ

$$H''(\lambda)[M\lambda^2 + C\lambda + K] + H'(\lambda)[2M\lambda + C] + H(\lambda)[2M\lambda + C] \\ + H(\lambda)2M = 0$$

and finally, putting $\lambda = 0$ again, we have

$$H''(0)K + 2H'(0)C + H(0)2M = 0$$

$$\frac{H''(0)K}{2} + (-H'(0)KH'(0)K) + H(0)M = 0$$

$$H(0)M = H'(0)KH'(0)K - \frac{H''(0)K}{2}$$

$$M = K(H'(0)KH'(0) - \frac{H''(0)}{2})K$$

and hence solutions for K , C and M are rapidly obtained. The serious difficulty that exists with this analysis is the initial inversion of $H(0)$ in order to obtain K . For this to be possible, $H(0)$ needs

to be non-singular or, in other words, all the modes of the structure must have been measured. If this is the case, these expressions - and others mentioned in the literature⁽³⁸⁾ - are perfectly valid and will provide the correct spatial matrices. In practice though, when measurements are made on a real structure, an incomplete set of data only will be obtained. That is, the number of measurement positions will greatly exceed the number of modes measured. We will have a so-called 'incomplete modal model' (model 2) consisting (thinking for the time being of the undamped case only) of an ($m \times m$) diagonal matrix of eigenvalues (square of the natural frequencies) Λ and an ($n \times m$) rectangular matrix of modal vectors Φ .

Starkey⁽⁹⁴⁾, in a recent paper, acknowledges this fact and introduces the idea of a generalised inverse in order to circumvent this difficulty, and proposes expressions of the form

$$K = \Phi(\Phi^T\Phi)^{-1}\Lambda(\Phi^T\Phi)^{-1}\Phi^T.$$

This type of result is attractive because it will satisfy the necessary condition of orthogonality

$$\Phi^TK\Phi = \Lambda$$

and hence, if he had derived a mass matrix in a similar fashion, satisfying

$$\Phi^TM\Phi = I$$

a complete system would have emerged consisting of two singular system matrices satisfying the two orthogonality requirements and hence the eigenvalue equation. However, his analysis fails to suggest such a system.

What is perhaps of more serious concern here is that the mass and stiffness matrices obtained by this method will have no meaningful

interpretation in terms of mass and stiffness distributions of the structure. Starkey quite rightly observes that this type of expression "does not include the subspace perpendicular to the eigenvectors from the experiments", but yet neglects to clarify exactly what information is to provide the data for this subspace. Ross⁽⁸⁹⁾, in an earlier paper, inferred that difficulties may be encountered when trying to develop matrices in this way with his comments: "from the spectral decomposition of a matrix, it is known that the higher-order eigenvectors determine the outward appearance of a matrix." He goes on to observe that the lowest strain energy states determine the outward appearance of the flexibility matrix, so a flexibility matrix may readily be constructed. Rodden⁽⁸⁶⁾, in a separate line of investigation, reaches this conclusion and goes on to demonstrate how this is done.

However, many authors also acknowledge the fact that there is additional information available in terms of analytical mass and stiffness matrices. If the analytical modes and frequencies correspond with those of the test then there is no call to direct attention to the generation of measured mass and stiffness matrices, since it is assumed that these will directly correspond with the analytical ones. However, the line of action necessary if the two in some way contradict each other has generated a lot of interest.

Much concern was directed to which set of data was correct, and earlier attempts^(6,8,46,62,88,97,98) which were made prior to the development of more sophisticated test equipment assumed that the most likely 'correct' piece of data was the analytical mass matrix, hence efforts were made to orthogonalise the measured data with respect to the mass matrix so that

$$\Phi^T M \Phi = I,$$

and then proceed to correct the stiffness matrix. One of the major criticisms of this type of exercise -is that the 'corrected' system still did not produce the measured modes, so it was debatable as to exactly how it had been corrected.

Berman and Flanelly⁽¹²⁾, in an earlier paper on the problem, considered some important points that one needs to be aware of for this type of analysis. They proposed an expression for an 'incomplete' stiffness matrix given by

$$K_{INC} = \sum_{i=1}^m M x_i \lambda_i x_i^T M.$$

Again, however, we may see that the dominant terms the high eigenvalues, were missing from the summation so that the form of this incomplete matrix may not, in practice, represent any tangible stiffness distribution. They acknowledged this by commenting that "since the terms containing the higher values of λ_i are not included, the dominant terms of K will be missing and thus K_{INC} will not resemble the true K matrix."

Another glaringly obvious fact about this type of result is that the mass matrix also needs to be known in advance. They consider this problem, and conclude that the "best information available as to what the 'true' values are, (i.e. elements of the mass matrix) is the approximation arrived at by the engineer" or, in effect, the analytical mass matrix, M_a . However, again there could be no guarantee that M_a would satisfy the orthogonality requirements with respect to the measured modes Φ . It was clear that what was needed was a best approximation to the mass distribution followed by a slight adjustment so that it also satisfied the orthogonality requirements.

It was not until 1979 that a generalised expression that satisfied these requirements finally emerged. In his excellent technical note, Berman⁽¹⁴⁾ describes how a change to M_a is sought (AM) so that

$$\phi^T (M_a + \Delta M) \phi = I.$$

He sets out to find that AM which has some minimum weighted Euclidean norm within the constraint of this condition. The following function is minimised

$$\epsilon = \left\| M_a^{-\frac{1}{2}} \Delta M M_a^{-\frac{1}{2}} \right\|$$

and Lagrange multipliers are introduced to incorporate the orthogonality constraint to give the following Lagrangian function

$$\psi = \epsilon + \sum_{i=1}^m \sum_{j=1}^m \lambda_{ij} (\phi^T \Delta M \phi - I + M_a)_{ij}$$

where $m_a = \phi^T M_a \phi$.

This equation is then differentiated with respect to each element of AM and the results are set to zero in order to satisfy the minimisation and the constraint. This process gives the matrix equation

$$2M_a^{-1} \Delta M M_a^{-1} + \phi \underline{\Lambda} \phi^T = 0$$

or $\Delta M = -\frac{1}{2} M_a \phi \underline{\Lambda} \phi^T M_a$.

A solution for $\underline{\Lambda}$ (the $(m \times m)$ matrix of λ_{ij}) may easily be extracted as

$$\underline{\Lambda} = -2m_a^{-1} (I - m_a) m_a^{-1}$$

so that

$$\Delta M = M_a \phi m_a^{-1} (I - m_a) m_a^{-1} \phi^T M_a$$

This result was encouraging insofar as it is:

(a) 'close' to the analytical matrix in the sense of a Euclidean norm;

(b) symmetrical;

(c) satisfies the orthogonality constraints.

This improved mass matrix allows the incomplete stiffness matrix to be also calculated as described previously. Alternatively, a similar method may be adopted to correct the analytical stiffness matrix - once the mass matrix has been corrected - as described by Baruch⁽⁷⁾ and Wei⁽¹⁰⁷⁾. The norm that is minimised here is

$$d = \|M^{-\frac{1}{2}}(K - K_a)M^{-\frac{1}{2}}\|$$

K_a is symmetric and can be singular if it includes rigid body modes (see below). K must also satisfy the constraints

$$K\Phi = M\Phi\Lambda,$$

$$K = K^T,$$

and $\Phi^T K \Phi = A$.

Again, Lagrange multipliers are introduced to incorporate these constraints and partial differentiation yields an expression for K of the form

$$K = K_a + M\Phi(\Phi^T K_a \Phi + \Lambda)\Phi^T M - K_a \Phi \Phi^T M - M \Phi \Phi^T K_a.$$

So a pattern is emerging whereby an analytical model is improved in stages using the data obtained from the modal test. In 1983, Berman and Nagy⁽¹⁵⁾ formalised this procedure, calling it AM1 (analytical model improvement). The method is essentially conducted in three steps:

1. M_a , K_a and the measured modal displacements and natural frequencies are used to obtain the 'full' modal vectors from which

Φ ($n \times m$) is formed (see Section 1.6).

2. M_a and the now known Φ are used to obtain M which satisfies the orthogonality relationship between the modes.

3. K_a and the known M , Φ and A are used to obtain K , which is symmetric and satisfies the eigenvalue equation. The M and K here do not represent the 'true' mass and stiffness matrices of the structure, as may be implied by the notation, but only corrected analytical matrices obtained using measured information.

Baruch^(9,10), in the light of the argument that it may be the stiffness matrix which is known with more reliability than the mass matrix because of "the significantly greater success of the finite-element static analyses (which use the stiffness matrix) as compared to corresponding dynamic analyses (which are both the mass and stiffness matrices.)"⁽¹³⁾, suggested that the stiffness matrix may be corrected first and then the mass matrix. Effectively the roles of the mass and stiffness matrices are reversed. Here, instead of initially normalising the modes with respect to the analytical mass matrix so that

$$x_i^T M_a x_i = 1,$$

as was necessary for the previous case, the modes are normalised so that

$$x_i^T K_a x_i = \lambda_i \quad (\lambda_i = \omega_i^2).$$

The important point to note here is that if the structure is not fixed in space, such as an aircraft or space vehicle, then there will exist rigid body modes. These are modes that have zero **frequency** and are brought about due to the lack of a fixed reference position. There is ^{normally} a maximum of six rigid body modes which satisfy

$$Kx_i^R = 0 \quad i = 1, \dots, 6.$$

So, if they are present, the stiffness matrix is singular. They are orthogonal with the mass matrix; so

$$x_i^R M x_j^R = \delta_j^i \quad i, j = 1, \dots, 6$$

therefore the mass matrix remains non-singular. Thus, if rigid body modes are present, the reverse approach cannot be implemented because of the singular nature of the stiffness matrix. The inclusion of rigid body modes does not affect the previous formulation. Having understood this, Lagrange multipliers may again be introduced in order to incorporate the necessary constraints. The expressions obtained in this way for stiffness and mass are given as

$$K = K_a + K_a \phi k^{-1} (\Lambda - k) k^{-1} \phi^T K_a$$

$$\text{and } M = M_a + K \phi k^{-1} (I + m) k^{-1} \phi^T K - K \phi \phi^T M_a - M_a \phi \phi^T K$$

where $k = \phi^T K_a \phi$.

Chen and Fuh, in a recent technical note⁽²⁴⁾, have adopted the idea of generalised inverse in order to rederive these types of expressions and introduce a weighting matrix W , but do not succeed in deriving a general form for an improved mass or stiffness matrix; nor, indeed, is it made clear that the mass and stiffness matrices do not have to be updated in any particular order. The same sort of comments also apply to O'Callahan and Leung⁽⁷³⁾ in attempts to use established pseudo-inverse techniques^(64,75) in order to redetermine the update expression for mass and stiffness.

Berman, in a more recent paper⁽¹⁶⁾, provoked further discussion with the justifiable observation that an expression of the

form

$$K = \sum_{i=1}^n M_{x_i} \lambda_i x_i^T M$$

could not identify a K matrix which represents the correct structural characteristics, since the higher modes used are those of the structure and not of the model. The modes in this expression are those of the finite-dimensional model. The high modes of the structure ($i \approx n$) are not the same as those of a valid model. This effectively means that the idea that the problem would be somehow 'solved' if only we could measure all the modes is a myth. It is not possible to measure the higher modes of a model since these are analytical functions associated with that model and do not represent any measurable parameter. Indeed, he quite rightly asserts that the validity of the model will only cover a frequency range up to approximately $\sqrt{(\lambda_n/2)}$.

One of the motivations for improving or updating mass and stiffness matrices is that it then offers the prospect of comparing an updated mass and stiffness with the original analytical matrices with the objective of an error analysis to see where the mathematical model may have been in error in the first instance. An 'error analysis' type of approach need not necessarily yield improved mass and stiffness, but may only serve to indicate the areas of poor modelling in the model. However, the text of this thesis sets out to demonstrate the close link that exists between error analysis and model improvement techniques.

In the light of this, Dobson⁽³²⁾ is perhaps a little bold with his sentiments that "it **is** not possible to convert differences between experimental and predicted results into spatial **modifica-**

tions within the FE model." In his contribution, he proposes the application of a flexibility error matrix in order to determine which parts of the mathematical model are in error. The error expression is extracted through the expression for flexibility with the corresponding analytical pieces of information being taken directly from the model thus

$$\epsilon = \Phi \Lambda^{-1} \Phi^T - \Phi_a \Lambda_a^{-1} \Phi_a^T$$

However, limited success is achieved here since, as will be discussed in Chapter 2, local changes in the material properties of the structure globally affect the flexibility of that structure, so it may be slightly optimistic to expect a 'flexibility' error matrix to indicate areas of poor modelling.

An alternative approach is proposed by Sidhu and Ewins⁽⁹¹⁾ whereby a stiffness error matrix is investigated. This is given as the difference between the exact stiffness matrix and that of the model

$$\epsilon = K - K_a$$

Rearranging and inverting both sides gives

$$K^{-1} = [I - K_a^{-1} \epsilon] K_a^{-1}$$

If the matrix $K_a^{-1} \epsilon$ satisfies the condition

$$(K_a^{-1} \epsilon)^\infty = 0$$

(i.e. $K_a^{-1} \epsilon$ is small in some sense), the expression in the square brackets can be rewritten using the binomial expansion as

$$K^{-1} = K_a^{-1} - K_a^{-1} \epsilon K_a^{-1} + ((K_a^{-1} \epsilon)^2 K_a^{-1})$$

or, to first order,

tions within the FE model." In his contribution, he proposes the application of a flexibility error matrix in order to determine which parts of the mathematical model are in error. The error expression is extracted through the expression for flexibility with the corresponding analytical pieces of information being taken directly from the model thus

$$\epsilon = \phi \Lambda^{-1} \phi^T - \phi_a \Lambda_a^{-1} \phi_a^T$$

However, limited success is achieved here since, as will be discussed in Chapter 2, local changes in the material properties of the structure globally affect the flexibility of that structure, so it may be slightly optimistic to expect a 'flexibility' error matrix to indicate areas of poor modelling.

An alternative approach is proposed by Sidhu and Ewins⁽⁹¹⁾ whereby a stiffness error matrix is investigated. This is given as the different between the exact stiffness matrix and that of the model

$$\epsilon = K - K_a$$

Rearranging and inverting both sides gives

$$K^{-1} = [I - K_a^{-1} \epsilon] K_a^{-1}$$

If the matrix $K_a^{-1} \epsilon$ satisfies the condition

$$(K_a^{-1} \epsilon)^\infty = 0$$

(i.e. $K_a^{-1} \epsilon$ is small in some sense), the expression in the square brackets can be rewritten using the binomial expansion as

$$K^{-1} = K_a^{-1} - K_a^{-1} \epsilon K_a^{-1} + ((K_a^{-1} \epsilon)^2 K_a^{-1})$$

or, to first order,

$$K^{-1} \approx K_a^{-1} - K_a^{-1} \epsilon K_a^{-1} + O(\epsilon^2)$$

or
$$\epsilon = K_a (K^{-1} - K_a^{-1}) K_a'$$

K^{-1} and K_a^{-1} are then determined as the flexibility matrices suggested by Dobson. A similar expression for the mass error matrix may be derived, of the form

$$\epsilon = M_a (M^{-1} - M_a^{-1}) M_a'$$

Sidhu and Ewins then go on to demonstrate how these error matrices may be applied in order to determine areas of poor modelling that may exist within the structure. Although these error expressions may look very different to the update expressions described previously, it will be seen through the course of this thesis that the two are quite closely related.

Other work in this area is directed towards utilising some sort of iterative procedure whereby the physical parameters of the model are modified (e.g. EI, mass/unit length) to encourage a closer agreement between analysis and test. Collins et al⁽²⁶⁾ offer a statistical approach and Chen and Garba⁽²²⁾ employ a matrix perturbation technique. The advantage of these methods is that the consistency of the model is preserved, but computational difficulties and problem formulation limit the adaptability of these methods to realistic structures.

Throughout the analysis of this problem, attention is directed to the undamped problem only, and the measured data are assumed to be real normal modes. However, in practice all structures are damped and will yield measured modes which are complex, often with significant imaginary parts. In this instance, the methods

already mentioned all come under question and nearly all authors tend to neglect this almost inevitable fact if so-called 'realistic' structures are to come under scrutiny. Some authors attempt to circumvent this problem with proposals for computing normal modes from complex ones (42,54,69,108). The type of approach that is adopted is usually either the introduction of measurement noise in order to facilitate the inversion of a singular matrix, or the introduction of an hypothesis such as the measured *modes* can be represented as a linear combination of the **normal modes** of the analytical system. These attempts tend to be unsuccessful, and can produce unsatisfactory and unstable solutions. In effect, the problem of damping is here eased out of the problem by attempting to eliminate its contribution to the set of measured data, and hence we return to an artificial undamped environment which is not truly representative of the real world.

The methods adopted to improve or update the spatial matrices describing a system discussed so far do not readily lend themselves to an extension to the dissipative case. One of the principle objectives of this thesis is to reassess the techniques mentioned here in order to unify the entire process of identification, thereby clarifying the objectives and expectations of the research in this area and allowing it to be extended to the case of viscous damping.

The initial introduction of the equations of motion of a dynamic system is usually done in terms of the mass-spring-damper one-degree-of-freedom system, as described in Section 1.2, but by the time a large system is being analysed in terms of modelling or testing, the damping matrix has usually either been completely cast aside or assumptions are made about its nature (usually proportional

damping or estimates gained from previous experience). Some attempts have been made to synthesise the concept of linear damping⁽⁶⁵⁾, but in general a technique for constructing a FE damping matrix in a similar fashion to the mass and stiffness continues to be excluded from any analysis. Until a satisfactory method emerges for doing this, experimentation will be the only source of information available concerning the damping characteristics of the structure. Clearly an unsatisfactory state of affairs will exist if experimentation increasingly tends towards the extraction of complex modes and damping factors, but yet consideration of the damping matrix is continually **ostracised** from any analysis. Fawzy and Bishop⁽³⁸⁾ analyse the equations of motion of a linear non-conservative system to **derive** the inherent relationships that exist, with no assumptions being made upon the properties of the system matrices. However, the analysis contains only statements of these identities and discussion concerning the implications is not forthcoming. The presentation of the orthogonality conditions that exist for this type of system continue to appear in the literature^(37,38,42), and Zhang and Lallement⁽¹⁰⁹⁾ realise that if the damped system is to tend towards the undamped system as the damping tends to zero then a different normalisation to the one usually quoted is required so that the phase shift of the modes is 0° or 180° .

As mentioned, this thesis is concerned with the viscous damping model. The alternative approach is to consider the hysteretic or structural damping approach. This is introduced as a result of the experimental observation that damping is independent of frequency, which is not reflected in the viscous damping model. The usual hysteretic, one-degree-of-freedom model adopted for transient

motion is

$$m\ddot{X}(t) + k(1 + ig)X(t) = 0.$$

This involves a complex operator, so therefore neither the real nor the imaginary parts of X alone are solutions. Physically, there appears to be no logical justification for the inclusion of the complex variable in the equation of motion. The more sensible model to adopt is an integro-differential equation which uses a convolution, thus

$$m\ddot{X}(t) + k(1 + g^*)X(t) = \theta$$

where a convolution between two functions is given as

$$\begin{aligned} f_1(t) * f_2(t) &= \int_0^t f_1(t - \tau)f_2(\tau)d\tau \\ &= \int_0^t f_1(\tau)f_2(t - \tau)d\tau. \end{aligned}$$

This formulation has a Laplace transform of

$$(\lambda^2 + \omega_1^2(1 + g(\lambda)))x(\lambda) = \theta.$$

The transfer function is given by

$$H(A) = \frac{1}{\lambda^2 + \omega_1^2(1 + \gamma \ln(\lambda))}$$

where the function $g(X) = \gamma \ln(\lambda)$ is necessary to ensure a constant imaginary part, in accordance with observations. Therefore we have a frequency response function of

$$H(i\Omega_j) = \frac{1}{-\Omega_j^2 + \omega_1^2(1 + \gamma \ln|\Omega_j| \pm iy \pi/2)}.$$

Thus, we may observe that hand-in-hand with constant damping is a change in stiffness. It may be possible, for certain frequency ranges, to neglect the change in stiffness if γ is small, so we have

$$H(i\Omega_j) \approx \frac{1}{(-\Omega_j^2 + \omega_1^2) + \frac{i\omega_1^2\gamma\pi}{2}}$$

which is the usual form adopted. However, this model has the difficulty of an infinitely negative stiffness as frequency tends to zero, which leads to an unbounded displacement response which is a totally unrealisable model. Attempts have been made to improve this with variations of $\ell_n(\lambda)$, all of which demonstrate that a region of constant damping requires a variation in stiffness. Reference (65) goes on to demonstrate that for the various formulations given, the displacement response for the equivalent viscous model is generally acceptable, thus justifying the use of the viscously damped model for dissipative systems.

Clearly, damping problems are an area where research potential is vast. Chapter 5 of this thesis considers the $(2n \times 2n)$ viscously damped problem and the results for the undamped case are rederived with the analytical damping matrix set to zero as would be anticipated if no analytical damping information is known.

The contents of this section are presented in order to provide a brief review of the work that has so far been presented on the problem of verification strategies. It is clearly a key issue in dynamic analysis, since if some sort of plausible agreement between test and analysis cannot be procured then the credibility of one, if not both, of these techniques will be seriously undermined and a confident appraisal of the dynamics of the structure under investigation will be denied. Early optimism concerning the apparent ease of formulation of measured mass and stiffness matrices from dynamic tests was rapidly extinguished. This is not to say that incomplete measured matrices may not be derived, but the very

inclusion of the word 'incomplete' implies that information is not available and the matrices so obtained may not reflect any tangible mass or stiffness distributions. It is a fact that the missing information represents that which is most predominant in terms of mass and stiffness distributions, but which is not readily available for measurement by the experimental dynamicist. However, all is not lost as a result of this, since further information is at hand in terms of the analytical mass and stiffness matrices. Two possible courses of action are the use of analytical matrices to provide the missing information, and to effectively complete the measured matrices with the best information available. Alternatively, this information may be removed from the analytical matrices in order to conduct an error analysis with matrices of a comparable nature.

Berman⁽¹⁶⁾ has quite rightly commented that discussion of the physical relationships between an analytical model and test data has been rare, and the objective of this thesis is to attain an understanding of these relationships. The formulae quoted so far are thus rederived within the framework of vector space theory in order to demonstrate how nearly all the analysis proceeds in the same fashion, with the same objectives. Reference (16) is rather less optimistic than previous publications, and expresses concern about some of the limitations that are to be expected. Although it is wise to proceed with caution, the nature of these limitations needs to be known. Not surprisingly, they are directly related to the quality and quantity of data obtained and it is an objective of this thesis to provide a feel for the sort of expectations one may anticipate and the amount of useful information one may expect

to extract. Discussion of this nature has been restricted because of its complexity and therefore the work presented herein has been directed to a more philosophical nature, bearing in mind the situation that a **practising** test engineer is likely to encounter, rather than attempting a straightforward application, which may not have been so useful without first understanding the problem at hand.

One of the central issues that is encountered in this analysis is the problem caused by the fact that measurements are not usually made at all the degree-of-freedom points of the model. This is rarely achievable in practice, since rotational **degrees-of-freedom** often exist in the analysis and equipment to measure this is not available to the experimentalist at present. A **compatibility** between a measured mode and an analytical one is essential prior to any analysis of the two, so clearly the problem is of key significance and will deny any further development if adequate consideration is not forthcoming. This fact, and its importance, is **recognised**, so that consideration of this problem is set aside and considered separately in Chapter 6 and thoughts upon this topic by others are reviewed in the next section.

1.6 Expansion of Measured Data

A central issue concerning the comparison of measured data with analytical matrices is the question of compatibility. An FE model, for example a dam structure, will have, say, 1500 nodes, 90% of which will be internal and therefore inaccessible to measurement. Furthermore, a modal test may be expected to identify no more than

perhaps the first 8-10 modes at, at most, 50 measured positions. In order to proceed with a comparison between these two sets of data, the order of the two sets will **have** to be equal. This involves either reducing the order of the analytical model or completing the measured modes in some fashion so that a direct comparison may ensue. In addition to the problem of the inability to measure internal degrees-of-freedom, there is also the problem of assessing the rotational motion at the external nodes. The current test equipment has the capacity to measure translational motion only, so we may see that much of the desired information concerning measurement will be unavailable. This is in addition to the problem of measuring the higher modes as previously mentioned. A reduction in the size of the model is considered undesirable, since it is advantageous to retain the form and structure of the model, so attention is directed towards the expansion of the measured modes. Consideration of this problem is given in Chapter 6, but is first briefly reviewed.

In essence, two possible strategies exist for completing the measured modes. Firstly, some sort of interpolation technique may be adopted in order to approximate the unknown information, and secondly the analytical model may again be used to provide the information with some kind of expansion process. The theory of **splines**^(2,17,90) is now a well-developed technique for interpolation purposes, and some efforts have been made to complete modes using these concepts. **Done**⁽³³⁾ discusses two-way **spline** curves for the analysis of the aeroelastic characteristics of aircraft. His attention is focused on the interpolation of node deflections which are given at the nodes of a structural grid in order to obtain the

desired information at the nodes of an aeroelastic grid. In general, the two do not coincide so the problem discussed there is similar to the one here, though it is usual for dynamic measurements to be made at positions corresponding to a node in the FE model. The use of surface splines has also received attention^(49,87). However, interpolation techniques have their limitations in any given circumstances since, although a useful tool, not a great deal of accuracy or reliability can be expected because the amount of known information (as compared to the amount of unknown) is very sparse. Large, unavoidable errors may emerge, especially with the higher, more complex modes.

The use of the mathematical model to complete the mode is often preferred in the literature and is, effectively, the same as interpolating using the shape functions from which the model is derived. In a rather different context, consideration at an early stage was given to reducing the number of terms in an FE model to reduce the computational difficulty experienced in determining the lower eigenvectors and eigenvalues for the problem^(47,56). However, the rapid increase in computer technology has meant that this is not such a significant problem as before. Guyan⁽⁴⁷⁾, in what is effectively a static analysis, proposes expressions for K and M in the reduced case as

$$K_{\text{FULL}} = \begin{bmatrix} K_{11} & K_{12} \\ K_{21} & K_{22} \end{bmatrix} \quad M_{\text{FULL}} = \begin{bmatrix} M_{11} & M_{12} \\ M_{21} & M_{22} \end{bmatrix} \quad \begin{array}{l} 1 = \text{measured} \\ 2 = \text{unmeasured} \end{array}$$

$$K_{\text{RED}} = K_{11} - K_{12}K_{22}^{-1}K_{21}$$

$$M_{\text{RED}} = M_{11} + (K_{22}^{-1}K_{12})^T M_{22} (K_{22}^{-1}K_{12}) - (K_{22}^{-1}K_{12})^T M_{21} - M_{12} (K_{22}^{-1}K_{12})$$

Using this idea, the reverse process may be implemented whereby the

unknown degrees-of-freedom are obtained from the known ones using this type of expression.

Berman and Nagy⁽¹⁵⁾, in a paper addressing the problem, formulate it as

$$\left\{ \begin{array}{cc} [K_{11} & K_{12}] \\ [K_{21} & K_{22}] \end{array} - \lambda_i \begin{array}{cc} [M_{11} & M_{12}] \\ [M_{21} & M_{22}] \end{array} \right\} \begin{array}{c} x_{1i} \\ x_{2i} \end{array} = 0$$

and so obtain

$$x_{2i} = - (K_{22} - \lambda_i M_{22})^{-1} (K_{21} - \lambda_i M_{21}) x_{1i}$$

If $\lambda_i = 0$, then this is equivalent to the Guyan reduction relationship. If $\lambda_i \neq 0$ then this method corresponds to the dynamic condensation method outlined by Paz and others^(74,76,77,78). The drawback with the dynamic condensation/expansion method is that it needs to be calculated for each natural frequency ω_i , and a costly inversion is involved which, although the method may be accurate, is also very slow. Proposals whereby this conversion may be avoided are presented in Chapter 6 in order for the best full experimental mode to be extracted from the information available.

1.7 Overview

The contents of this chapter have introduced the subject matter of this thesis. It has identified two methods of approach for the dynamic assessment of structures, and reviewed some of the work that has emerged which attempts to bring the two together in order to obtain the best approximation of the structure's dynamic characteristics. Rarely, in the published work, is there any discussion upon the 'nature' of the problem, and confusion often prevails as a result of the apparent lack of success of methods proposed.

Chapter 1 has attempted to highlight some of the more significant comments that have hitherto appeared in the literature, and to outline the motivation of this **area of** research.

Chapter 2 follows this up with a discussion upon the application of the FE method and contains details of modal tests, both investigations being carried out on a simple uniform beam in order to display the very contrasting nature of the information extracted by each method. This is then extended to a consideration of the contrasting stiffness/flexibility type of data under investigation in each case.

The theory of vector spaces is introduced in Chapter 3 in order to revisit the problem armed with these tools. A simple analysis of the single matrix case is included. Chapter 4 then goes on to deal with the undamped problem, and this is then naturally extended to the damped problem in Chapter 5. The difficulties caused by not being able to measure at all the FE nodes are discussed in Chapter 6, as already mentioned, and Chapter 7 brings the entire problem together with an overall assessment in the light of the knowledge gained, including recommendations and proposals for future work in this area.

CHAPTER 2

PRELIMINARY WORK

2.1 Preliminaries

Having now established the area of research, namely the correlation of experimental measurements with theory, in the first instance an examination of both techniques in more specific detail is required. To this end, simple structures are investigated in this chapter in order to obtain an awareness of the methods of approach of both theoretical finite-element analysis and experimental modal analysis. The contents of this chapter therefore contain the details of the development of mathematical models describing simple structures and some of the experimental techniques used for testing such structures. The purpose of this is to obtain first-hand knowledge of both methods and allow some of the features that must be considered during such processes to be highlighted. The chapter builds to a general discussion upon the contrasting nature of the two methods to establish some undeniable facts and focus the analysis of the subsequent chapters on the difficulties arising from the real world with its many observable phenomena.

2.2 Setting Up an FE Model

The work in this section will be concentrated on simple specific examples. The motivation was to develop working mathematical models with which the analysis of the ensuing chapters could be investigated and tested. The structures studied are:

1. uniform cantilever;
2. uniform simply-supported beam;
3. simply-supported beam with non-proportional damping;

and for the remainder of this thesis these will be known as Examples 1, 2 and 3. The majority of the text of this thesis concentrates upon the detection of error and improvement of mathematical models of structures, so to go hand-in-hand with these three models, alternative versions were developed which were known to be incorrect, but were **labelled** 'the analytical model', requiring improvement or adjustment. Thus, for each of the three examples there exist two versions of the mass matrix and two of the stiffness matrix. Those which correctly describe the structure or the true FE matrices are simply called M and K, and the incorrect analytical versions are **labelled** M_a and K_a . Although experimental techniques receive attention in this chapter, for the purposes of the development and investigation of the error expressions and so on in the remainder of this thesis it was considered prudent to adopt two FE models, one to represent the analytical environment and the other to represent the real world or that which would be measured **experimentally**. Therefore the additional problems that are encountered when making good measurements are avoided and the two separate problems may be addressed individually. The theme of this thesis **concentrates** on the second part of this problem, or that which is concerned with the course of action required when good experimental measurements disagree with analytical predictions. That is not to say that the first stage, the acquisition of good measurements, is in any way a simple or trivial task. This problem has received widespread attention and is addressed in this chapter to attempt to provoke some constructive discussion upon experimental techniques for people wishing to verify their mathematical model using modal analysis.

The 'two model' approach is defended with the argument that it would be fruitless to devote time and effort to obtaining good dynamic measurements of a structure if one were unaware of what to do with them, once obtained. For example, it is often the case that an experimentalist will measure complex modes of vibration and yet the analysis in the literature is all too often based upon real modes, so already the first dilemma is encountered. The analysis of this thesis starts from a very simple position and attempts to build and expand the theory in stages to arrive at a plausible assessment, by adding in at each stage the increasing difficulties that would be envisaged with the comparison of experiment with theory. It is submitted that by the end of the thesis all the relevant practical considerations have been covered and dealt with. The use of two mathematical models, one for experiment and one for analysis, is the only way *effectively* to do this. If the development of a theory was attempted using a mathematical model and experimental measurements then one is simultaneously confronted with the problems of curvefitting, interpolation, complex v normal modes, damping estimates, normalisation and so on, at the onset. Each problem in turn, if it is to be properly understood, needs to be individually isolated and analysed.

Example 1 - Uniform Cantilever

Example 1 is a uniform cantilever that is split up into five finite elements (see Diagram 2.1). For each of the elements, four shape functions were used which possess either unit displacement or unit gradient at either end of the element and 0 displacement or gradient at the ends other than this (see Table 2.1). The

expressions for mass and stiffness are well established and given by References (71) and (110)

$$k_{ij} = \int_0^l EI(y) \psi_i'(y) \psi_j'(y) dy$$

$$m_{ij} = \int_0^l m(y) \psi_i(y) \psi_j(y) dy$$

Performing these integrations for each pair of shape functions results in the production of the element stiffness and mass matrices, thus

$$K^e = \frac{EI}{l^3} \begin{bmatrix} 12 & 6l & -12 & 6l \\ 6l & 4l^2 & -6l & 2l^2 \\ -12 & -6l & 12 & -6l \\ 6l & 2l^2 & -6l & 4l^2 \end{bmatrix}$$

$$M^e = \frac{ml}{420} \begin{bmatrix} 156 & 22l & 54 & -13l \\ 22l & 4l^2 & 13l & -3l^2 \\ 54 & 13l & 156 & -22l \\ -13l & -3l^2 & -22l & 4l^2 \end{bmatrix}$$

For convenience, l , m and EI are set equal to 1. These elemental matrices are then assembled over the five elements and boundary conditions are introduced at $x = 0$ (that is, the first two rows and columns are eliminated) to give the two global matrices given by Figure 2.1. The modes and frequencies of this system are then evaluated by solving the equation

$$Kx_i = \lambda_i Mx_i$$

where $\lambda_i = \omega_i^2$

The analytical model for this example is taken as a cantilever with

the second element having half the mass per unit length and a quarter of the second moment of area of the original (see Diagram 2.2). For this element, the element mass and stiffness matrices are given by

$$K^e = \begin{bmatrix} 3.0 & 1.5 & -3.0 & 1.5 \\ 1.5 & 1.0 & -1.5 & 0.5 \\ -3.0 & -1.5 & 3.0 & -1.5 \\ 1.5 & 0.5 & -1.5 & 1.0 \end{bmatrix}$$

and

$$M^e = \begin{bmatrix} 78 & 11 & 27 & -6.5 \\ 11 & 2 & 6.5 & -1.5 \\ 27 & 6.5 & 78 & -11 \\ -6.5 & -1.5 & -11 & 2 \end{bmatrix}$$

and the global mass and stiffness matrices are given in Figure 2.2.

Example 2 - Uniform Simply-Supported Beam

The same beam element was used in this example, the only differences being that, for convenience, the length of the beam was set to 3.1415926 (π) and different boundary conditions were imposed (i.e. translational coordinates at each end eliminated - see Diagram 2.3). The mass and stiffness matrices for this are given by Figure 2.3. This has the convenience of ease of comparison with the theoretical modes which are sine functions with eigenfrequencies w_i^2 (i.e. 1, 16, 81, 256, 625 etc.). The modes and frequencies are given in Figure 2.4, with the modes being **normalised** so that

$$\Phi^T M \Phi = I.$$

It is important to realise at this stage that the eigenvalues and eigenvectors in Figure 2.4 correspond to the solution of the finite

dimensional eigenvalue problem. They do not all describe the first 10 modes of a simply-supported beam (i.e. the first 10 sine functions), but are merely approximations. However, the approximation is generally considered to be good for the first $n/2$ modes when arranged in order of ascending frequency, hence the appeal of the FE method when continuous analytical solutions are not available, which is the usual practical situation. The analytical model for this example was taken as a simply-supported beam with the first element having half the mass and half the second moment of area (see Diagram 2.4). The analytical matrices are given in Figure 2.5.

Example 3 - Simply-Supported Beam with Non-Proportional Damping

In this example a non-proportional viscous damping matrix is introduced where the damping is set at 1% of the stiffness in the first element and zero everywhere else. The damping matrix is given in Figure 2.6. The eigenvectors and eigenvalues are now complex and are normalised so that

$$-\Phi^T M \Phi \Lambda + \Lambda \Phi^T M \Phi + \Phi^T C \Phi = 2A$$

for reasons expanded upon later. The solution to this problem is given in Figures 2.7 and 2.8.

The analytical model was taken to be the same as in Example 2, with the analytical damping matrix being assumed to be zero (as would be the most probable situation). One may observe that damping is relatively small in the first mode and increases for the higher modes. The real part of the complex mode approximates the normal mode for the lower modes which is an observation often made in practical situations (see Appendix 1 for a comparison with estimates obtained using a perturbation analysis). The interpretation

of the real and imaginary parts of the eigenvalues of this problem are given later on in this chapter. These three models are used throughout this thesis for preliminary investigations into the construction of incomplete spatial matrices, error analysis and so on.

2.3 Experimental Modal Analysis

Two approaches for modal analysis are generally adopted. They involve exciting the structure at either one point or many points. Both methods are briefly discussed here to outline some of the more important points that need to be considered when conducting a modal test.

2.3(a) Multiple Input Testing

Multiple input testing has been in existence for a longer time than its counterpart, single input. Its use was developed rapidly in the mid-60s, principally in the aircraft industry, when the use of computer power was not as readily accessible as it is today. Broadly speaking, multiple input testing involves the attachment of several electromagnetic exciters to the structure under investigation, with the objective of exciting one of the normal modes of that structure by tuning the various force levels of each exciter, until a state of resonance is reached. The mode is then measured and the process is repeated for another mode of vibration. Early work on this technique (51) was perhaps a little ambitious, with attempts to automate this procedure using an analogue machine, so that the force level of each exciter was controlled automatically, such that once the process was set in motion the machine would tune

itself in to a state where it was exciting a normal mode and thus relieve the engineer of any manual adjustments. This machine was given the acronym **GRAMPA** (Ground Resonance Automatic Multipoint Apparatus). The technique envisaged a fully-automated system which would rapidly converge to a normal mode and hence reduce the experimental time and the need for expertise in the tedious manual adjustment of exciter force levels. Despite this, it achieved limited success and was hampered by a continual divergence away from the frequency of the mode being excited.

The consequence of this was to adopt a compromise situation where only one exciter is controlled automatically which monitors the frequency of vibration, but the remaining exciters are adjusted manually until all are tuned into the normal mode. This version was given the acronym **MAMA** (Manual Automatic Multipoint Apparatus) (101).

At Bristol University the need to develop MAMA by incorporating computer technology was identified and an updated version, **MAMA-2**, was constructed which utilised a NASCOM micro-computer for control of the hardware. **MAMA-2** utilises up to five electromagnetic exciters which are attached to the structure at five different locations. The principal exciter, usually fixed at a position of large amplitude of the mode being considered, is set in motion at the frequency of that mode. An accelerometer is fixed near to the principal exciter and a resonance is said to have been established when a quadrature phase shift has been observed between the force level and the accelerometer. The phase angle is monitored on the **MAMA** VDU. Automatic frequency control is then imposed which allows the frequency of the principal exciter to be automatically adjusted to maintain a quadrature phase shift while the force levels of the

other exciters are set in motion. The force levels of these exciters are then adjusted in turn until a normal mode is being excited. The involvement of the author on the MAMA project was to develop software for the automatic frequency control, to conduct some preliminary tests, and to produce documentation for its use, a copy of which appears as Appendix 2. Some useful subsequent results were obtained using MAMA-2 for the dynamic analysis of concrete arch dams⁽¹⁰³⁾.

Further work on MAMA-2 was not pursued for the purposes of this thesis. This is because the introduction of computer technology for use with this type of equipment has not greatly enhanced its potential but highlighted the inherent difficulties of this technique. The principal drawback with this type of approach is that some preconception of the mode shape is required before an analysis can begin. This is a potentially dangerous situation and the user must exercise extreme caution and judgement to ensure that he does not impose his premeditated opinion of what the mode shape should look like upon his interpretation of the observations that are made. No phase variation on the force input is currently available on MAMA-2. This means that real modes are assumed from the onset and no facility for accommodating complex modes is available. In real life this situation is reversed. There is invariably a change of phase between different positions, sometimes small if damping is light. Therefore a phase variation of as much as $\pm 10\%$ from quadrature is considered acceptable when exciting a normal mode and damping is light. Already we may observe that an approximate confirmation of a preconceived mode shape is all that may be expected. In addition, setting up of the apparatus is time-consuming

and tricky. The positioning of the exciters needs to be considered in advance and careful attachment by suspending the exciters is required. There is no facility for automating the setting up of apparatus at present, so these difficulties are inevitably going to continue to present themselves. On top of this, some authors⁽⁵⁵⁾ express concern that prolonged excitation of one mode may actually result in structural damage, the very thing that it is desirable to prevent.

Multipoint excitation has not benefitted greatly from advances in computer technology and at present, in the opinion of the author, fails to keep pace with the rapid advances being made with the single point excitation method, which is much easier to set up and implement.

2.3(b) Single Point Excitation

Single point excitation techniques have generally undergone significant development in recent years due to the fact that they more readily lend themselves to processing using digital computer technology. The method assumes a linear structure so that to establish a picture of the dynamic behaviour of a structure either an accelerometer measuring response may be fixed and the excitation position moved to different positions on the structure, or the excitation position is fixed and the accelerometer moved to different positions. It is more usual for the latter to be adopted, though some caution is needed to ensure that the excitation position does not coincide with a node of one of the principal modes of vibration.

The response of the structure is almost invariably measured with the use of accelerometers, but the excitation may be produced

with either one electromagnetic exciter or an instrumental hammer. When conducting a modal test, perhaps the single most important consideration is repeatability. If the equipment can be dismantled, calibration checks made and reassembled with a repeat of the test producing the same measurements, then the confidence in the procedure and subsequent analysis will grow. It is rarely wasted effort, therefore, to ensure that the apparatus has been set up sensibly. The attachment of the equipment is an important consideration. Accelerometers may be attached using a variety of techniques ranging from hand-held to threaded screws. Clearly, the more firmly they are attached, the more confidence will be given to the reliability of the readings. Electromagnetic exciters, if they are to be used, are best attached via a thin rod which has the advantage of being very stiff in one direction (that of the excitation) and flexible in other directions, thereby ensuring that the exciter does not impose unwanted additional reactionary forces which would contaminate the readings. The length of the attachment rod is important: not too long so as to introduce the dynamic behaviour of the rod into the system, **but not** so short that the required **flexibility** in perpendicular directions is not attained. Once the **correct** attachment has been chosen and implemented, the sort of signal that may be imposed may vary from sine-sweep to periodic random, to random - depending on the test situation and the type of information sought.

The general procedure for setting up apparatus, exciting the structure and dealing with the sorts of problems that need to be identified (e.g. aliasing, leakage) are now well documented⁽³⁷⁾. It is not the purpose of this thesis to review these phenomena in

any detail since they are now well understood and hardware has emerged which analyses the data with these problems overcome (e.g. by introducing a windowing technique). The most significant outstanding difficulty appears to be the assessment of modal parameters once frequency response function data has been obtained. That is, the development of model 2 once model 1 has been established. This is essentially a curvefitting problem, and is necessary if good modal parameters are to be extracted for the subsequent comparison with a theoretical model. Therefore the approach that has been adopted and implemented at Bristol is described here, and this is then supplemented with examples using an impact testing transient technique which will be described at that stage.

2.4 Development of the Curvefitting Program

If we consider, for the present, a one-degree-of-freedom system, then the equation of motion describing that system is given by

$$m\ddot{x}(t) + c\dot{x}(t) + kx(t) = F(t).$$

If we take the **Laplace** transform of this equation and assume zero initial displacement and velocity, we have

$$(\lambda^2 m + \lambda c + k)x(\lambda) = f(\lambda).$$

That is

$$(\lambda^2 + 2\mu_1\omega_1\lambda + \omega_1^2)x(\lambda) = f(\lambda)$$

where $2\mu_1\omega_1 = \frac{c}{m}$

and $\omega_1^2 = \frac{k}{m}$.

The transfer function is then given by

$$H(\lambda) = \frac{x(\lambda)}{f(\lambda)} = \frac{1}{\lambda^2 + 2\mu_1\omega_1\lambda + \omega_1^2}$$

where λ is complex and equal to, say, $\xi + iw$. We may solve

$$\lambda^2 + 2\mu_1\omega_1\lambda + \omega_1^2 = 0$$

to get $\lambda = -\mu_1\omega_1 \pm \omega_1\sqrt{1 - \mu_1^2}$.

So, $H(X)$ may be factorised about its poles to give

$$H(X) = \frac{a' + ia''}{(\lambda + \mu_1\omega_1 - i\omega_1\sqrt{1 - \mu_1^2})} + \frac{a' - ia''}{(\lambda + \mu_1\omega_1 + i\omega_1\sqrt{1 - \mu_1^2})}$$

Therefore

$$1 = (a' + ia'')(\xi + iw + \mu_1\omega_1 + i\omega_1\sqrt{1 - \mu_1^2}) \\ + (a' - ia'')(\xi + iw + \mu_1\omega_1 - i\omega_1\sqrt{1 - \mu_1^2})$$

and taking real and imaginary parts gives

$$1 = a'\xi + a'\mu_1\omega_1 - a''w + a''\omega_1\sqrt{1 - \mu_1^2} + a'\xi + a'\mu_1\omega_1 \\ + a''w + a''\omega_1\sqrt{1 - \mu_1^2}$$

so $1 = 2(a'\xi + a'\mu_1\omega_1 + a''\omega_1\sqrt{1 - \mu_1^2})$

and $0 = a''\xi + a''\mu_1\omega_1 + a'w - a'\omega_1\sqrt{1 - \mu_1^2} + a'w \\ + a'\omega_1\sqrt{1 - \mu_1^2} - a''\xi - a''\mu_1\omega_1$

so $0 = a'w \Rightarrow a' = 0$

and $a'' = \frac{-1}{2\omega_1\sqrt{1 - \mu_1^2}}$

This is the transfer function for a one-degree-of-freedom system.

It is usual for the frequency response function only to be measured, which is simply the transfer function measured along the frequency axis. λ is replaced with $i\Omega_j$ where Ω_j is the j th measured frequency ($j = 1, \dots, \overset{A}{M}$), thus

$$H(i\Omega_j) = \frac{a' + ia''}{(i\Omega_j + \mu_1\omega_1 - i\omega_1\sqrt{1 - \mu_1^2})} + \frac{a' - ia''}{(i\Omega_j + \mu_1\omega_1 + i\omega_1\sqrt{1 - \mu_1^2})}$$

We may also observe that the real and imaginary parts of the frequency response function are given by

$$\text{Re}(H(i\Omega_j)) = \frac{(\omega_1^2 - \Omega_j^2)}{(\omega_1^2 - \Omega_j^2) + 4\mu_1^2\omega_1^2\Omega_j^2} \quad j = 1, \dots, \hat{M}$$

$$\text{and } \text{Im}(H(i\Omega_j)) = \frac{-2\mu_1\omega_1\Omega_j}{(\omega_1^2 - \Omega_j^2)^2 + 4\mu_1^2\omega_1^2\Omega_j^2}, \quad j = 1, \dots, \hat{M}$$

These are shown, for a one-degree-of-freedom system, in Figure 2.9.

In a similar fashion, an expression for the frequency response function may be obtained for a multiple degree of freedom system (see Section 5.11) to give

$$H(i\Omega_j) = \sum_{k=1}^n \frac{a_k}{i\Omega_j - \lambda_k} + \frac{a_k}{i\Omega_j - \bar{\lambda}_k} \quad j = 1, \dots, \hat{M}$$

where a_k = residue of kth mode;

$$\lambda_k = -\mu_k\omega_k + i\omega_k\sqrt{1 - \mu_k^2};$$

ω_k = undamped natural frequency of kth mode;

μ_k = % critical damping of kth mode.

The purpose of the **curvefit** is to give the best parameters for a_k and λ_k so that the mathematical expression given here approximates the measured frequency response function in a minimum least squares sense. For the single degree-of-freedom example we let

$$\epsilon = \sum_{j=1}^{\hat{M}} (H_j - H(i\Omega_j))$$

where H_j = measured frequency response at frequency Ω_j ;

$H(i\Omega_j)$ = analytical frequency response at frequency Ω_j with unknown parameters a' , a'' , μ_1, ω_1 .

The mathematical parameters need to be set so as to make

$$\begin{aligned} \|\epsilon\|^2 &= \langle \epsilon, \epsilon \rangle \\ &= \sum_{j=1}^{\hat{M}} \{(H_j - H(i\Omega_j))(\bar{H}_j - \overline{H(i\Omega_j)})\} \end{aligned}$$

a minimum. A Newton-Raphson iteration scheme was developed to perform this minimisation. It possesses quadratic convergence with a sequence of linear equations. So,

$$\frac{\partial \langle \epsilon, \epsilon \rangle}{\partial \alpha} = \sum_{j=1}^{\hat{M}} (H_j - H(i\Omega_j)) \frac{\partial H(i\Omega_j)}{\partial \alpha} + (\bar{H}_j - \bar{H}(i\Omega_j)) \frac{\partial H(i\Omega_j)}{\partial \alpha}$$

$$= f(\alpha), \text{ say,}$$

where $\alpha = a', a'', p', p''$

and $p' = -\mu_1 \omega_1, p'' = \omega_1 \sqrt{1 - \mu_1^2}$.

The iteration scheme to solve $f(a) = 0$ is given as

$$\{D(f(\alpha^{(p)}))\}(\delta^{(p)}) = -f(\alpha^{(p)}),$$

$$\{\delta^{(p)}\} = \{\alpha^{(p+1)}\} - \{\alpha^{(p)}\}.$$

So, if we have initial estimates of the unknown parameter vector $\{\alpha^{(0)}\}$, a better approximation is given by $\{\alpha^{(0)}\} + \{\delta^{(0)}\}$ where $\{\delta^{(0)}\}$ is the solution of the above equation. The D denotes partial differentiation with respect to the α parameters. $\{D(f(\alpha^{(p)}))\}$ is therefore a matrix, known as the Jacobian matrix. The scheme may readily be extended to many degrees-of-freedom with the number of equations to solve being four times the number of modes present. Hence, the formal differentiation may be carried out and the iteration procedure applied to provide the best approximation to a_k and λ_k given a_0 and λ_0 .

This procedure was programmed for preliminary tests on the Bristol University mainframe computer. In order to determine its usefulness, some artificial one-degree-of-freedom test data were generated with which to try the program. Only an initial estimate of the pole was required since the initial estimate for the residue could be found by solving the linear least squares problem with the pole initial estimate. For the test data the following parameters were set:

$$\mu_1 = 0.03, \omega_1 = 4$$

so $\lambda = -0.12 \pm 3.99819953$.

and $a' + ia'' = 0 - 0.1250562i$.

The program was run using differing initial estimates and the results are given in Table 2.2. As can be seen from this, convergence is obtained if

$$-1 < \text{DAMPING ESTIMATE} < -0.07$$

$$3.93 < \text{NATURAL FREQUENCY ESTIMATE} < 4.07$$

That is, from this test the indication is that an initial estimate error of about 40% is good enough for the damping and an error of not more than 1.75% is required for the frequency. This was considered acceptable since it is usual for the frequency estimate to be obtained quite accurately from a modal test.

The Hilbert transform says that the real and imaginary parts of an analytical function contain the same information (one being derivable from the other using the transform) so a further test was conducted to identify whether $\text{MIN}|\text{Re}(H)|^2$, $\text{MIN}|\text{Im}(H)|^2$ or $\text{MIN}(|\text{Re}(H)|^2 + |\text{Im}(H)|^2)$ show any signs of differing stability criteria. The outcome of this test is summarised in Tables 2.2, 2.3 and 2.4. This showed that using $\text{MIN}|\text{Im}(H)|^2$ was perhaps not as advisable as the other two possibilities. It was decided to use $\text{MIN}|\text{Re}(H)|^2$ since this reduced the amount of data that needed to be processed by a half.

In the final preliminary test some artificial noise was introduced on the data with the use of a pseudo-random variable. 2% and 5% noise was introduced to simulate actual measurements. The outcome of this test is given in Tables 2.5 and 2.6. This showed that the introduction of noise did not affect the quality of the convergence, but only increased the number of iterations required for convergence to be obtained.

Two-degree-of-freedom **data were** also generated to investigate the usefulness of the algorithm for identifying close peaks. In general, the outcome was encouraging, provided that the initial natural frequency estimates were fairly good.

A further development of the curvefitting program was the inclusion of a NAG⁽¹¹²⁾ linear least squares algorithm, which uses an improved version of Newton-Raphson iteration. The standard version may run into difficulties with poor initial estimates, especially if the Jacobian matrix $(D(f(\alpha^{(p)})))$ is rank deficient or the sum of squares is not small near the solution. The modified technique is based on the singular value decomposition of the Jacobian **matrix**⁽⁷⁰⁾, thus

$$J = D(f(\alpha^{(p)})) = U \begin{bmatrix} S \\ 0 \end{bmatrix} V^T$$

where $S (= \text{diag}[S_1 \dots S_{4n}])$ is a matrix of singular values of J with $S_{i+1} \leq S_i$. U and V are $(\hat{M} \times \hat{M})$ and $(4n \times 4n)$ orthonormal matrices. S is then partitioned to provide an iterative algorithm for the solution. The use of this routine removes the ill-conditioned nature of J . The introduction of this improved version of the **curvefit** permitted a relaxing of the fairly severe initial estimate restriction on the natural frequency and allowed a more reliable degree of convergence. The inclusion of the NAG routine was also useful insofar as it provides information **as** to the quality of the curvefit, indicating whether convergence has been obtained, or how close the final values are to a minimum, or whether divergence has occurred, thus allowing the user the option of rerunning the program until a satisfactory solution is found.

Two programs were completed and written in PASCAL on the Bristol University mainframe computer (Multics), using the FORTRAN NAG library subroutines. They were called SDOF, a single-degree-of-freedom program for well-separated peaks with a fast run time, and MDOF, a multi-degree-of-freedom **curvefit** program for multiple closely-spaced peaks with a slower run time.

2.5 Experimental Impact Testing

In order to assess the sort of problems likely to be encountered in practice, a cantilever was tested to gain an insight into experimental techniques and to allow an application of the **curve-fitting** program to actual measured data. The cantilever that was examined possessed the characteristics itemised in Table 2.7. It was clamped to a large concrete block with four heavy-duty screws running through a thick steel plate, as shown in Diagram 2.5. Five perspex blocks, for attachment of the accelerometers, were glued on to the cantilever. The accelerometers could then be attached using a threaded screw. The apparatus was set up as in Diagram 2.6. The instrumented hammer contained a force transducer from which the input was measured. Impacts were made at the tip of the cantilever and the accelerometer was moved to each of the five locations in turn. The data was processed on a Solartron 1200 signal processor, with several averages being taken, and care was taken to ensure a good coherence (a measure of repeatability, ranging from 0 to 1 with 1 being the optimum value). Due to data transfer difficulties at the time of the test (which have subsequently been overcome), the measurements were read off the signal processor (after it had calculated the real part of the frequency response function) and

are given in Tables 2.8 and 2.9, for the first two modes which were being investigated. These numbers were then fed into the Bristol University mainframe computer for further analysis using the curvefitting software. The results using SDOF for the two well-spaced modes are given in Figure 2.10, and the magnitude values are plotted for comparison with the analytical modes predicted from an FE model in Figure 2.11. As can be seen, in general a good agreement is observed, with the errors being introduced most probably because the necessary boundary conditions could not be entirely satisfied. The analytical frequencies are in good agreement with those measured, but there is no analytical damping value with which to compare the measured ones, which were found to be about 0.2% of **critical** in both modes.

For further tests, the cantilever was damaged by sawing a quite severe notch in it in the second element from the fixed end. The test was then repeated, and the measurements obtained from the signal processor for the damaged cantilever are given in Tables 2.10 and 2.11, and the **curvefit** results in Figure 2.12. Figures 2.13 and 2.14 show how the eigenvalues have moved as a result of the introduction of the notch. The most significant observation is the increase in damping from 0.2% to 0.64% in the first mode and 0.47% in the second mode. However, although an increase in damping is indicative that damage has occurred, it is a global parameter, and no information about the location of the damage can be expected with this observation. The first two modes are replotted in Figures 2.15 and 2.16, and it can be seen that the first mode has hardly changed, but the second mode has become much more flexible near the fixed end.

The objectives of the cantilever experiments were as follows:

- (a) to demonstrate the effectiveness of the **curvefit** program for establishing measured modes and frequencies;
- (b) to illustrate the need for a comprehensive theory for the detection of errors or poor modelling;
- (c) to show that damping values are important and are sensitive to structural changes or inaccuracies, and that any theory should cater for this, while acknowledging that currently no entirely satisfactory analytical method exists for assessing damping properties.

The experiments with a simple cantilever had indicated the potential use of the curvefitting program. Its implementation for larger, more realistic cases would relieve the experimental engineer of a subjective assessment of the frequency response function data to try to approximate the modal parameters. The motivation was identified, therefore, for a further development of the program for use on the PDP **11/34** which is a mini-computer used in the Civil Engineering Department for processing and analysis of dynamic test measurements. This involved an entire rewriting of the program from PASCAL to FORTRAN, a loading of the program and associated NAG software onto the PDP **11/34**, and an allocation of sufficient computer memory organisation to allow the program to run. An inevitable consequence of this, because of the length of the NAG routines, was to use single precision instead of double precision. The direct loading of data from the Solartron 1200 signal processor has been developed at Bristol University (by members of the Earthquake Engineering Research Group), so a potentially efficient and direct

procedure for extracting modal properties from dynamic tests is beginning to emerge, which may either be used in the laboratory on models, with the equipment **directly** at hand, or information may be stored on magnetic tape for subsequent analysis on return to the laboratory. The user manual for the PDP **11/34 curvefit** program is given in Appendix 3, with a listing of the two programs in Appendices 4 and 5.

To investigate this, an analysis of some of the transient data collected recently from a small suspension bridge (Dolarue) in North Wales by members of the Earthquake Engineering Research Group was conducted. As an illustrative example of the **curvefit**-ing program's use for the purposes of this thesis, the first two lateral modes were investigated once the data had been transferred onto the PDP **11/34**. Data was collected from 9 positions along the bridge. The quality of the data was assessed, and a note made of the modes visible in each channel (see Figure 2.17). SDOF was then used to **curvefit** each channel for each mode present and the results are given in Tables 2.12 and 2.13. The results of the **curvefit** produced estimates of the first two lateral modes of the structure, given by the following two complex vectors:

$$\begin{array}{l}
 \mathbf{L1} = \begin{bmatrix} 0.11 - 0.003i \\ 0.15 + 0.03i \\ 0.18 + 0.12i \\ 0.18 + 0.08i \\ 0.125 + 0.025i \\ 0.134 - 0.043i \\ 0.0072 - 0.0007i \end{bmatrix} \\
 \mathbf{L2} = \begin{bmatrix} 0.15 - 0.04i \\ 0.34 - 0.02i \\ 0.20 - 0.00i \\ 0 \\ -0.082 + 0.053i \\ -0.284 + 0.157i \\ -0.246 + 0.173i \\ -0.005 + 0.173i \end{bmatrix}
 \end{array}$$

The missing elements are from data channels where there was excessive noise so as to make any analysis unreliable. The natural frequencies and damping estimates of these first two modes were extracted by taking a weighted mean of the estimates, weighted by the subjective assessment of the quality of the data as given in Figure 2.17. They are

$$\omega_1 = 1.69\text{Hz} \quad \mu_1 = 0.60\%$$

$$\omega_2 = 6.98\text{Hz} \quad \mu_2 = 0.69\%$$

$|L1|$ and $|L2|$ were calculated for plotting and are given as

| $ L1 $ = | | $ L2 $ = | |
|----------|------|----------|-------|
| | 0.11 | | 0.16 |
| | 0.15 | | 0.34 |
| | | | 0.20 |
| | 0.22 | | 0 |
| | 0.20 | | -0.10 |
| | 0.13 | | -0.32 |
| | 0.14 | | -0.25 |
| | 0 | | -0.17 |

These modes are plotted in Figure 2.18. As may be observed, the modes illustrate that the bridge is essentially behaving as a simply-supported beam in the lateral direction. Some variation of the global parameters was observed, especially with damping. This is, to some extent, to be expected, as the mathematical model itself is an idealistic simplification, and the best option is to acknowledge this fact and extract the best parameters which most closely reflect the behaviour of the structure. The analysis of the suspension bridge has been encouraging, with the potential advantages of employing a **curvefit** program demonstrated.

2.6 Comparison of FE Method and Modal Analysis

Two differing methods, both encompassing the same objectives, have been discussed hitherto. **One is** an analytical technique, the other an experimental technique. The validity of both methods hinges upon whether they predict the same dynamic response, in terms of the predominant mode shapes and frequencies. If a contradiction in the results of the two methods is observed, something is wrong with the overall assessment. A calculation of the structure's dynamic response or internal stresses and so on can no longer be considered as good enough if the modes and frequencies predicted by the model used are not directly backed up and verified with a modal test on the structure itself. All too often this agreement is lacking, and the approach is then either to adopt some haphazard trial-and-error adjustment of the mathematical model to improve it, which usually results in a worsening of the situation, or to dismiss the warnings brought to light by a modal test as being due to 'experimental error'. As experimental techniques and expertise grow, neither of these arguments is satisfactory. Some thought must be directed towards reconciling these difficulties with a more formal approach that may be implemented on a more routine basis. No ideal solution to this problem exists. In this thesis a 'best solution given the circumstances' is presented. It is possible to extract useful information, but not without first identifying the contrasting nature of the two methods and the inherent difficulties associated with a marriage of the two.

If we compare the FE method and modal analysis, the first observation is that the mathematical model is built up in terms of **stiffness**, where the stiffness is defined as

k_{ij} = force at node i due to unit displacement at node j , all other displacements being zero.

On the other hand, a modal analysis-type of measurement is of a flexibility nature, where the flexibility is defined as

f_{ij} = displacement of node i due to force at node j , all other forces being zero.

To measure stiffness we need to apply forces at all the nodes of the structure to make displacements zero, which is practically impossible. To measure flexibility we need to apply zero forces at other nodes which is easy - and what is done in practice. So in a modal test we are measuring dynamic flexibilities which are, from the definition, independent of the number of degrees of freedom. The stiffness matrix is not, since all the degrees of freedom included need to be constrained to be zero. If we consider the usual dynamic FE model, we have

$$Kx_i = \lambda_i Mx_i$$

and each interpolation function has the same degree of complexity of the form



therefore the stiffness matrix is banded and the order of numbers anywhere in the matrix is the same; that is, it is of uniform complexity. Therefore FE stiffnesses are of the order of complexity of the highest mode. A summation of the form

$$\sum_{i=1}^n x_i x_i^T$$

will thus give small contributions if in ascending order of modes.

This infers that what we measure in a modal test are not necessarily those vectors which dominate the form of the mathematical model. The lower eigenvectors are of principal interest, but the higher analytical eigenvectors dictate the outward appearance of the mathematical model. This will inevitably restrict the verification or correction of mass and stiffness parameters using experimental modal analysis. A theory that is built up needs to account for this and take the necessary precautionary steps. The text of this thesis uses vector space theory to construct a plausible approach, with the initial inevitable limitations being acknowledged and accepted.

2.7 Some Uses of the Mathematical Model

If agreement between the FE analysis and modal test is reached, then the mathematical model is considered to be a good representation of the structure and can be used for further analysis. This is an extremely desirable state of affairs, since the principal modes of vibration will be known, at given frequencies with possibly an additional knowledge of damping estimates. The distribution of the structure in terms of mass and stiffness will also be **known, so** an accurate assessment will have been made.

The mathematical model may be used to calculate the dynamic response of a structure to a given excitation. The two methods in general use are direct integration methods where the equations of motion are integrated using a numerical step-by-step procedure, and the mode superposition method, where the motion is assumed to be a linear combination of the principal modes of vibration and the problem is decoupled into n separate linear differential

equations by use of a modal transformation. Of the direct integration methods, the central difference method (which is essentially an explicit integration procedure), is perhaps the best-known, but other popular methods exist which use an implicit integration technique such as the Houbolt, Wilson θ , and **Newmark β** methods. The methods are all useful, and are well-documented⁽¹¹⁾ and therefore not reiterated here. Some research has been conducted⁽¹⁰⁶⁾ in order to establish which method is most accurate with the general conclusion being that if accuracy is a priority and the quantity of data is small, the mode superposition method is preferred; but if the quantity of data is large, the **Newmark β** method is most suitable.

Once the dynamic response of the structure has been calculated, the maximum displacements and internal stresses may be assessed. Areas of high displacement and excessive stress may be identified and corrected, not necessarily with the addition of extra mass or stiffer material at that point, but perhaps with a redistribution of mass that will reduce dynamic movement. An assessment of the durability of the structure may be made, and its lifespan when subjected to constant loading may be forecast. Alternatively, its performance may be predicted in an earthquake situation with violent external loading, and so on. If the exact form of loading is not known, for example wind loading, a non-deterministic solution may be sought. In general, a good mathematical model opens the door to a confident assessment of the structure's likely dynamic performance, resulting in longer-lasting, safer and cheaper structures being constructed.

2.0 Sensitivity Analysis

If we have an incorrect model and are trying to correct it by changing some of the **parameters**, or have a correct model with which we wish to estimate the effect of parameter changes, then it is possible to estimate the change in frequencies and mode shapes as a result of changes in mass and stiffness using a sensitivity first order analysis. We have

$$(M\lambda_i - K)x_i = \theta.$$

If the mass and stiffness distributions are altered so that M becomes $M + \delta M$ and K becomes $K + \delta K$ then we have

$$[(M + \delta M)(\lambda_i + \delta\lambda_i) - (K + \delta K)](x_i + \delta x_i) = \theta$$

which, to first order, gives

$$(M\lambda_i - K)\delta x_i + (\delta M\lambda_i - \delta K)x_i + M\delta\lambda_i x_i = \theta.$$

If we premultiply by x_i^T then we have

$$\delta\lambda_i = -x_i^T(\delta M\lambda_i - \delta K)x_i$$

giving the change in natural frequency of mode i due to the change in the mass and stiffness distributions. Also, if we premultiply by x_j^T ($j \neq i$) we have

$$x_j^T(M\lambda_i - K)\delta x_i + x_j^T(\delta M\lambda_i - \delta K)x_i = 0$$

and if we now assume that

$$\delta x_i = \sum_{\substack{k=1 \\ k \neq i}}^n \mu_k x_k$$

then

$$\sum_{\substack{k=1 \\ k \neq i}}^n \mu_k x_j^T(M\lambda_i - K)x_k + x_j^T(\delta M\lambda_i - \delta K)x_i = 0$$

$$\text{or } \mu_j(\lambda_i - \lambda_j) + x_j^T(\delta M \lambda_i - \delta K)x_i = 0;$$

that is

$$\mu_j = \frac{x_i^T(\delta M \lambda_i - \delta K)x_i}{(\lambda_i - \lambda_j)}$$

$$\text{so } \delta x_i = \sum_{\substack{j=1 \\ j \neq i}}^n \frac{x_j(\delta M \lambda_i - \delta K)x_i}{(\lambda_i - \lambda_j)} x_j$$

which gives an approximation to the change in mode i due to a change in mass and stiffness.

2.9 Overview

Both the FE method and modal analysis have been investigated in some detail in this chapter. Simple structures have been used with which to outline the basics of both methods. The contrasting nature of the two methods has been observed and the need for the two to show some signs of agreement identified. An illustration of the application of these methods has set the scene for the analysis of the following chapters which attempt to bring together the two methods to permit a more unified approach where each method is contributing valid information as to the dynamic performance of the structure under investigation.

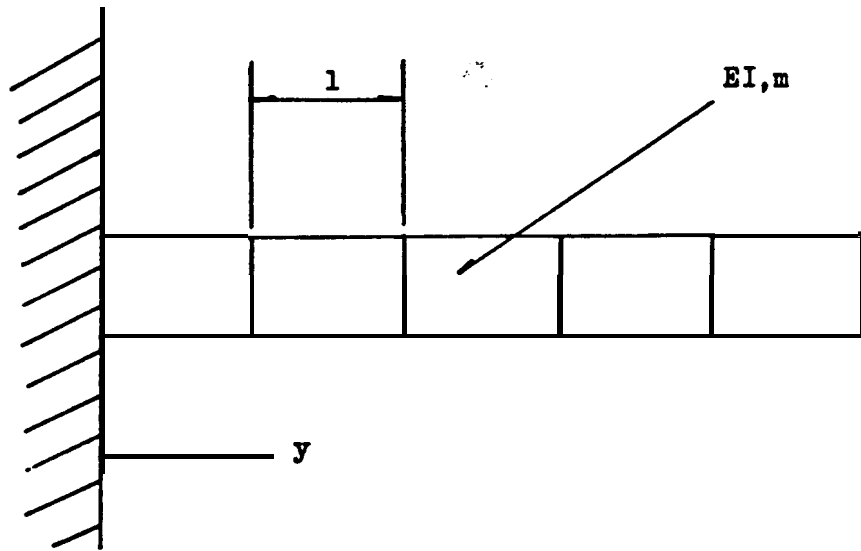


Diagram 2.1

Correct 'Measured' Cantilever

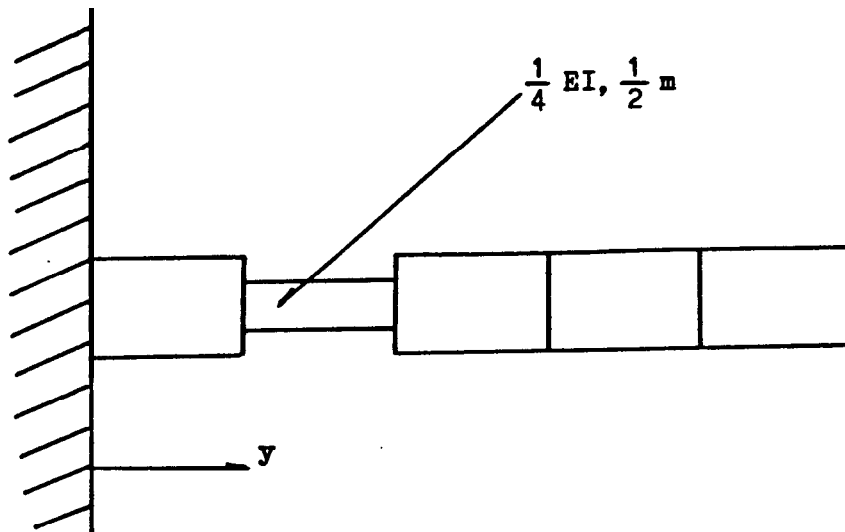


Diagram 2.2

Incorrect 'Analytical' Cantilever

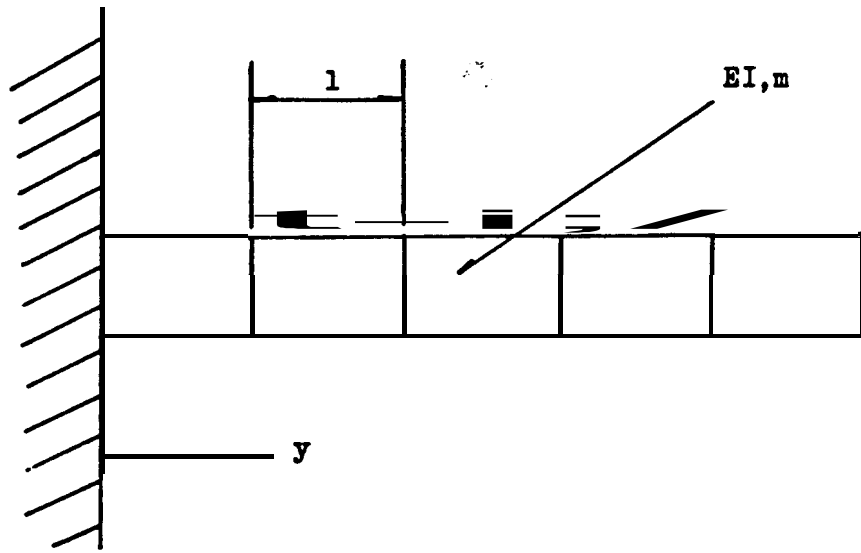


Diagram 2.1

Correct 'Measured' Cantilever

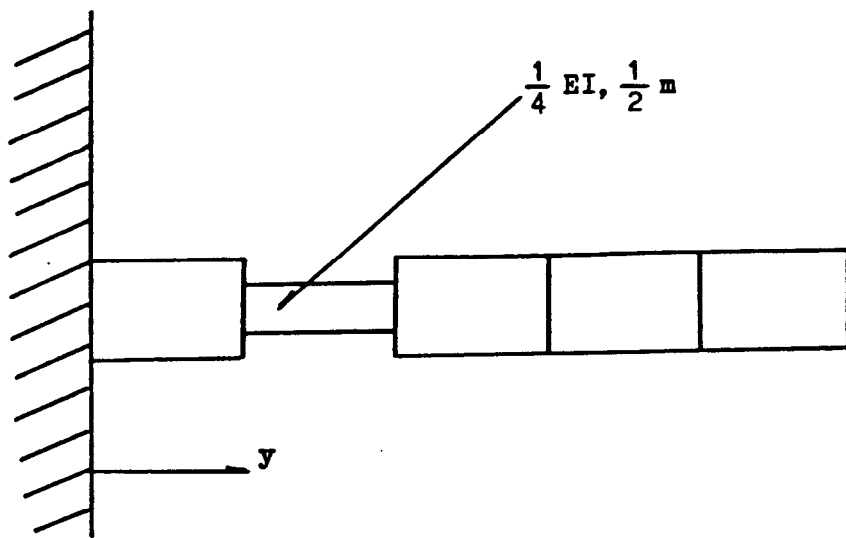


Diagram 2.2

Incorrect 'Analytical' Cantilever

Diagram 2.3

Correct 'Measured' Beam

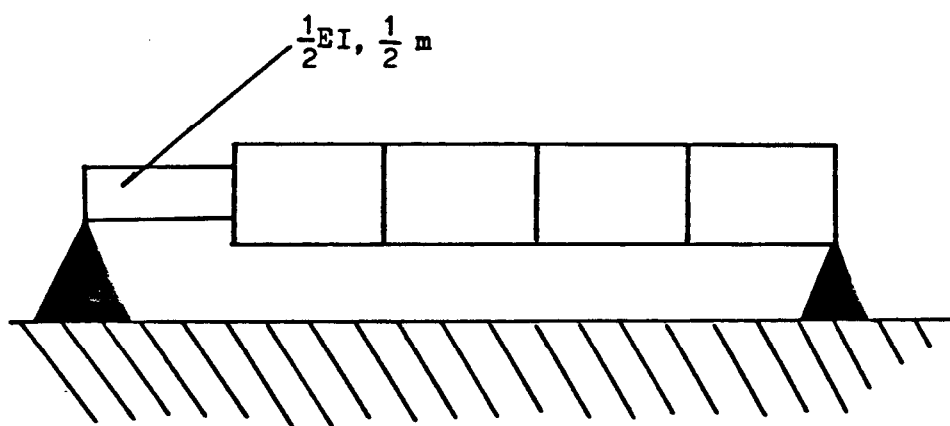


Diagram 2.4

Incorrect 'Analytical' Beam

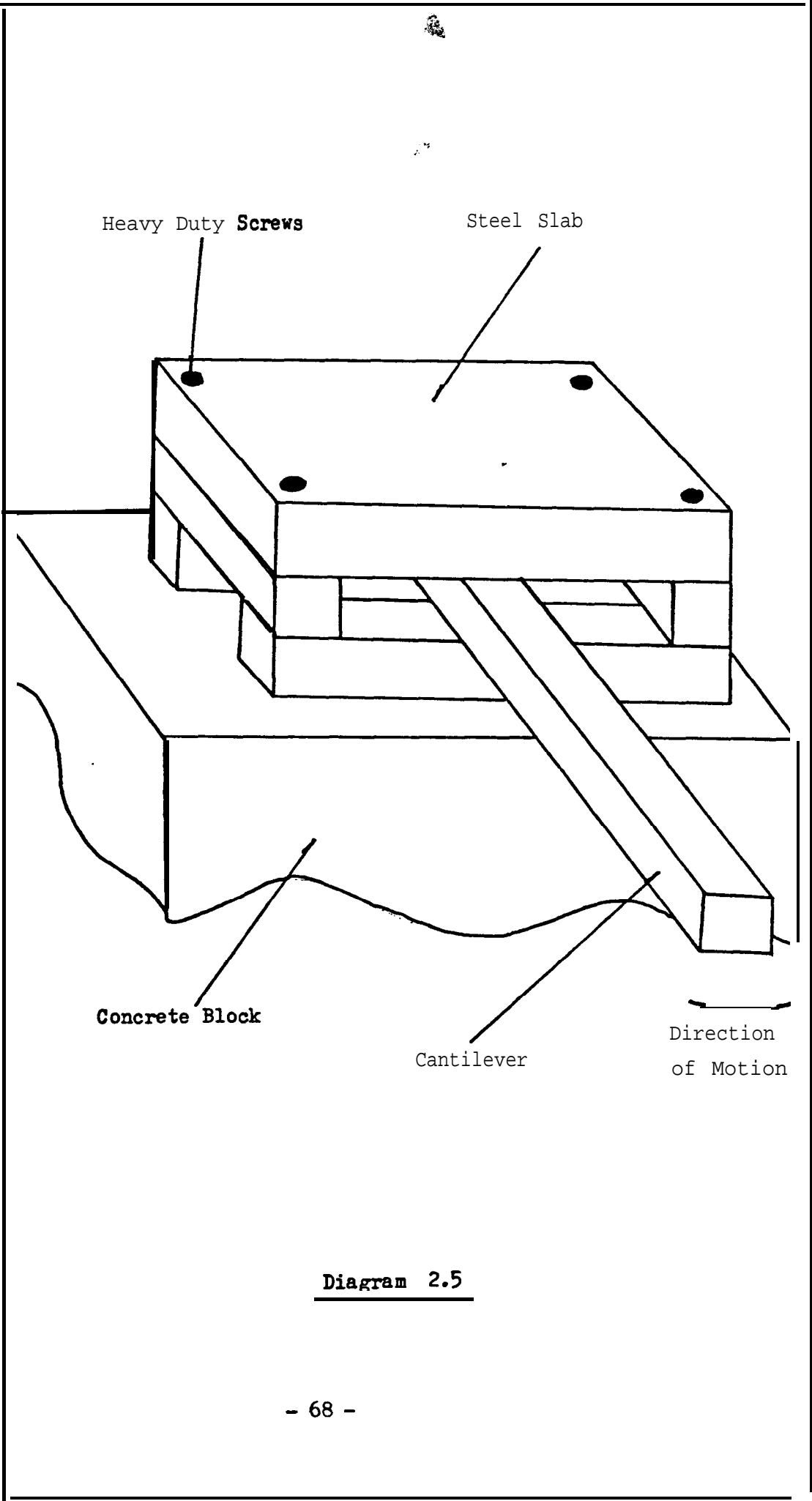


Diagram 2.5

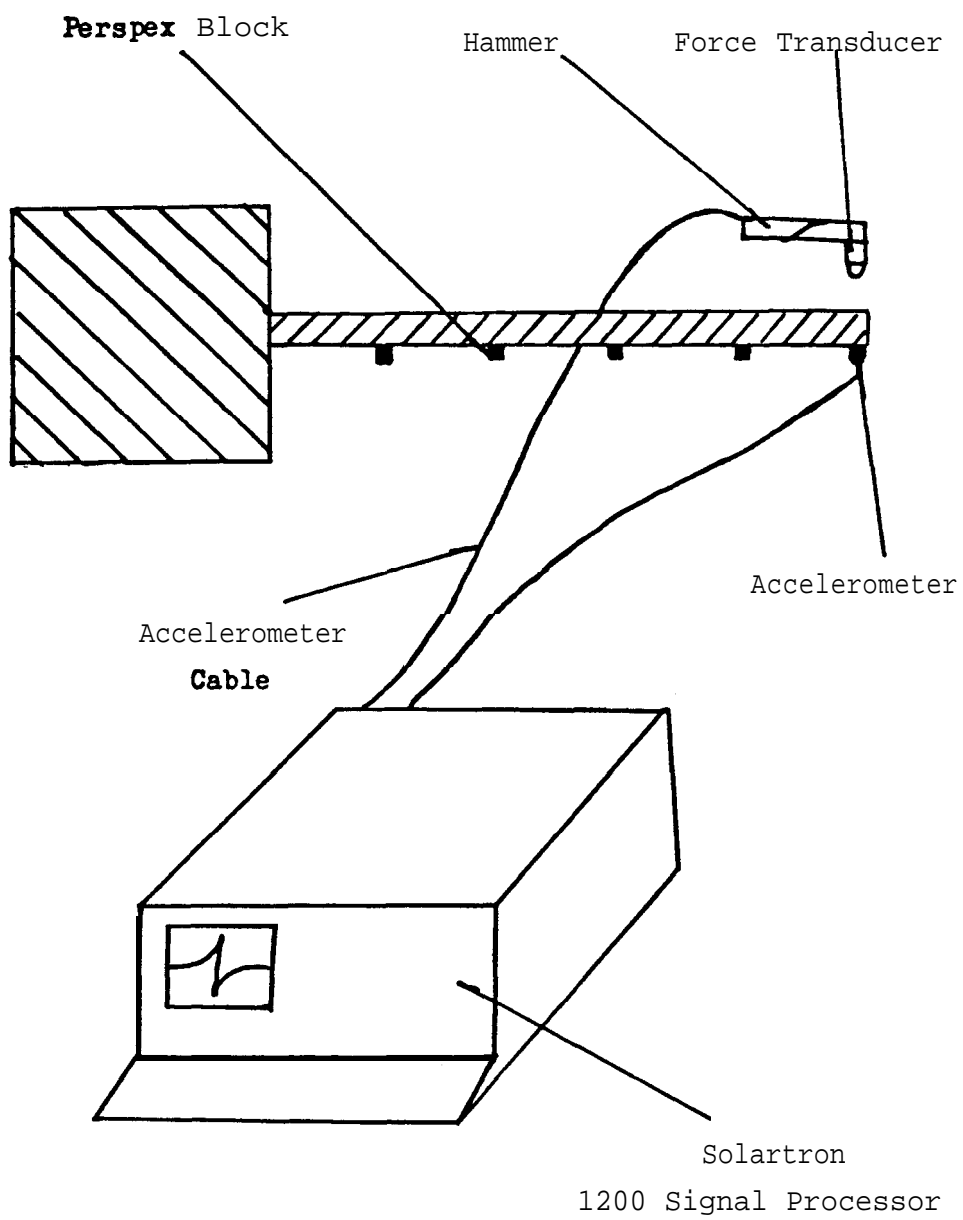


Diagram 2.6

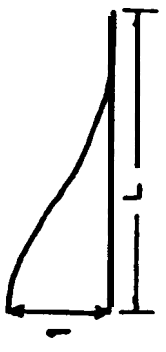
| | | | |
|---|---|--|--|
|  |  |  |  |
| $\Psi_1(y) = 1 - 3\left(\frac{y}{L}\right)^2 + 2\left(\frac{y}{L}\right)^3$ | $\Psi_2(y) = \left(1 - \left(\frac{y}{L}\right)\right)^2$ | $\Psi_3(y) = 3\left(\frac{y}{L}\right)^2 - 2\left(\frac{y}{L}\right)^3$ | $\Psi_4(y) = \left(\frac{y}{L}\right)^2 \left(\left(\frac{y}{L}\right) - 1\right)$ |
| $\Psi_1'(y) = \left(\frac{6y}{L}\right) - \left(\frac{6y}{L^2}\right)$ | $\Psi_2'(y) = \left(1 - \left(\frac{y}{L}\right)\right)^2 - \left(\frac{2y}{L}\right) \left(1 - \frac{y}{L}\right)$ | $\Psi_3'(y) = \left(\frac{6y}{L^2}\right) - \left(\frac{6y^2}{L^3}\right)$ | $\Psi_4'(y) = \left(\frac{2y}{L}\right) \left(\left(\frac{y}{L}\right) - 1\right) + \frac{y^2}{L^2}$ |
| $\Psi_1(0) = 1$ | $\Psi_2(0) = 0$ | $\Psi_3(0) = 0$ | $\Psi_4(0) = 0$ |
| $\Psi_1(L) = 0$ | $\Psi_2(L) = 0$ | $\Psi_3(L) = 1$ | $\Psi_4(L) = 0$ |
| $\Psi_1'(0) = 0$ | $\Psi_2'(0) = 1$ | $\Psi_3'(0) = 0$ | $\Psi_4'(0) = 0$ |
| $\Psi_1'(L) = 0$ | $\Psi_2'(L) = 0$ | $\Psi_3'(L) = 0$ | $\Psi_4'(L) = 1$ |

Table 2.1: Shape Functions

| Damping Estimate | Frequency Estimate | Convergence ? | Number of Iterations |
|------------------|--------------------|---------------|----------------------|
| -5 | 3.998 | X | |
| -2 | 3.998 | X | |
| -1.5 | 3.998 | X | |
| -1 | 3.998 | ✓ | 8 |
| -0.5 | 3.998 | ✓ | 6 |
| -0.1 | 3.998 | ✓ | 4 |
| -0.07 | 3.998 | ✓ | 6 |
| -0.06 | 3.998 | X | |
| -0.05 | 3.998 | X | |
| 0.01 | 3.998 | X | |
| 0.5 | 3.998 | X | |
| -0.12 | 3.9 | X | |
| | | X | |
| -0.12 | 3.93 | ✓ | 7 |
| -0.12 | 3.95 | ✓ | 6 |
| -0.12 | 4.05 | ✓ | 6 |
| -0.12 | 4.07 | ✓ | 8 |
| -0.12 | 4.08 | X | |
| -0.12 | 4.1 | X | |
| -0.12 | 4 | ✓ | 3 |
| -1 | 3.93 | ✓ | 8 |
| -1 | 4.07 | ✓ | 7 |
| -0.07 | 3.93 | X | |
| -0.07 | 4.07 | X | |

Table 2.2: Convergence Test Using $\text{MIN}(|\text{RE}(H)|^2 + |\text{IM}(H)|^2)$

| Damping Estimate | Frequency Estimate | Convergence ? | Number of Iterations |
|------------------|--------------------|---------------|----------------------|
| -1 | 3.998 | X | |
| -0.5 | 3.998 | X | |
| -0.1 | 3.998 | ✓ | 5 |
| -0.06 | 3.998 | ✓ | 6 |
| -0.05 | 3.998 | ✓ | 7 |
| -0.04 | 3.998 | ✓ | 6 |
| -0.03 | 3.998 | X | |
| -0.01 | 3.998 | X | |
| -0.12 | 3.92 | X | |
| -0.12 | 3.93 | ✓ | 8 |
| -0.12 | 4 | ✓ | 3 |
| -0.12 | 4.07 | ✓ | 8 |
| -0.12 | 4.08 | X | |
| -0.07 | 3.93 | ✓ | 10 |
| - 0.07 | 4.07 | X | |

Table 2.3: Convergence Test Using $\text{MIN } |\text{Re}(H)|^2$

| Damping Estimate | Frequency Estimate | Convergence? | Number of Iterations |
|------------------|--------------------|--------------|----------------------|
| -1 | 3.998 | x | - |
| -0.5 | 3.998 | x | - |
| -0.1 | 3.998 | ✓ | 6 |
| -0.07 | 3.998 | x | - |
| -0.06 | 3.998 | x | - |
| -0.05 | 3.998 | x | - |
| -0.12 | 3.93 | x | - |
| -0.12 | 3.97 | x | - |
| -0.12 | 3.98 | ✓ | 6 |
| -0.12 | 4 | ✓ | 4 |
| -0.12 | 4.02 | ✓ | 6 |
| -0.12 | 4.05 | x | - |

Table 2.4: Convergence Test Using $\text{MIN}|\text{Im}(H)|^2$

| Damping Estimate | Frequency Estimate | Convergence ? | Number of Iterations |
|------------------|--------------------|---------------|----------------------|
| -0.06 | 3.998 | X | - |
| -0.07 | 3.998 | ✓ | 8 |
| -0.12 | 4 | ✓ | 5 |
| -0.2 | 3.998 | ✓ | 5 |
| -0.8 | 3.998 | ✓ | 8 |
| -1 | 3.998 | ✓ | 9 |
| -1.2 | 3.998 | X | - |
| -1.5 | 3.998 | X | - |
| -0.12 | 3.92 | X | - |
| -0.12 | 3.93 | ✓ | 9 |
| - 0.12 | 4.07 | ✓ | 9 |
| -0.12 | 4.09 | X | - |

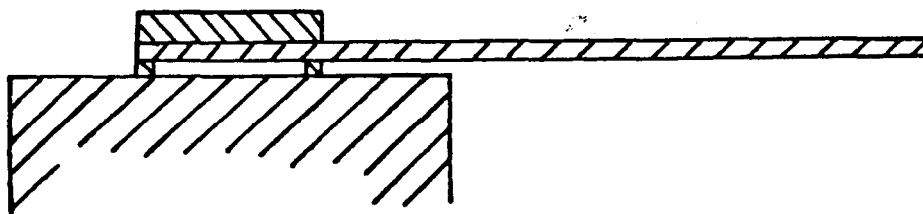
Table 2.5: Convergence Test with 2% Noise

Added

| Damping Estimate | Frequency Estimate | Convergence ? | Number of Iterations |
|------------------|--------------------|---------------|----------------------|
| -0.1 | 4 | ✓ | 7 |
| -1 | 3.998 | ✓ | 11 |
| -1.2 | 3.998 | × | |
| -0.07 | 3.998 | ✓ | 9 |
| -0.06 | 3.998 | × | |
| -0.12 | 4.07 | ✓ | 10 |
| -0.12 | 4.08 | × | |
| -0.12 | 3.93 | ✓ | 10 |
| -0.12 | 3.92 | × | |
| -0.12 | 4 | ✓ | 6 |

Table 2.6 Convergence Test with 5 % Noise

Added



| | |
|--|---|
| Total Length of Cantilever | 0.545m |
| Density of Steel | 7850 kg/m ³ |
| Cross-Sectional Area | 0.000256m² |
| Young's Modulus (E_{dynamic}) | 0.168825x10¹² N/m² |
| Second Moment of Area | 5.46133x10⁻⁹ m⁴ |
| EI | 922 Nm ² |
| Mass/Unit Length | 2.0096 kg/m |

First two Analytical Frequencies :-

$$\omega_1 = (1.875)^2 \sqrt{\left(\frac{EI}{ml^4}\right)} = 253.52 \quad f_1 = 40.35 \text{ Hz}$$

$$\omega_2 = (4.694)^2 \sqrt{\left(\frac{EI}{ml^4}\right)} = 1588.926 \quad f_2 = 252.88 \text{ Hz}$$

Table 2.7: Cantilever Parameters

| | CHAN 1 | CHAN 2 | CHAN 3 | CHAN 4 | CHAN 5 |
|-------------|----------------|----------------|----------------|---------|----------|
| PEAK; | 40.44 | 40.36 | 40.4 | 40.44 | 40.48 |
| COHERENCE : | 0.945 | 0.98 | 0.991 | 0.993 | 0.984 |
| VALUE: | 82.969 | 46.811 | 39.489 | 28.936 | 13.876 |
| FREQ. | | | | | |
| 38.96 | -4.9471 | -5.0647 | -2.8054 | -1.4097 | -0.47234 |
| 39.12 | -5.6487 | -5.8991 | -3.124 | -1.624 | -0.53952 |
| 39.4 | -7.5447 | -7.6189 | -4.2896 | -2.1398 | -0.69049 |
| 39.6 | -9.6938 | -9.478 | -5.5237 | -2.7256 | -0.86591 |
| 39.8 | -13.225 | -11.718 | -7.4224 | -3.7499 | -1.1631 |
| 39.88 | -14.806 | -12.537 | -8.4223 | -4.353 | -1.3345 |
| 39.92 | -16.277 | -12.861 | -9.0396 | -4.7249 | -1.4412 |
| 39.96 | -17.407 | -12.987 | -9.6196 | -5.1765 | -1.5669 |
| 40.04 | -20.2 | -12.472 | -10.737 | -6.1646 | -1.8961 |
| 40.08 | -21.779 | -11.513 | -11.338 | -6.7466 | -2.0985 |
| 40.12 | -23.657 | -9.4229 | -11.382 | -7.3716 | -2.3577 |
| 40.16 | -24.603 | -6.5182 | -10.869 | -8.0276 | -2.6876 |
| 40.2 | -24.532 | -1.6036 | -9.5708 | -8.481 | -3.0793 |
| 40.24 | -22.277 | 5.9795 | -6.6433 | -8.543 | -3.5393 |
| 40.28 | -17.336 | 16.164 | -1.5438 | -7.7363 | -4.0598 |
| 40.32 | -6.6777 | 29.838 | 7.584 | -5.0461 | -4.3911 |
| 40.36 | 13.112 | 41.256 | 14.305 | 0.9599 | -3.8501 |
| 40.4 | 47.672 | 41.359 | 34.107 | 8.8345 | -2.5746 |
| 40.44 | 82.238 | 16.202 | 27.051 | 24.381 | 9.88382 |
| 40.48 | 25.53 | 8.2891 | 8.0098 | 15.303 | 10.68 |
| 40.52 | 19.718 | 14.403 | 10.933 | 6.5811 | 6.0942 |
| 40.56 | 21.797 | 11.802 | 9.97855 | 7.3408 | 3.9404 |
| 40.76 | 12.773 | 8.644 | 6.3667 | 4.323 | 1.9454 |
| 40.88 | 10.49 | 7.4102 | 5.2927 | 3.4679 | 1.4599 |
| 41.4 | 5.8464 | 4.6501 | 3.0514 | 1.8376 | 0.71487 |

Table 2.8: Mode 1, Undamaged Cantilever

| | CHAN 1 | CHAN 2 | CHAN 3 | CHAN 4 | CHAN 5 |
|------------|---------|---------|----------|----------|----------|
| PEAK: | 254.4 | (254.5) | 254.5 | 254.8 | 255.2 |
| COHERENCE: | 0.961 | (0.805) | D.953 | 0.9621 | 0.978 |
| VALUE: | 21.048 | (0.879) | 12.027 | 18.768 | 16.04 |
| FREQ. | | | | | |
| 247.6 | -0.9661 | 0.16492 | 1.0276 | 1.1816 | 0.55869 |
| 250.9 | -1.3497 | 0.23122 | 1.9476 | 2.2123 | 1.055 |
| 251.9 | -1.184 | 0.25914 | 2.5487 | 2.9696 | 1.3674 |
| 253.2 | 2.2014 | 0.43575 | 3.6652 | 4.741 | 2.1814 |
| 253.5 | 4.896 | 0.50119 | 3.6934 | 5.4153 | 2.5197 |
| 253.6 | 6.2554 | 0.55936 | 3.5735 | 5.5806 | 2.6515 |
| 253.7 | 7.667 | 0.62256 | 3.3463 | 5.6294 | 2.7815 |
| 253.8 | 9.4824 | 0.59705 | 3.0592 | 5.8052 | 2.9302 |
| 253.9 | 11.56 | 0.65585 | 2.5466 | 5.833 | 3.1338 |
| 254 | 13.564 | 0.71732 | 1.7685 | 5.6453 | 3.3359 |
| 254.1 | 15.494 | 0.7735 | 0.79926 | 5.1963 | 3.5619 |
| 254.2 | 17.781 | 0.80829 | -0.5261: | 4.6572 | 3.7667 |
| 254.3 | 19.561 | 0.83804 | -1.8453 | 3.4939 | 3.9728 |
| 254.4 | 20.591 | 0.83502 | -3.7168 | 1.8231 | 4.2349 |
| 254.5 | 20.723 | 0.81613 | -5.4993 | -0.37421 | 4.3291 |
| 254.6 | 19.666 | 0.74387 | -7.1399 | -3.3022 | 4.3142 |
| 254.7 | 17.399 | 0.58768 | -8.7072 | -6.8184 | 4.1738 |
| 254.8 | 14.234 | 0.38391 | -9.1982 | -10341 | 3.433 |
| 254.9 | 11.485 | 0.15859 | -9.0404 | -12.956 | 2.2074 |
| 255 | 9.4878 | 0.24712 | -8.1436 | -14.158 | -0.15563 |
| 255.1 | 8.4658 | 0.45612 | -7.0012 | -13.676 | -3.6637 |
| 255.2 | 7.8342 | 0.31898 | -6.2095 | -11.923 | -8.6073 |
| 255.3 | 7.1919 | 0.27951 | -5.7288 | -10.199 | -11.472 |
| 255.4 | 6.6667 | 0.25172 | -5.3416 | -9.2983 | -12.437 |
| 255.5 | 6.2209 | 0.20411 | -4.9771 | -8.4604 | -11.072 |
| 255.6 | 5.8003 | 0.34639 | -4.6284 | -7.7852 | -9.2148 |

Table 2.9: Mode 2, Undamaged Cantilever

| | CHAN 1 | CHAN 2 | CHAN 3 | CHAN 4 | CHAN 5 |
|-------------|---------|---------|---------------|----------|----------|
| PEAK: | 39.3 | 39.2 | 39.2 | 39.4 | 39.6 |
| COHERENCE: | 0.983 | 0.9716 | 0.9538 | 0.979 | 0.96307 |
| VALUE: | 30.451 | 20.625 | 15.673 | 10.264 | 6.3083 |
| FREQ. | | | | | |
| 33.2 | -1.1442 | -0.9873 | -0.6535 | -0.3377 | -0.13404 |
| 35.2 | -1.9073 | -1.6942 | -1.1128 | -0.56015 | -0.22077 |
| 36.3 | -3.209 | -2.8994 | -1.9062 | -0.93527 | -0.35872 |
| 37.3 | -4.5706 | -4.1399 | -2.757 | -1.3606 | -0.49023 |
| 37.9 | -6.8576 | -5.3784 | -4.1084 | -2.051 | -0.6918 |
| 38 | -7.4512 | -6.2449 | -4.405 | -2.2113 | -0.74823 |
| 38.2 | -8.7441 | -7.031 | -5.0742 | -2.6661 | -0.87317 |
| 38.4 | -10.123 | -7.3528 | -5.6831 | -3.1171 | -0.99075 |
| 38.5 | -10.525 | -7.1108 | -5.8137 | -3.3247 | -1.0748 |
| 38.6 | -10.592 | -6.3193 | -5.5642 | -3.4504 | -1.1773 |
| 38.7 | -10.02 | -4.6541 | -4.8015 | -3.5121 | -1.2703 |
| 38.8 | -8.6577 | -2.0813 | -3.5011 | -3.3517 | -1.3492 |
| 38.9 | -6.1904 | 1.7095 | -1.4089 | -2.9252 | -1.4483. |
| 39 | -2.2609 | 6.4409 | 1.4785 | -2.1515 | -1.5474 |
| 39.1 | 3.5518 | 11.533 | 5.1602 | -0.89761 | -1.6217 |
| 39.2 | 11.23 | 16.052 | 9.2822 | 1.0089 | -1.567 |
| 39.3 | 19.851 | 18.143 | 12.766 | 3.7203 | -1.1978 |
| 39.4 | 26.74 | 15.647 | 13.542 | 6.9675 | -0.3291 |
| 39.5 | 25.145 | 8.1118 | 9.9473 | 9.5845 | 1.4704 |
| 39.6 | 8.6528 | 2.0551 | 3.0889 | 7.8262 | 4.531 |
| 39.7 | 5.1616 | 7.4436 | 3.9548 | 1.0778 | 4.9365 |
| 39.8 | 8.8013 | 5.6843 | 4.7986 | 3.1932 | 1.532 |
| 40 | 7.5613 | 5.0286 | 3.9302 | 2.4734 | 1.3961 |
| 40.9 | 4.2227 | 3.1454 | 2.3604 | 1.4158 | 0.65842 |
| 41.8 | 3.0021 | 2.3497 | 1.7095 | 4.0009 | 0.45059 |
| \$4.6 | 1.6877 | 1.3943 | 0.99072 | 0.55722 | 0.24804 |

Table 2.10: Mode 1, Damaged Cantilever - 79 -

| | CHAN 1 | CHAN 2 | CHAN 3 | CHAN 4 | CHAN 5 |
|------------|-----------|----------|----------------|----------|----------|
| PEAK: | 249.6 | 249.4 | 249.4 | 250 | 251.2 |
| COHERENCE: | 0.92102 | 0.90329 | 0.93878 | 0.9934 | 0.93964 |
| VALUE: | 9.1452 | 0.45525 | 4.978 | 9.8443 | 6.4326 |
| FREQ. | | | | | |
| 240.4 | -1.0365 | 0.024813 | 8.498793 | 0.81329 | 0.3373 |
| 242.6 | -0.076561 | 0.025161 | 0.68118 | 1.1332 | 0.47319 |
| 244.6 | 0.1319 | 0.05896 | 0.86719 | 1.5684 | 0.65204 |
| 246 | 0.60767 | 0.11713 | 0.87778 | 2.0747 | 0.83609 |
| 246.8 | 1.3035 | 0.18723 | 0.63422 | 2.4191 | 0.98251 |
| 248 | 3.7332 | 0.3607 | -0.73953 | 2.7981 | 1.2312 |
| 248.2 | 4.3962 | 0.3736 | -1.1533 | 2.7538 | 1.2822 |
| 248.4 | 5.176 | 0.39963 | -1.6592 | 2.6699 | 1.3109 |
| 248.6 | 5.9575 | 0.42499 | -2.1558 | 2.3994 | 1.3205 |
| 248.8 | 6.7893 | 0.43054 | -2.7191 | 1.9709 | 1.3331 |
| 249 | 7.6611 | 0.42439 | -3.2581 | 1.3763 | 1.2919 |
| 249.2 | 8.4131 | 0.41939 | -3.7515 | 9.59247 | 1.2129 |
| 249.4 | 8.8911 | 0.40229 | -4.1768 | -0.46367 | 1.1171 |
| 249.6 | 9.1362 | 0.35121 | -4.3486 | -1.8209 | 0.96353 |
| 249.8 | 8.9385 | 0.26375 | -4.4749 | -3.5394 | 0.84262 |
| 250 | 8.3047 | 0.13882 | -4.1274 | -4.9265 | 0.26497 |
| 250.2 | 7.3555 | 0.21502 | -3.7231 | -6.2852 | -0.29849 |
| 250.4 | 6.228 | 0.18322 | -3.3143 | -7.375 | -1.074 |
| 250.6 | 4.9958 | 0.1804 | -2.9569 | -7.7791 | -1.9302 |
| 250.8 | 4.1002 | 0.18816 | -2.6589 | -7.6062 | -2.8901 |
| 251 | 3.4355 | 0.1738 | -2.4766 | -6.9553 | -3.8437 |
| 251.2 | 3.0641 | 0.15743 | -2.335 | -6.1116 | -4.668 |
| 251.4 | 2.79 | 0.15678 | -2.1849 | -5.353 | -5.3008 |
| 251.6 | 2.5588 | 0.15932 | -2.0603 | -4.8208 | -5.5872 |
| 253.8 | 1.2623 | 0.11879 | -1.2756 | -2.5385 | -2.1213 |
| 259.2 | 0.60873 | 0.10083 | -0.6904 | -1.2298 | -0.91141 |

Table 2.11: Mode 2, Damaged Cantilever

| CHANNEL | DAMPING FACTOR | % CRITICAL DAMPING | DAMPED NATURAL FREQUENCY | UNDAMPED NATURAL FREQUENCY | REAL PART OF RESIDUE | IMAG. PART OF RESIDUE | ERROR |
|---|----------------|--------------------|--------------------------|----------------------------|----------------------|-----------------------|-------|
| B | (-0.1) | (6.35) | 31.69) | (1.70) | (0.11) | (0.02) | 7 |
| C | -0.023 | 1.37 | 1.695 | 1.695 | 0.11 | -0.003 | 3 |
| D | -0.016 | 0.914 | 1.70 | 1.70 | 0.149 | 0.03 | 3 |
|  | -0.0022 | 0.128 | 1.683 | 1.683 | 0.06 | 0.04 | 2 |
| F | -0.017 | 1.03 | 1.67 | 1.67 | 0.18 | 0.12 | 3 |
| G | -0.018 | 1.05 | 1.68 | 1.68 | 0.18 | 0.08 | 3 |
| H | -0.0012 | 0.071 | 1.7036 | 1.70 | 0.125 | 0.025 | 2 |
| I | -0.0012 | 0.071 | 1.717 | 1.717 | 0.1338 | -0.043 | 3 |
| J | -0.0015 | 0.085 | 1.700 | 1.700 | 0.0072 | -0.0007 | 2 |

Table 2.12: SDOF Curvefit Results (1L)

| CHANNEL | DAMPING FACTOR | % CRITICAL FACTOR | DAMPED NATURAL FREQUENCY | UNDAMPED NATURAL FREQUENCY | REAL PART OF RESIDUE | IMAG PART OF RESIDUE | ERROR |
|---------|----------------|-------------------|--------------------------|----------------------------|----------------------|----------------------|----------|
| B | - | | | | | | |
| C | -0.09 | 1.31 | 6.96 | 6.96 | 0.04 | -0.15 | 0 |
| D | -0.051 | 0.72 | 7.00 | 7.00 | 0.02 | -0.34 | 3 |
| E | -0.056 | 0.80 | 7.02 | 7.02 | 0.00 | -0.20 | 3 |
| F | - | | | | | | |
| G | -0.034 | 0.48 | 6.97 | 6.97 | -0.053 | 0.082 | 8 |
| H | -0.069 | 0.99 | 6.98 | 6.98 | -0.157 | 0.284 | 6 |
| I | -0.034 | 0.48 | 7.01 | 7.01 | -0.073 | 0.246 | 3 |
| J | -0.029 | 0.43 | 6.89 | 6.89 | -0.0173 | -0.005 | 8 |

Table 2.13: SDOF **Curvefit** Results (2L)

$$M = \begin{bmatrix} 312.0 & 0.0 & 54.0 & -13.0 & 0.0 \\ 0.0 & 9.0 & 13.0 & -3.0 & 0.0 \\ 54.0 & 13.0 & 312.0 & 0.0 & 54.0 \\ -13.0 & -3.0 & 0.0 & 8.0 & 13.0 \\ 0.0 & 0.0 & 54.0 & 13.0 & 312.0 \\ 0.0 & 0.0 & -13.0 & -3.0 & 0.0 \\ 0.0 & \mathbf{0.0} & 0.0 & 0.0 & 54.0 \\ 0.0 & 0.0 & 0.0 & 0.0 & -13.0 \\ 0.0 & 0.0 & 0.0 & 0.0 & 0.0 \\ 0.0 & 0.0 & 0.0 & 0.0 & 0.0 \end{bmatrix}$$

$$K = \begin{bmatrix} 24.0 & 0.0 & -12.0 & 8.0 & 0.0 \\ 0.0 & 8.0 & -8.0 & 2.0 & 0.0 \\ -12.0 & -8.0 & 24.0 & 0.0 & -12.0 \\ 8.0 & 2.0 & 0.0 & 8.0 & -8.0 \\ 0.0 & 0.0 & -12.0 & -8.0 & 24.0 \\ 0.0 & 0.0 & 8.0 & 2.0 & 0.0 \\ 0.0 & 0.0 & 0.0 & 0.0 & -12.0 \\ 0.0 & 0.0 & 0.0 & 0.0 & 8.0 \\ \mathbf{0.0} & \mathbf{0.0} & \mathbf{0.0} & \mathbf{0.0} & \mathbf{0.0} \\ 0.0 & 0.0 & 0.0 & 0.0 & 0.0 \end{bmatrix}$$

Figure 2.1: 'Measured' Ca

Matric

- 40 -

$$M_a = \begin{bmatrix} 234.0 & -11.0 & 27.0 & -8.5 & 0.0 & 0.0 & 0.0 & 0.0 & 0.0 & 0.0 \\ -11.0 & 6.0 & 6.5 & -1.5 & 0.0 & 0.0 & 0.0 & 0.0 & 0.0 & 0.0 \\ 27.0 & 6.5 & 234.0 & 11.0 & 54.0 & -13.0 & 0.0 & 0.0 & 0.0 & 0.0 \\ -6.5 & -1.5 & 17.0 & 6.0 & 13.0 & -3.0 & 0.0 & 0.0 & 0.0 & 0.0 \\ 0.0 & 0.0 & 54.0 & 13.0 & 312.0 & 0.0 & 54.0 & -13.0 & 0.0 & 0.0 \\ 0.0 & 0.0 & -13.0 & -3.0 & 0.0 & 8.0 & 13.0 & -3.0 & 0.0 & 0.0 \\ 0.0 & 0.0 & 0.0 & 0.0 & 54.0 & 13.0 & 312.0 & 0.0 & 54.0 & -13.0 \\ 0.0 & 0.0 & 0.0 & 0.0 & -13.0 & -3.0 & 0.0 & 8.0 & 13.0 & -3.0 \\ 0.0 & 0.0 & 0.0 & 0.0 & 0.0 & 0.0 & 0.0 & 13.0 & 156.0 & -22.0 \\ 0.0 & 0.0 & 0.0 & 0.0 & 0.0 & 0.0 & -13.0 & -3.0 & -22.0 & 4.0 \end{bmatrix}$$

$$K_a = \begin{bmatrix} 15.0 & -4.5 & -3.0 & 1.5 & 0.0 & 0.0 & 0.0 & 0.0 & 0.0 & 0.0 \\ -4.5 & 5.0 & -1.5 & 0.5 & 0.0 & 0.0 & 0.0 & 0.0 & 0.0 & 0.0 \\ -3.0 & -1.5 & 15.0 & 4.5 & -12.0 & 6.0 & 0.0 & 0.0 & 0.0 & 0.0 \\ 1.5 & 0.5 & 4.5 & 5.0 & -6.0 & 2.0 & 0.0 & 0.0 & 0.0 & 0.0 \\ 0.0 & 0.0 & -12.0 & -6.0 & 24.0 & 0.0 & -12.0 & 6.0 & 0.0 & 0.0 \\ 0.0 & 0.0 & 6.0 & 2.0 & 0.0 & 8.0 & -6.0 & 2.0 & 0.0 & 0.0 \\ 0.0 & 0.0 & 0.0 & 0.0 & -12.0 & -6.0 & 24.0 & 0.0 & -12.0 & 6.0 \\ 0.0 & 0.0 & 0.0 & 0.0 & 6.0 & 2.0 & 0.0 & 6.0 & -6.0 & 2.0 \\ 0.0 & 0.0 & 0.0 & 0.0 & 0.0 & 0.0 & -12.0 & -6.0 & 12.0 & -6.0 \\ 0.0 & 0.0 & 0.0 & 0.0 & 0.0 & 0.0 & 6.0 & 2.0 & -6.0 & 4.0 \end{bmatrix}$$

Figure 2.2: 'Analytical! Cantilever Mass and
Stiffness Matrices

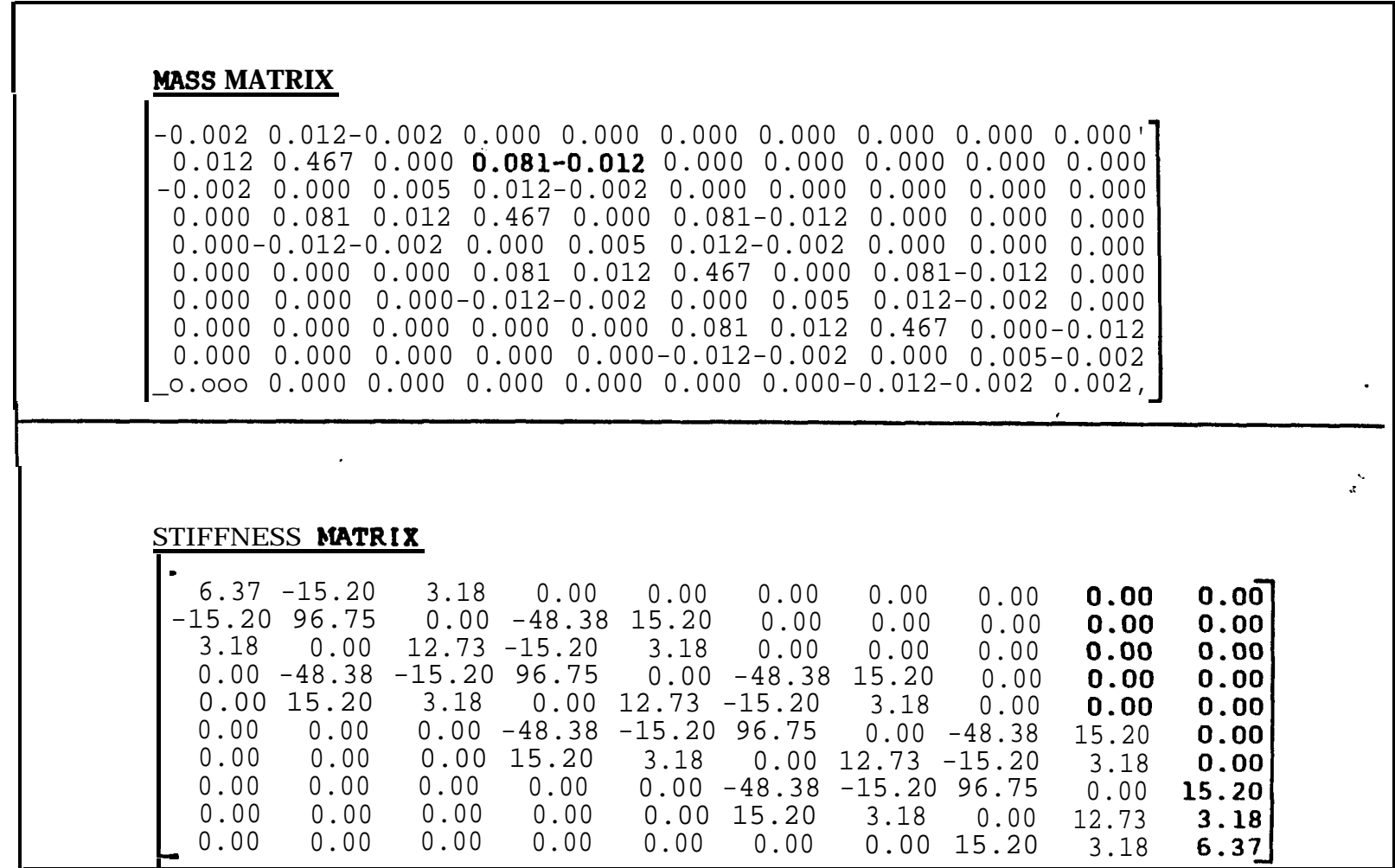


Figure 2.3: Correct (Measured) Mass and Stiffness Matrices of a Uniform Simply-Supported

Beam

EIGENVALUES

1.00021
 16.05306
 82.29164
 267.93070
 769.94872
 1604.32752
 3401.01224
 6860.57149
 12427.70447
 16168.92315

| | |
|---|--|
| <p>Eigenvector number.. 1</p> <p>0.79805530 0.46908518 0.64564030 0.75899576 0.24661265 0.75899576 -0.24661265 0.46908518 -0.64564030 -0.79805530</p> | <p>Eigenvector number.. 3</p> <p>-2.42965342 -0.77117777 0.75080420 0.47661407 1.96563090 0.47661407 -1.96563090 -0.77117777 -0.75080420 2.42965342</p> |
| <p>Eigenvector number.. 2</p> <p>-1.60101553 -0.76135436 -0.49474101 -0.47054287 1.29524877 0.47054287 1.29524877 0.76135436 -0.49474101 -1.60101553</p> | <p>Eigenvector number.. 4</p> <p>3.29392705 0.49465689 -2.66484296 -0.80037166 1.01787944 0.80037166 1.01787944 -0.49465689 -2.66484296 3.29392705</p> |

Figure 2.4: Correct (Measured) Modes and Frequencies of a
Simply Supported Uniform Beam

| | |
|--|--|
| <p>Eigenvector number.. 5</p> <p>-4.91819602 0.00000000 4.91819602 -0.00000000 -4.91819602 0.00000000 4.91819602 -0.00000000 -4.91819602 4.91819602</p> | <p>Eigenvector number.. 8</p> <p>-12.33800175 0.63554701 -3.81265222 0.39278965 9.98165310 -0.39278965 9.98165310 -0.63554701 -3.81265222 -12.33800175</p> |
| <p>Eigenvector number.. 6</p> <p>6.81740864 -0.45028622 -5.51539945 0.72857840 2.10669513 -0.72857840 2.10669513 0.45028622 -5.51539945 6.81740864</p> | <p>Eigenvector number.. 9</p> <p>-16.24231073 0.25314256 -13.14030541 0.40959327 -5.01915004 0.40959327 5.01915004 0.25314256 13.14030541 16.24231073</p> |
| <p>Eigenvector number.. 7</p> <p>-9.08402648 0.72247637 2.80711856 -0.44651495 7.34913180 -0.44651495 -7.34913180 0.72247637 -2.80711856 9.08402648</p> | <p>Eigenvector number.. 10</p> <p>13.01232356 0.00000000 13.01232356 0.00000000 13.01232356 0.00000000 13.01232356 0.00000000 13.01232356 0.00000000 13.01232356</p> |

Figure 2.4 (cont.)

MASS MATRIX

| | | | | | | | | | | |
|--------|--------|--------|--------|--------|--------|--------|--------|--------|--------|--------------|
| 0.001 | 0.006 | -0.001 | 0.000 | 0.000 | 0.000 | 0.000 | 0.000 | 0.000 | 0.000 | 0.000 |
| 0.006 | 0.350 | -0.010 | 0.081 | -0.006 | 0.000 | 0.000 | 0.000 | 0.000 | 0.000 | 0.000 |
| -0.001 | -0.010 | 0.004 | 0.012 | -0.001 | -0.010 | 0.000 | 0.000 | 0.000 | 0.000 | 0.000 |
| 0.000 | 0.081 | 0.012 | 0.467 | 0.000 | 0.081 | -0.012 | 0.000 | 0.000 | 0.000 | 0.000 |
| 0.000 | -0.012 | -0.002 | 0.000 | 0.005 | 0.012 | -0.002 | 0.000 | 0.000 | 0.000 | 0.000 |
| 0.000 | 0.000 | 0.000 | 0.081 | 0.012 | 0.467 | 0.000 | 0.081 | -0.012 | 0.000 | 0.000 |
| 0.000 | 0.000 | 0.000 | -0.012 | -0.002 | 0.000 | 0.005 | 0.012 | -0.002 | 0.000 | 0.000 |
| 0.000 | 0.000 | 0.000 | 0.000 | 0.000 | 0.081 | 0.012 | 0.467 | 0.000 | -0.012 | 0.000 |
| 0.000 | 0.000 | 0.000 | 0.000 | 0.000 | -0.012 | -0.002 | 0.000 | 0.005 | -0.002 | 0.000 |
| 0.000 | 0.000 | 0.000 | 0.000 | 0.000 | 0.000 | 0.000 | -0.012 | -0.002 | 0.002 | 0.002 |

STIFFNESS MATRIX

| | | | | | | | | | | |
|-------------|--------|--------|--------|--------|--------|-------------|-------------|-------------|-------------|-------------|
| 3.18 | -7.60 | 1.59 | 0.00 | 0.00 | 0.00 | 0.00 | 0.00 | 0.00 | 0.00 | 0.00 |
| -7.60 | 72.56 | -7.60 | -48.38 | 7.60 | 0.00 | 0.00 | 0.00 | 0.00 | 0.00 | 0.00 |
| 1.59 | -7.60 | 9.55 | -15.20 | 1.59 | 0.00 | 0.00 | 0.00 | 0.00 | 0.00 | 0.00 |
| 0.00 | -48.38 | -15.20 | 96.75 | 0.00 | -48.38 | 15.20 | 0.00 | 0.00 | 0.00 | 0.00 |
| 0.00 | 15.20 | 3.18 | 0.00 | 12.73 | -15.20 | 3.18 | 0.00 | 0.00 | 0.00 | 0.00 |
| 0.00 | 0.00 | 0.00 | -48.38 | -15.20 | 96.75 | 0.00 | -48.38 | 15.20 | 0.00 | 0.00 |
| 0.00 | 0.00 | 0.00 | 15.20 | 3.18 | 0.00 | 12.73 | -15.20 | 3.18 | 0.00 | 0.00 |
| 0.00 | 0.00 | 0.00 | 0.00 | 0.00 | -48.38 | -15.20 | 96.75 | 0.00 | 15.20 | 0.00 |
| 0.00 | 0.00 | 0.00 | 0.00 | 0.00 | 15.20 | 3.18 | 0.00 | 12.73 | 3.18 | 0.00 |
| 0.00 | 0.00 | 0.00 | 0.00 | 0.00 | 0.00 | 0.00 | 15.20 | 3.18 | 6.37 | 6.37 |

Figure 2.5: Incorrect (Analytical) Mass and Stiffness Matrices of a Uniform Simply-Supported
Beam

DAMPING MATRIX

| | | | | | | | | | | |
|--------------|--------|--------|-------|-------|-------|-------|-------|-------|-------|--------------|
| 0.064 | -0.152 | 0.032 | 0.000 | 0.000 | 0.000 | 0.000 | 0.000 | 0.000 | 0.000 | 0.000 |
| -0.152 | 0.484 | -0.152 | 0.000 | 0.000 | 0.000 | 0.000 | 0.000 | 0.000 | 0.000 | 0.000 |
| 0.032 | -0.152 | 0.064 | 0.000 | 0.000 | 0.000 | 0.000 | 0.000 | 0.000 | 0.000 | 0.000 |
| 0.000 | 0.000 | 0.000 | 0.000 | 0.000 | 0.000 | 0.000 | 0.000 | 0.000 | 0.000 | 0.000 |
| 0.000 | 0.000 | 0.000 | 0.000 | 0.000 | 0.000 | 0.000 | 0.000 | 0.000 | 0.000 | 0.000 |
| 0.000 | 0.000 | 0.000 | 0.000 | 0.000 | 0.000 | 0.000 | 0.000 | 0.000 | 0.000 | 0.000 |
| 0.000 | 0.000 | 0.000 | 0.000 | 0.000 | 0.000 | 0.000 | 0.000 | 0.000 | 0.000 | 0.000 |
| 0.000 | 0.000 | 0.000 | 0.000 | 0.000 | 0.000 | 0.000 | 0.000 | 0.000 | 0.000 | 0.000 |
| 0.000 | 0.000 | 0.000 | 0.000 | 0.000 | 0.000 | 0.000 | 0.000 | 0.000 | 0.000 | 0.000 |
| 0.000 | 0.000 | 0.000 | 0.000 | 0.000 | 0.000 | 0.000 | 0.000 | 0.000 | 0.000 | 0.000 |

Figure 2.6: Damping Matrix for a Uniform Simply-Supported Beam with
Non-Proportional Damping

| EIGENVALUES | | |
|-------------|----|-------------|
| -0.00024 | +i | 1.000109 |
| -0.00024 | +i | -1.000109 |
| -0.01229 | +i | 4.007036 |
| -0.01229 | +i | -4.007036 |
| -0.09466 | +i | 9.076626 |
| -0.09466 | +i | -9.076626 |
| -0.30394 | +i | 16.384171 |
| -0.30394 | +i | -16.384171 |
| -0.768027 | +i | 27.790997 |
| -0.768027 | +i | -27.790997 |
| -1.333621 | +i | 40.146059 |
| -1.333621 | +i | -40.146059 |
| -2.299626 | +i | 59.217929 |
| -2.299626 | +i | -59.217929 |
| -4.617110 | +i | 87.723826 |
| -4.617110 | +i | -87.723826 |
| -40.916446 | +i | 99.577774 |
| -40.916446 | +i | -99.577774 |
| -1.570939 | +i | 121.357080 |
| -1.570939 | +i | -121.357080 |

Figure 2.7: Eigenvalues of Uniform Simply Supported
Beam with Non-Proportional Damping

| | | | |
|----------------------|------------|----------------|-------------|
| EIGENVECTOR 1 | | EIGENVECTOR 5 | |
| 0.79804828 +i | -0.0008845 | 2.42874327 +i | -0.0839267 |
| 0.46908380 +i | -0.0002342 | 0.77215438 +i | 0.00500067 |
| 0.64564659 +i | 0.00058926 | -0.74863749 +i | 0.11453139 |
| 0.75899742 +i | 0.00007504 | -0.4763304 +i | 0.01286049 |
| 0.24661641 +i | 0.00037269 | -1.96975738 +i | -0.0644648 |
| 0.75899871 +i | 0.00021499 | -0.4776535 +i | -0.0174445 |
| -0.2466123 +i | 0.00006760 | 1.96667746 +i | 0.00142318 |
| 0.46908733 +i | 0.00016825 | 0.77161587 +i | 0.00472798 |
| -0.64564295 +i | -0.0001983 | 0.75249932 +i | 0.03338632 |
| -0.79805911 +i | -0.0003033 | -2.43188841 +i | -0.0350207 |
| EIGENVECTOR 2 | | EIGENVECTOR 6 | |
| 0.79804828 +i | 0.00088454 | 2.42874327 +i | 0.0639267 1 |
| 0.46908360 +i | 0.00023428 | 0.77215438 +i | -0.0050006 |
| 0.64564659 +i | -0.0005892 | -0.74663749 +i | -0.1145313 |
| 0.75899742 +i | -0.0000750 | -0.4763304 +i | -0.0128804 |
| 0.24661641 +i | -0.0003728 | -1.96975738 +i | 0.06446482 |
| 0.75899871 +i | -0.0002149 | -0.4776535 +i | 0.07 744456 |
| -0.2466123 +i | -0.0000676 | 1.96867746 +i | -0.0014231 |
| 0.46908733 +i | -0.0001682 | 0.77161587 +i | -0.0047279 |
| 0.64564295 +i | 0.00019833 | 0.75249932 +i | -0.0333863 |
| 0.79805911 +i | 0.00030338 | -2.43188841 +i | 0.03502075 |
| EIGENVECTOR 3 | | EIGENVECTOR 7 | |
| 1.60063222 +i | 0.01694926 | -3.29436566 +i | 0.11675713 |
| 0.76134713 +i | 0.00234402 | -0.4986783 +i | -0.0419077 |
| -0.4953804 +i | -0.0200945 | 2.66829007 +i | -0.2252383 |
| -0.4707129 +i | -0.0044576 | 0.80342192 +i | 0.02867941 |
| 1.29532791 +i | -0.0008148 | -1.01336236 +i | 0.18483988 |
| 0.47055460 +i | -0.0006742 | -0.80096786 +i | 0.00263282 |
| 1.29561779 +i | 0.00944367 | -1.02520948 +i | -0.1600463 |
| 0.76149596 +i | 0.00308637 | 0.49429990 +i | -0.0095409 |
| -0.4947652 +i | 0.00036550 | 2.66944398 +i | 0.09219724 |
| 1.60135284 +i | -0.0078835 | -3.29673638 +i | -0.0603341 |
| EIGENVECTOR 4 | | EIGENVECTOR 8 | |
| 1.60063222 +i | -0.0169492 | -3.29436566 +i | -0.1167571 |
| 0.76134713 +i | -0.0023440 | -0.4986783 +i | 0.04190775 |
| -0.4953804 +i | 0.02009450 | 2.66829007 +i | 0.22523833 |
| -0.4707129 +i | 0.00445760 | 0.80342192 +i | -0.0286794 |
| 1.29532791 +i | 0.00081480 | -1.01336236 +i | -0.1848398 |
| 0.47055460 +i | 0.00067424 | -0.80096788 +i | -0.0026326 |
| 1.29561779 +i | -0.0094436 | -1.02520948 +i | 0.16004631 |
| 0.76149596 +i | -0.0030863 | 0.49429990 +i | 0.00954094 |
| -0.4947652 +i | -0.0003655 | 2.66944398 +i | -0.0921972 |
| 1.60135284 +i | 0.00788358 | -3.29673638 +i | 0.06033418 |

Figure 2.8: Eigenvectors of Uniform Simply-Supported
Beam with Non-Proportional Damping

| | |
|---|--|
| <p>EIGENVECTOR 9</p> <p>-4.86309617 +i 0.39 156067</p> <p>-0.0073714 +i -0.0929540</p> <p>4.99524698 +i -0.1671134</p> <p>0.004 16455 +i 0.10009398</p> <p>-4.96310114 +i -0.1318510</p> <p>-0.002442 1 +i -0.0655089</p> <p>4.94454322 +i 0.19429566</p> <p>0.00112707 +i 0.03277538</p> <p>-4.93327299 +i -0.2371513</p> <p>4.92948488 +i 0.25 128642</p> | <p>EIGENVECTOR 13</p> <p>7.70823039 +i -2.14134378</p> <p>-0.70891578 +i 0.06993765</p> <p>-4.13874081 +i -2.51285774</p> <p>0.52118352 +i 0.12679480</p> <p>-7.41866311 +i 0.88296407</p> <p>0.43007458 +i -0.0836168</p> <p>8.02361606 +i 1.10993801</p> <p>-0.75347279 +i -0.0240873</p> <p>2.72496814 +i -0.4750263</p> <p>-9.50646662 +i -0.4889860</p> |
| <p>EIGENVECTOR 10</p> <p>-4.86309617 +i -0.3915606</p> <p>-0.00737 14 +i 0.09295406</p> <p>4.99524698 +i 0.16711345</p> <p>0.00416455 +i -0.1000939</p> <p>-4.96310114 +i 0.13185100</p> <p>-0.002442 1 +i 0.06550899</p> <p>4.94454322 +i -0.1942956</p> <p>0.00112707 +i -0.0327753</p> <p>-4.9332 7299 +i 0.23715136</p> <p>4.92948488 +i -0.2512864</p> | <p>EIGENVECTOR 14</p> <p>7.70823039 +i 2.14134378</p> <p>-0.70891578 +i -0.0699376</p> <p>-4.13874081 +i 2.51285774</p> <p>0.52118352 +i -0.1267948</p> <p>-7.41866311 +i -0.88296407</p> <p>0.43007458 +i 0.08361688</p> <p>8.02361606 +i -1.10993801</p> <p>-0.75347279 +i 0.02408733</p> <p>2.72496814 +i 0.47502833</p> <p>-9.50646662 +i 0.48898806</p> |
| <p>EIGENVECTOR 11</p> <p>-6.49884647 +i 0.62921861</p> <p>0.44238085 +i -0.0979085</p> <p>5.80399407 +i 0.79627146</p> <p>-0.74090650 +i 0.03594341</p> <p>-2.21029950 +i -1.11377107</p> <p>0.74023466 +i 0.03015839</p> <p>-2.09483630 +i 0.65224691</p> <p>-0.4568743 +i -0.0366172</p> <p>5.55398970 +i -0.0785197</p> <p>-6.87061007 +i -0.1729018</p> | <p>EIGENVECTOR 15</p> <p>7.45324447 +i -6.24122905</p> <p>-0.68625485 +i 0.06868798</p> <p>-2.10000870 +i -6.14541687</p> <p>-0.2104462 +i 0.21590885</p> <p>14.29690639 +i -2.24227152</p> <p>0.54679930 +i 0.08123459</p> <p>-9.82439128 +i 1.56820700</p> <p>0.64951987 +i -0.047 1842</p> <p>5.86043927 +i 1.72043321</p> <p>14.36016423 +i 0.94252876</p> |
| <p>EIGENVECTOR 12</p> <p>-6.49884647 +i -0.62921861</p> <p>0.44238085 +i 0.09790854</p> <p>5.80399407 +i -0.79627146</p> <p>-0.74090650 +i -0.0359434</p> <p>-2.21029950 +i 1.11377107</p> <p>0.74023466 +i -0.0301583</p> <p>-2.09483630 +i -0.6522469 1</p> <p>-0.4568743 +i 0.03661729</p> <p>5.55398970 +i 0.07851970</p> <p>-6.87061007 +i 0.17290189</p> | <p>EIGENVECTOR 16</p> <p>7.45324447 +i 6.24122905</p> <p>-0.68625485 +i -0.0668879</p> <p>-2.10000870 +i 6.14541667</p> <p>-0.2104462 +i -0.2159088</p> <p>14.29690639 +i 2.24227152</p> <p>0.54679930 +i -0.0812345</p> <p>-9.82439128 +i -1.56820700</p> <p>0.64951987 +i 0.04718420</p> <p>5.86043927 +i -1.72043321</p> <p>14.36016423 +i -0.94252876</p> |

Figure 28 (cont.)

| EIGENVECTOR 17 | | |
|----------------|----|----------------|
| 26.675420 | 11 | +i -9.61793553 |
| 0.52915315 | | +i 0.54295220 |
| 19.83261166 | | +i -1.57958265 |
| 0.44551446 | | +i 0.05151553 |
| -7.30067665 | 4i | 5.91671735 |
| 0.16257968 | | +i -0.1486024 |
| -0.1552809 | | +i 4.16051563 |
| 0.01957921 | | +i -0.1018729 |
| 1.75767996 | | +i 0.99315436 |
| 1.88679567 | | +i -0.2395551 |

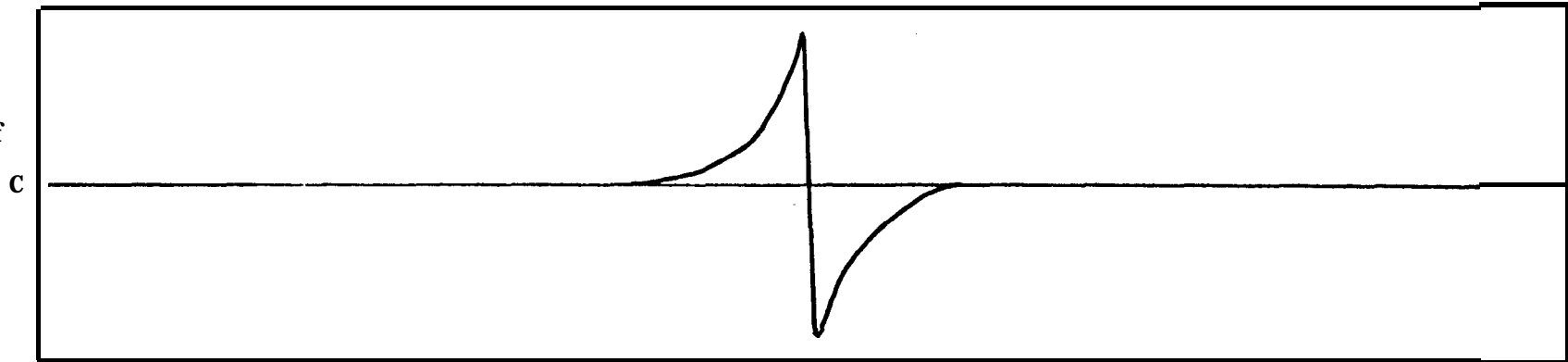
| EIGENVECTOR 18 | | |
|----------------|----|----------------|
| 26.67542011 | | +i 9.61793553 |
| 0.52915315 | | +i -0.54295220 |
| 19.83261168 | 4i | 1.57958265 |
| 0.44551446 | | +i -0.0515155 |
| -7.30067665 | | +i -5.91671735 |
| 0.16257968 | | +i 0.14860240 |
| -0.1552809 | 4i | -4.16051563 |
| 0.01957921 | | +i 0.10187293 |
| 1.75767996 | | +i -0.99315436 |
| 1.88679567 | | +i 0.23955516 |

| EIGENVECTOR 19 | | |
|----------------|----|----------------|
| -0.70964409 | | +i 4.21619012 |
| 0.25471659 | | +i -0.0495710 |
| 2.61180108 | 4i | 3.74569192 |
| 0.25902052 | 4i | -0.0729415 |
| 9.01791709 | | +i 2.16618231 |
| 0.19218298 | 4i | -0.0616198 |
| 14.44910849 | | +i 0.53144312 |
| 0.10207651 | | +i -0.0349668 |
| 17.98876480 | | +i -0.64014133 |
| 19.21658627 | | +i -1.06414531 |

| EIGENVECTOR 20 | | |
|----------------|----|-----------------|
| -0.70964409 | 4i | -4.21619012 |
| 0.25471659 | | +i 0.04957 103 |
| 2.61180108 | | +i -3.74569 192 |
| 0.25902052 | 4i | 0.07294152 |
| 9.01791709 | 4i | -2.16618231 |
| 0.19218298 | | +i 0.06161981 |
| 14.44910849 | | +i -0.53144312 |
| 0.10207651 | | +i 0.03496687 |
| 17.98876480 | | +i 0.64014133 |
| 19.21658627 | | +i 1.06414531 |

Figure 2.8 (cont.)

Real part of
Frequency
Response
Function



- 76 -

Imaginary
part of
Frequency
Response
Function

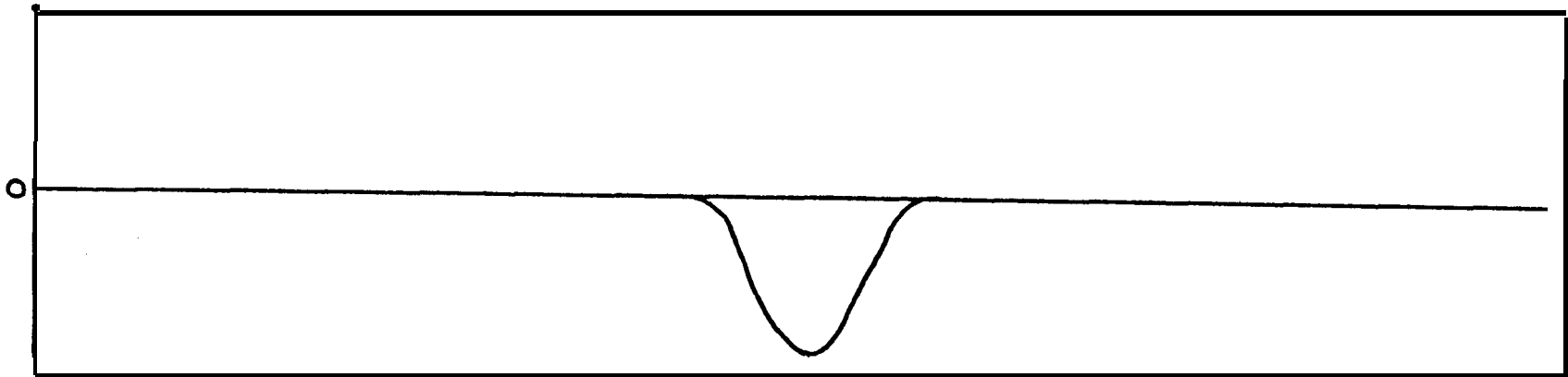


Figure 2.9

| | U.D. FREQ. | D. FREQ. | DAMPING FACTOR | ζ CRIT. | RE | IM |
|-----|------------|-----------------|----------------|---------------|----------------|-----------|
| | MODE 1 | | | | | |
| (1) | 40.37 | 40.37 | -0.0741 | 0.183533 | 2.29445 | 5.491102 |
| (2) | 40.2847 | 40.2846 | -0.10312 | 0.255711 | 2.3507 | 4.022547 |
| (3) | 40.3287 | 40.3285 | -0.0984 | 0.244 | 1.192357 | 3.181806 |
| (4) | 40.385 | 40.3849 | -0.07612 | 0.1884 | 0.655109 | 1.866827 |
| (5) | 40.4498 | 40.4498 | -0.0468 | 0.1158 | 0.22195 | 0.610550 |
| | MODE 2 | | | | | |
| (1) | 254.325 | 254.324 | -0.582144 | 0.228897 | 11.852656 | 2.656811 |
| (2) | 254.25595 | 254.25443 | -0.879 | 0.345723 | 0.694002 | -0.102144 |
| (3) | 254.454 | 254.4539 | -0.53189 | 0.209032 | -2.77474 | -5.603733 |
| (4) | 254.6978 | 254.6974 | -0.46166 | 0.181258 | -3.480396 | -7.888621 |
| (5) | 255.133 | 255.172 | -0.32878 | 0.128847 | -2.48746 | -4.706277 |

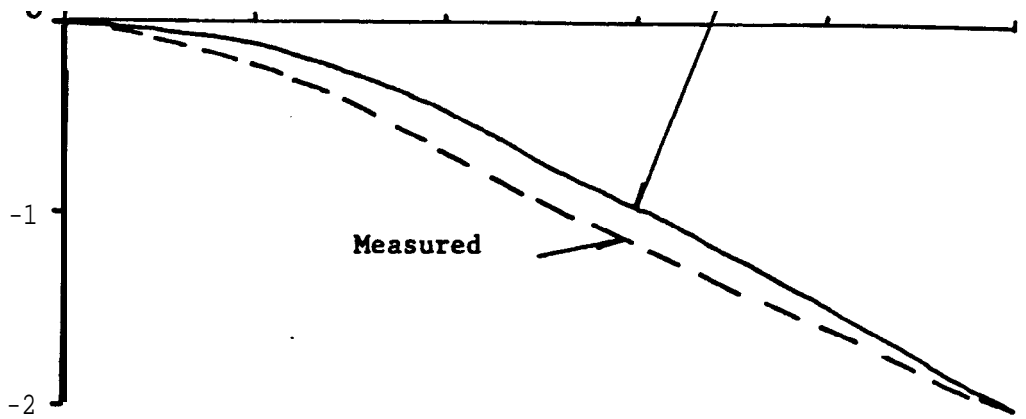
MODE 1

| <u>MOD</u> | <u>PHASE</u> | <u> N </u> |
|------------|--------------|------------|
| 5.951193 | 67.32 | 2 |
| 4.659042 | 59.698 | 1.5657 |
| 3.397882 | 64.457 | 1.1419 |
| 1.978436 | 70.663 | 0.6649 |
| 0.64964 | 70.022 | 0.2183 |

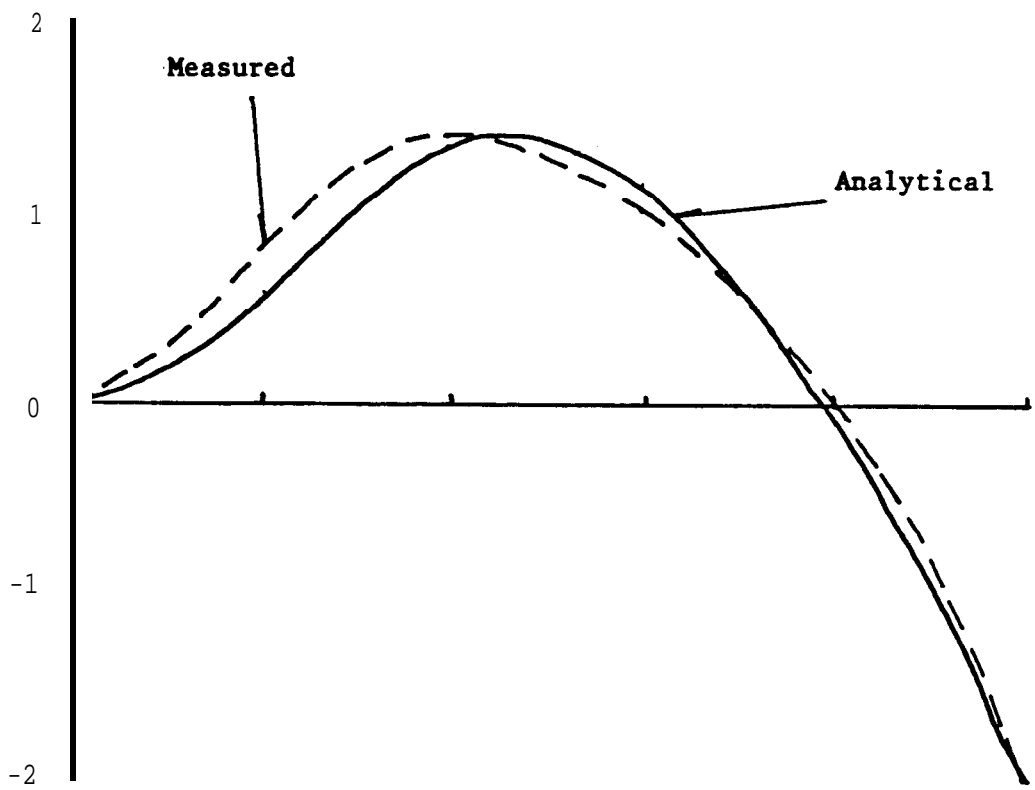
MODE 2

| <u>MOD</u> | <u>PHASE</u> | <u> N </u> |
|-----------------|--------------|------------|
| 12.14677 | 12.634 | 2 |
| 0.70147 | | 0.1155 |
| 6.25308 | 243.65 | -1.02958 |
| 8.62227 | 246.19 | -1.41968 |
| 5.323203 | 242.14 | -0.87648 |

Figure 2.10: **Curvefit** Results -Undamaged Cantilever



Mode 1



Mode 2

Figure 2.11

| | U.D. FREQ. | D.FREQ. | DAMPING FACTOR | Z CRIT. | RE | IM |
|-----|------------|-----------|----------------|----------|-----------|----------|
| | MODE 1 | | | | | |
| (1) | 39.1696 | 39.16874 | -0.26283 | 0.671 | 3.03679 | 7.376032 |
| (2) | 39.00954 | 39.008466 | 0.289495 | 0.742112 | 2.475344 | 5.630936 |
| (3) | 39.084196 | 39.083144 | -0.289495 | 0.733691 | 1.681678 | 4.275594 |
| (4) | 39.274357 | 39.2735 | -0.252542 | 0.643021 | 1.011412 | 2.409633 |
| (5) | 39.524173 | 39.523832 | -0.164121 | 0.415242 | 0.458141 | 0.873377 |
| | MODE 2 | | | | | |
| (1) | 249.4656 | 249.46269 | -1.21668 | 0.487717 | 11.20954 | 0.74112 |
| (2) | 248.4981 | 248.49744 | -1.68177 | 0.676749 | 0.708874 | 0.106716 |
| (3) | 249.03436 | 249.03689 | -1.31323 | 0.527346 | -4.66496 | -4.45960 |
| (4) | 249.94155 | 249.9392s | -1.07594 | 0.428338 | -5.15853 | -9.31251 |
| (5) | 251.03272 | 251.03022 | -1.12062 | 0.446405 | -4.647265 | -5.79940 |

MODE 1

| <u>MOD</u> | <u>PHASE</u> | <u> N </u> |
|------------|--------------|------------|
| 7.9767124 | 67.622 | 2 |
| 6.1509974 | 66.2698 | 1.442238 |
| 4.5944254 | 68.5292 | 1.151959 |
| 2.6132901 | 67.23 | 0.6552298 |
| 0.9862456 | 62.32 | 0.2472812 |

MODE 2

| <u>MOD</u> | <u>PHASE</u> | <u> N </u> |
|------------|--------------|------------|
| 11.234 | 86.21739 | 2 |
| 0.71686 | 81.4388 | 0.1276 |
| 6.45368 | 226.29 | -1.1489549 |
| 10.645817 | 241.016 | -1.8952852 |
| 7.4316995 | 231.3 | -1.3230727 |

Figure 2.12: **Curvefit** Results -Damaged Cantilever

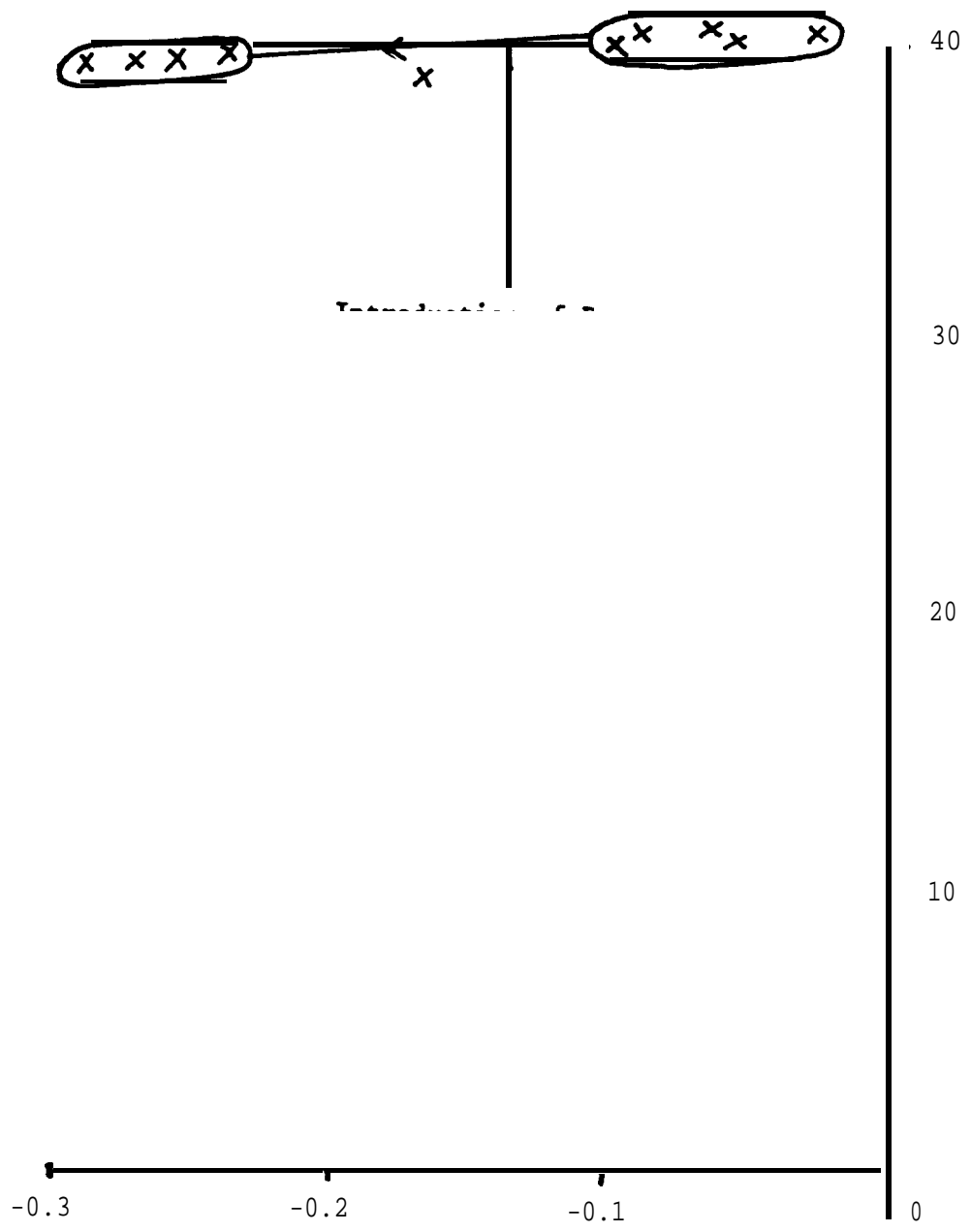


Figure 2.13: Mode 1 -Pole Location

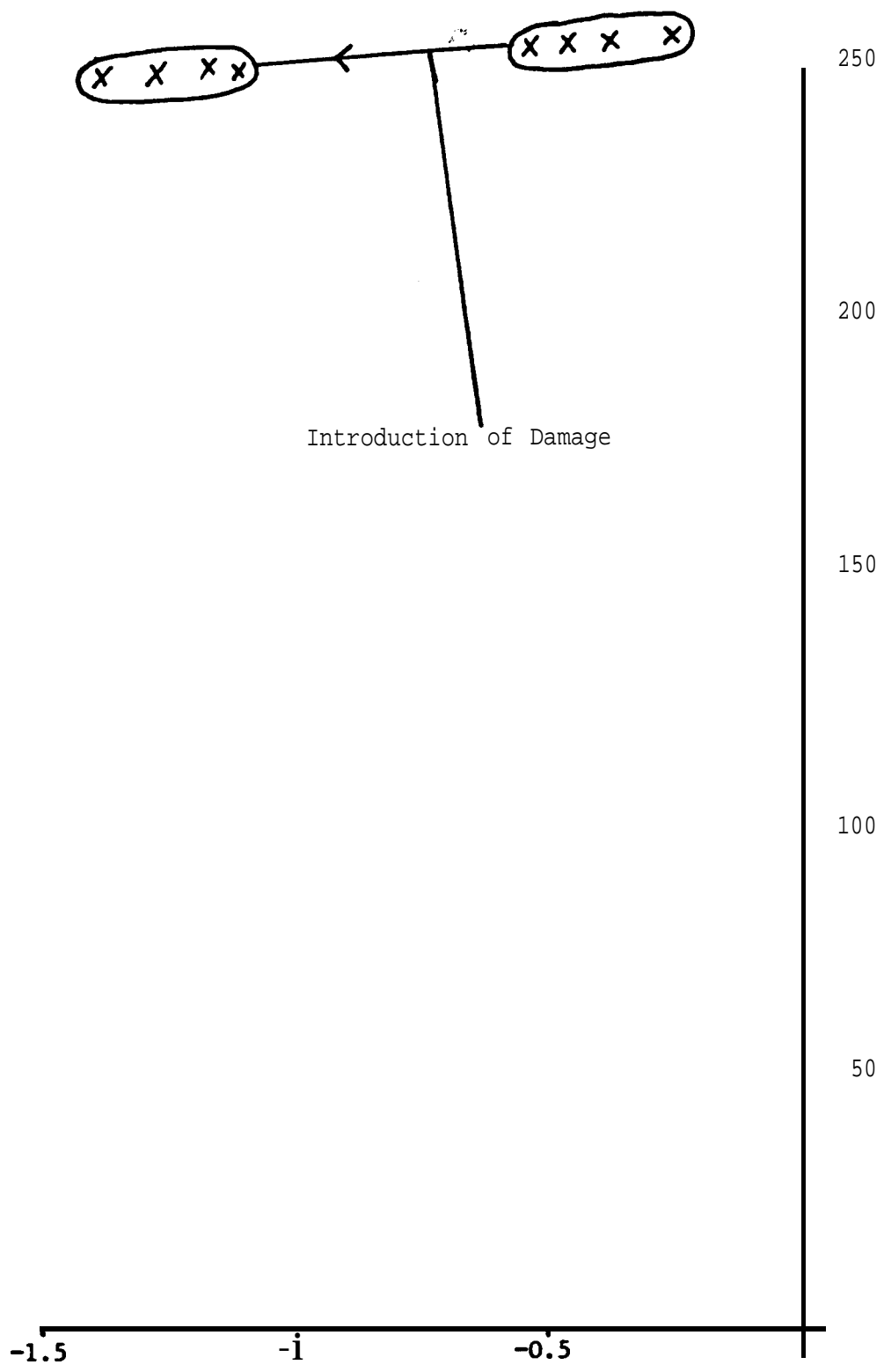


Figure 2.14: Mode 2 -Pole Location

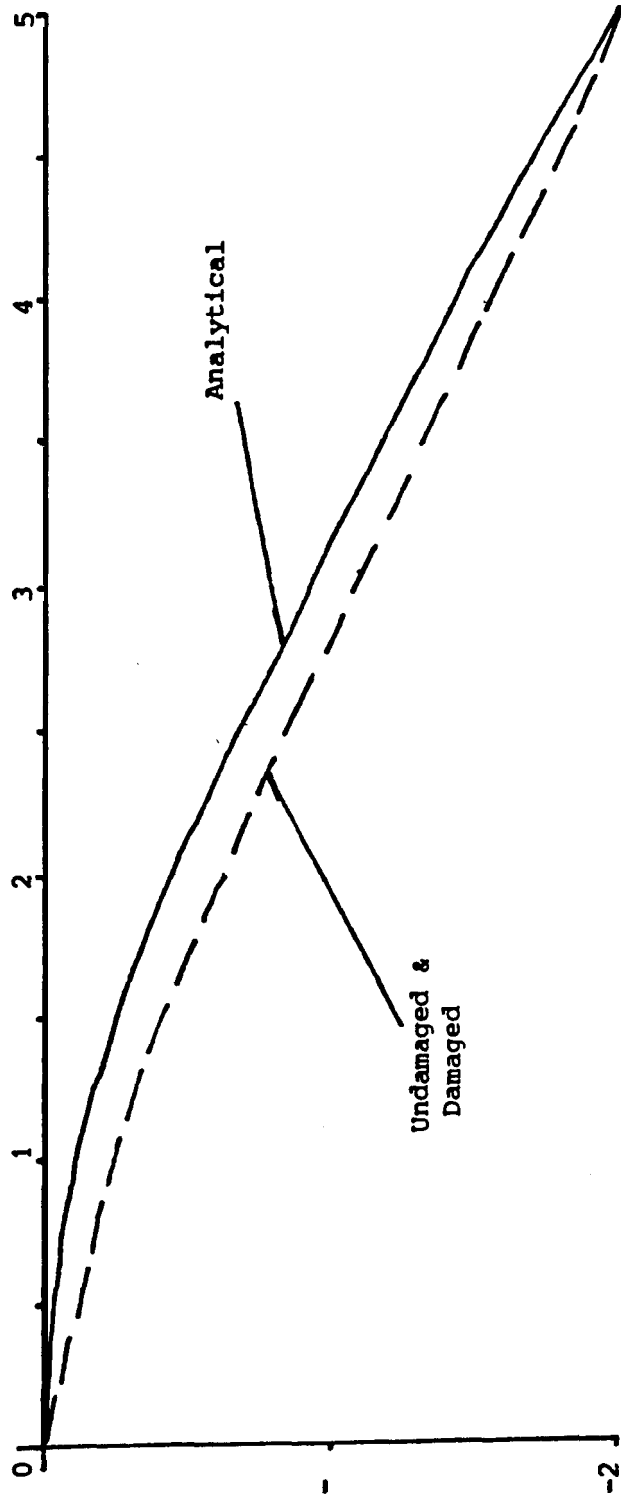


Figure 2.15: Mode 1

-- 101 --

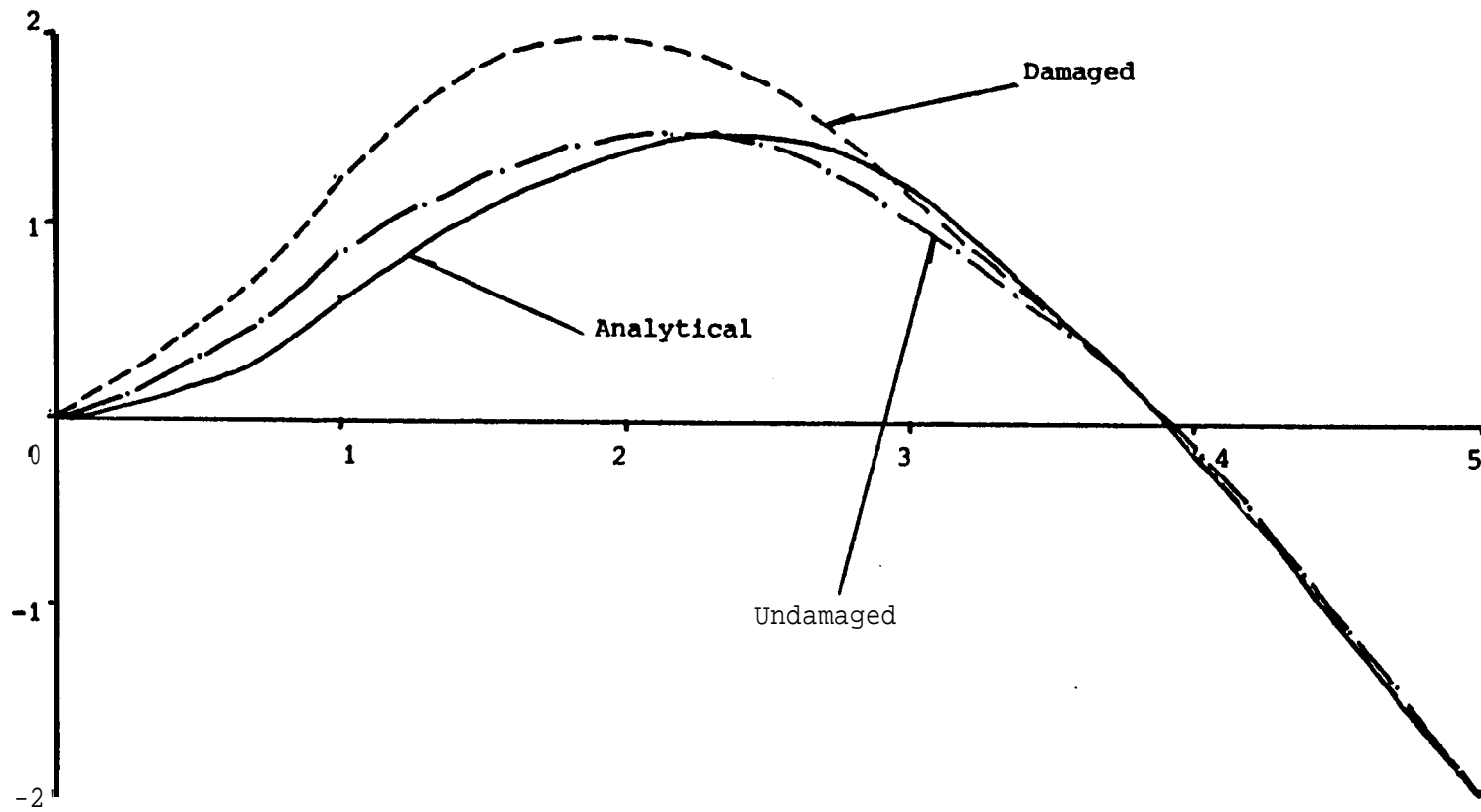
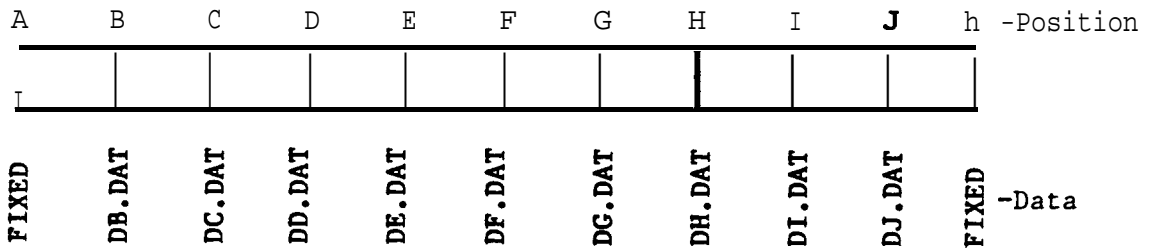


Figure 2.16: Mode 2

HAMMER

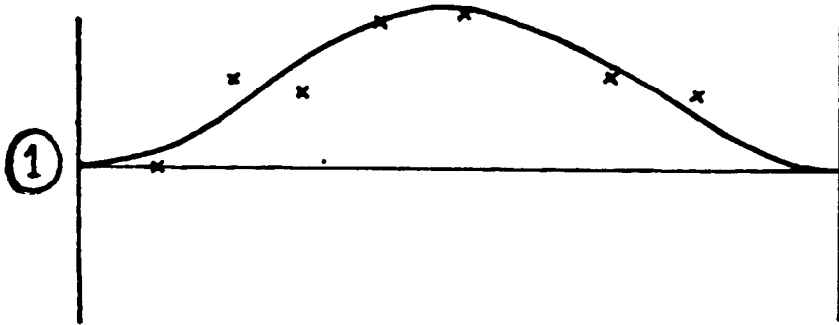


| | ESTIMATED FREQUENCIES | ESTIMATED RANGE |
|------------------------------|-----------------------|-----------------|
| FIRST LATERAL (1L) | 1.64 | 1.3 - 2.2 |
| SECOND LATERAL (2L) | 6.95 | 6.5 - 7.6 |

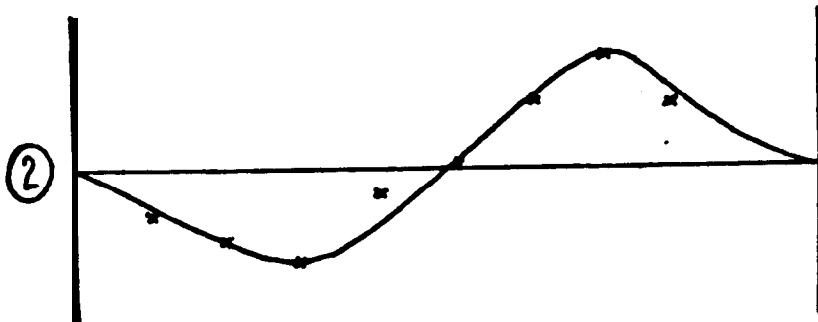
| CHANNEL | QUALITY OF DATA (10=good 1=poor) | MODES VISIBLE |
|---------------|-------------------------------------|---------------------|
| DB.DAT | 1 | (1L) |
| DC.DAT | 3 | 1L (2L) |
| DD.DAT | 6 | 1L 2L |
| DE.DAT | 5 | 1L 2L |
| DF.DAT | 10 | 1L |
| DG.DAT | 8 | 1L 2L |
| DH.DAT | 7 | 1L 2L |
| DI.DAT | 6 | 1L 2L |
| DJ.DAT | 6 | 1L 2L |

Figure 2.17: **Suspension Bridge Data**

k j i h g f e d c b a



Mode 1L $\omega = 1.69$ Hz $\mu = 0.60$ %



Mode 2L $\omega = 6.96$ Hz $\mu = 0.69$ %

Figure 2.18: Suspension Bridge Modes

THEORETICAL DEVELOPMENT3.1 Preliminaries

The first two chapters of this thesis have set out to review and analyse some of the theoretical and mathematical considerations of dynamic analysis. As a result, some unanswered questions have emerged, principally the dilemma that occurs between the comparison of theoretical results using a method such as finite-elements and experimental results which emerge as a result of modal tests. In the literature, some formal attempts have been made to directly compare and analyse the two simultaneously, but the efforts have been far from exhaustive. No effort has been made with regard to the comparison of measured complex modes with analytical, real matrices.

It is the opinion of the author that the reason for this has been the lack of an adequate mathematical tool with which to analyse the problem. Matrix algebra, on its own, could never reveal the underlying fundamentals of the problem, and so results obtained will nearly always need to be viewed with scepticism. The introduction of vector space theory as a possible tool with which to analyse the problem offers the prospect of a more fundamental grasp of the situation and provides a good framework in which to argue and justify results obtained.

However, prior to the analysis, the necessary groundwork needs to be laid and fully understood. It is by no means the objective of this thesis to offer a comprehensive survey of the

techniques and ideas of vector space theory: on the contrary, the number of ideas needed to pursue ~~the remainder~~ of this thesis with a full understanding is surprisingly small. So that this volume may stand as a complete entity in its own right, the necessary definitions will be quoted⁽⁶⁶⁾ and expanded upon, bearing in mind the objectives and goals of the ensuing chapters.

3.2 Fundamentals

The most direct way to introduce vector space theory is with the definition of a vector space.

Definition 1

A vector space \mathcal{V} is a set of elements called vectors with an operation called addition, and an operation called scalar multiplication which satisfy the following axioms:

(a) Addition Axioms: To every pair of vectors $x, y \in \mathcal{V}$, there corresponds a unique vector $x + y \in \mathcal{V}$, the sum of x and y such that

(i) $x + y = y + x$ (commutative law);

(ii) $(x + y) + z = x + (y + z)$ (associative law);

(iii) there exists a unique zero vector $\theta \in \mathcal{V}$ such that $x + \theta = x \forall x \in \mathcal{V}$ (identity element for addition);

(iv) for every vector x there exists a unique vector $(-x) \in \mathcal{V}$ such that $x + (-x) = \theta$ (additive inverse): the vector $x + (-y)$ is normally written $x - y$.

(b) Scalar Multiplication Axioms: To every scalar α and every vector $x \in \mathcal{V}$ there corresponds a unique vector $\alpha x \in \mathcal{V}$ such that

(v) $\alpha(\beta x) = (\alpha\beta)x$ for every scalar β ;

- (vi) $1x = x$ $0x = \theta$ $\forall x \in \mathcal{V}$;
- (vii) $a(x + y) = ax + ay$;
- (viii) $(a + \beta)x = ax + \beta x$.
- (distributive laws)

One can easily show that the vector $-1x$ is the vector $(-x)$ of axiom (iv).

Thus, if we consider the space of real n -tuples and let $x = (\xi_1, \xi_2, \dots, \xi_n)$ and $y = (\eta_1, \eta_2, \dots, \eta_n)$. We define

$$x + y = (\xi_1 + \eta_1, \xi_2 + \eta_2, \dots, \xi_n + \eta_n)$$

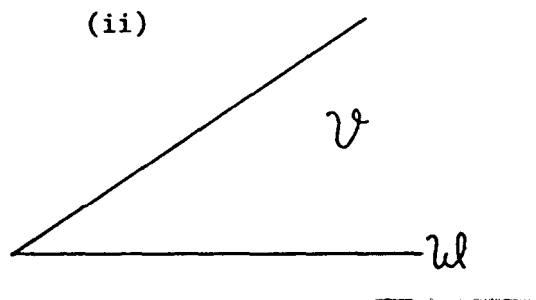
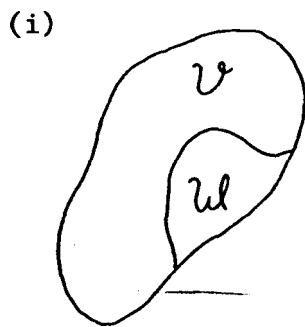
and $ax = (a\xi_1, a\xi_2, \dots, a\xi_n)$.

This concrete definition of addition and scalar multiplication on ordered n -tuples satisfies the axioms for a vector space, as is easily verified. The zero vector is $(0, 0, \dots, 0)$. This space is generally denoted by \mathbb{R}_n . The next thing to define is a subspace.

Definition 2

A non-empty subset \mathcal{W} of a vector space \mathcal{V} is called a subspace of \mathcal{V} if \mathcal{W} is itself a vector space under the rules for addition and scalar multiplication as defined for \mathcal{V} .

Possible pictorial representations for vector spaces and subspaces are:



For much of the analysis we will be concerned directly with inner product spaces. An inner **product** space is denoted by $(\mathcal{V}, \langle \cdot, \cdot \rangle)$ and consists of a vector space \mathcal{V} and an operation between elements of that vector space called an inner product. The definition of an inner product is as follows.

Definition 3

An inner product on a vector space \mathcal{V} is a scalar valued function $\langle x, y \rangle$, defined for all ordered pairs of vectors $x, y \in \mathcal{V}$ and which satisfies the following axioms:

- (i) $\langle x, y \rangle = \overline{\langle y, x \rangle}$ $\forall x, y \in \mathcal{V}$;
- (ii) $\langle \alpha x + \beta y, z \rangle = \alpha \langle x, z \rangle + \beta \langle y, z \rangle$;
- (iii) $\langle x, x \rangle \geq 0$; $\langle x, x \rangle = 0$ if, and only if, $x = \theta$.

The following property follows from axioms 1 and 2:

- (iv) $\langle x, \gamma y + \delta z \rangle = \overline{\gamma} \langle x, y \rangle + \overline{\delta} \langle x, z \rangle$.

The bar denotes complex conjugate. Thus, if we consider the space of complex n -tuples (\mathbb{C}^n) then

$$\langle x, y \rangle = \sum_{i=1}^n \xi_i \overline{\eta_i} \quad (= \underline{x}^T \underline{y})$$

This also **allows** us to introduce the norm of a vector, given by

$$\|x\| = \langle x, x \rangle^{\frac{1}{2}} = \left(\sum_{i=1}^n \xi_i^2 \right)^{\frac{1}{2}}$$

For the analysis of the undamped problem, a real inner product space will be required, often called a Euclidean space. This is because the operators involved (typically matrices) are **symmetric** and positive-definite, allowing an analysis using real arithmetic. For the damped problem, the space and its dual will be

analysed. This will be mentioned later.

Next we need to define a basis. in which to describe elements of the vector space. This is defined as:

Definition 4

A set, s , of linearly independent vectors is an algebraic basis for the space \mathcal{V} if $[s] = \mathcal{V}$, i.e. s spans the whole space \mathcal{V} .

Thus for \mathcal{R}_n , if we have n vectors x_i $i = 1, \dots, n$ any other vector may be expressed as a linear combination of these vectors, viz:

$$x = \sum_{i=1}^n \alpha_i x_i$$

where the α_i are scalar multipliers $[x_i]$ $i = 1, \dots, n$ is said to span the whole space \mathcal{R}_n . A vector space does not have a unique basis; however, the number of vectors in any basis for \mathcal{V} is unique. We will primarily be concerned with a basis of eigenvectors.

Definition 5

The dimension, $\dim \mathcal{V}$, of a vector space is the number of elements in any basis.

We shall be concerned mainly with vector spaces having a finite basis, i.e. finite dimensional. The dimension of the vector space will be typically n ($\dim(\mathcal{V}) = n$) where n is the number of elements in the FE model.

Ideally we wish our basis sets to be orthonormal with respect to the inner product. By orthonormal we mean (typically for **eigenvectors**)

$$\langle x_i, x_j \rangle = \frac{x_i^T x_j}{-1-1} = \sum_{r=1}^n \xi_r^i \xi_r^j = 0$$

and $\langle x_i, x_i \rangle = \frac{x_i^T x_i}{-1-1} = \sum_{r=1}^n (\xi_r^i)^2 = 1$

where the x_i are basis vectors. If we have a weighted inner product, involving a positive definite transformation (see below) the orthonormality conditions are given as

$$\langle x_i, x_j \rangle_A = \frac{x_i^T A x_j}{-1-1} = 0$$

$$\langle x_i, x_i \rangle_A = \frac{x_i^T A x_i}{-1-1} = 1$$

where A is such a transformation. Thus a set of eigenvectors, x_i , $i = 1, \dots, m$ will define a subspace \mathcal{V}_m and the orthogonal complement space \mathcal{V}_m^\perp will be spanned by x_i , $i = m+1, \dots, n$, since all the vectors in one subspace are mutually orthogonal to those in the other. So we may say

$$\mathcal{V}_n = \mathcal{V}_m \oplus \mathcal{V}_m^\perp$$

where \oplus denotes the addition of two subspaces when the intersection is equal to the null (empty) space. Thus

$$\dim(\mathcal{V}_n) = \dim(\mathcal{V}_m) + \dim(\mathcal{V}_m^\perp).$$

We may now introduce symmetric positive-definite operators of the form $T: \mathcal{V}_n \rightarrow \mathcal{V}_n$ where, relative to an orthonormal basis, T is represented by a square, symmetric positive-definite matrix array (\underline{T}). T is a linear transformation where a linear transformation is defined as

Definition 6

The function (or mapping)

$$T: \mathcal{V} \rightarrow \mathcal{V}$$

is called a linear transformation of \mathcal{V} onto itself if

$$(i) \quad T(\mathbf{x} + \mathbf{y}) = T\mathbf{x} + T\mathbf{y};$$

(ii) $T(\alpha\mathbf{x}) = \alpha T\mathbf{x} \quad \forall \mathbf{x} \in \mathcal{V}$ and all scalars α . T is a symmetric transformation if

$$\langle \mathbf{x}, T\mathbf{x} \rangle = \langle T\mathbf{x}, \mathbf{x} \rangle \quad \forall \mathbf{x}$$

and T is positive-definite if

$$\langle \mathbf{x}, T\mathbf{x} \rangle = \langle \mathbf{x}, \mathbf{x} \rangle_T > 0 \quad \forall \mathbf{x} \neq \theta$$

The principal concern of this thesis will be the formulation of projected forms of T so that

$$\text{Proj}(T)_{\mathcal{V}_m} : \mathcal{V}_m \rightarrow \mathcal{V}_m$$

That is, $\text{Proj}(T)_{\mathcal{V}_m}$ can only operate on and produce vectors that lie within the subspace \mathcal{V}_m . Then, for $\mathbf{x} \in \mathcal{V}_m$,

$$(\text{Proj}(T)_{\mathcal{V}_m})\mathbf{x} = \text{Proj}(T\mathbf{x})_{\mathcal{V}_m}$$

that is, the component of $T\mathbf{x}$ in \mathcal{V}_m and for $\mathbf{x} \notin \mathcal{V}_m$

$$(\text{Proj}(T)_{\mathcal{V}_m})\mathbf{x} = \theta.$$

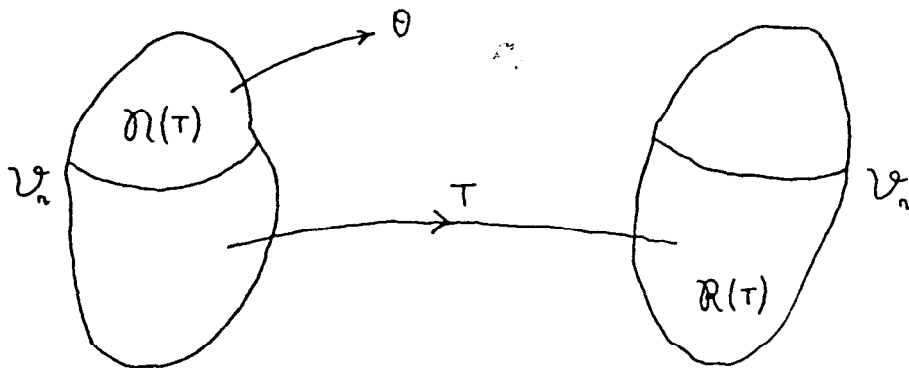
The projected transformations behave exactly the same as T in the subspace onto which they have been projected and map everything outside that subspace to zero. We need some more definitions:

Definition 7

The range space of T , $\mathcal{R}(T)$, is the subspace of vectors produced after the operation of T on vectors in \mathcal{V}_n : $\mathcal{R}(T)$ is a subspace of \mathcal{V}_n .

Definition 8

The null space of T , $\mathcal{N}(T)$, is the subspace of vectors which map to zero when operated on by T : $\mathcal{N}(T)$ is a subspace of \mathcal{V}_n .



We may say that

$$\rho(\text{Proj}(T) \mathcal{V}_m) = \dim(\mathcal{R}(\text{Proj}(T) \mathcal{V}_m)) = m$$

and $\nu(\text{Proj}(T) \mathcal{V}_m) = \dim(\mathcal{N}(\text{Proj}(T) \mathcal{V}_m)) = n - m.$

However, it is not true to say that

$$T = \text{Proj}(T) \mathcal{V}_m \oplus \text{Proj}(T) \mathcal{V}_m^\perp$$

since the effect of T in mapping vectors from \mathcal{V}_m to \mathcal{V}_m^\perp and vice versa will have been eliminated. This may be illustrated with a partitioned matrix

$$\underline{T} = \begin{bmatrix} \text{Proj}(\underline{T}) \mathcal{V}_m & \underline{T}_{12} \\ \underline{T}_{21} & \text{Proj}(\underline{T}) \mathcal{V}_m^\perp \end{bmatrix}$$

\underline{T}_{12} and \underline{T}_{21} are not included in the sum of the two projections.

In order that a full understanding of the undamped problem is gained, an initial analysis of the single matrix case

$$(\lambda_i I - \underline{T}) \underline{x}_i = \theta$$

or $\underline{T} \Phi = \Phi \Lambda$

will first be studied, with (where appropriate) a (3x3) symmetric matrix example

$$\underline{T} = \begin{bmatrix} 3 & -1 & 0 \\ -1 & 2 & -1 \\ 0 & -1 & 3 \end{bmatrix}$$

Then, as a preliminary study for the damped case, a single **unsymmetric** matrix will be studied.

3.3 Change of Basis

Before attempting to approximate \underline{T} using its eigenvectors and eigenvalues, it is essential to realise that \underline{T} is merely a matrix representation of the linear transformation T . Although the linear transformation is fixed, its matrix representation can take on many forms, depending upon the basis (axis system) in which we choose to describe it.

For example, \underline{T} maps the point $\bar{A}(1,1,1)$ to $\bar{B}(2,0,2)$ and T is represented using the standard basis $e_i = \{(1,0,0), (0,1,0), (0,0,1)\}$. However, we may choose to describe T using an alternative basis $b_i = \{(1,1,0), (0,1,1), (1,0,1)\}$. These are the coordinates of the new basis vectors (axes) b_i relative to the old basis e_i which is the only way we can describe them.

Alternatively, we may choose to describe the vectors e_i in terms of the vectors b_i , which are then as follows: $\{\frac{1}{2}(1,-1,1), \frac{1}{2}(1,1,-1), \frac{1}{2}(-1,1,1)\}$. Relative to the new basis b_i the point \bar{A} is now $\frac{1}{2}(1,1,1)$ and \bar{B} is $(0,0,2)$. To determine the form of T relative to this new basis we must transform the coordinates of \underline{T} .

$$\begin{aligned} \underline{T}_{\text{NEW BASIS}} &= \{\text{old basis in terms of new basis}\} \\ &\quad \times \underline{T}_{\text{OLD BASIS}} \times \{\text{new basis in terms of old basis}\} \end{aligned}$$

with

{old basis in terms of new basis} = {new basis in terms of old basis}⁻¹.

So

$$\begin{aligned} \underline{T}_{\text{NEW BASIS}} &= \frac{1}{2} \begin{bmatrix} 1 & 1 & -1 \\ 1 & 1 & 1 \\ 1 & -1 & 1 \end{bmatrix} \begin{bmatrix} 3 & -1 & 0 \\ -1 & 2 & -1 \\ 0 & -1 & 3 \end{bmatrix} \begin{bmatrix} 1 & 0 & 1 \\ 1 & 1 & 0 \\ 0 & 1 & 1 \end{bmatrix} \\ &= \begin{bmatrix} -1 & 2 & -1 \\ 0 & -1 & -4 \end{bmatrix} \end{aligned}$$

T is the same operator, that is it still maps the point \bar{A} to the point \bar{B} , but because we have chosen to represent it using a different basis set b_i , it appears completely different and is no longer symmetrical. The loss of symmetry is a result of choosing a non-orthogonal basis. In nearly all cases the basis vectors are merely rotated and so remain orthogonal, and hence preserve symmetry.

Furthermore, if we choose to represent T using a basis set of eigenvectors, \underline{T} is diagonalised with the diagonal terms being the eigenvalues.

$$\begin{aligned} \underline{T}_{\text{EIGENVECTOR BASIS}} &= \begin{bmatrix} 1/\sqrt{6} & 2/\sqrt{6} & 1/\sqrt{6} \\ 1/\sqrt{2} & 0 & -1/\sqrt{2} \\ 1/\sqrt{3} & -1/\sqrt{3} & 1/\sqrt{3} \end{bmatrix} \begin{bmatrix} 3 & -1 & 0 \\ -1 & 2 & -1 \\ 0 & -1 & 3 \end{bmatrix} \begin{bmatrix} 1/\sqrt{6} & 1/\sqrt{2} & 1/\sqrt{3} \\ 2/\sqrt{6} & 0 & -1/\sqrt{3} \\ 1/\sqrt{6} & -1/\sqrt{2} & 1/\sqrt{3} \end{bmatrix} \\ &= \begin{bmatrix} 1 & 0 & 0 \\ 0 & 3 & 0 \\ 1 & 0 & 4 \end{bmatrix} \end{aligned}$$

$$\underline{T}_{\text{EIGENVECTOR BASIS}} = \Phi^T \underline{T}_{\text{OLD BASIS}} \Phi$$

$$\underline{T}_{\text{EIGENVECTOR BASIS}} = \Lambda(\text{diagonal matrix of eigenvalues}).$$

So, any operator T is merely a 'stretching' in three directions

(that of the eigenvector) by a given amount (that of the eigenvalue).

3.4 Approximating the Single Symmetric Operator

The first objective is to approximate T in terms of a basis of an incomplete set of eigenvectors and eigenvalues. The problem may be posed as

$$\begin{array}{ccccc}
 (n \times n) & & (n \times n) & & (n \times n) \\
 T & = & T_m & + & T_r \\
 \uparrow & & \uparrow & & \uparrow \\
 \text{actual} & & \text{restriction of } T & & \text{remainder} \\
 \text{operator} & & \text{to subspace spanned} & & \\
 & & \text{by first } m \text{ eigenvectors} & &
 \end{array}$$

We know that the operators $T : \mathcal{V}_n + \mathcal{V}_n$ themselves form a vector space (which we shall denote as $\mathcal{L}(\mathcal{V}_n, \mathcal{V}_n)$) and on this space we may define an inner product as

$$\langle A, B \rangle = \text{tra } \underline{A}^T \underline{B}, \quad (\text{tra} = \text{trace})$$

and the norm will be

$$\|A\|^2 = \langle A, A \rangle = \text{tra } A^T A = \sum_{i=1}^n \sum_{j=1}^n a_{ij}^2$$

which is a Euclidean norm.

A suitable basis for this space are the n P_i operators,

where

$$\underline{P}_i = \underline{x}_i \underline{x}_i^T$$

and the \underline{x}_i are the eigenvectors of \underline{T} .

They are a suitable orthonormal basis since

$$\langle P_i, P_j \rangle = \text{tra} \{ \underline{P}_i^T \underline{P}_j \} = 0$$

and $\langle P_i, P_i \rangle = \text{tra} \{ \underline{P}_i^T \underline{P}_i \} = \text{tra} \{ \underline{x}_i \underline{x}_i^T \underline{x}_i \underline{x}_i^T \} = 1$

The \underline{P}_i are symmetric and of rank 1. They are projection matrices in the sense that

$$\underline{P}_i \underline{x}_i = \underline{x}_i$$

and $\underline{P}_i \underline{x}_j = \theta$.

Thus, the first m \underline{P}_i matrices will be a suitable basis in which to describe \underline{T}_m ,

$$\underline{T}_m = \sum_{i=1}^m \mu_i \underline{P}_i.$$

In order to extract the best approximation to the required matrix T , the norm

$$\|T - \sum_{i=1}^m \mu_i \underline{P}_i\|$$

needs to be minimised. This means finding that point in the subspace spanned by the \underline{P}_i , $i = 1, \dots, m$ which is nearest to T in the sense of the given norm.

$$\begin{aligned} \text{So } \epsilon &= \left\| T - \sum_{i=1}^m \mu_i \underline{P}_i \right\|^2 \\ &= \left\langle T - \sum_{i=1}^m \mu_i \underline{P}_i, T - \sum_{j=1}^m \mu_j \underline{P}_j \right\rangle \\ &= \langle T, T \rangle - \sum_{i=1}^m \mu_i \langle \underline{P}_i, T \rangle - \sum_{j=1}^m \mu_j \langle T, \underline{P}_j \rangle \\ &\quad + \sum_{i=1}^m \sum_{j=1}^m \mu_i \mu_j \langle \underline{P}_i, \underline{P}_j \rangle. \end{aligned}$$

To minimise, we differentiate with respect to μ_i ,

$$\frac{\partial \epsilon}{\partial \mu_i} = 0$$

$$\text{so, } \langle \underline{P}_i, T \rangle - \sum_{j=1}^m \mu_j \langle \underline{P}_i, \underline{P}_j \rangle = 0.$$

$$\langle P_i, T \rangle = \text{tra } \underline{T} \underline{x}_i \underline{x}_i^T = \text{tra } \lambda_i \underline{x}_i \underline{x}_i^T = \lambda_i$$

and
$$\sum_{j=1}^m \mu_j \langle P_i, P_j \rangle = \mu_i$$

so the best approximation to \underline{T} is obtained if

$$\mu_i = \lambda_i$$

hence
$$T = \sum_{i=1}^m \lambda_i \underline{x}_i \underline{x}_i^T.$$

If $m = n$ then we may call this the spectral expansion of \underline{T}

$$\underline{T} = \sum_{i=1}^n \lambda_i \underline{x}_i \underline{x}_i^T = \Phi \Lambda \Phi^T.$$

For the simple, illustrative example, we have

$$\underline{T} = \begin{bmatrix} 3 & -1 & 0 \\ -1 & 2 & -1 \\ 0 & -1 & 3 \end{bmatrix}$$

with eigensolutions:

$$\underline{x}_1 = (1; 1/\sqrt{6}(1, 2, 1)),$$

$$\underline{x}_2 = (3; 1/\sqrt{2}(1, 0, -1))$$

and
$$\underline{x}_3 = (4; 1/\sqrt{3}(1, -1, 1)).$$

So, the spectral solution for \underline{T} is given by

$$\underline{T} = \frac{1}{6} \begin{bmatrix} 1 & 2 & 1 \\ 2 & 4 & 2 \\ 1 & 2 & 1 \end{bmatrix} + \frac{3}{2} \begin{bmatrix} 1 & 0 & -1 \\ 0 & 0 & 0 \\ -1 & 0 & 1 \end{bmatrix} + \frac{4}{3} \begin{bmatrix} 1 & -1 & 1 \\ -1 & 1 & -1 \\ 1 & -1 & 1 \end{bmatrix}$$

Our best approximation to \underline{T} , if knowledge of the first two eigenvectors only is available, is therefore:

$$\underline{T}_m = \frac{1}{6} \begin{bmatrix} 1 & 2 & 1 \\ 2 & 4 & 2 \\ 1 & 2 & 1 \end{bmatrix} + \frac{3}{2} \begin{bmatrix} 1 & 0 & -1 \\ 0 & 0 & 0 \\ -1 & 0 & 1 \end{bmatrix} = \frac{1}{3} \begin{bmatrix} 5 & 1 & -4 \\ 1 & 2 & 1 \\ -4 & 1 & 5 \end{bmatrix}$$

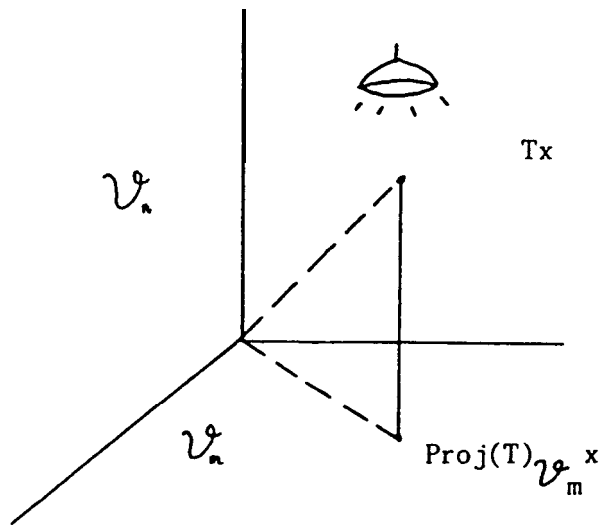
Although we have $\frac{2}{3}$ of the necessary information for the construction of \underline{T} , the form of \underline{T}_m is very different to that of \underline{T} . \underline{T}_m represents the projected solution of \underline{T} , which will, henceforth, be written as $\text{Proj}(\underline{T})_{\mathcal{V}_m}$ to make this point apparent. It is a projected solution in the sense that it only operates on vectors in the subspace into which it has been projected. All others are mapped to zero. Examples are

$$\text{Proj}(\underline{T})_{\mathcal{V}_m} \begin{bmatrix} 3 \\ 3 \\ -3 \\ 3 \end{bmatrix} = \frac{1}{3} \begin{bmatrix} 5 & 1 & -4 \\ 1 & 2 & 1 \\ 1 & 5 & 3 \end{bmatrix} \begin{bmatrix} 3 \\ 1 \\ -3 \\ 3 \end{bmatrix} = \theta$$

$$\text{Proj}(\underline{T})_{\mathcal{V}_m} \begin{bmatrix} 2 \\ 1 \\ 3 \end{bmatrix} = \frac{1}{3} \begin{bmatrix} 5 & 1 & -4 \\ 1 & 2 & 1 \\ 1 & 5 & 3 \end{bmatrix} \begin{bmatrix} 2 \\ 1 \\ 3 \end{bmatrix} = \frac{1}{3} \begin{bmatrix} -1 \\ 7 \\ 8 \end{bmatrix} = \frac{7}{6} \begin{bmatrix} 1 \\ 2 \\ 1 \end{bmatrix} - 3 \begin{bmatrix} 1 \\ 0 \\ -1 \end{bmatrix}$$

$$\underline{T} \begin{bmatrix} 1 \\ 3 \end{bmatrix} = \begin{bmatrix} 3 & -1 & 0 \\ -1 & 0 & -12 & -13 \end{bmatrix} \begin{bmatrix} 1 \\ 2 \\ 3 \end{bmatrix} = \begin{bmatrix} 5 \\ -3 \\ 8 \end{bmatrix} = \frac{7}{6} \begin{bmatrix} 1 \\ 2 \\ 1 \end{bmatrix} - 3 \begin{bmatrix} 1 \\ 0 \\ -1 \end{bmatrix} + \frac{16}{3} \begin{bmatrix} 1 \\ -1 \\ 1 \end{bmatrix}$$

So we can see that on the subspace that $\text{Proj}(\underline{T})_{\mathcal{V}_m}$ is restricted to, it operates exactly as \underline{T} . Thus $\text{Proj}(\underline{T})_{\mathcal{V}_m}$ may be considered as the shadow caused by \underline{T} by shining a light onto the subspace \mathcal{V}_m .



so $\text{Proj}(\underline{T})_{\mathcal{V}_m}$ knows nothing about $\begin{pmatrix} 1 \\ -1 \\ 1 \end{pmatrix}$.

The projection operators P_i are of key significance here. For an incomplete set of eigenvectors we may define a projection operator P with range \mathcal{V}_m as

$$P = \Phi \Phi^T = \sum_{i=1}^m \underline{x}_i \underline{x}_i^T$$

where Φ is an $(n \times m)$ incomplete matrix of eigenvectors. P has the following attractive properties:

$$\begin{aligned} P \underline{x}_i &= \underline{x}_i & i &= 1, \dots, m \\ P \underline{x}_{-i} &= \theta & i &= m+1, \dots, n. \end{aligned}$$

Another important point is that P is idempotent. That is, over the space to which it is restricted, it is equal to the identity operator, so

$$P^2 = \Phi \Phi^T \Phi \Phi^T = \Phi \Phi^T = P$$

and $P = I$ on \mathcal{V}_m .

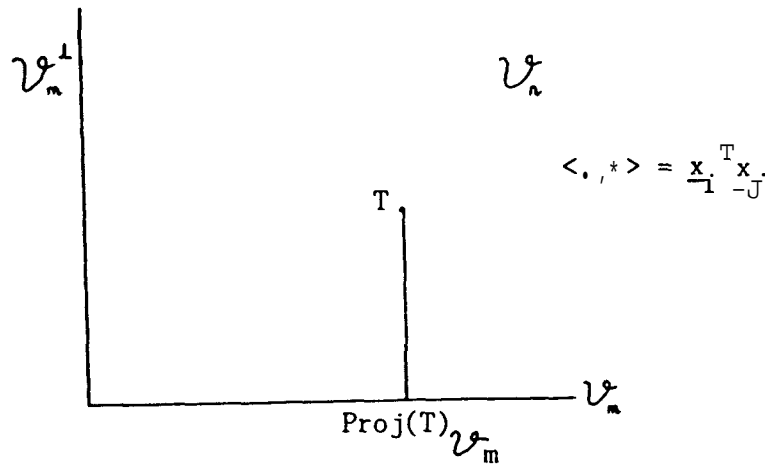
Therefore, to formulate the projected solution of \underline{T} on the subspace of known eigenvectors (m) we need to perform two operations:

- (a) Premultiply \underline{T} by P in order to ensure that images in the known **subspace** only are produced.
- (b) Postmultiply \underline{T} by P in order to ensure that it operates only on vectors in the **subspace** and maps others to zero.

We have

$$\begin{aligned} \text{Proj}(\underline{T})_{\mathcal{V}_m} &= P \underline{T} P \\ &= \Phi \Phi^T \underline{T} \Phi \Phi^T \\ &= \Phi \Lambda \Phi^T = \sum_{i=1}^m \lambda_i \underline{x}_i \underline{x}_i^T \end{aligned}$$

which is the same result as obtained earlier. Diagrammatically, this may be expressed as



For the simple example we may say that

$$\dim \mathcal{R}(\text{Proj}(\underline{\mathbf{T}})_{\mathcal{V}_m}) = 2 = \text{rank}(\text{Proj}(\underline{\mathbf{T}})_{\mathcal{V}_m})$$

$$\dim \mathcal{N}(\text{Proj}(\underline{\mathbf{T}})_{\mathcal{V}_m}) = 1 = \text{nullity}(\text{Proj}(\underline{\mathbf{T}})_{\mathcal{V}_m}).$$

This simple but key idea provides the tool with which to analyse the entire problem and will be the central theme in nearly all the subsequent analysis.

3.5 The Approximation and Its Uses

The analysis so far has described how, if only a limited number of the eigensolutions of $\underline{\mathbf{T}}$ are available, the matrix can be approximated in terms of these solutions. The resultant matrix is singular and is a projected solution of the true matrix $\underline{\mathbf{T}}$. We may, if we wish, want to compare the projected matrix with an analytical matrix, $\underline{\mathbf{T}}_a$. However, it would be foolhardy to engage in a direct comparison since $\text{Proj}(\underline{\mathbf{T}})_{\mathcal{V}_m}$ and $\underline{\mathbf{T}}_a$ operate on different spaces

(\mathcal{V}_m and \mathcal{V}_n respectively). A more definitive error analysis would be obtained if $\text{Proj}(\underline{T})\mathcal{V}_m$ were compared with $\text{Proj}(\underline{T}_a)\mathcal{V}_m$, where \underline{T}_a had been projected onto the same subspace as T . An identical procedure for projection is involved,

$$\begin{aligned}\text{Proj}(\underline{T}_a)\mathcal{V}_m &= P\underline{T}_aP \\ &= \phi\phi^T\underline{T}_a\phi\phi^T\end{aligned}$$

so that

$$\begin{aligned}\epsilon &= \text{Proj}(\underline{T})\mathcal{V}_m - \text{Proj}(\underline{T}_a)\mathcal{V}_m \\ &= \phi(\Lambda - \phi^T\underline{T}_a\phi)\phi^T\end{aligned}$$

For example, if \underline{T}_a is given by

$$\underline{T}_a = \begin{bmatrix} 3 & -1 & 0 \\ -1 & 2 & -1 \\ 0 & -1 & 8 \end{bmatrix} \left(\text{recalling that } \underline{T} = \begin{bmatrix} 3 & -1 & 0 \\ -1 & 2 & -1 \\ 0 & -1 & 3 \end{bmatrix} \right)$$

$$\begin{aligned}\text{then } \phi\phi^T\underline{T}_a\phi\phi^T &= \frac{1}{9} \begin{bmatrix} 2 & 1 & -1 \\ 1 & 2 & 1 \\ -1 & 1 & 2 \end{bmatrix} \begin{bmatrix} 3 & -1 & 0 \\ -1 & 2 & -1 \\ 0 & -1 & 8 \end{bmatrix} \begin{bmatrix} 2 & 1 & -1 \\ 1 & 2 & 1 \\ -1 & 1 & 2 \end{bmatrix} \\ &= \frac{1}{9} \begin{bmatrix} 20 & -2 & -22 \\ -2 & 11 & 13 \\ -22 & 13 & 35 \end{bmatrix}\end{aligned}$$

so that

$$\epsilon = \frac{1}{9} \begin{bmatrix} -5 & 5 & 10 \\ 5 & -5 & -10 \\ 10 & -10 & -20 \end{bmatrix} = \frac{5}{9} \begin{bmatrix} -1 & 1 & 2 \\ 1 & -1 & -2 \\ 2 & -2 & 4 \end{bmatrix}.$$

The bottom right-hand corner indicates the largest error which, with a comparison of \underline{T}_a and \underline{T} , may be seen to be the case.

Alternatively, \underline{T}_a may be projected onto the orthogonal complement space and then **directly added** on to $\text{Proj}(\underline{T})\underline{y}_m$. Since this projection would operate entirely in the orthogonal complement space, its addition to the projected solution will not affect its properties. The appropriate operator here is given by

$$(I - \Phi\Phi^T) = (I - P)$$

so that

$$(I - P)\underline{x}_i = \underline{x}_i - \underline{x}_i = 0 \quad i = 1, \dots, m$$

$$\text{and } (I - P)\underline{x}_i = \underline{x}_i \quad i = m+1, \dots, n.$$

We have

$$\begin{aligned} \text{Proj}(\underline{T}_a)\underline{y}_m^\perp &= (I - P)\underline{T}_a(I - P) \\ &= (I - \Phi\Phi^T)\underline{T}_a(I - \Phi\Phi^T) \\ &= \Phi\Phi^T\underline{T}_a\Phi\Phi^T + \underline{T}_a - \underline{T}_a\Phi\Phi^T - \Phi\Phi^T\underline{T}_a. \end{aligned}$$

For the example,

$$\begin{aligned} \text{Proj}(\underline{T}_a)\underline{y}_m^\perp &= \frac{1}{9} \begin{bmatrix} -1 & 1 & -1 \\ 1 & -1 & 1 \\ -1 & 1 & -1 \end{bmatrix} \begin{bmatrix} 3 & -1 & 0 \\ -1 & 2 & -1 \\ 0 & -1 & 8 \end{bmatrix} \\ &= \frac{1}{9} \begin{bmatrix} 17 & -17 & 17 \\ -17 & 17 & -17 \\ 17 & -17 & 17 \end{bmatrix} \end{aligned}$$

So the 'hybrid' solution, \underline{T}^H , is given by

$$\begin{aligned} \underline{T}^H &= P \left[\text{Proj}(\underline{T})\underline{y}_m \oplus \text{Proj}(\underline{T}_a)\underline{y}_m^\perp \right] \\ &= \frac{1}{9} \left(\begin{bmatrix} 15 & 3 & -12 \\ 3 & 6 & 3 \\ -12 & 3 & 15 \end{bmatrix} + \begin{bmatrix} 17 & -17 & 17 \\ -17 & 17 & -17 \\ 17 & -17 & 17 \end{bmatrix} \right) \end{aligned}$$

$$= \frac{1}{9} \begin{vmatrix} 32 & -14 & 5 \\ -14 & 23 & -14 \\ 5 & -14 & 32 \end{vmatrix} = \begin{vmatrix} 3.56 & -1.56 & 0.561 \\ -1.56 & 2.56 & -1.56 \\ 0.56 & -1.56 & 3.561 \end{vmatrix}$$

which would be considered the best **approximation to \underline{T}** , given the information available. We observe

$$(a) \quad \underline{T}^H(1,2,1) = (1,2,1)$$

$$(b) \quad \underline{T}^H(1,0,-1) = 3(1,0,-1)$$

$$(c) \quad \underline{T}^H(1,-1,1) = \frac{17}{3}(1,-1,1)$$

$$(d) \quad \underline{T}_a(1,-1,1) = \frac{5}{6}(1,2,1) - \frac{5}{2}(1,0,-1) + \frac{17}{3}(1,-1,1)$$

verifying that the restriction of \underline{T}^H to \mathcal{V}_m^\perp behaves as \underline{T}_a .

3.6 The Unsymmetric Operator

The analysis so far has pertained to the inner product space $(\mathcal{V}_n, \langle \cdot, \cdot \rangle)$ where the inner product has been defined as

$$\langle \underline{x}_i, \underline{x}_j \rangle = \underline{x}_i^T \underline{x}_j = \sum_{i=1}^n \xi_i \bar{\eta}_i$$

where the ξ_i 's and the η_i 's are the elements of \underline{x}_i and \underline{x}_j respectively. If we now wish to extend the analysis to consider the unsymmetric case (with a direct analogy to the damped problem) we have

$$(\lambda_i I - \underline{T}) \underline{x}^i = \theta$$

where \underline{T} is now $(n \times n)$ and not symmetrical. We will need to use, instead of an inner product on \mathcal{V}_n , the linear functional on the primal space \mathcal{V}_n and its algebraic dual \mathcal{V}_n^* . In order to clarify the situation we require some new definitions:

Definition 9

A linear transformation ℓ from a vector space \mathcal{V} into the vector space of real (or complex) scalars is said to be a linear functional on \mathcal{V} .

We also need to define a suitable basis for this linear functional.

Definition 10

Let $\{x^1, \dots, x^n\}$ be a basis for \mathcal{V}_n and let y_j be the linear functional on \mathcal{V}_n , defined by $y_j(x^i) = \delta_j^i$, $j = 1, \dots, n$, then $\{y_1, \dots, y_n\}$ is a basis for \mathcal{V}_n^* ; it is called the dual basis of $\{x^i\}$.

The new basis defines the algebraic dual of \mathcal{V}_n , denoted by \mathcal{V}_n^* , which is isomorphic to \mathcal{V}_n . That is, they are both finite-dimensional of dimension n and isomorphic to (indistinguishable from) the space of complex numbers \mathbb{C}_n .

The value of the linear functional is usually represented by

$$\begin{aligned} y_j(x^i) &= [y_j, x^i] = [x^i, y_j] \\ &= \sum_{r=1}^n \xi_i^r \eta_i^r \end{aligned}$$

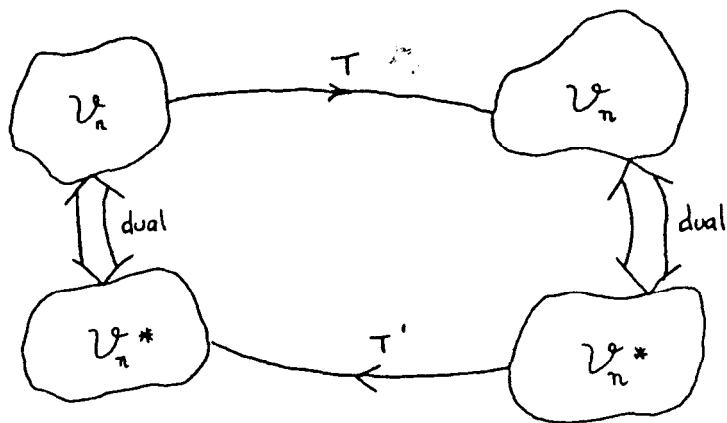
There is no complex conjugate here, as for the inner product. We have

$$T : \mathcal{V}_n \rightarrow \mathcal{V}_n$$

$$T' : \mathcal{V}_n^* \rightarrow \mathcal{V}_n^* \text{ (see diagram overleaf)}$$

where \mathcal{V}_n^* denotes the dual space for T and T' is the dual of T .

If T has a matrix representation \underline{T} relative to a basis in \mathcal{V}_n then



T' has a matrix representation \underline{T}' relative to the dual basis in \mathcal{V}_n^* . So, in general for the damped problem, the analysis requires the use of two basis sets, one for each of the isomorphic spaces \mathcal{V}_n and \mathcal{V}_n^* .

For the ensuing analysis we assume that the eigenvalues for T are distinct and the problem is diagonalisable (which generally reflects the case for light damping). We have

$$(\lambda_i I - T)x^i = \theta \quad i = 1, \dots, n$$

$$\text{and } (\lambda_i I - T')y_j = \theta \quad j = 1, \dots, n$$

so that

$$[x^i, y_j] = \delta_j^i$$

if the eigenvalues are suitably normalised, and

$$[Tx^i, y_j] = [x^i, T'y_j] = \lambda_i \delta_j^i.$$

So a vector $z \in \mathcal{V}_n = \mathcal{V}_n^*$ can be written as

$$z = \sum_{i=1}^n \alpha_i x^i$$

or as

$$z = \sum_{i=1}^n \beta^i y_i.$$

In the same manner as before, we may now introduce projection matrices

$$P_i = x^i y_i^T$$

so that

$$P_i x^i = x^i,$$

$$P_i x^j = \theta,$$

$$P_i^2 = P_i$$

and $P_i P_j = \theta.$

Also $P_i^T = y_i x^{iT}$

so that

$$P_i^T y_i = y_i,$$

$$P_i^T y_j = \theta,$$

$$(P_i^T)^2 = P_i^T$$

and $P_i^T P_j^T = \theta.$

We may also say that

$$\sum_{i=1}^m P_i$$

is a projection of \mathcal{V}_n onto \mathcal{V}_m along \mathcal{V}_m^\perp , where \mathcal{V}_m is the subspace of \mathcal{V}_n spanned by the first m eigenvectors $[x_i]$, $i = 1, \dots, m$.

We have no inner product here so the concept of orthogonality is extended to **normed** spaces with the symbol \perp representing an annihilator, as in Reference (60).

It is plain to see that

$$\sum_{i=1}^n \underline{P}_i = \sum_{i=1}^n \underline{P}_i^T = \underline{I}.$$

If we let

$$\underline{P}_{ij} = \underline{x}^i \underline{y}_j^T$$

then $\underline{P}_{ij}^2 = 0$ unless $i = j$

$$\begin{aligned} \text{and } \underline{P}_{ij} \underline{P}_{jk} &= 0 & j \neq k \\ &= \underline{P}_i & j = k \end{aligned}$$

and $\underline{P}_{ii} = \underline{P}_i$

as above.

The \underline{P}_{ij} are n^2 independent basis vectors for the space $\mathcal{L}(\mathcal{V}_n, \mathcal{V}_n)$ and hence we may write

$$\underline{T} = \sum_{i=1}^n \sum_{j=1}^n \alpha_{ij} \underline{P}_{ij} = \sum_{i=1}^n \sum_{j=1}^n \alpha_{ij} \underline{x}^i \underline{y}_j^T$$

whence

$$\begin{aligned} [y_\ell, T x^k] &= \text{if, } \sum_{j=1}^n \alpha_{ij} (y_\ell^T (\underline{x}^i \underline{y}_j^T \underline{x}^k)) \\ &= \sum_{i=1}^n \alpha_{ik} (y_\ell^T \underline{x}^i) = \alpha_{\ell k} \end{aligned}$$

$$\text{but } [y_\ell, T x^k] = \lambda_k \delta_\ell^k$$

$$\text{hence } \alpha_{\ell k} = \lambda_k \delta_\ell^k.$$

$$\text{So } \underline{T} = \sum_{i=1}^n \lambda_i \underline{P}_i$$

which is analogous to the result obtained for the symmetric case.

Again, we may consider this as the spectral expansion of \underline{T} .

If we let

$$P = \sum_{i=1}^m \underline{x}^i \underline{y}_i^T$$
$$= \Phi \Pi^T$$

we have

$$\text{Proj}(\underline{T}) \underline{v}_n = P \underline{T} P$$
$$= \Phi \Pi^T \underline{T} \Phi \Pi^T$$
$$= \Phi \Lambda \Pi^T$$

$$\text{with } \mathcal{R}(\text{Proj}(\underline{T}) \underline{v}_n) = [x^i] \quad i = 1, \dots, m$$
$$\mathcal{N}(\text{Proj}(\underline{T}) \underline{v}_n) = [x^i] \quad i = m+1, \dots, n.$$

Having thus established an analogous framework with which to analyse the damped or unsymmetric problem, error and hybrid matrices may then be calculated in a similar fashion to that of the symmetric problem.

3.7 Overview

The analysis has demonstrated that matrices are merely representations of more fundamental objects called linear transformations. A linear transformation may take on several matrix disguises depending on the basis (axis system) in which we choose to describe it. Since, for the following analysis the basis implied is usually the standard \mathbf{e}_i basis $\{(1,0,\dots,0), (0,1,\dots,0), \dots, (0,0,\dots,1)\}$ the formal distinction between the operator and its representation with respect to this basis will be omitted. If the analysis moves to an eigenvector basis, the operator will usually be described by a diagonal matrix (namely I or A).

A foundation on which further analysis may be constructed has now been provided. It has been shown that pre- and post-multiplication by certain idempotent matrices can force a matrix to exhibit predetermined range and null spaces. As a result, projected solutions are readily formulated. This enables a restricted version of a given matrix to be established. The stage has now been set to derive mass and stiffness matrices which are restricted to the sub-space spanned by the measured modes. These 'incomplete' measured matrices will represent the best possible approximation to the true matrices with the information available.

As indicated in this chapter, these matrices have the potential uses of determination of errors or improvement of existing mathematical models. The analysis has been built up from the consideration of the single symmetric operator and then an outline of how this may be extended to the single unsymmetric operator has been detailed. The analysis of the next chapter is that of the double symmetric operator problem or the undamped problem, and then, in Chapter 5, the double unsymmetric operator problem or the damped problem is dealt with which, by that stage, is no more than a natural extension of the work that has gone before.

THE UNDAMPED PROBLEM4.1 Preliminaries

Having now established a mathematical framework in which further analysis can be conducted, it is possible to consider the undamped eigenvalue problem

$$(\lambda_i M - K)x_i = 0$$

or $M\Phi\Lambda = K\Phi.$

In this case, we know that M and K are diagonalisable and we assume isolated roots. Before commencing further analysis, it is worth restating the problem in terms of what information is available and what is sought. From the experimental measurements, which are assumed to have been made correctly, there is a set of measured data consisting of an $(n \times m)$ unnormalised modal matrix Φ of measured modes and an $(m \times m)$ matrix of natural frequencies Λ . From the theoretical analysis, there are assumed to exist finite-element mass and stiffness matrices M_a and K_a . Using these, the analytical eigenvalues and eigenvectors have been calculated, Λ_a, Φ_a , and these correspond to the theoretical natural frequencies and mode shapes of the system. The objective of the experimental work will have been to show that the mathematical model is accurate and acceptable. If the measurements agree with those predicted by the model then it is reasonable to assume that the model is accurate, is a good representation of the structure and may be used for further analysis. The contents of this chapter address themselves to the course of action necessary if there is disagreement between the two.

In essence, two questions arise which are related, and which will both be considered in this chapter. They are:

1. Is it possible to determine error matrices which show where the **error** in the mathematical modelling has occurred?
2. What are the correct mass and stiffness matrices?

The first, and most important decision to make is what inner product to select. Although any inner product may be used, there are, in reality, no more than five with a realistic case for selection. These are:

| | Inner Product | Normalisation |
|---|---|--|
| 1 | $\langle \dots \rangle_M = x_i^T M x_j$ | $x_i^T M x_i = 1$ |
| 2 | $\langle \dots \rangle_K = x_i^T K x_j$ | $x_i^T K x_i = \lambda_i$ (measured) |
| 3 | $\langle \dots \rangle_I = x_i^T x_j$ | $x_i^T x_i = 1$ |
| 4 | $\langle \dots \rangle_{M_a} = x_i^T M_a x_j$ | $x_i^T M_a x_i = 1$ |
| 5 | $\langle \dots \rangle_{K_a} = x_i^T K_a x_j$ | $x_i^T K_a x_i = \lambda_i$ (measured) |

1 and 2 are clearly the correct or best choice since the measured modes will then be mutually orthogonal

i.e. $x_i^T M x_j = 0$

and $x_i^T K x_j = 0$.

The problem here is that M and K, the correct mass and stiffness matrices are, in general, unknown and so any results obtained using these, which have M and K in their solution, will be of little or no use since they cannot be computed. 3 has little to recommend it, other than the fact that it was the one used in the

single matrix case. The modes will not be orthogonal to one another if this inner product is chosen.

The most appropriate choice of inner product is most commonly 4, since it is generally thought that the analytical mass matrix is a better approximation than the analytical stiffness matrix. 5 may be used if no rigid body modes are present. If they are, the stiffness matrix will not be positive-definite and an inner product axiom would be violated if they were included in the analysis. No other type of inner product is generally considered. In all the ensuing analysis, the inner product will be stated at the beginning of the derivation.

4.2 Inverse Mass and Stiffness Expressions

Two initial results may first be derived; that is, expressions for the inverses of the mass and stiffness matrices. Since these results do not explicitly contain M and K, the correct inner product can be used to derive the expressions

$$\text{inner product (in } \mathcal{L}(\mathcal{V}_n, \mathcal{V}_n)) = \langle A, B \rangle_M = \text{tra } A^T M B.$$

So the norm will be

$$\langle A, A \rangle_M = \text{tra } A^T M A = \|A\|_M^2.$$

An approximation for the inverse of the mass matrix may now be determined in terms of the matrix dyads Q_i , where

$$Q_i = \mathbf{x}_i \mathbf{x}_i^T.$$

The following norm is minimised with respect to the coordinates ψ_i ,

$$\epsilon = \|M^{-1} - \sum_{i=1}^m \psi_i Q_i\|_M^2$$

$$\begin{aligned}
&= \langle M^{-1} - \sum_{i=1}^m \psi_i Q_i, M^{-1} - \sum_{j=1}^m \psi_j Q_j \rangle_M \\
&= \langle M^{-1}, M^{-1} \rangle_M - \sum_{i=1}^m \psi_i \langle Q_i, M^{-1} \rangle_M - \sum_{j=1}^m \psi_j \langle M^{-1}, Q_j \rangle_M \\
&\quad + \sum_{i=1}^m \sum_{j=1}^m \psi_i \psi_j \langle Q_i, Q_j \rangle_M.
\end{aligned}$$

Differentiating with respect to ψ_i gives

$$\sum_{j=1}^m \psi_j \langle Q_i, Q_j \rangle_M - \langle Q_i, M^{-1} \rangle_M = 0.$$

But $\langle Q_i, M^{-1} \rangle_M = \text{tra } Q_i M M^{-1} = \text{tra } Q_i = \|x_i\|^2$

where $\|x_i\|^2 = x_i^T x_i$ (no mass matrix)

and $\langle Q_i, Q_j \rangle = 0 \quad i \neq j$

thus $\langle Q_i, Q_i \rangle_M = \text{tra } Q_i^T M Q_i = \text{tra } Q_i = \|x_i\|^2$

giving $\psi_i = \frac{\|x_i\|^2}{\|x_i\|^2} = 1$

so that

$$M_B^{-1} \text{ (approximation to } M^{-1}) = \sum_{i=1}^m Q_i = \sum_{i=1}^m x_i x_i^T = \phi \phi^T.$$

Similarly, minimising for the flexibility matrix K^{-1} ,

$$\begin{aligned}
\varepsilon &= \|K^{-1} - \sum_{i=1}^m \xi_i Q_i\|_M^2 \\
&= \langle K^{-1} - \sum_{i=1}^m \xi_i Q_i, K^{-1} - \sum_{j=1}^m \xi_j Q_j \rangle_M \\
&= \langle K^{-1}, K^{-1} \rangle_M - \sum_{i=1}^m \xi_i \langle Q_i, K^{-1} \rangle_M - \sum_{j=1}^m \xi_j \langle K^{-1}, Q_j \rangle_M \\
&\quad + \sum_{i=1}^m \sum_{j=1}^m \xi_i \xi_j \langle Q_i, Q_j \rangle_M.
\end{aligned}$$

Differentiating with respect to ξ_i ,

$$\sum_{j=1}^m \xi_j \langle Q_i, Q_j \rangle_M - \langle Q_i, K^{-1} \rangle_M = 0,$$

so $\langle Q_i, K^{-1} \rangle_M = \text{tra } Q_i^T M K^{-1} = \text{tra } K^{-1} M Q_i = \frac{\|x_i\|^2}{\lambda_i},$

and $\xi_i = \frac{\|x_i\|^2}{\lambda_i \|x_i\|^2} = \frac{1}{\lambda_i}$

So $K_B^{-1} = \sum_{i=1}^m \frac{1}{\lambda_i} Q_i = \phi \Lambda^{-1} \phi^T.$

Effectively what has been accomplished is the approximation of M^{-1} and K^{-1} in terms of the measured modes and natural frequencies.

The resulting approximations are restricted to the space spanned by the vectors $M\phi$ and, in effect, represent projected solutions

$$M_B^{-1} = \phi \phi^T \quad K_B^{-1} = \phi \Lambda^{-1} \phi^T$$

where $\mathcal{R}(M_B^{-1}) = \mathcal{R}(K_B^{-1}) = [x_i] \quad i = 1, \dots, m$

$$\mathcal{N}(M_B^{-1}) = \mathcal{N}(K_B^{-1}) = [Mx_i] \quad i = m+1, \dots, n.$$

We can rederive these expressions thinking of them as projections.

If we decompose \mathcal{V}_n so that

$$\mathcal{V}_n = \mathcal{U} + \mathcal{W} \quad \text{where } \mathcal{U} = [x_i] \quad i = 1, \dots, m$$

$$\text{and } \mathcal{W} = [x_i] \quad i = m+1, \dots, n,$$

then here \mathcal{U} and \mathcal{W} are not orthogonal with respect to $\langle \dots \rangle_M$.

If we introduce, with respect to the inner product $\langle \dots \rangle_M$, the projection operator

$$P_M = \phi \phi^T$$

we may note that P_M is not an orthogonal projection (since $P_M \neq P_M^T$).

PM is the projection onto \mathcal{U} along \mathcal{W} and $P_M^T (= M\Phi\Phi^T)$ is the projection onto \mathcal{W}^\perp along \mathcal{U}^\perp where \perp denotes orthogonality with respect to $\langle \dots \rangle_M$.

So P_M : projection onto $[x_i]$ along $[x_i]$
 $i=1 \dots m$ $i=m+1 \dots n$

and P_M^T : projection onto $[Mx_i]$ along $[Mx_i]$
 $i=1 \dots m$ $i=m+1 \dots n$

Thus $\mathcal{R}(P_M) = [x_i]$; $\mathcal{N}(P_M) = [x_i]$
 $i=1 \dots m$ $i=m+1 \dots n$

and $\mathcal{R}(P_M^T) = [Mx_i]$; $\mathcal{N}(P_M^T) = [Mx_i]$
 $i=1 \dots m$ $i=m+1 \dots n$

We also need to note that

$$(P_M)^2 = (P_M^T)^2 = I$$

or that the projection operators are idempotent. If we consider the inverse mass matrix, M^{-1} , we see that it operates on the vectors Mx_i , $i = 1, \dots, n$ to produce the vectors x_i , $i = 1, \dots, n$. A projected solution would need to operate only on the vectors Mx_i , $i = 1, \dots, m$ to produce the vectors x_i , $i = 1, \dots, m$. Thus

$$\mathcal{R}(\text{Proj}(M^{-1})) = [x_i] \quad i = 1, \dots, m$$

$$\mathcal{N}(\text{Proj}(M^{-1})) = [Mx_i] \quad i = m+1, \dots, n.$$

This is ensured by a premultiplication by P_M and a post-multiplication by P_M^T . The resulting solution is an orthogonal decomposition of \mathcal{V}_n with respect to $\langle \dots \rangle_M$. Thus,

$$\begin{aligned} \text{Proj}_M(M^{-1})\mathcal{V}_m &= \text{projection of } M^{-1} \text{ using mass inner product} \\ &\quad \text{onto space spanned by experimental modes} \\ &\quad (\Phi) \text{ along its orthogonal complement} \\ &= P_M M^{-1} P_M^T \end{aligned}$$

$$= \Phi \Phi^T M M^{-1} M \Phi \Phi^T$$

$$= \Phi \Phi^T$$

$$\begin{aligned} \text{and } \text{Proj}_M(K^{-1}) \mathcal{V}_m &= P_M K^{-1} P_M^T \\ &= \Phi \Phi^T M K^{-1} M \Phi \Phi^T \\ &= \Phi \Lambda^{-1} \Phi^T \end{aligned}$$

so the same results are obtained by a projection onto the relevant subspaces.

4.3 Projection of Measured Matrices

The expressions for the projected inverse mass and stiffness matrices have been successfully derived, but are of little use to us. The projected solutions for the mass and stiffness matrices themselves are now sought since clearly the complete matrices cannot be derived from a set of incomplete data. Again we wish the projected solutions to behave as the complete operator on the subspace onto which it has been projected. Thus they will need to have

- (a) range space given by $[Mx_i]$ $i = 1, \dots, m;$
- (b) null space given by $[x_i]$ $i = m+1, \dots, n.$

In order to facilitate this, a post-multiplication by P_M and a pre-multiplication by P_M^T are required. The projected solution for each of the five inner products under consideration will now be derived.

- (a) Inner product $\langle \dots \rangle_M$
normalisation $x_i^T M x_i = 1$

$$P_M = \Phi \Phi^T M.$$

Therefore

$$\begin{aligned} \text{Proj}_M(M) \mathcal{V}_m &= P_M^T M P_M \\ &= M \Phi \Phi^T M \Phi \Phi^T M \\ &= M \Phi \Phi^T M \end{aligned}$$

and

$$\begin{aligned} \text{Proj}_M(K) \mathcal{V}_m &= P_M^T K P_M \\ &= M \Phi \Phi^T K \Phi \Phi^T M \\ &= M \Phi \Lambda \Phi^T M. \end{aligned}$$

(b) Inner product $\langle \dots \rangle_K$

$$\text{normalisation } x_i^T K x_i = \lambda_i$$

$$P_K = \Phi \Lambda^{-1} \Phi^T K$$

Therefore

$$\begin{aligned} \text{Proj}_K(M) \mathcal{V}_m &= P_K^T M P_K \\ &= K \Phi \Lambda^{-1} \Phi^T M \Phi \Lambda^{-1} \Phi^T K \\ &= K \Phi \Lambda^{-2} \Phi^T K \end{aligned}$$

and

$$\begin{aligned} \text{Proj}_K(K) \mathcal{V}_m &= P_K^T K P_K \\ &= K \Phi \Lambda^{-1} \Phi^T K \Phi \Lambda^{-1} \Phi^T K \\ &= K \Phi \Lambda^{-1} \Phi^T K. \end{aligned}$$

The projected solutions using either $\langle \dots \rangle_M$ or $\langle \dots \rangle_K$ satisfy the orthogonality conditions and the eigenvalue equation. However, the problems here are obvious. In order to find a projected solution, the complete matrix needs to be known (either mass or stiffness). Clearly the use of these inner products is inappropriate.

The object was to demonstrate this and outline the method for other projected solutions.

(c) Inner product $\langle \cdot, \cdot \rangle_I$

$$\text{normalisation } x_i^T x_i = 1$$

If we consider PM we observe that its full form is given as

$$PM = \phi(\phi^T M \phi)^{-1} \phi^T M$$

As we are free to choose the inner product we may replace M by any suitable matrix. If we use the identity matrix, I, we have

$$PI = \phi(\phi^T \phi)^{-1} \phi^T$$

so that

$$\begin{aligned} \text{Proj}_I(M) \mathcal{V}_m &= P_I^T M P_I \\ &= \phi(\phi^T \phi)^{-1} \phi^T M \phi(\phi^T \phi)^{-1} \phi^T \\ &= \phi(\phi^T \phi)^{-2} \phi^T \end{aligned}$$

$$\begin{aligned} \text{and } \text{Proj}_I(K) \mathcal{V}_m &= P_I^T K P_I \\ &= \phi(\phi^T \phi)^{-1} \phi^T K \phi(\phi^T \phi)^{-1} \phi^T \\ &= \phi(\phi^T \phi)^{-1} \Lambda (\phi^T \phi)^{-1} \phi^T. \end{aligned}$$

Again, these expressions satisfy the orthogonality and eigenvalue equation conditions and may be thought of as generalised inverses for M^{-1} and $K^{-1(94)}$. However, the use of $\langle \cdot, \cdot \rangle_I$ here is inappropriate and the matrices so generated would not represent any recognisable mass or stiffness distribution. Inner products which use either the analytical mass or stiffness are most appropriate since we hope that these would reflect the true mass and stiffnesses reasonably closely.

(d) Inner product $\langle \dots \rangle_{M_a}$

$$\text{normalisation } x_i^T M_a x_i = 1$$

$$P_{M_a} = \phi^T m^{-1} \phi^T M_a \text{ where } m^{-1} = (\phi^T M_a \phi)^{-1}$$

$$\begin{aligned} \text{so } \text{Proj}_{M_a}(M) \mathcal{V}_m &= P_{M_a}^T M P_{M_a} \\ &= M_a \phi m^{-1} \phi^T M \phi m^{-1} \phi^T M_a \\ &= M_a \phi m^{-2} \phi^T M_a \end{aligned}$$

$$\begin{aligned} \text{and } \text{Proj}_{M_a}(K) \mathcal{V}_m &= P_{M_a}^T K P_{M_a} \\ &= M_a \phi m^{-1} \phi^T K \phi m^{-1} \phi^T M_a \\ &= M_a \phi m^{-1} \Lambda m^{-1} \phi^T M_a \end{aligned}$$

and finally, for the fifth inner product:

(e) Inner product $\langle \dots \rangle_{K_a}$

$$\text{normalisation } x_i^T K_a x_i = \lambda_1$$

We need to note here that K_a may not be positive definite if rigid body modes are present, thus the argument here needs to be restricted to flexible modes

$$P_{K_a} = \phi^T k^{-1} \phi^T K_a \text{ where } k = \phi^T K_a \phi$$

$$\begin{aligned} \text{so } \text{Proj}_{K_a}(M) \mathcal{V}_m &= P_{K_a}^T M P_{K_a} \\ &= K_a \phi k^{-1} \phi^T M \phi k^{-1} \phi^T K_a \\ &= K_a \phi k^{-2} \phi^T K_a \end{aligned}$$

$$\begin{aligned}
\text{and } \text{Proj}_{K_a}(K)_{\mathcal{V}_m} &= P_{K_a}^T K P_{K_a} \\
&= K_a \Phi_k^{-1} \Phi^T K \Phi_k^{-1} \Phi^T K_a \\
&= K_a \Phi_k^{-1} \Lambda_k^{-1} \Phi^T K_a .
\end{aligned}$$

Thus, five incomplete expressions for measured mass and stiffness matrices have been presented, all of which are restricted to a **subspace** of \mathcal{V}_n defined by the choice of inner product.

In order to make comparisons, for error analysis of these projected matrices, the analytical matrices need to be projected into the appropriate subspaces as well. Since the use of inner products 1, 2 and 3 are, in most circumstances, impossible or inappropriate, the arguments henceforth will be limited to the $\langle \dots \rangle_{M_a}$ and $\langle \dots \rangle_{K_a}$ choices.

4.4 Projection of Analytical Matrices

A simple comparison of the projected matrices generated in the last section with K_a or M_a cannot really be justified as a correct measure of error since $\text{Proj}(M)_{\mathcal{V}_m}$ and $\text{Proj}(K)_{\mathcal{V}_m}$ are restricted to \mathcal{V}_m only, whereas K_a and M_a operate on the whole of the space \mathcal{V}_n . A more reasonable comparison would be with the projections of K_a and M_a onto the same subspace, i.e. the **subspace determined** by the measured modes. Thus the two error matrices for the two inner products still under examination may be formulated as:

Inner product $\langle \dots \rangle_{M_a}$

$$P_{M_a} = \Phi_m^{-1} \Phi^T M_a$$

So $\text{Proj}_{M_a}(M_a)\mathcal{V}_m$ = Projection of M_a using analytical mass inner product onto subspace spanned by the experimental modes

$$= P_{M_a}^T M_a P_{M_a}$$

$$= M_a \phi_m^{-1} \Phi^T M_a \phi_m^{-1} \Phi^T M_a$$

giving $\epsilon_{\text{MASS}}^1 = \text{Proj}_{M_a}(M)\mathcal{V}_m - \text{Proj}_{M_a}(M_a)\mathcal{V}_m$

$$= M_a \phi_m^{-1} (I - m) m^{-1} \Phi^T M_a$$

and $\text{Proj}_{M_a}(K_a)\mathcal{V}_m = P_{M_a}^T K_a P_{M_a}$

$$= M_a \phi_m^{-1} \Phi^T K_a \phi_m^{-1} \Phi^T M_a$$

giving $\epsilon_{\text{STIFFNESS}}^1 = \text{Proj}_{M_a}(K)\mathcal{V}_m - \text{Proj}_{M_a}(K_a)\mathcal{V}_m$

$$= M_a \phi_m^{-1} (\Lambda \Phi^T K_a \Phi) m^{-1} \Phi^T M_a$$

Inner product $\langle \dots \rangle_{K_a}$

$$P_{K_a} = \Phi k^{-1} \Phi^T K_a$$

So $\text{Proj}_{K_a}(M_a)\mathcal{V}_m = P_{K_a}^T M_a P_{K_a}$

$$= K_a \Phi k^{-1} \Phi^T M_a \Phi k^{-1} \Phi^T K_a$$

giving $\epsilon_{\text{MASS}}^2 = \text{Proj}_{K_a}(M)\mathcal{V}_m - \text{Proj}_{K_a}(M_a)\mathcal{V}_m$

$$= K_a \Phi k^{-1} (I - \Phi^T M_a \Phi) k^{-1} \Phi^T K_a$$

and $\text{Proj}_{K_a}(K_a)\mathcal{V}_m = P_{K_a}^T K_a P_{K_a}$

$$= K_a \Phi k^{-1} \Phi^T K_a \Phi k^{-1} \Phi^T K_a$$

$$= K_a \Phi k^{-1} \Phi^T K_a$$

$$\begin{aligned} \text{giving } \epsilon_{\text{STIFFNESS}}^2 &= \text{Proj}_{K_a}(K) \mathcal{V}_m - \text{Proj}_{K_a}(K_a) \mathcal{V}_m \\ &= K_a \phi k^{-1} (\Lambda - k) k^{-1} \phi^T K_a \end{aligned}$$

A study of how some of these errors are built up, in the form of 3-D matrix surfaces, as more and more modes are added is shown in Figures 4.1 and 4.2. The example used is that of the cantilever (example 1) described in Chapter 2. Figures 4.3 and 4.4 attempt to give a geometrical view of what is happening and which errors are being measured.

As an alternative approach, but perhaps with less fundamental justification, error matrices may be formulated by projecting the analytical matrices onto the corresponding analytical space determined by the vectors ϕ_a, \mathcal{V}_m^A , where each of the x_{ai} corresponds to a measured mode x_i . Since the two basis sets will not span exactly the same space they will only be approximately comparable. To avoid unnecessary repetition, only the mass error matrix using the analytical mass inner product and the stiffness error matrix using the analytical stiffness inner product will be derived using this idea.

Inner product $\langle \dots \rangle_{M_a}$

normalisation $x_{ai}^T M_a x_{ai} = 1$

$$P_{M_a}' = \phi_a \phi_a^T M_a$$

$$\begin{aligned} \text{So, } \text{Proj}_{M_a}(M_a) \mathcal{V}_m^A &= M_a \phi_a \phi_a^T M_a \phi_a \phi_a^T M_a \\ &= M_a \phi_a \phi_a^T M_a \end{aligned}$$

$$\begin{aligned} \text{giving } \epsilon_{\text{MASS}}^3 &= \text{Proj}_{M_a}^{(M)} \mathcal{V}_m - \text{Proj}_{M_a}^{(M_a)} \mathcal{V}_m^A \\ &= M_a \phi_m^{-2} \phi_a^T M_a - M_a \phi_a \phi_a^T M_a \end{aligned}$$

Inner product $\langle \dots \rangle_{K_a}$

$$\text{normalisation } x_{ai}^T K_a x_{ai} = \lambda_{ai}$$

$$P'_{K_a} = \phi_a \Lambda_a^{-1} \phi_a^T K_a$$

$$\begin{aligned} \text{so } \text{Proj}_{K_a}^{(K_a)} \mathcal{V}_m^A &= K_a \phi_a \Lambda_a^{-1} \phi_a^T K_a \phi_a \Lambda_a^{-1} \phi_a^T K_a \\ &= K_a \phi_a \Lambda_a^{-1} \phi_a^T K_a \end{aligned}$$

$$\begin{aligned} \text{giving } \epsilon_{\text{STIFFNESS}}^4 &= \text{Proj}_{K_a}^{(K)} \mathcal{V}_m - \text{Proj}_{K_a}^{(K_a)} \mathcal{V}_m^A \\ &= K_a (\phi_k^{-1} \Lambda_k^{-1} \phi_k^T - \phi_a \Lambda_a^{-1} \phi_a^T) K_a \end{aligned}$$

Sidhu and Ewins⁽⁹¹⁾, using a different approach, propose expressions of this kind, but use an additional approximation. Their analysis proceeds as follows:

$$E = K - K_a$$

$$K^{-1} = (I + K_a^{-1} E)^{-1} K_a^{-1}$$

$$K^{-1} = K_a^{-1} - K_a^{-1} E K_a^{-1} + (K_a^{-1} E)^2 K_a^{-1} \dots$$

$$= K_a^{-1} - K_a^{-1} E K_a^{-1} + O(\epsilon^2) \text{ where } \epsilon = (K_a^{-1} E).$$

So, ignoring the small error term, they have,

$$\phi_a \Lambda_a^{-1} \phi_a^T = K_a^{-1} - K_a^{-1} (K - K_a) K_a^{-1}$$

$$K_a \phi_a \Lambda_a^{-1} \phi_a^T K_a = K_a - K + K_a$$

which is equivalent to

$$\begin{aligned}\Phi^T K_a \Phi \Lambda^{-1} \Phi^T K_a \Phi &= 2\Phi^T K_a \Phi - A \\ k\Lambda^{-1}k &= 2k - A\end{aligned}$$

or $k\Lambda^{-1} + \Lambda k^{-1} = 2I.$

This implies that the approximation used by Ewins and Sidhu is that $k = A$, and similarly for the mass representation the approximation is $m = I$. Hence the error expressions proposed by them are

$$\begin{aligned}\epsilon_{\text{MASS}}^5 &= M_a (\Phi\Phi^T - \Phi_a \Phi_a^T) M_a \\ \epsilon_{\text{STIFFNESS}}^6 &= K_a (\Phi\Lambda^{-1}\Phi^T - \Phi_a A_a^{-1}\Phi_a^T) K_a\end{aligned}$$

ϵ_{MASS}^5 and $\epsilon_{\text{STIFFNESS}}^6$ are shown in Figures 4.5 and 4.6. For geometrical interpretation the diagram of Figures 4.7 and 4.8 attempts to describe exactly what the situation is. A full table of all possible results is given in Table 4.1. As explained previously, the motivation for the derivation of $\epsilon(M^{-1})$ and $\epsilon(K^{-1})$ is limited, although the results are easily established. This is because these properties exhibit global changes as a result of a change in mass or stiffness, so the error matrices produced will not provide any useful information.

Having conducted a fairly comprehensive survey of possible error matrix expressions using a few of the tools of vector space theory, a critical examination of how much useful information may be extracted from them is postponed until later in the chapter. Before that, the second objective in Section 4.1 is now studied,

4.5 Improvement/Correction of Mass and Stiffness

The expressions for mass and stiffness derived in Section 4.3 represent experimentally derived matrices. We have seen that

if there are to be no unknowns in these expressions then the analysis needs to be conducted in an inner product space other than those defined by M and K, since these are, to all intents and purposes, unknown. The fact that analytical matrices M_a and K_a pop up in expressions for experimental matrices need not concern us too greatly. This is inevitable because of the choice of inner product. Emphasis has been placed on inner product choice, and this needs to be clearly established and defined prior to any analysis.

All the matrices produced for mass and stiffness to date satisfy the conditions of orthogonality and the eigenvalue equation. For example, the mass and stiffness matrices produced using perhaps the most preferable inner product $\langle \cdot, \cdot \rangle_{M_a}$ are

$$\left. \begin{aligned} \text{Proj}_{M_a}(M) \mathcal{V}_m &= M_a \phi_m^{-2} \phi^T M_a \\ \text{Proj}_{M_a}(K) \mathcal{V}_m &= M_a \phi_m^{-1} \Lambda_m^{-1} \phi^T M_a \end{aligned} \right\} m = \phi^T M_a \phi$$

and $\phi^T \text{Proj}_{M_a}(M) \mathcal{V}_m \phi = \phi^T M_a \phi_m^{-2} \phi^T M_a \phi = I$

$$\phi^T \text{Proj}_{M_a}(K) \mathcal{V}_m \phi = \phi^T M_a \phi_m^{-1} \Lambda_m^{-1} \phi^T M_a \phi = A$$

$$\begin{aligned} \text{Proj}_{M_a}(M) \mathcal{V}_m \phi \Lambda &= M_a \phi_m^{-2} \phi^T M_a \phi \Lambda = M_a \phi_m^{-1} \Lambda \\ &= \text{Proj}_{M_a}(K) \mathcal{V}_m \phi \end{aligned}$$

In spite of these extremely encouraging properties, the mass and stiffness matrices will still give cause for concern. They look nothing like the true mass and stiffness distributions. This is an unfortunate fact, due to the fact that they are projected

solutions. We know, and indeed with all the measuring equipment available in the world can only ever hope to know, an incomplete knowledge of a finite representation of mass and stiffness using measurements on a continuous structure. As will be expanded upon in Section 4.6, there is no way we can ever 'measure' all the modes of a finite degree-of-freedom representation without moving beyond the bounds of feasibility.

We have seen that, for an objective comparison with analytical matrices, we need to project the analytical mass and stiffness into some comparable subspace. However, in order to formulate our best approximation of the true, but unknown, stiffness and mass matrices our formulations should operate on the entire space \mathcal{V}_n under consideration instead of just the subspace \mathcal{V}_m spanned by the measured modes. Then the question arises of exactly how we are to do this with an incomplete set of measurements. As a result of the fact that we have no 'measured' information with which to complete the solution, it would seem reasonable to assert that, in the absence of any information to the contrary, we should assume that our analytical matrices, which operate on the whole space, may be 'added on' to our incomplete matrices so as to extend the operators from \mathcal{V}_m to \mathcal{V}_n . This will then produce hybrid matrices consisting of a measured matrix over the space for which we have information \mathcal{V}_m , and an analytical matrix over the space for which we have no information \mathcal{V}_m^\perp (the orthogonal complement of \mathcal{V}_m). All that remains for us to do is to perform the necessary calculations in order to formulate these matrices. M_a and K_a will clearly have to be projected onto the orthogonal complement space in order to facilitate a direct vector space addition. Again, only the two

most appropriate inner products will be considered.

$$\text{Inner product } \langle \dots \rangle_{M_a}$$

Orthogonal Complement Projection Operator = I - Original Projection Operator

$$= I - P$$

where P : projection onto $[x_i]$ along $[x_i]$

$$i=1 \dots m \quad i=m+1 \dots n$$

and I - P : projection onto $[x_i]$ along $[x_i]$

$$i=m+1 \dots n \quad i=1 \dots m$$

Now $\text{Proj}_{M_a}(M_a) \psi_m^\perp$ = Projection of M_a using analytical mass inner product onto orthogonal complement of subspace determined by experimental modes

$$= (I - P_{M_a})^T M_a (I - P_{M_a})$$

$$= (I - M_a \phi_m^{-1} \phi^T) M_a (I - \phi_m^{-1} \phi^T M_a)$$

$$= M_a + M_a \phi_m^{-1} \phi^T M_a \phi_m^{-1} \phi^T M_a - 2 M_a \phi_m^{-1} \phi^T M_a$$

$$= M_a - M_a \phi_m^{-1} \phi^T M_a$$

$M_a = M_a \phi_m^{-1} \phi^T M_a$

So the hybrid for the mass matrix becomes

$$M_{M_a}^H = \text{Proj}_{M_a}(M) \psi_m \oplus \text{Proj}_{M_a}(M_a) \psi_m^\perp$$

$$= M_a \phi_m^{-2} \phi^T M_a + M_a - M_a \phi_m^{-1} \phi^T M_a$$

$$= M_a + M_a \phi_m^{-1} (I - \phi_m) \phi^T M_a$$

also $\text{Proj}_{M_a}(K_a) \psi_m = (I - P_{M_a})^T K_a (I - P_{M_a})$

$$= (I - M_a \phi_m^{-1} \phi^T) K_a (I - \phi_m^{-1} \phi^T M_a)$$

$$= K_a + M_a \phi_m^{-1} \phi^T K_a \phi_m^{-1} \phi^T M_a - M_a \phi_m^{-1} \phi^T K_a$$

$$- K_a \phi_m^{-1} \phi^T M_a$$

and so

$$K_{M_a}^H = \text{Proj}_{M_a}^{(K)} \mathcal{V}_m \oplus \text{Proj}_{M_a}^{(K_a)} \mathcal{V}_m^\perp$$

$$= M_a \phi_m^{-1} \Lambda m^{-1} \phi^T M_a + K_a + M_a \phi_m^{-1} \phi^T K_a \phi_m^{-1} \phi^T M_a - M_a \phi_m^{-1} \phi^T K_a$$

$$- K_a \phi_m^{-1} \phi^T M_a$$

$$= K_a + M_a \phi_m^{-1} (\Lambda + \phi^T K_a \phi)_m^{-1} \phi^T M_a - M_a \phi_m^{-1} \phi^T K_a - K_a \phi_m^{-1} \phi^T M_a$$

These are expressions similar to those derived by Berman and others, by different methods^(15,24,107).

There is no logical reason why the mass matrix hybrid should be formulated before the stiffness matrix. Now M_a is cropping up for two reasons:

- (a) because all calculations are done in the inner product space defined by M_a ;
- (b) because the projection of M_a onto the orthogonal complement space is being used to complete the incomplete measured matrix.

K_a exists for the second reason only. If we wish, we can eliminate the occurrence of the Gram matrix, m , in the expression for $K_{M_a}^H$ by using M_a^H :

$$M_a^H \phi = M_a \phi + M_a \phi_m^{-2} \phi^T M_a \phi - M_a \phi_m^{-1} \phi^T M_a \phi$$

$$= M_a \phi_m^{-1}$$

and $\phi^T M_a^H = m^{-1} \phi^T M_a$

Using this, we may write $K M_a^H$ as

$$K M_a^H = M_a^H \phi (\Lambda + \phi^T K_a \phi) \phi^{-1} M_a^H - M_a^H \phi \phi^T K_a - K_a \phi \phi^T M_a^H.$$

Since the incomplete measured matrices have only been added to in the orthogonal complement space, the necessary orthogonality and eigenvalue equation conditions are bound to have been unaffected. There can be no 'coupling' between the two spaces.

The whole procedure may be repeated for the other inner product:

Inner product $\langle \dots \rangle_{K_a}$

$$\begin{aligned} \text{so } \text{Proj}_{K_a}(M_a) \mathcal{V}_m^\perp &= (I - P_{K_a})^T M_a (I - P_{K_a}) \\ &= (I - K_a \phi k^{-1} \phi^T) M_a (I - \phi k^{-1} \phi^T K_a) \\ &= M_a + K_a \phi k^{-1} \phi^T M_a \phi k^{-1} \phi^T K_a - K_a \phi k^{-1} \phi^T M_a \\ &\quad - M_a \phi k^{-1} \phi^T K_a, \end{aligned}$$

The hybrid matrix under this inner product is

$$\begin{aligned} M_{K_a}^H &= \text{Proj}_{K_a}(M) \mathcal{V}_m \oplus \text{Proj}_{K_a}(M_a) \mathcal{V}_m^\perp \\ &= K_a \phi k^{-2} \phi^T K_a + M_a + K_a \phi k^{-1} \phi^T M_a \phi k^{-1} \phi^T K_a - K_a \phi k^{-1} \phi^T M_a \\ &\quad - M_a \phi k^{-1} \phi^T K_a \\ &= M_a + K_a \phi k^{-1} (I + \phi^T M_a \phi) k^{-1} \phi^T K_a - K_a \phi k^{-1} \phi^T M_a \\ &\quad - M_a \phi k^{-1} \phi^T K_a \end{aligned}$$

$$\text{also, } \text{Proj}_{K_a}(K_a) \mathcal{V}_m^\perp = (I - K_a \phi k^{-1} \phi^T) K_a (I - \phi k^{-1} \phi^T K_a)$$

$$\begin{aligned}
&= K_a + K_a \phi k^{-1} \phi^T K_a \phi k^{-1} \phi^T K_a - 2 K_a \phi k^{-1} \phi^T K_a \\
&= K_a - K_a \phi k^{-1} \phi^T K_a
\end{aligned}$$

$$\begin{aligned}
\text{and so } K_{K_a}^H &= \text{Proj}_{K_a} (K) \mathcal{L}_m \oplus \text{Proj}_{K_a} (K_a) \mathcal{L}_m \\
&= K_a \phi k^{-1} \Lambda k^{-1} \phi^T K_a + K_a - K_a \phi k^{-1} \phi^T K_a \\
&= K_a + K_a \phi k^{-1} (\Lambda - k) k^{-1} \phi^T K_a
\end{aligned}$$

These expressions correspond to those proposed by Baruch⁽⁹⁾ but obtained by a different method.

Again, if desired, the expressions may be made more attractive by replacing $K_a k^{-1}$ by $K_{K_a}^H$ in the $M_{K_a}^H$ expression thus:

$$M_{K_a}^H = M_a + K_{K_a}^H \phi (I + \phi^T M_a \phi) \phi^T K_{K_a}^H - K_{M_a}^H \phi \phi^T M_a - M_a \phi \phi^T K_{K_a}^H.$$

(See Table 4.2 for a summary of hybrid matrices.)

Clearly the concept of orthogonal projections within a predetermined inner product space provides us with sufficient tools with which to build a complete analysis. There is nothing to stop a further analysis using a different inner product and projecting onto different subspaces. However, all the results occurring in the literature to date have appeared within this simple framework.

Geometrical diagrams of what is going on are given in Figures 4.9 and 4.10. We now go on to consider how each projection is related to the problem as a whole to give some idea of exactly how much may be expected from the error analysis and exactly how close the $M_{M_a}^H$, $M_{K_a}^H$, $K_{M_a}^H$ and $K_{K_a}^H$ matrices will be to the true objectives, M and K . This may be done by consideration of the continuous example and the underlying principles and approximations of

the FE method.

4.6 The Continuous Structure

The error matrices derived in Section 4.4 and summarised in Table 4.1 provide a good framework with which to attempt to identify the errors that may arise in finite-element modelling, as will be indicated by experimentation on the structure itself. Some insight into how much information one may expect to extract from these expressions may be sought. This can only be obtained by examining the fundamentals of the finite-element method itself, which is the purpose of this section. The language of vector spaces will be retained, but now we deal with a vector space \mathcal{V} whose elements are functions f defined on some physical region Γ (the structure) and for which

$$\int_{\Gamma} mf^2$$

is finite, where m is a positive function (the mass) defined on Γ ; we define an inner product on \mathcal{V} by

$$\langle f, g \rangle_M = \int_{\Gamma} mfg.$$

Figure 4.11 is designed to illustrate the following argument in terms of the familiar bending beam. Let T be a positive definite operator defined on a physical region Γ ; T possesses a denumerably infinite set of eigenfunctions f_k and eigenvalues μ_k which are solutions of

$$Tf - \mu mf = 0$$

together with a consistent set of boundary conditions.

The eigenfunctions are an orthonormal basis for \mathcal{V} and hence

for any $g \in \mathcal{V}$ we can write

$$g = \sum_{k=1}^{\infty} \langle g, f_k \rangle_M f_k$$

usually referred to as the Fourier series for g relative to $\{f_k\}$.

A finite element analysis begins by replacing the operator equation $Tf - \mu f = 0$ by its weak form

$$B_a(f, g) - \mu \langle f, g \rangle_{M_a} = 0 \quad \forall g \in \mathcal{V}$$

where $B_a(f, g)$ is a bilinear symmetric functional usually obtained from

$$\int_{\Gamma} g T f$$

by an integration by parts and incorporation of the natural boundary conditions. The displacement field f is then approximated by a finite linear combination of local interpolation functions n_i , $i = 1, \dots, n$. These are functions which vanish over most of Γ and are smooth enough for $B_a(n_i, n_j)$ to exist. The n_i are not the so-called shape functions of the FE method, but the functions obtained as a result of combining a group of shape functions over contiguous elements; in the usual implementation of the finite element method the n_i are the functions obtained after assembly and the imposition of the essential boundary conditions.

The k th eigenfunction f_k is then approximated by the function

$$a^k f_k = \sum_{i=1}^n a^{x_{ki}} n_i$$

where the $a^{x_{ki}}$ are the entries of the vector a^k satisfying

$$(K_a - \lambda_k M_a) a^k = 0:$$

λ_k is an upper bound for μ_k . The stiffness matrix K_a has elements

$$k_{k\ell} = B_a(n_k, n_\ell)$$

and the mass matrix M_a has elements

$$m_{k\ell} = \langle n_k, n_\ell \rangle_a M.$$

The matrix K_a is, in effect, a projection of the differential operator T onto a finite dimensional space $\mathcal{V}_n \subset \mathcal{V}$ and the nature of the interpolation functions n_k tends to preserve its 'differential' properties in the sense that

- (i) $k_{k\ell} = 0$ for disjoint subregions;
- (ii) local changes in properties of the structure are locally reflected in K (this is in contrast to a flexibility matrix for the structure which is a projection of an integral operator).

The eigenfunction basis for T , on the other hand, does not preserve these properties for it consists of globally defined functions whose complexity (curvature) increases with increasing k ; a linear combination of the lower eigenfunctions may singularly fail to reflect local changes in T . The central difficulty in using measured eigenvectors to 'update' the K matrix resides in this essential difference in character between the two basis sets. The more local are the changes (errors) in the structural model, the more poorly they will be reflected in the (lower) eigenvectors.

So, the main point here concerns the **localisation** of errors. The smallest unit that the finite element method can deal with is the element itself: no detail of the changes within an element of the structure will be reflected in the k_{ij} , hence we cannot expect better discrimination than this. But as has already been pointed out, the lower global modes of the structure have a discrimination

length of many elements and it will be clear that only by including modes with a number of nodes of **the same** order as the finite-element nodes could we hope to discriminate at this level.

Reference (20) contains an analytical experiment designed to demonstrate the rate of convergence of the series for mass and stiffness matrices as more modes are included.

The result of this shows that a faster convergence of the mass matrix may be expected (of the order $1/k^n$) provided that M_a is not so inaccurate as to make the choice of $\langle \dots \rangle_{M_a}$ inappropriate. The stiffness matrix, though less sensitive to the inner product choice, exhibits much slower convergence ($1/k^2$).

If we examine the error matrices of Figures 4.1, 4.2, 4.5 and 4.6 we may see that for Figures 4.1 and 4.5 little information is extracted as to errors in the mass matrix; this is because the original analytical mass matrix is so badly in error that its use in defining an inner product is inappropriate. In the same example we can see that for the stiffness the error matrices obtained are far more encouraging. This is not because of the **fact that** the choice of K_a as an inner product is more appropriate, but because the stiffness error matrix is less sensitive to inner product selection. This is due to the fact that since the lower modes contribute more to the mass matrix than the stiffness matrix, inappropriate scaling will distort the picture more, as can be brought about by wrong inner product selection. The fact that the first few modes show negligible error values arises as a direct consequence of the argument just expounded. The modes are too smooth. The fourth and fifth **modes**, on the other hand, begin to pick up

the region in error quite nicely, since they are modes of the same order of complexity as the region in error. In all the analysis the size of the region of error detected can only be as small as the complexity of the most complex mode. So if the most complex mode is one with n nodes, only a region of error covering $1/n$ th or more of the structure can we hope to detect.

As for the 6th to 10th modes, not too much emphasis should be placed upon them, since they represent essentially artificial results. The trouble is that two 'analytical' models are being used. This does not reflect the situation likely to be encountered in practical situations. The higher eigenvectors of an analytical model have no physical significance. Any finite element model, because of its finite nature, ceases to have a direct relation with a continuous structure after, at most, 50% of the modes and natural frequencies. Although it is quite possible to neatly show the error between two mathematical models using most or all of the modes and the correct inner product $\langle \cdot, \cdot \rangle_M$, it is also pointless. It represents an ideal situation which we could never hope to achieve in practice.

It is extremely unlikely that in any realistic situation the number of measured modes (m) is going to exceed half the number of degrees of freedom of an FE model. In practice, it is likely to be much, much less.

The analysis of a simply-supported beam allows us to illustrate some of the points just described more explicitly. Using example 2, here the M_a is not so inaccurate that its use in defining the inner product space is inappropriate. Also, we know that

the analytical modes of a simply-supported beam are the simple sine functions, $\sin kx$, so we may use a finite discretisation of these for our 'measured' modes. Figure 4.12 shows

- (a) faster convergence of mass matrix;
- (b) good error detection when complexity of modes = size of error region;
- (c) rapid distortion for number of modes greater than $N/2$.

4.7 Hybrid Matrices

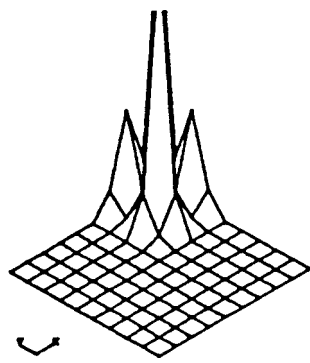
For similar reasons to those expressed in Section 4.6, one may expect the hybrid matrices in reality to look similar to the original analytical matrices M_a and K_a , and not the correct mass and stiffness - although they will perhaps be a better approximation to the true mass and stiffness than the original M_a and K_a . This is a result of the fact that the higher, more complex modes of the matrices, which dominate the 'form' or outward appearance of the matrix, are still provided by the analytical matrix. So if only a few smooth modes are measured and the M_a and K_a matrices are in error, generation of the hybrid matrices will necessarily impose fairly minimal changes upon M_a and K_a . An attempt to describe the situation diagrammatically is given in Figures 4.13 and 4.14. There comes a stage where the addition of further measured modes will no longer provide useful information about the true finite dimensional mass and stiffness, and so the problem has to be completed using M_a and K_a . These dominate the outward **appearance**. Again, clearly the most useful information is provided by modes of a complexity sufficient to describe areas where M_a and K_a are in error.

4.8 Overview

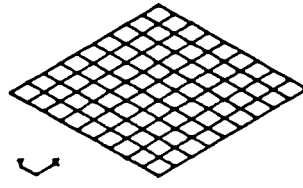
A critical study of the **undamped** eigenvalue problem within the framework of vector space theory enables a great deal of clarification for error analysis and mathematical model improvement. The following factors have emerged:

1. Inner product choice is fundamental in any analysis (with the associated normalisation).
2. M^{-1} and K^{-1} can be derived in terms of Φ and A only.
3. Measured mass and stiffness matrices are incomplete and operate only on the space determined by the measured modes.
4. Analytical matrices need to be projected into a comparable **subspace** before suitable comparisons can be formulated.
5. Hybrid matrices consisting of measured M and K over the measured space and analytical M and K over the unmeasured space may be readily formulated.
6. Error detection of the order of the most complex measured mode only can be expected.
7. Mass error exhibits fast convergence.
8. Mass error is strongly dependent on inner product choice and associated normalisation.
9. Stiffness error shows a slower rate of convergence.
10. Stiffness error is not so dependent on inner product choice.

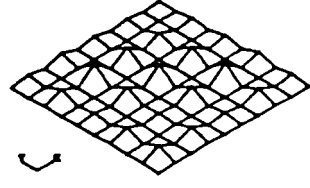
The study of Chapter 4 permits the experimental engineer to work within an organised mathematical framework so that the verification of mathematical models using experimental measurements may be conducted in a more enlightened atmosphere.



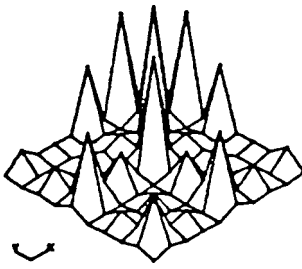
Correct



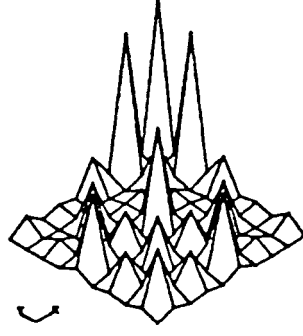
2



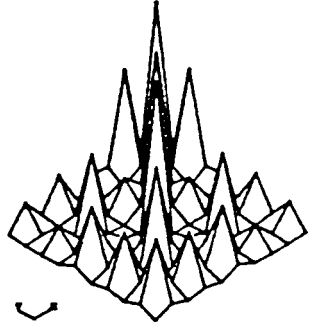
3



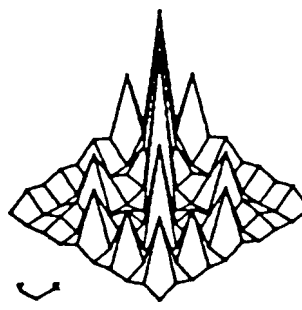
4



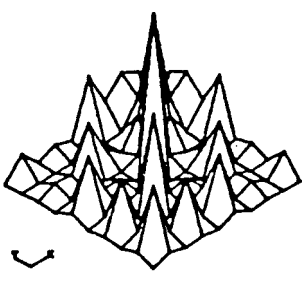
5



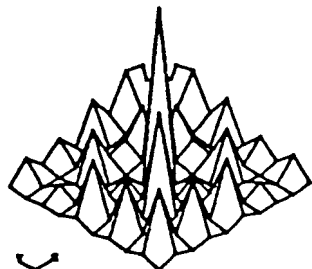
6



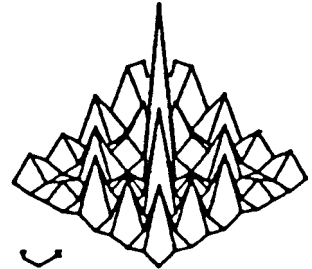
7



8



9



10

Figure 4.1: $\epsilon_{\text{Mass}}^1 = \text{Proj}_{M_a}(M)_{\mathcal{L}} - \text{Proj}_{M_a}(M_a)_{\mathcal{L}}$

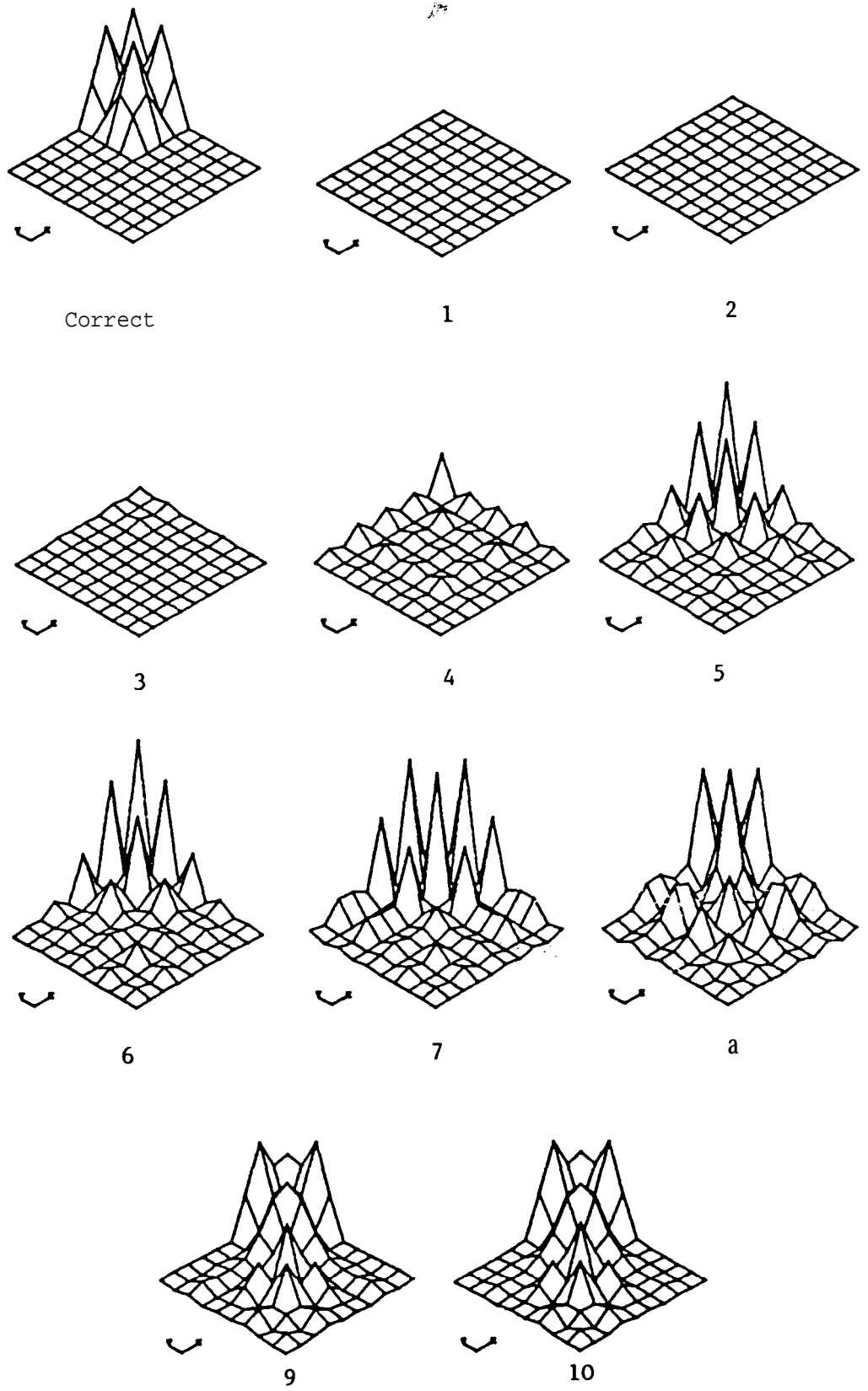


Figure 4.2: $\epsilon_{\text{Stiffness}}^{2\omega} = \text{Proj}_{K_a}(K) \psi_m - \text{Proj}_{K_a}(K_a) \psi_m$

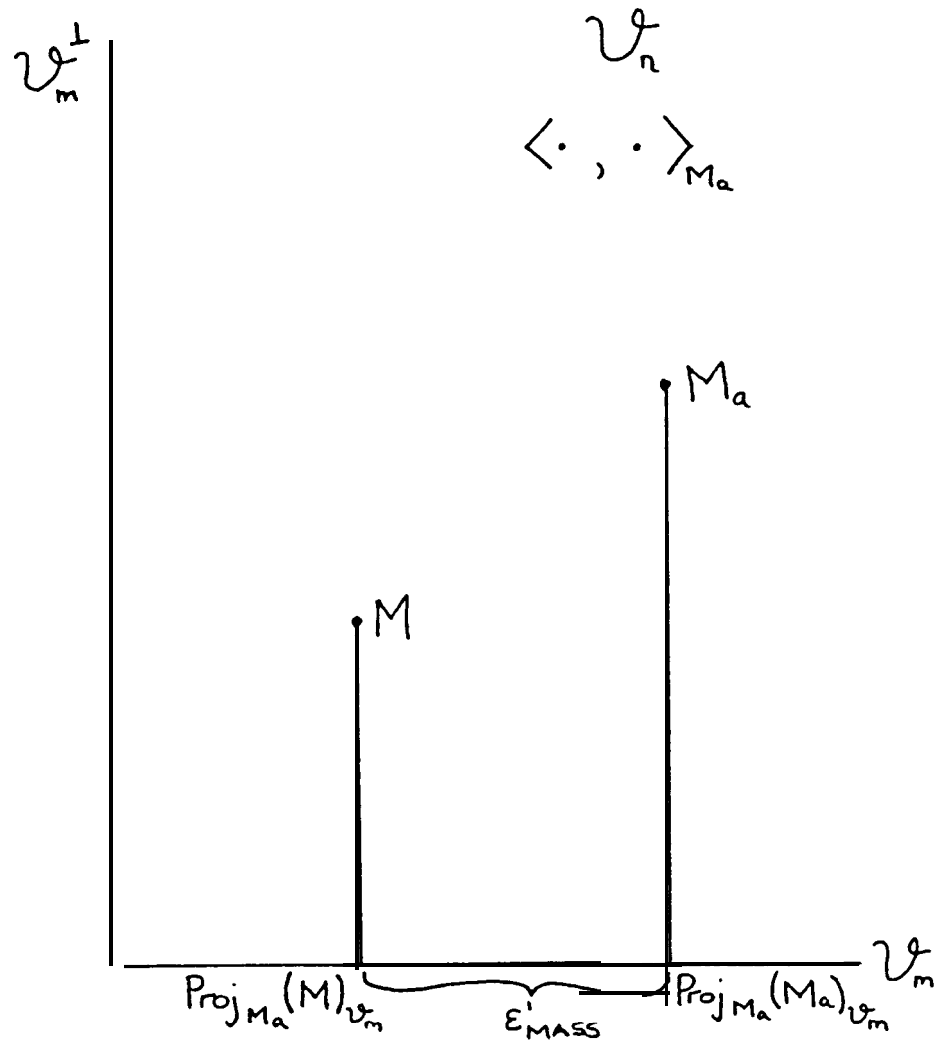


Figure 4.3: Mass Error ϵ'

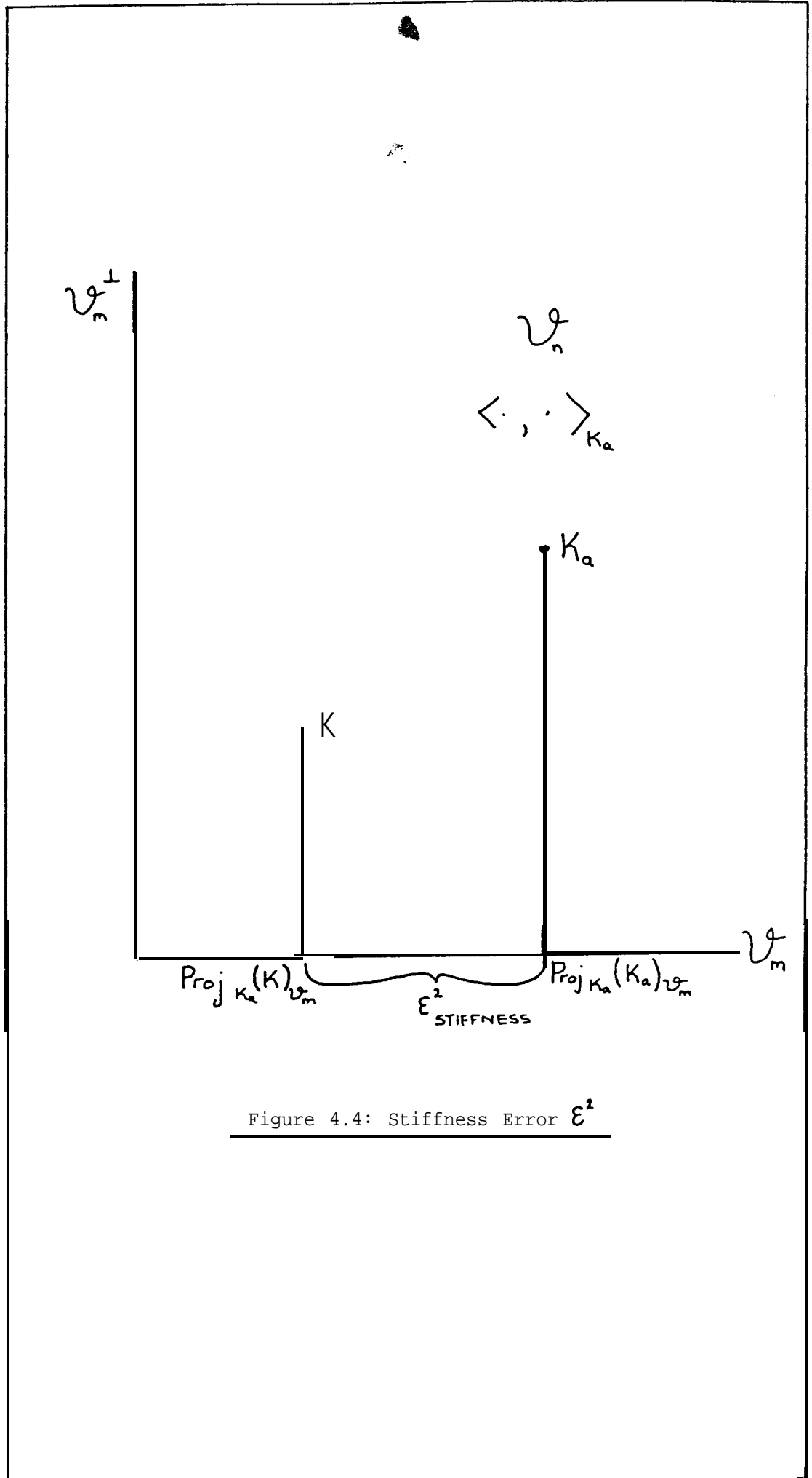


Figure 4.4: Stiffness Error ϵ^2

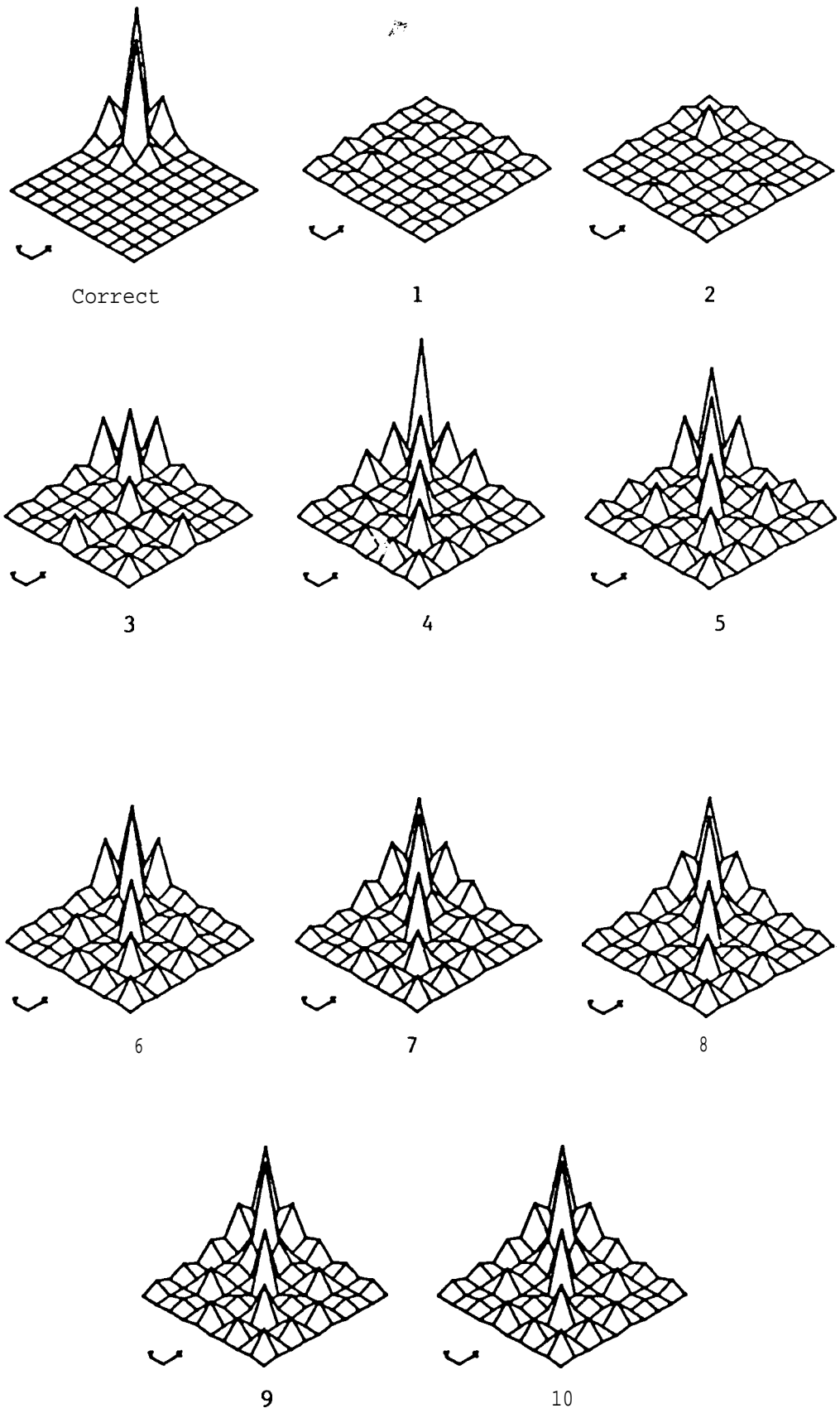


Figure 4.5: $\mathcal{E}_{\text{Mass}}^{\text{D}} = \text{Proj}_{M_4} (M) \underline{v} - \text{Proj}_{M_4} (M_e) \underline{v}^A$

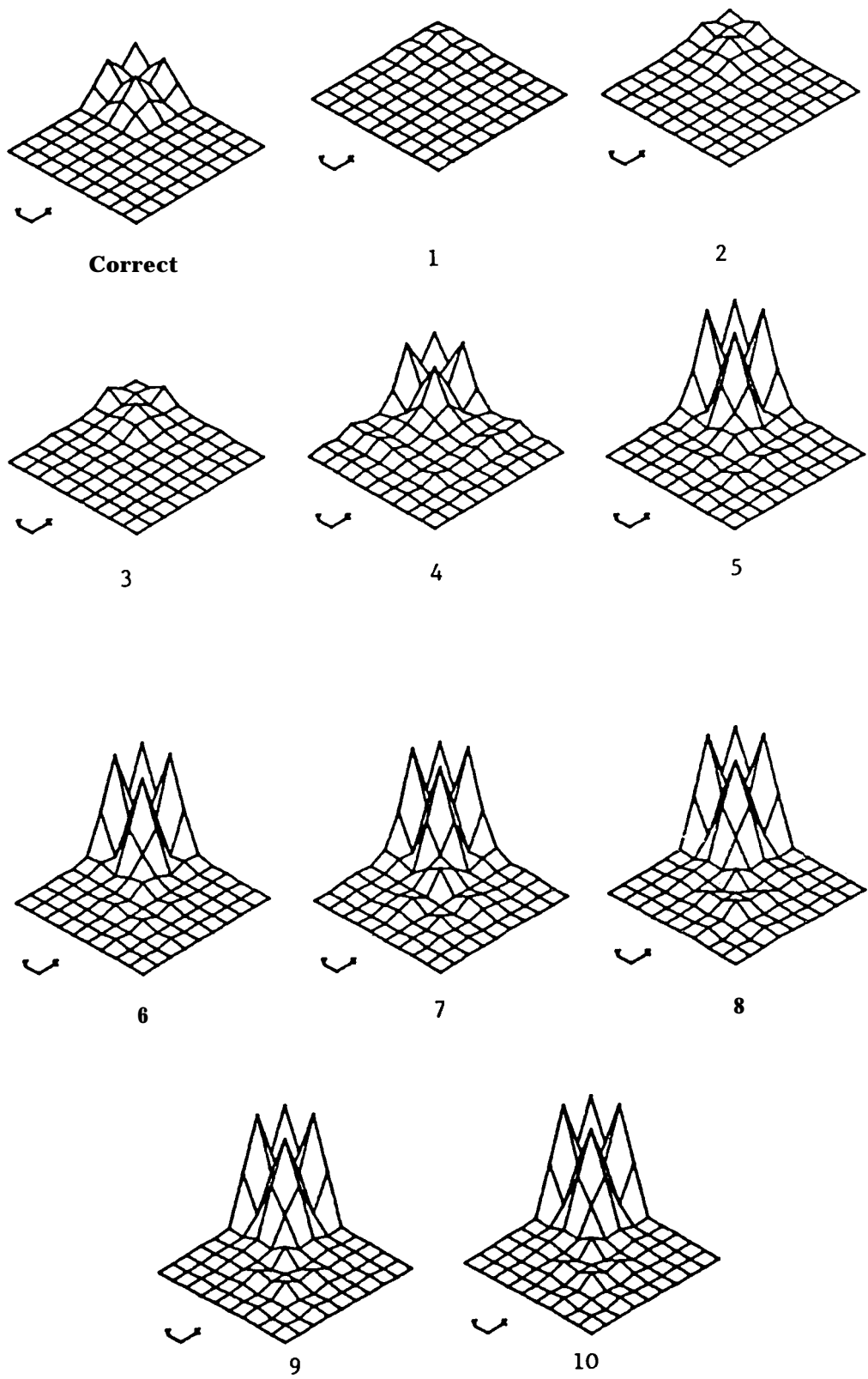


Figure 4.6: $\hat{\epsilon}_{\text{Stiffness}}^{\beta} = \text{Proj}_{K_a}(K)_{\mathcal{U}_m} - \text{Proj}_{K_a}(K_a)_{\mathcal{U}_m}$

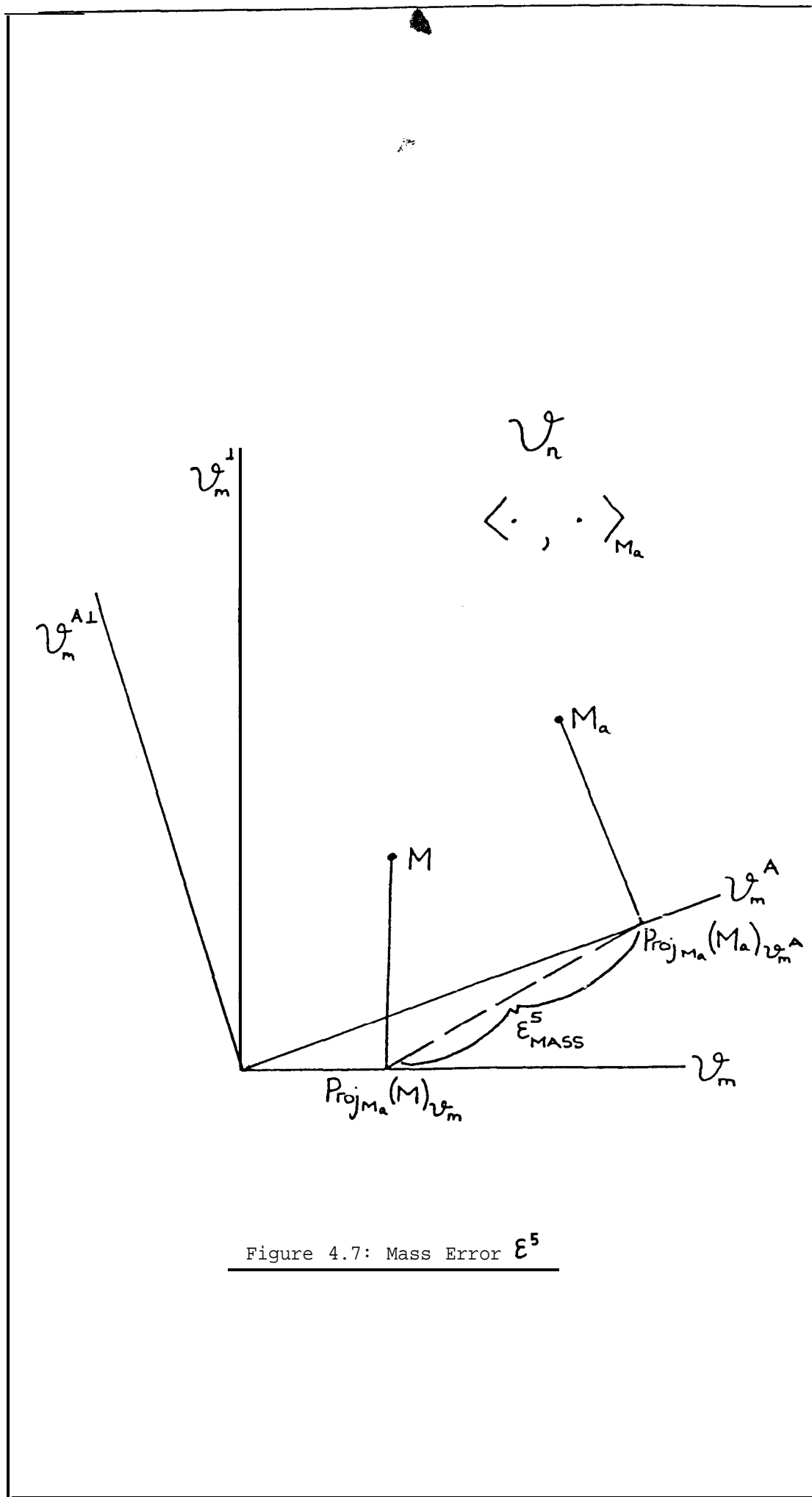


Figure 4.7: Mass Error ϵ^5

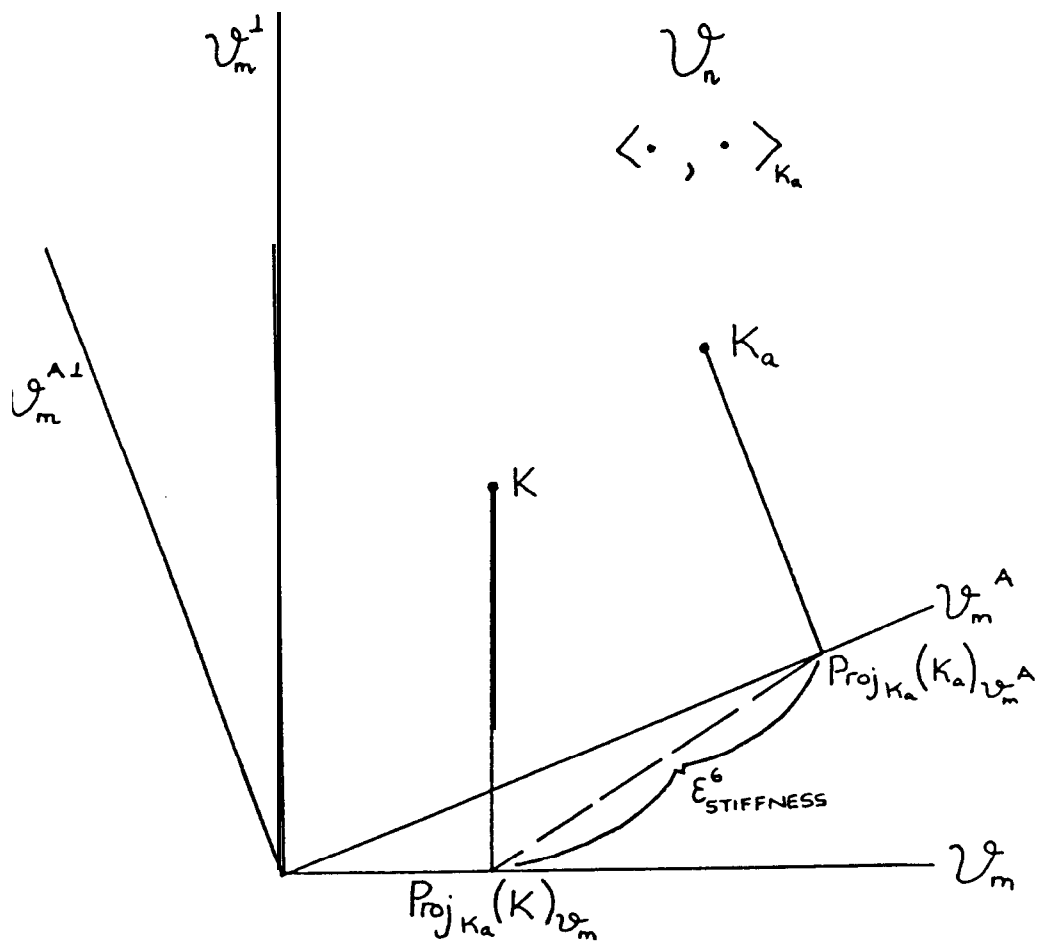


Figure 4.8: Stiffness Error ϵ^6

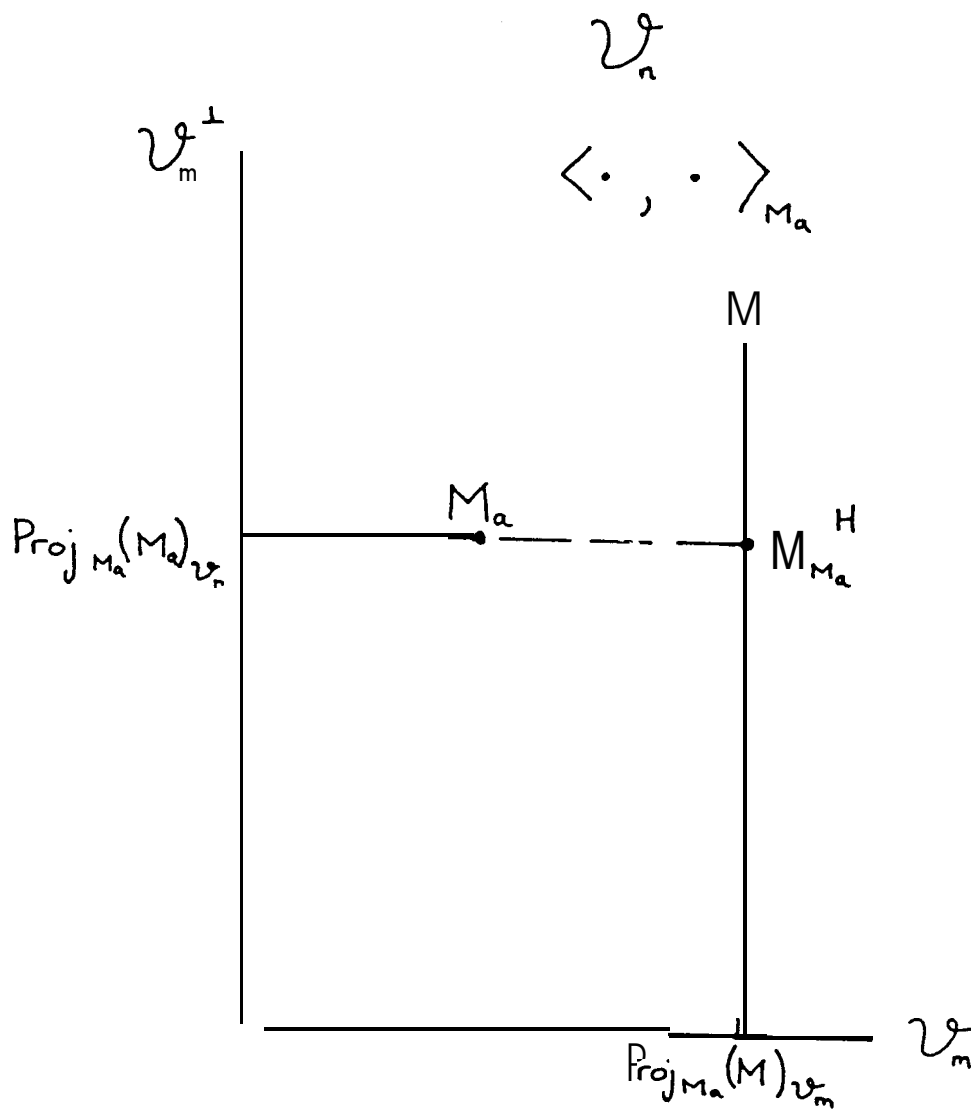


Figure 4.9: Mass Matrix Hybrid

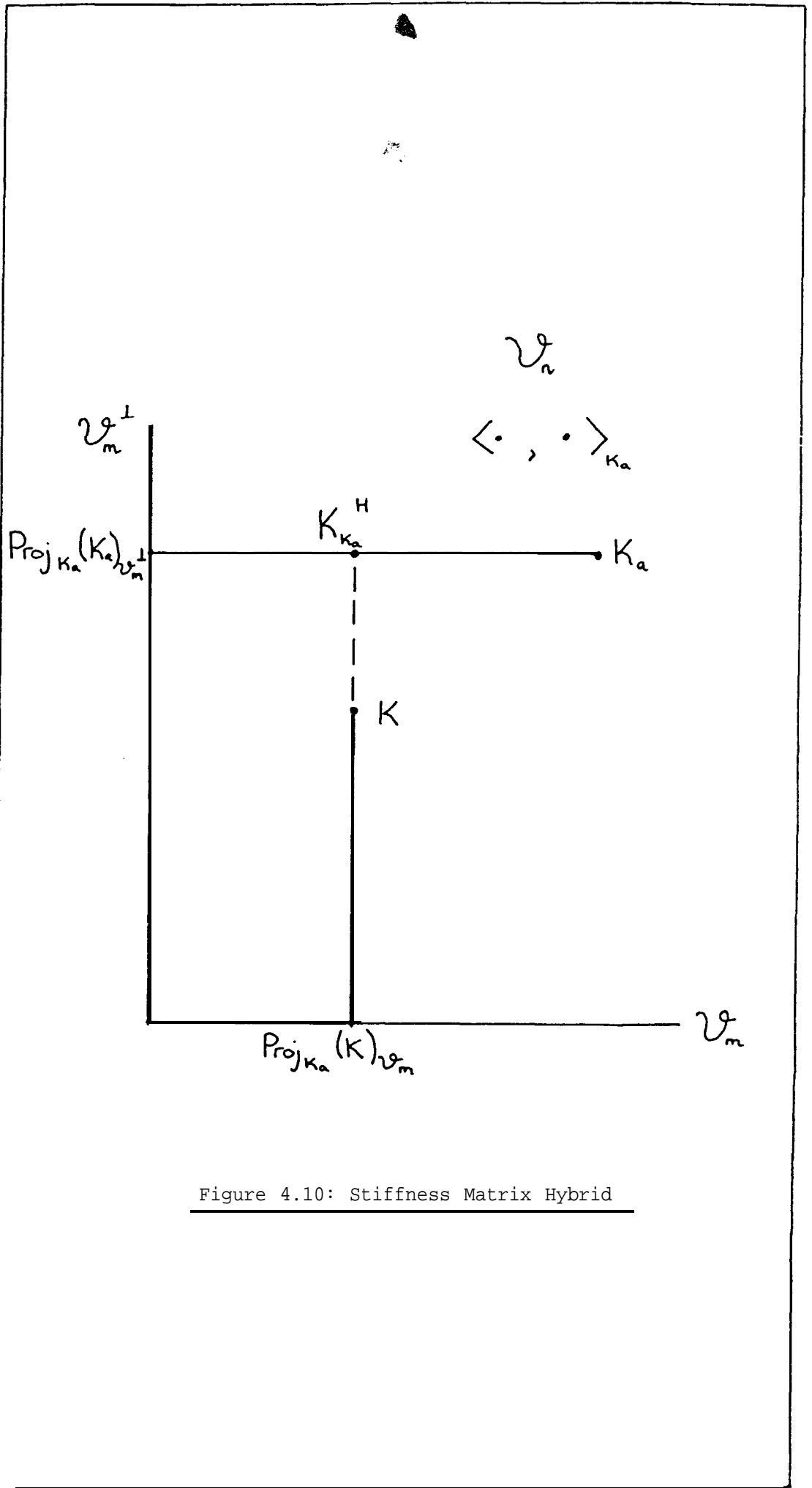


Figure 4.10: Stiffness Matrix Hybrid

The Operator T

$$Tf = (EI f'')'' \text{ on } \Gamma = (0, L)$$

with $\left\{ \begin{array}{l} \text{a essential} \\ \text{b natural} \end{array} \right\}$ boundary conditions at $0, L$

The Eigenvalue Equation

$$(EI f'')'' - \mu mf = 0$$

The Bilinear Functional B_a

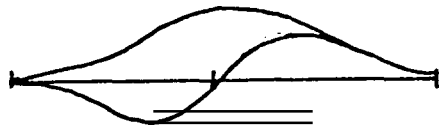
$$B_a(f, g) = \int_0^L EI f'' g''$$

The Weak Eigenvalue Equation

$$\int_0^L EI f'' g'' - \int_0^L m_a f g = 0 \quad \forall g \in \mathcal{V}$$



Shape Functions



Interpolation Functions

Figure 4.11: Bending Beam

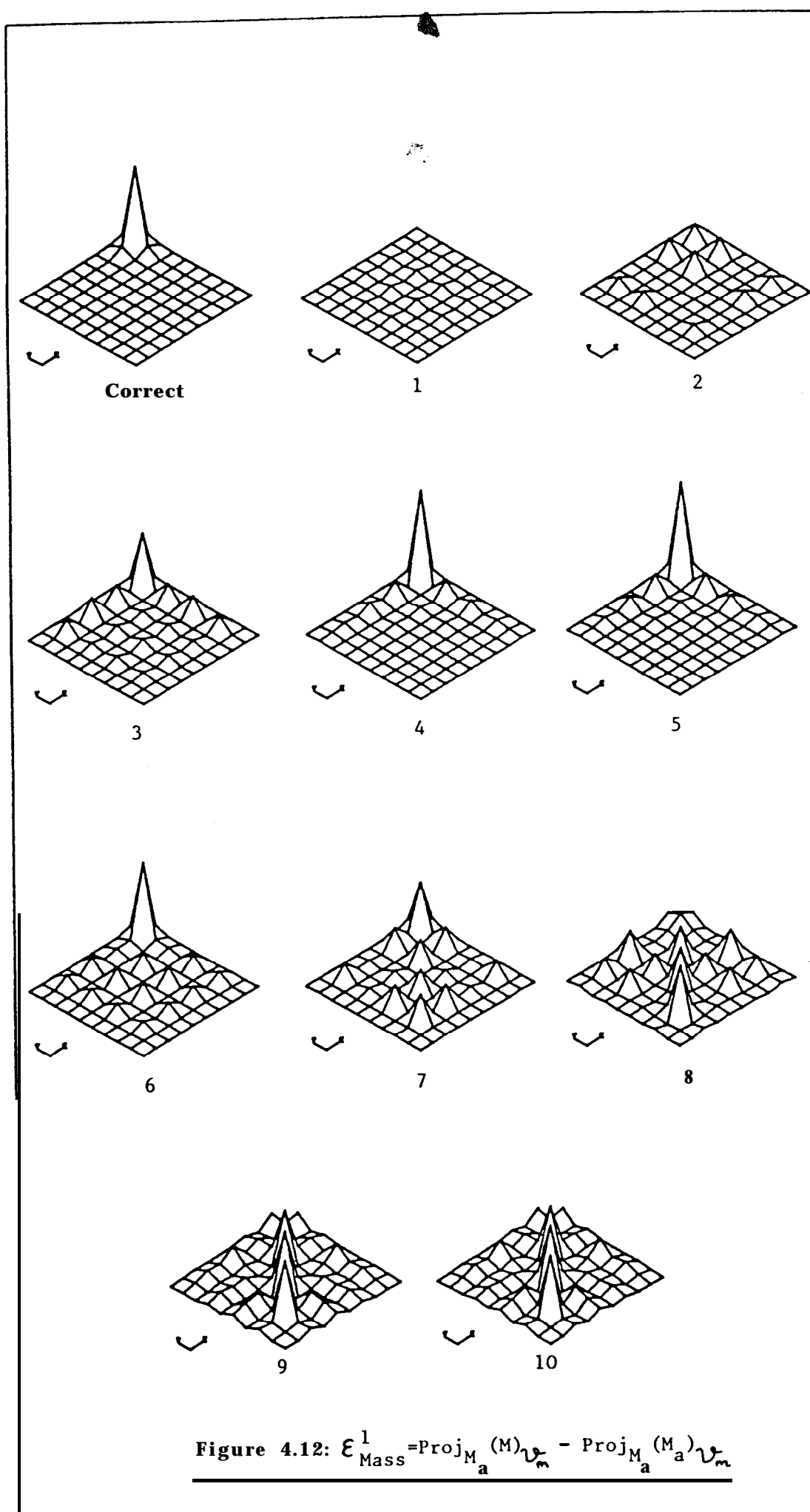


Figure 4.12: $\mathcal{E}_{\text{Mass}}^1 = \text{Proj}_{M_a}^{(M)} \psi_m - \text{Proj}_{M_a}^{(M_a)} \psi_m$

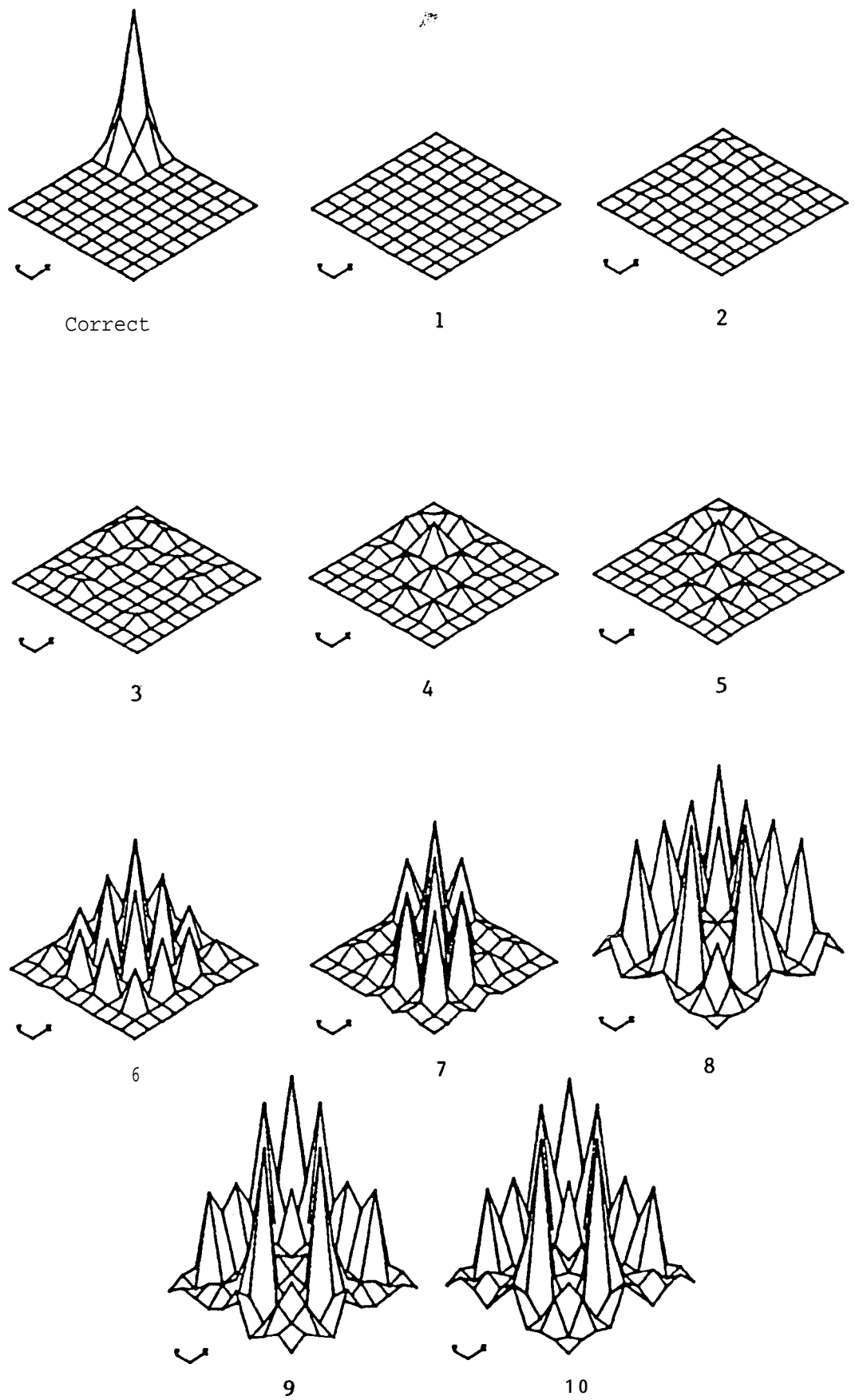


Figure 4.12 (cont.): $\mathcal{E}_{\text{Stiffness}}^1 = \text{Proj}_{M_a}(K) v_m - \text{Proj}_{M_a}(K_a) v_m$

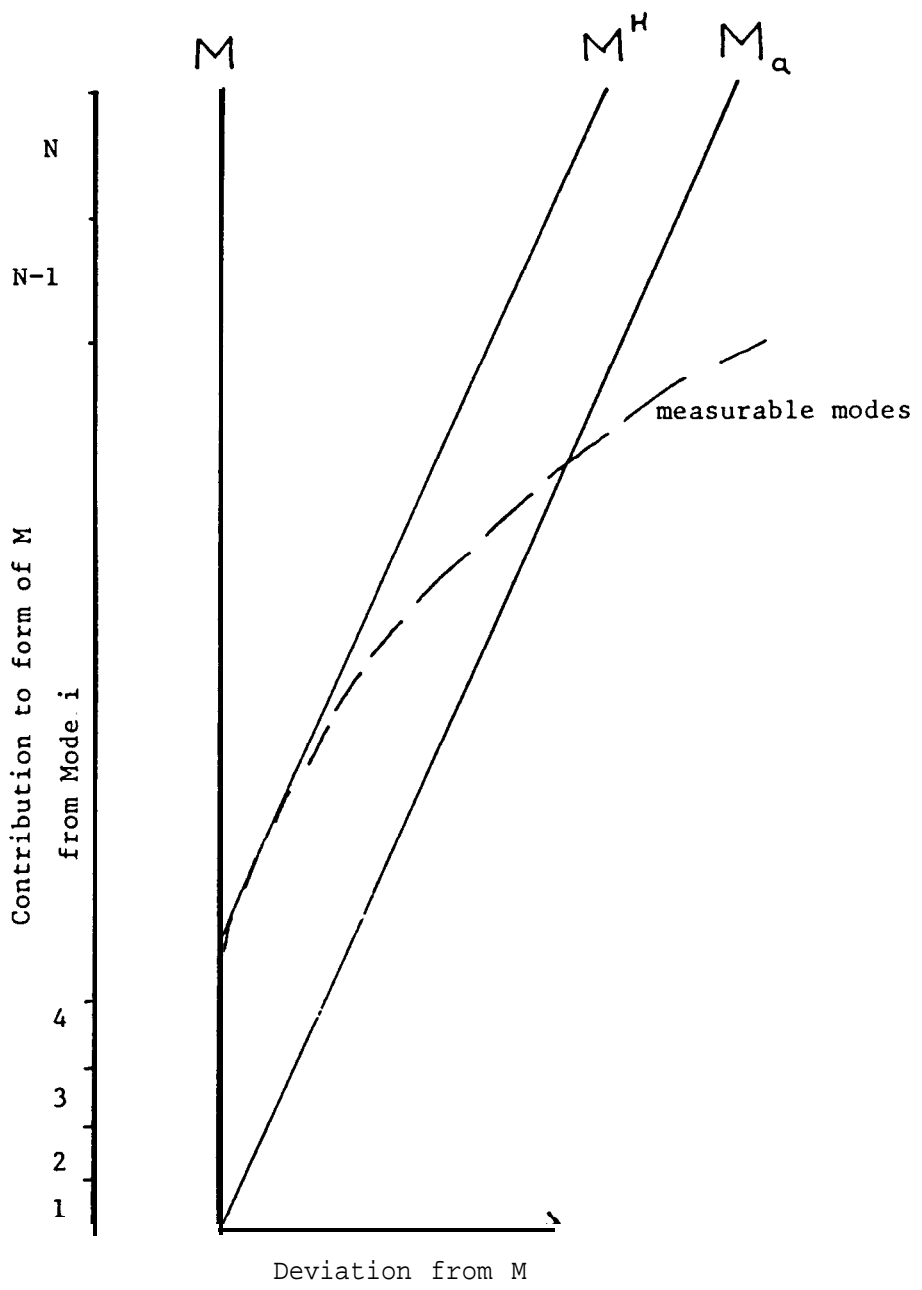


Figure 4.13: Mass Hybrid

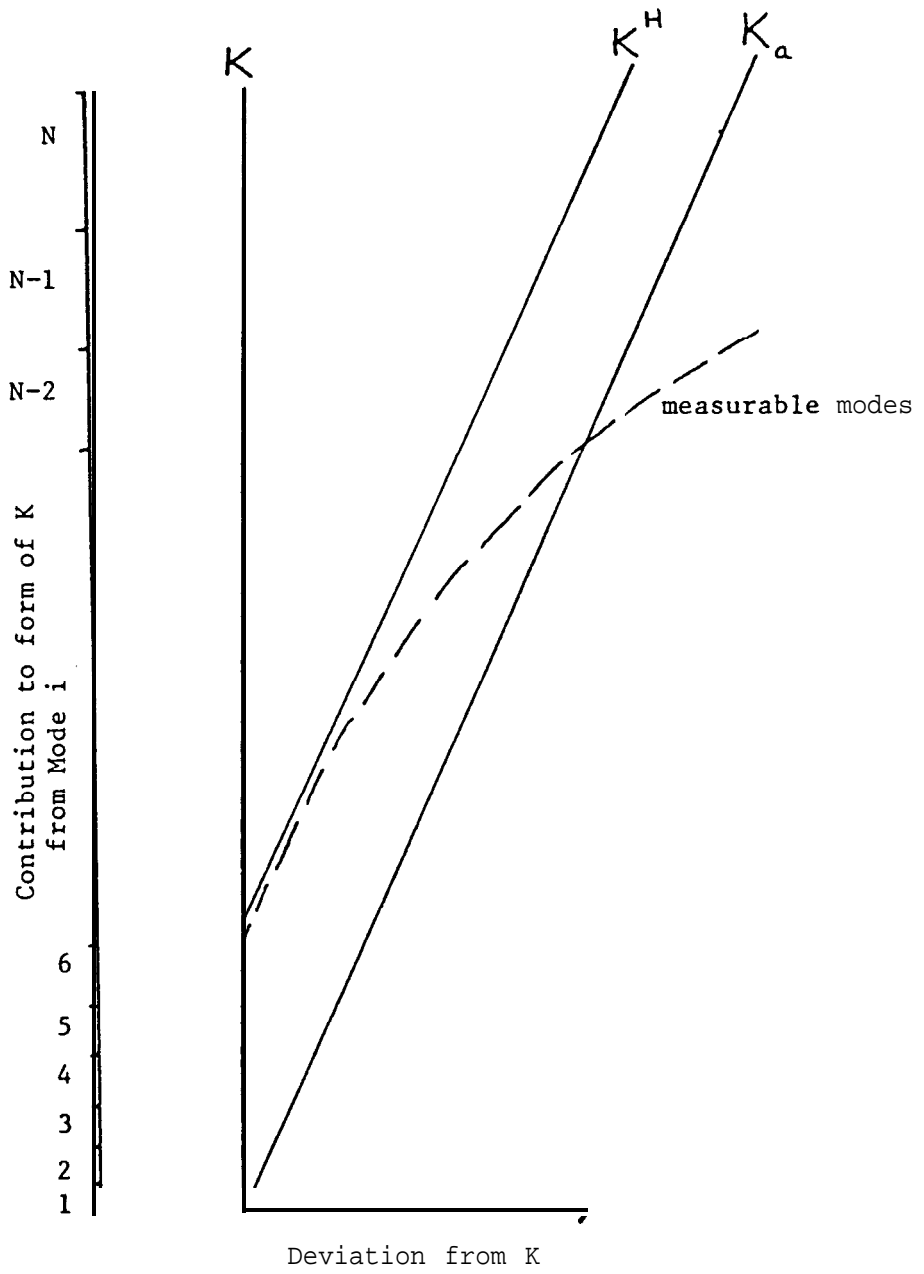


Figure 4.14: Stiffness Hybrid

| | | $\mathcal{V}_n : \langle \dots, \rangle M_a$ | $\mathcal{V}_n : \langle \dots, \rangle K_a$ |
|---|--|--|---|
| M | Proj(K) \mathcal{V}_m - Proj(K _a) \mathcal{V}_m | $\epsilon^1 = M_a \phi_m^{-1} (I - m^{-1} \phi_m^T M_a)$ | $\epsilon^2 = K_a \phi_k^{-1} (I - \phi_a^T M_a \phi) I^{-1} \phi_a^T K_a$ |
| | Proj(K) \mathcal{V}_m | $\epsilon^3 = M_a (\phi_m^{-2} \phi^T - \phi_a \phi_a^T) M_a$ | $\epsilon^4 = K_a (\phi_k^{-2} \phi^T - \phi_a \Lambda^{-2} \phi_a^T) K_a$ |
| | - Proj(K _a) \mathcal{V}_m^A | NO APPROXIMATION | $\epsilon^5 = K_a (\phi \Lambda^{-2} \phi^T - \phi_a \Lambda \phi_a^T) K_a$ |
| | Proj(K) \mathcal{V}_m - Proj(K _a) \mathcal{V}_m | APPROXIMATION k=Λ m=I | $\epsilon^2 = K_a \phi_k^{-1} (\Lambda - k) k^{-1} \phi_a^T K_a$ |
| K | Proj(K) \mathcal{V}_m - Proj(K _a) \mathcal{V}_m | $\epsilon^1 = M_a \phi_m^{-1} (\Lambda - \phi_a^T K_a \phi) m^{-1} \phi_a^T M_a$ | $\epsilon^2 = K_a \phi_k^{-1} (\Lambda - k) k^{-1} \phi_a^T K_a$ |
| | Proj(K) \mathcal{V}_m | $\epsilon^3 = M_a (\phi_m^{-1} \Lambda m^{-1} \phi^T - \phi_a \Lambda_a \phi_a^T) M_a$ | $\epsilon^4 = K_a (\phi_k^{-1} \Lambda k^{-1} \phi^T - \phi_a \Lambda_a^{-1} \phi_a^T) K_a$ |
| | - Proj(K _a) \mathcal{V}_m^A | NO APPROXIMATION k=Λ m=I | $\epsilon^5 = M_a (\phi \Lambda \phi^T - \phi_a \Lambda_a \phi_a^T) M_a$ |
| | Proj(K) \mathcal{V}_m - Proj(K _a) \mathcal{V}_m | APPROXIMATION k=Λ m=I | $\epsilon^6 = K_a (\phi \Lambda^{-1} \phi^T - \phi_a \Lambda_a^{-1} \phi_a^T) K_a$ |

TABLE 4.1: Error Matrices

| | |
|---|---|
| $\mathcal{V}_n^{\langle \dots \rangle M_a}$ | $M^H = M_a + M_a \phi_m^{-1} (I - m)^{-1} \phi^T M_a$ |
| $\mathcal{V}_n^{\langle \dots \rangle K_a}$ | $M^H = M_a + K_a \phi k^{-1} (I + \phi^T M_a \phi) k^{-1} \phi^T M_a$ $- K_a \phi k^{-1} \phi^T M_a - M_a \phi k^{-1} \phi^T K_a$ |
| | $K^H = K_a + M_a \phi_m^{-1} (\Lambda + \phi^T K_a \phi) m^{-1} \phi^T M_a$ $- M_a \phi_m^{-1} \phi^T K_a - K_a \phi_m^{-1} \phi^T M_a$ |
| | $K^H = K_a + K_a \phi k^{-1} (\Lambda + k) k^{-1} \phi^T K_a$ |

TABLE 4.2: Hybrid Matrices

CHAPTER 5

THE DAMPED PROBLEM

5.1 Preliminaries

The analyses of the preceding chapters have now pointed the way for an analysis of the viscously damped system, or that which may be described by the eigenvalue equation

$$M\Phi\Lambda^2 + C\Phi\Lambda + K\Phi = 0.$$

Here, Φ is an $(n \times 2n)$ matrix of eigenvectors, consisting of n eigenvectors and their complex conjugates. Λ is now a $(2n \times 2n)$ diagonal matrix of eigenvalues, consisting of n eigenvalues and their complex conjugates. The analysis is conducted in the complex space, \mathcal{C} , with the necessary additional terminology and considerations. The usual strategy is to set the problem up as a $(2n \times 2n)$ first order problem. Some of the possible formulations are

$$(1) \quad S = \begin{bmatrix} C & M \\ I & 0 \end{bmatrix} \quad T = \begin{bmatrix} K & 0 \\ 0 & -I \end{bmatrix}.$$

That is

$$SX\Lambda + TX = 0 \text{ where } X = \begin{bmatrix} \Phi \\ \Phi\Lambda \end{bmatrix}$$

$$\text{So } \begin{bmatrix} C & M \\ I & 0 \end{bmatrix} \begin{bmatrix} \Phi \\ \Phi\Lambda \end{bmatrix} [\Lambda] + \begin{bmatrix} K & 0 \\ 0 & -I \end{bmatrix} \begin{bmatrix} \Phi \\ \Phi\Lambda \end{bmatrix} = 0$$

$$\text{or } M\Phi\Lambda^2 + C\Phi\Lambda + K\Phi = 0$$

$$\text{and } \Phi\Lambda - \Phi\Lambda = 0.$$

$$(2) \quad S = \begin{bmatrix} 0 & M \\ I & 0 \end{bmatrix} \quad T = \begin{bmatrix} K & C \\ 0 & -I \end{bmatrix}.$$

That is

$$SX\Lambda + TX = 0 \text{ where } X = \begin{bmatrix} \Phi \\ \Phi\Lambda \end{bmatrix}.$$

$$\text{So } \begin{bmatrix} 0 & M \\ I & 0 \end{bmatrix} \begin{bmatrix} \phi \\ \phi\lambda \end{bmatrix} + \begin{bmatrix} K & C \\ 0 & -I \end{bmatrix} \begin{bmatrix} \phi \\ \phi\lambda \end{bmatrix} = 0$$

$$\text{or } M\phi\lambda^2 + C\phi\lambda + K\phi = 0$$

$$\text{and } \phi\lambda - \phi\lambda = 0.$$

$$(3) \quad S = \begin{bmatrix} C & M \\ M & 0 \end{bmatrix} \quad T = \begin{bmatrix} K & 0 \\ 0 & -M \end{bmatrix}.$$

That is

$$SXA + TX = 0 \text{ where } X = \begin{bmatrix} \phi \\ \phi\lambda \end{bmatrix}.$$

$$\text{So } \begin{bmatrix} C & M \\ M & 0 \end{bmatrix} \begin{bmatrix} \phi \\ \phi\lambda \end{bmatrix} + \begin{bmatrix} K & 0 \\ 0 & -M \end{bmatrix} \begin{bmatrix} \phi \\ \phi\lambda \end{bmatrix} = 0$$

$$\text{or } M\phi\lambda^2 + C\phi\lambda + K\phi = 0$$

$$\text{and } M\phi\lambda - M\phi\lambda = 0.$$

For the analysis of this chapter we use, instead of an inner product on \mathcal{V}_{2n} , a linear functional on \mathcal{V}_{2n} and its dual space \mathcal{V}_{2n}^* , represented by

$$x(y) = y(x) = [y, x] = [y, x]$$

$$y(x) = \sum_{i=1}^{2n} \xi^i \eta_i$$

where $x = \{\xi^1, \dots, \xi^{2n}\} \in \mathcal{V}_{2n}$ and $y = \{\eta_1, \dots, \eta_{2n}\} \in \mathcal{V}_{2n}^*$.

The eigenvector sets $\{x^i\}$ and $\{y_i\}$ (X and Y) are dual basis sets for the isomorphic spaces \mathcal{V}_{2n} and \mathcal{V}_{2n}^* . We know a vector z can be written as either

$$z = \sum_{i=1}^{2n} \zeta_i x^i \quad \text{or} \quad z = \sum_{i=1}^{2n} \zeta^i y_i.$$

In a matrix sense, the eigencolumns of the dual are the eigenrows of the primal. So, in order to find the dual basis we solve for the transpose problem, thus

$$S^T Y \Lambda + T^T Y = 0.$$

So, for example 1 we have,

$$S^T = \begin{bmatrix} C & I \\ M & O \end{bmatrix} \quad T^T = \begin{bmatrix} K & 0 \\ 0 & I \end{bmatrix}$$

that is

$$\begin{bmatrix} C & I \\ M & O \end{bmatrix} \begin{bmatrix} Y_1 \\ Y_2 \end{bmatrix} \begin{bmatrix} \Lambda \\ \Lambda \end{bmatrix} + \begin{bmatrix} K & 0 \\ 0 & -I \end{bmatrix} \begin{bmatrix} Y_1 \\ Y_2 \end{bmatrix} = 0.$$

$$\text{So } CY_1 \Lambda + Y_2 \Lambda + KY_1 = 0$$

$$\text{and } MY_1 \Lambda - Y_2 = 0$$

which gives

$$Y_2 = MY_1 \Lambda \text{ and } Y_1 = \Phi$$

$$\text{i.e. } Y = \begin{bmatrix} \Phi \\ M\Phi \Lambda \end{bmatrix}$$

which is the dual or reciprocal set of eigenvectors.

We have

$$SXA + TX = 0$$

$$\text{and } S^T Y \Lambda + T^T Y = 0.$$

From the definition of the dual transformation the following conditions hold:

$$[Sx^i, y_j] = k_i \delta_j^i = [x^i, S'y_j]$$

$$\text{and } [Tx^i, y_j] = -k_i \lambda_i \delta_j^i = [x^i, T'y_j]$$

where the k_i are constants, yet to be assigned. These conditions may be expressed in a more familiar form^(38,42), setting $k_i = 1$ for all i , as

$$|\Phi^T \Phi \Lambda^T M| \begin{bmatrix} C & M \\ I & O \end{bmatrix} \begin{bmatrix} \Phi \\ \Phi \Lambda \end{bmatrix} = I$$

$$\text{or } \Phi^T C \Phi + \Phi^T M \Phi \Lambda + \Lambda \Phi^T M \Phi = I$$

$$\text{and } \begin{bmatrix} \Phi^T & \Lambda \Phi^T M \end{bmatrix} \begin{bmatrix} K & 0 \\ 0 & -I \end{bmatrix} \begin{bmatrix} \Phi \\ \Phi \Lambda \end{bmatrix} = -\Lambda$$

$$\text{or } \Phi^T K \Phi - \Lambda \Phi^T M \Phi \Lambda = -A .$$

However, if we decide to employ formulation 3 we may observe that S and T are symmetric, so the eigenvector basis for the dual space is the same as the eigenvector basis of the primal, or the problem is apparently self-dual. We have

$$x^{iT} S_{xj} = k_{ij} \delta_j^i$$

$$x^{iT} T_{xj} = -\lambda k_{ij} \delta_j^i .$$

It is because of this attractive feature that this formulation is adopted for the remainder of this chapter. However, merely making S and T symmetrical does not permit a side-step of the necessary analysis, with a return to inner product spaces, as the operators involved are not really symmetric in the fundamental sense, even though this fact is well disguised by using the third formulation. This is expanded upon in the next section.

5.2 Symmetric Formulation Paradox

We have set

$$S = \begin{bmatrix} C & M \\ M & 0 \end{bmatrix} \text{ and } T = \begin{bmatrix} K & 0 \\ 0 & -M \end{bmatrix}$$

which was first proposed by Hurty and Rubenstein in 1964⁽⁵²⁾. If we permit the use of an inner product we may observe the paradox that ensues:

$$\begin{aligned}
\langle Sx^i, x^i \rangle &= \begin{bmatrix} \bar{x}_i^T & \lambda_i \bar{x}_i^T \end{bmatrix} \begin{bmatrix} C & M \\ M^* & 0 \end{bmatrix} \begin{bmatrix} x_i \\ \lambda_i x_i \end{bmatrix} \\
&= \bar{x}_i^T C x_i + \bar{\lambda}_i \bar{x}_i^T M x_i + \lambda_i \bar{x}_i^T M x_i \\
&= 0
\end{aligned}$$

from orthogonality relationship, since this is an off diagonal term.

Also

$$\langle Tx^i, x^i \rangle = 0$$

by similar reasoning.

Here, it is worth restating the essential difference between inner product and linear functional:

$$\begin{aligned}
\langle x, y \rangle &= \sum_{i=1}^{2n} \xi^i \bar{\eta}_i & x, y \in \mathcal{V}_{2n} \\
[x, y] &= \sum_{i=1}^{2n} \xi^i \eta_i & x \in \mathcal{V}_{2n} \quad y \in \mathcal{V}_{2n}^* \\
x^i &= \{\xi^1, \dots, \xi^{2n}\} & y_i = \{\eta_1, \dots, \eta_{2n}\},
\end{aligned}$$

noting the use of the complex conjugate formulation for the inner product, but not with the linear functional. In essence, the S and T matrices here are not positive definite so analysis using inner product spaces is not permissible (see definition of inner product, axiom 3).

5.3 Normalisation

Before **embarking** on a projection analysis for the damped problem, a mention of normalisation is required. The usual **normalisation** that is adopted is

$$x^T S x = I$$

$$\begin{aligned}
\langle Sx^i, x^i \rangle &= \begin{bmatrix} \bar{x}_i^T & \lambda_i \bar{x}_i^T \end{bmatrix} \begin{bmatrix} C & M \\ M^* & 0 \end{bmatrix} \begin{bmatrix} x_i \\ \lambda_i x_i \end{bmatrix} \\
&= \bar{x}_i^T C x_i + \bar{\lambda}_i \bar{x}_i^T M x_i + \lambda_i \bar{x}_i^T M x_i \\
&= 0
\end{aligned}$$

from orthogonality relationship, since this is an off diagonal term.

Also

$$\langle Tx^i, x^i \rangle = 0$$

by similar reasoning.

Here, it is worth restating the essential difference between inner product and linear functional:

$$\langle x, y \rangle = \sum_{i=1}^{2n} \xi_i^i \bar{\eta}_i \quad x, y \in \mathcal{V}_{2n}$$

$$[x, y] = \sum_{i=1}^{2n} \xi_i^i \eta_i \quad x \in \mathcal{V}_{2n} \quad y \in \mathcal{V}_{2n}^*$$

$$x^i = \{\xi^1, \dots, \xi^{2n}\} \quad y_i = \{\eta_1, \dots, \eta_{2n}\},$$

noting the use of the complex conjugate formulation for the inner product, but not with the linear functional. In essence, the S and T matrices here are not positive definite so analysis using inner product spaces is not permissible (see definition of inner product, axiom 3).

5.3 Normalisation

Before **embarking** on a projection analysis for the damped problem, a mention of normalisation is required. The usual **normalisation** that is adopted is

$$x^T S x = I$$

and $x^T T x = -A$

or $\phi^T C \phi + \Lambda \phi^T M \phi + \phi^T M \phi \Lambda = I$

and $\phi^T K \phi - \Lambda \phi^T M \phi \Lambda = -A$

or, in other words, $k_i = 1$ for all i . This is perfectly valid, and would appear the most suitable at first glance. However, if, using this normalisation, we let $C = 0$ then we have, for the first equation when $i = j$:

$$2\lambda_i x_i^T M x_i = 1$$

or $x_i^T M x_i = \frac{1}{2\lambda_i} = \frac{1}{2i\omega_i} = \frac{-i}{2\omega_i}$

A phase shift of 45° will prevail when damping is zero. For the analysis here we wish

$$x_i^T M x_i = 1 \text{ if } C = 0$$

to allow compatibility with the undamped problem. To facilitate this we let

$$k_i = 2X_i \quad \forall i$$

so we have

$$x^T S x = 2\Lambda$$

$$x^T T x = -2\Lambda^2$$

i.e. $\phi^T C \phi + \Lambda \phi^T M \phi + \phi^T M \phi \Lambda = 2\Lambda$

and $\phi^T K \phi - \Lambda \phi^T M \phi \Lambda = -2\Lambda^2$

The advantages associated with this normalisation become apparent as the theory is developed and C is put equal to zero for comparison with the undamped problem.

5.4 Projection of Inverse S and T Matrices

We now consider the problem where we have an incomplete set of measured complex modes, Φ , which is now $(n \times 2m)$ and an incomplete set of measured eigenvalues A $(2m \times 2m)$. **From this** information, an incomplete basis \mathcal{V}_{2m} may be formulated as the matrix X $(2n \times 2m)$, so decomposing \mathcal{V}_{2n} into the direct sum, we have

$$\mathcal{V}_{2n} = \mathcal{V}_{2m} \oplus \mathcal{V}'_{2m}$$

We may introduce, as before, two projection operators, using $[...]_S$ as

$$P_S = \frac{1}{2} X \Lambda^{-1} X^T S$$

and $P_S^T = \frac{1}{2} S X \Lambda^{-1} X^T$.

In effect, P_S is the projection onto $[x^i]$ ($i = 1, \dots, 2m$) along $[x^i]$ ($i = 2m+1, \dots, 2n$). Thinking in terms of normed spaces, P_S is an annihilator of $[x^i]$ ($i = 2m+1, \dots, n$). P_S^T is the projection onto $[Sx^i]$ ($i = 1, \dots, 2m$) along $[Sx^i]$ ($i = 2m+1, \dots, 2n$) (annihilator of $[Sx^i]$ ($i = 2m+1, \dots, n$)). So here orthogonality has been extended to include normed spaces with the use of linear functionals, i.e. $[...]$ (that is, an orthogonal space is replaced, in effect, by the annihilator of the original).

We may also readily observe that the fact that we are dealing here with a primal vector space and its dual is of little significance, since both are expressed using the same set of basis vectors, which is the advantage of employing a symmetric formulation. We may readily deduce that

$$S^{-1} = \begin{bmatrix} 0 & M^{-1} \\ M^{-1} & -M^{-1} C M^{-1} \end{bmatrix}$$

so we have, with respect to $[\dots]_S$

$$\begin{aligned} \text{Proj}_S(S^{-1})\mathcal{V}_{2m} &= P_S S^{-1} P_S^T \\ &= \frac{1}{4} X \Lambda^{-1} X^T S S^{-1} S X \Lambda^{-1} X^T \\ &= \frac{1}{4} X \Lambda^{-1} X^T S X \Lambda^{-1} X^T \\ &= \frac{1}{2} X \Lambda^{-1} X^T \end{aligned}$$

That is

$$\begin{aligned} \begin{bmatrix} \text{Proj}_S(0)\mathcal{V}_{2m} & \text{Proj}_S(M^{-1})\mathcal{V}_{2m} \\ \text{Proj}_S(M^{-1})\mathcal{V}_{2m} & \text{Proj}_S(-M^{-1}CM^{-1})\mathcal{V}_{2m} \end{bmatrix} &= \frac{1}{2} \begin{bmatrix} \Phi & [\Lambda^{-1}] [\Phi^T & \Phi \Lambda^T] \\ \Phi \Lambda & \end{bmatrix} \\ &= \frac{1}{2} \begin{bmatrix} \Phi \Lambda^{-1} \Phi^T & \Phi \Phi^T \\ \Phi \Phi^T & \Phi \Lambda \Phi^T \end{bmatrix} \end{aligned}$$

So, equating corresponding elements,

$$\text{Proj}_S(M^{-1})\mathcal{V}_{2m} = \frac{1}{2} \Phi \Phi^T = \frac{1}{2} \sum_{i=1}^{2m} x_i x_i^T = \text{Re} \left\{ \sum_{i=1}^m x_i x_i^T \right\}$$

where Re signifies the real part. This may be used since we are summing vectors and their complex conjugates. This is analogous to the undamped case since if $C = 0$ then no imaginary part would exist. Also we have

$$-\text{Proj}_S(M^{-1}CM^{-1})\mathcal{V}_{2m} = \frac{1}{2} \Phi \Lambda \Phi^T$$

$$\text{and } \text{Proj}_S(0)\mathcal{V}_{2m} = \frac{1}{2} \Phi \Lambda^{-1} \Phi^T$$

This second projection is not equal to zero unless $m=n$ and, for comparison with the undamped case, if $C = 0$ then both these projections are equal to zero for all m . Also, since

$$T^{-1} = \begin{bmatrix} K^{-1} & 0 \\ 0 & M^{-1} \end{bmatrix}$$

$$\begin{aligned}
\text{then } \text{Proj}_S(T^{-1})\mathcal{V}_{2m} &= P_S T^{-1} P_S^T \\
&= \frac{1}{4} X \Lambda T_{ST}^{-1} S X \Lambda^{-1} X^T \\
&= -\frac{1}{4} X \Lambda^{-1} X^T S X \Lambda^{-2} X^T \\
&= -\frac{1}{2} X \Lambda^{-2} X^T
\end{aligned}$$

$$\begin{aligned}
\text{so } & \left[\begin{array}{cc} \text{Proj}_S(K^{-1})\mathcal{V}_{2m} & \text{Proj}_S(0)\mathcal{V}_{2m} \\ \text{Proj}_S(0)\mathcal{V}_{2m} & -\text{Proj}_S(M^{-1})\mathcal{V}_{2m} \end{array} \right] \\
&= -\frac{1}{2} \begin{bmatrix} \Phi \\ \Phi \Lambda \end{bmatrix} [\Lambda^{-2}] \begin{bmatrix} \Phi^T & \Lambda \Phi^T \end{bmatrix} \\
&= -\frac{1}{2} \begin{bmatrix} \Phi \Lambda^{-2} \Phi^T & \Phi \Lambda^{-1} \Phi^T \\ \Phi \Lambda^{-1} \Phi^T & \Phi \Phi^T \end{bmatrix}
\end{aligned}$$

which gives

$$\text{Proj}_S(M^{-1})\mathcal{V}_{2m} = 3 \Phi \Phi^T$$

$$\text{and } \text{Proj}_S(0)\mathcal{V}_{2m} = -\frac{1}{2} \Phi \Lambda^{-1} \Phi^T$$

as before. Also

$$\begin{aligned}
\text{Proj}_S(K^{-1})\mathcal{V}_{2m} &= -\frac{1}{2} \Phi \Lambda^{-2} \Phi^T = -\frac{1}{2} \sum_{i=1}^{2m} \frac{x_i \cdot x_i^T}{\lambda_i^2} \\
&= -\text{Re} \left(\sum_{i=1}^m \frac{x_i \cdot x_i^T}{\lambda_i} \right)
\end{aligned}$$

which is again analogous with the undamped problem.

We also have the two orthogonality conditions

$$\Lambda \Phi^T M \Phi + \Phi^T M \Phi \Lambda + \Phi^T C \Phi = 2\Lambda$$

$$\text{and } \Phi^T K \Phi - \Lambda \Phi^T M \Phi \Lambda = -2\Lambda^2$$

from which a third may be derived involving K and C only, thus:

$$\Phi^T K \Phi + 2\Lambda^2 = \Lambda \Phi^T M \Phi \Lambda$$

$$\Lambda(\Lambda \Phi^T M \Phi \Lambda) + (\Lambda \Phi^T M \Phi \Lambda)\Lambda + \Lambda \Phi^T C \Phi \Lambda = 2\Lambda^3$$

$$\Lambda(\Phi^T K \Phi + 2\Lambda^2) + (\Phi^T K \Phi + 2\Lambda^2)\Lambda + \Lambda \Phi^T C \Phi \Lambda = 2\Lambda^3$$

$$\Lambda \Phi^T K \Phi + \Phi^T K \Phi \Lambda + \Lambda \Phi^T C \Phi \Lambda = -2\Lambda^3$$

so
$$\Phi^T K \Phi \Lambda^{-1} + \Lambda^{-1} \Phi^T K \Phi + \Phi^T C \Phi = -2\Lambda$$

This section has illustrated that again only expressions for the inverse matrices are derived. It is possible to derive further relationships between mass, damping and stiffness for a complete system, but these are of little use.

As for the undamped case, in order to derive measured mass, damping and stiffness matrices we require some additional information, and the adoption of a suitable linear functional. Now we may go on to consider how we may do this using, as that additional information, analytical mass and stiffness M_a and K_a .

5.5 Incomplete M, C and K

For the derivation of expressions for incomplete mass and stiffness matrices we need to reintroduce the analytical system, this time describing it as a $(2n \times 2n)$ problem. We have

$$S_a = \begin{bmatrix} 0 & M_a \\ M_a & 0 \end{bmatrix} \quad T_a = \begin{bmatrix} K_a & 0 \\ 0 & -M_a \end{bmatrix} \quad \text{and} \quad X_a = \begin{bmatrix} \Phi_a \\ \Phi_a \Lambda_a \end{bmatrix}$$

The analytical damping matrix is assumed to be zero, which would reflect the most likely situation in practice, but the analysis could be carried through with $C_a \neq 0$. We know that

$$X_a^T S_a X_a = 2\Lambda_a$$

$$X_a^T T_a X_a = -2\Lambda_a^2$$

and $T_a X_a + S_a X_a \Lambda_a = 0.$

The following two matrices are set up, preceded first by an appropriate normalisation (that is

$$2\lambda_i x_i^T M_a x_i = 2\lambda_i \text{ for } [\dots]_{S_a}$$

and $x_i^T K_a x_i - \lambda_i^2 x_i^T M_a x_i = -2\lambda_i^2$

for $[\dots]_{T_a}$).

So define

$$s = \Lambda \Phi^T M_a \Phi + \Phi^T M_a \Phi \Lambda = X^T S_a X$$

and $t = \Phi^T K_a \Phi - \Lambda \Phi^T M_a \Phi \Lambda = X^T T_a X.$

If we first consider the two projection operators for $[\dots]_{S_a}$, that is

$$P_{S_a} = X s^{-1} X^T S_a$$

where $P_{S_a}(x^i) = x^i \quad i = 1, \dots, 2m$

and $P_{S_a}(x^i) = \theta \quad i = 2m+1, \dots, 2n$

with $P_{S_a}^T = S_a X s^{-1} X^T$

where $P_{S_a}^T(S_a x^i) = S_a x^i \quad i = 1, \dots, 2m$

and $P_{S_a}^T(S_a x^i) = \theta \quad i = 2m+1, \dots, 2n$

then we may formulate a projected solution for the true S matrix,

thus

$$\text{Proj}_{S_a}(S) \mathcal{V}_{2m} = P_{S_a}^T S P_{S_a}$$

$$= S_a X_s^{-1} X^T S X_s^{-1} X^T S_a$$

$$= 2S_a X_s^{-1} \Lambda_s^{-1} X^T S_a$$

so

$$\begin{bmatrix} \text{Proj}_{S_a} (C) \mathcal{V}_{2m} & \text{Proj}_{S_a} (M^1) \mathcal{V}_{2m} \\ \text{Proj}_{S_a} (M^2) \mathcal{V}_{2m} & \text{Proj}_{S_a} (O^1) \mathcal{V}_{2m} \end{bmatrix}$$

$$= 2 \begin{bmatrix} 0 & M_a \\ M_a & 0 \end{bmatrix} \begin{bmatrix} \Phi \\ \Phi \Lambda \end{bmatrix} s^{-1} \Lambda_s^{-1} \begin{bmatrix} \Phi^T & \Lambda \Phi^T \end{bmatrix} \begin{bmatrix} 0 & M_a \\ M_a & 0 \end{bmatrix}$$

That is

$$\text{Proj}_{S_a} (C) \mathcal{V}_{2m} = 2M_a \Phi \Lambda_s^{-1} \Lambda_s^{-1} \Lambda \Phi^T M_a$$

$$\text{Proj}_{S_a} (M^1) \mathcal{V}_{2m} = 2M_a \Phi s^{-1} \Lambda_s^{-1} \Lambda \Phi^T M_a$$

$$\text{Proj}_{S_a} (M^2) \mathcal{V}_{2m} = 2M_a \Phi \Lambda_s^{-1} \Lambda_s^{-1} \Phi^T M_a$$

$$\text{Proj}_{S_a} (O^1) \mathcal{V}_{2m} = 2M_a \Phi s^{-1} \Lambda_s^{-1} \Phi^T M_a$$

Also

$$\text{Proj}_{S_a} (T) \mathcal{V}_{2m} = P_{S_a}^T T P_{S_a}$$

$$= S_a X_s^{-1} X^T T X_s^{-1} X^T S_a$$

$$= -2S_a X_s^{-1} \Lambda^2 s^{-1} X^T S_a$$

So

$$\begin{bmatrix} \text{Proj}_{S_a} (K) \mathcal{V}_{2m} & \text{Proj}_{S_a} (O^2) \mathcal{V}_{2m} \\ \text{Proj}_{S_a} (O^3) \mathcal{V}_{2m} & -\text{Proj}_{S_a} (M^3) \mathcal{V}_{2m} \end{bmatrix}$$

$$= -2 \begin{bmatrix} M_a & \Phi \\ M_a & 0 \end{bmatrix} \begin{bmatrix} \Phi \\ \Phi \Lambda \end{bmatrix} s^{-1} \Lambda^2 s^{-1} \begin{bmatrix} \Phi^T & \Lambda \Phi^T \end{bmatrix} \begin{bmatrix} 0 & M_a \\ M_a & 0 \end{bmatrix}$$

that is

$$\text{Proj}_{S_a}(K) \mathcal{V}_{2m} = -2M_a \Phi \Lambda S^{-1} \Lambda^2 S^{-1} \Lambda \Phi^T M_a$$

$$\text{Proj}_{S_a}(M^3) \mathcal{V}_{2m} = 2M_a \Phi S^{-1} \Lambda^2 S^{-1} \Phi^T M_a$$

$$\text{Proj}_{S_a}(O^2) \mathcal{V}_{2m} = -2M_a \Phi S^{-1} \Lambda^2 S^{-1} \Lambda \Phi^T M_a$$

$$\text{Proj}_{S_a}(O^3) \mathcal{V}_{2m} = -2M_a \Phi \Lambda S^{-1} \Lambda^2 S^{-1} \Phi^T M_a$$

Here we see that there are three expressions for an incomplete mass matrix. The expressions satisfy the following two orthogonality relationships,

$$\begin{aligned} \Phi^T(\text{Proj}_{S_a}(C) \mathcal{V}_{2m}) \Phi + \Phi^T(\text{Proj}_{S_a}(M^2) \mathcal{V}_{2m}) \Phi \Lambda + \Lambda \Phi^T(\text{Proj}_{S_a}(M^1) \mathcal{V}_{2m}) \Phi \\ + \Phi \Lambda^T(\text{Proj}_{S_a}(O^1) \mathcal{V}_{2m}) \Phi \Lambda = 2\Lambda \end{aligned}$$

$$\begin{aligned} \text{and } \Phi^T(\text{Proj}_{S_a}(K) \mathcal{V}_{2m}) \Phi + \Lambda \Phi^T(\text{Proj}_{S_a}(M^3) \mathcal{V}_{2m}) \Phi \Lambda + \Lambda \Phi^T(\text{Proj}_{S_a}(O^2) \mathcal{V}_{2m}) \Phi \\ + \Phi^T(\text{Proj}_{S_a}(O^3) \mathcal{V}_{2m}) \Phi \Lambda = -2\Lambda^2. \end{aligned}$$

Alternatively, we may formulate expressions for incomplete matrices using $[\dots]_T$, thus

$$P_{T_a} = X t^{-1} X^T T_a$$

$$P_{T_a}^T = T_a X t^{-1} X^T$$

Using this approach, the projected S matrix will be

$$\begin{aligned} \text{Proj}_{T_a}(S) \mathcal{V}_{2m} &= T_a X t^{-1} X^T S X t^{-1} X^T T_a \\ &= 2T_a X t^{-1} \Lambda t^{-1} X^T T_a \end{aligned}$$

$$\text{So } \begin{bmatrix} \text{Proj}_{T_a}(C) \mathcal{V}_{2m} & \text{Proj}_{T_a}(M^1) \mathcal{V}_{2m} \\ \text{Proj}_{T_a}(M^2) \mathcal{V}_{2m} & \text{Proj}_{T_a}(O^1) \mathcal{V}_{2m} \end{bmatrix}$$

$$= 2 \begin{bmatrix} K_a & 0 \\ 0 & -M_a \end{bmatrix} \begin{bmatrix} \phi \\ \phi \Lambda \end{bmatrix} t^{-1} \Lambda t^{-1} \begin{bmatrix} \phi^T & \Lambda \phi^T \\ 0 & -M_a^T \end{bmatrix} \begin{bmatrix} K_a & 0 \\ 0 & -M_a^T \end{bmatrix}$$

That is

$$\begin{aligned} \text{Proj}_{T_a}(C) \mathcal{V}_{2m} &= 2K_a \phi t^{-1} \Lambda t^{-1} \phi^T K_a \\ \text{Proj}_{T_a}(M^1) \mathcal{V}_{2m} &= 2K_a \phi t^{-1} \Lambda t^{-1} \Lambda \phi^T M_a \\ \text{Proj}_{T_a}(M^2) \mathcal{V}_{2m} &= -2M_a \phi \Lambda t^{-1} \Lambda t^{-1} \phi^T K_a \\ \text{Proj}_{T_a}(O^1) \mathcal{V}_{2m} &= 2M_a \phi \Lambda t^{-1} \Lambda t^{-1} \Lambda \phi^T M_a \end{aligned}$$

Finally, for the projected solution of the T matrix,

$$\begin{aligned} \text{Proj}_{T_a}(T) \mathcal{V}_{2m} &= T_a X t^{-1} X^T T X t^{-1} X^T T_a \\ &= -2T_a X t^{-1} \Lambda^2 t^{-1} X^T T_a \end{aligned}$$

so

$$\begin{bmatrix} \text{Proj}_{T_a}(K) \mathcal{V}_{2m} & \text{Proj}_{T_a}(O^2) \mathcal{V}_{2m} \\ \text{Proj}_{T_a}(O^3) \mathcal{V}_{2m} & -\text{Proj}_{T_a}(M^3) \mathcal{V}_{2m} \end{bmatrix} = -2 \begin{bmatrix} K_a & 0 \\ 0 & M_a \end{bmatrix} \begin{bmatrix} \phi \\ \phi \Lambda \end{bmatrix} t^{-1} \Lambda^2 t^{-1}$$

$$\begin{bmatrix} \phi^T & \Lambda \phi^T \\ 0 & -M_a^T \end{bmatrix} \begin{bmatrix} K_a & 0 \\ 0 & -M_a^T \end{bmatrix}$$

that is

$$\begin{aligned} \text{Proj}_{T_a}(K) \mathcal{V}_{2m} &= -2K_a \phi t^{-1} \Lambda^2 t^{-1} \phi^T K_a \\ \text{Proj}_{T_a}(O^2) \mathcal{V}_{2m} &= 2K_a \phi t^{-1} \Lambda^2 t^{-1} \Lambda \phi^T M_a \\ \text{Proj}_{T_a}(O^3) \mathcal{V}_{2m} &= 2M_a \phi \Lambda t^{-1} \Lambda^2 t^{-1} \phi^T K_a \\ \text{Proj}_{T_a}(M^3) \mathcal{V}_{2m} &= 2M_a \phi \Lambda t^{-1} \Lambda^2 t^{-1} \Lambda \phi^T M_a \end{aligned}$$

Again, we may observe that the following orthogonality conditions are satisfied:

$$\begin{aligned} & \Phi^T(\text{Proj}_{T_a}(C))\mathcal{V}_{2m} \Phi + \Lambda \Phi^T(\text{Proj}_{T_a}(M^2))\mathcal{V}_{2m} \Phi + \Phi^T(\text{Proj}_{T_a}(M^1))\mathcal{V}_{2m} \Phi \Lambda \\ & + \Lambda \Phi^T(\text{Proj}_{T_a}(O^1))\mathcal{V}_{2m} \Phi \Lambda = 2\Lambda \end{aligned}$$

$$\begin{aligned} \text{and } & \Phi^T(\text{Proj}_{T_a}(K))\mathcal{V}_{2m} \Phi + \Lambda \Phi^T(\text{Proj}_{T_a}(O^3))\mathcal{V}_{2m} \Phi + \Phi^T(\text{Proj}_{T_a}(O^2))\mathcal{V}_{2m} \Phi \Lambda \\ & + \Phi \Lambda^T(\text{Proj}_{T_a}(M^3))\mathcal{V}_{2m} \Phi \Lambda = -2\Lambda^2. \end{aligned}$$

It can be seen that for the incomplete case the projection of the 0 matrix is not itself 0 (although it will be for a complete system) and thus plays a role in satisfying the necessary conditions. Also, the expressions for incomplete mass matrices are similar, but not identical. These observations are discussed later in this chapter. The next section demonstrates how this analysis is the logical extension of the undamped problem by showing that the three incomplete expressions for mass are all identical and equal to the original undamped expression when the damping matrix is set to zero.

5.6 Comparison with Undamped Problem

$$\text{We know that } X = \begin{bmatrix} \Phi \\ \Phi \Lambda \end{bmatrix}$$

but that the Φ is really a matrix of eigenvectors and their complex conjugates, thus $[\Phi \quad \bar{\Phi}]$. With the normalisation that has been adopted it is known that as damping tends to zero so do the imaginary parts of the eigenvectors. In the limit we have $[\Phi \quad \Phi]$ (Φ now real). Also, we know that A may be expressed as

$$\begin{bmatrix} A & | & 0 \\ \hline 0 & | & \Lambda \end{bmatrix}$$

and as damping tends to zero it becomes

$$\begin{bmatrix} i\Omega & | & 0 \\ \hline 0 & | & -i\Omega \end{bmatrix}$$

where Ω is the diagonal matrix of measured natural frequencies.

Now, if we consider the s matrix under these conditions, then

$$\begin{aligned} s &= \begin{bmatrix} \phi^T \\ \hline \phi^T \end{bmatrix} M_a \begin{bmatrix} \phi & | & \phi \end{bmatrix} \begin{bmatrix} i\Omega & | & 0 \\ \hline 0 & | & -i\Omega \end{bmatrix} + \begin{bmatrix} i\Omega & | & 0 \\ \hline 0 & | & -i\Omega \end{bmatrix} \begin{bmatrix} \phi^T \\ \hline \phi^T \end{bmatrix} M_a \begin{bmatrix} \phi & | & \phi \end{bmatrix} \\ &= i \begin{bmatrix} \phi^T M_a \phi \Omega + \Omega \phi^T M_a \phi & -\phi^T M_a \phi \Omega + \Omega \phi^T M_a \phi \\ \phi^T M_a \phi \Omega - \Omega \phi^T M_a \phi & -\phi^T M_a \phi \Omega - \Omega \phi^T M_a \phi \end{bmatrix} \\ &= i \begin{bmatrix} A & -B \\ B & -A \end{bmatrix} \end{aligned}$$

where $A = \phi^T M_a \phi \Omega + \Omega \phi^T M_a \phi$

and $B = \phi^T M_a \phi \Omega - \Omega \phi^T M_a \phi$

We may then formulate the inverse as

$$\begin{aligned} s^{-1} &= -i \begin{bmatrix} B^{-1} & A^{-1} \\ A^{-1} & -B^{-1} \end{bmatrix} (AB^{-1} - BA^{-1})^{-1} \\ &= -i \begin{bmatrix} (A - BA^{-1}B)^{-1} & -(AB^{-1}A - B)^{-1} \\ (AB^{-1}A - B)^{-1} & -(A - BA^{-1}B)^{-1} \end{bmatrix} \begin{matrix} \uparrow \\ \uparrow \end{matrix} -i \begin{bmatrix} E & -F \\ F & -E \end{bmatrix}, \text{ say.} \end{aligned}$$

This allows us to consider

$$\phi s^{-1} \Lambda = \begin{bmatrix} \phi & | & \phi \end{bmatrix} \begin{bmatrix} E & -F \\ F & -E \end{bmatrix} \begin{bmatrix} \Omega & | & 0 \\ \hline 0 & | & -\Omega \end{bmatrix}$$

with the complex variable i cancelling. So,

$$\phi s^{-1} \Lambda = \begin{bmatrix} \phi & | & \phi \end{bmatrix} \begin{bmatrix} E\Omega & F\Omega \\ F\Omega & E\Omega \end{bmatrix} = \begin{bmatrix} \phi E\Omega + \phi F\Omega & | & \phi F\Omega + \phi E\Omega \end{bmatrix}$$

$$\begin{aligned}
\text{where } \Phi E \Omega + \Phi F \Omega &= \Phi((A^{-1} + B^{-1})(AB^{-1} - BA^{-1})^{-1})\Omega \\
&= \Phi((A^{-1} + B^{-1})((A - B)(A^{-1} + B^{-1}))^{-1})\Omega \\
&= \Phi(A - B)^{-1}\Omega \\
&= \frac{1}{2}\Phi m^{-1}\Omega^{-1}\Omega = \frac{1}{2}\Phi m^{-1}
\end{aligned}$$

recalling that

$$m = \Phi^T M_a \Phi.$$

This calculation may be repeated for $\Phi \Lambda s^{-1}$, thus

$$\begin{aligned}
\Phi \Lambda s^{-1} &= [\Phi \mid \Phi] \begin{bmatrix} \Omega & \mid & 0 \\ \hline 0 & \mid & -\Omega \end{bmatrix} \begin{bmatrix} E & -F \\ F & -E \end{bmatrix} \\
&= [\Phi \mid \Phi] \begin{bmatrix} \Omega E & -\Omega F \\ -\Omega F & \Omega E \end{bmatrix} \\
&= [\Phi \Omega E - \Phi \Omega F \mid -\Phi \Omega F + \Phi \Omega E]
\end{aligned}$$

where $\Phi \Omega E - \Phi \Omega F = \Phi \Omega(E - F)$

$$\begin{aligned}
&= \Phi \Omega(B^{-1} - A^{-1})[(A + B)(B^{-1} - A^{-1})]^{-1} \\
&= \Phi \Omega(B^{-1} - A^{-1})(B^{-1} - A^{-1})^{-1}(A + B)^{-1} \\
&= \Phi \Omega(A + B)^{-1} \\
&= \frac{1}{2}\Phi \Omega \Omega^{-1} m^{-1} = \frac{1}{2}\Phi m^{-1}
\end{aligned}$$

as before.

From this we may say that

$$\begin{aligned}
(a) \quad 2M_a \Phi s^{-1} \Lambda s^{-1} \Lambda \Phi^T M_a &= 2M_a \Phi \Lambda s^{-1} \Lambda s^{-1} \Phi^T M_a \\
&= 2M_a \Phi s^{-1} \Lambda^2 s^{-1} \Phi^T M_a \\
&= \{ M_a \Phi m^{-2} \Phi^T M_a \text{ ((} n \times n \text{) version)} \}.
\end{aligned}$$

$$(b) \quad 2M_a \Phi \Lambda s^{-1} \Lambda s^{-1} \Lambda \Phi^T M_a = 2M_a \Phi s^{-1} \Lambda s^{-1} \Phi^T M_a$$

$$\begin{aligned}
&= -2M_a \phi s^{-1} \Lambda^2 s^{-1} \Lambda \phi^T M_a \\
&= -2M_a \phi \Lambda s^{-1} \Lambda^2 s^{-1} \phi^T M_a - 0.
\end{aligned}$$

$$(c) \quad -2M_a \phi \Lambda s^{-1} \Lambda^2 s^{-1} \Lambda \phi^T M_a = \{-M_a \phi m^{-1} \Lambda^2 m^{-1} \phi^T M_a \text{ ((n} \times \text{n) version)}\}.$$

Effectively, the two are one and the same problem. The same may also be found to be true if we use $[...]_{T_a}$ to conduct the analysis. This is encouraging insofar as we may see that we have moved from a $(n \times n)$ undamped problem to a $(2n \times 2n)$ undamped problem (but permitting the inclusion of damping if so desired) without affecting the original expressions. It may therefore be asserted that the $(2n \times 2n)$ problem is just a natural extension of the $(n \times n)$ problem.

5.7 Error Expressions

Error expressions for the damped case may now be formulated, in a similar fashion to that described in Chapter 4. For brevity, calculations using $[...]_{S_a}$ only are described here. Full tables of possible error expressions are given in Tables 5.1 to 5.4. Firstly, to derive an error expression, S_a and T_a must be projected onto the corresponding subspace so that

$$\begin{aligned}
\epsilon_{\text{error}}^1 &= P_{S_a}^T (S - S_a) P_{S_a} \\
&= S_a \chi s^{-1} \chi^T (S - S_a) \chi s^{-1} \chi^T S_a \\
&= S_a \chi s^{-1} (2\Lambda - s) s^{-1} \chi^T S_a \\
&= \begin{bmatrix} 0 & M_a \\ M_a & 0 \end{bmatrix} \begin{bmatrix} \phi \\ \phi \Lambda \end{bmatrix} s^{-1} (2\Lambda - s) s^{-1} \begin{bmatrix} \phi^T & \Lambda \phi^T \end{bmatrix} \begin{matrix} 0 & M_a \\ I_a^{M_a} & 0 \end{matrix}
\end{aligned}$$

so that

$$C_{\text{error}} = M_a \phi \Lambda s^{-1} (2\Lambda - s) s^{-1} \Lambda \phi^T M_a$$

$$M_{\text{error}}^1 = M_a \phi s^{-1} (2\Lambda - s) s^{-1} \Lambda \phi^T M_a$$

$$M_{\text{error}}^2 = M_a \phi \Lambda s^{-1} (2\Lambda - s) s^{-1} \phi^T M_a$$

$$O'_{\text{error}} = M_a \phi s^{-1} (2\Lambda - s) s^{-1} \phi^T M_a$$

and for the T matrix

$$\begin{aligned} \epsilon^2 &= P S_a^T (T - T_a) P S_a \\ &= S_a X s^{-1} X^T (T - T_a) X s^{-1} X^T S_a \\ &= S_a X s^{-1} (2\Lambda^2 - X^T T_s X) s^{-1} X^T S_a \\ &= S_a X s^{-1} (2\Lambda^2 - t) s^{-1} X^T S_a \\ &= \begin{bmatrix} 0 & M_a \\ M_a & 0 \end{bmatrix} \begin{bmatrix} \phi \\ \phi \Lambda \end{bmatrix} s^{-1} (2\Lambda^2 - t) s^{-1} \begin{bmatrix} \phi^T & \phi \Lambda^T \end{bmatrix} \begin{bmatrix} 0 & M_a \\ M_a & 0 \end{bmatrix} \end{aligned}$$

$$\text{so, } K_{\text{error}} = M_a \phi \Lambda s^{-1} (2\Lambda^2 - t) s^{-1} \Lambda \phi^T M_a$$

$$M_{\text{error}}^3 = M_a \phi s^{-1} (2\Lambda^2 - t) s^{-1} \phi^T M_a$$

$$O_{\text{error}}^2 = M_a \phi \Lambda s^{-1} (2\Lambda^2 - t) s^{-1} \phi^T M_a$$

$$O_{\text{error}}^3 = M_a \phi s^{-1} (2\Lambda^2 - t) s^{-1} \Lambda \phi^T M_a.$$

Alternatively S_a and T_a may be projected onto the subspace described by the corresponding analytical modes. Here, the analytical modes are assumed to be real (i.e. analytical system has no, or possibly proportional, damping).

$$\text{So, } \epsilon^3 = S_a (X s^{-1} 2\Lambda s^{-1} X^T - \frac{1}{2} X_a \Lambda_a^{-1} X_a^T) S_a$$

$$\begin{aligned}
&= \begin{bmatrix} 0 & M_a \\ M_a & 0 \end{bmatrix} \begin{bmatrix} [\phi] s^{-1} 2\Lambda s^{-1} [\phi^T & \Lambda \phi^T] \\ [\phi \Lambda] \end{bmatrix} \\
&- \frac{1}{2} \begin{bmatrix} \phi_a \\ \phi_a \Lambda_a \end{bmatrix} \Lambda_a^{-1} \begin{bmatrix} \phi_a^T & \Lambda_a \phi_a^T \end{bmatrix} \begin{bmatrix} 0 & M_a \\ M_a & 0 \end{bmatrix}
\end{aligned}$$

that is

$$C_{\text{error}} = M_a \phi \Lambda s^{-1} 2\Lambda s^{-1} \Lambda \phi^T M_a - \frac{1}{2} M_a \phi_a \Lambda_a \phi_a^T M_a$$

$$M_{\text{error}}^1 = M_a \phi s^{-1} 2\Lambda s^{-1} \Lambda \phi^T M_a - \frac{1}{2} M_a \phi_a \phi_a^T M_a$$

$$M_{\text{error}}^2 = M_a \phi \Lambda s^{-1} 2\Lambda s^{-1} \phi^T M_a - \frac{1}{2} M_a \phi_a \phi_a^T M_a$$

$$O'_{\text{error}} = M_a \phi s^{-1} 2\Lambda s^{-1} \phi^T M_a - \frac{1}{2} M_a \phi_a \Lambda_a^{-1} \phi_a^T M_a$$

and for the T matrix

$$\begin{aligned}
\epsilon^4 &= S_a (X s^{-1} 2\Lambda^2 s^{-1} X^T - \frac{1}{2} X_a X_a^T) S_a \\
&= \begin{bmatrix} 0 & M_a \\ M_a & 0 \end{bmatrix} \begin{bmatrix} [\phi] s^{-1} 2\Lambda^2 s^{-1} [\phi^T & \Lambda \phi^T] \\ [\phi \Lambda] \end{bmatrix} \\
&- \frac{1}{2} \begin{bmatrix} \phi_a \\ \phi_a \Lambda_a \end{bmatrix} \begin{bmatrix} \phi_a^T & \Lambda_a \phi_a^T \end{bmatrix} \begin{bmatrix} 0 & M_a \\ M_a & 0 \end{bmatrix}
\end{aligned}$$

$$K_{\text{error}} = M_a \phi \Lambda s^{-1} 2\Lambda^2 s^{-1} \Lambda \phi^T M_a - \frac{1}{2} M_a \phi_a \Lambda_a^2 \phi_a^T M_a$$

$$M_{\text{error}}^3 = M_a \phi s^{-1} 2\Lambda^2 s^{-1} \phi^T M_a - \frac{1}{2} M_a \phi_a \phi_a^T M_a$$

$$O_{\text{error}}^2 = M_a \phi s^{-1} 2\Lambda^2 s^{-1} \Lambda \phi^T M_a - \frac{1}{2} M_a \phi_a \Lambda_a \phi_a^T M_a$$

$$O_{\text{error}}^3 = M_a \phi \Lambda s^{-1} 2\Lambda^2 s^{-1} \phi^T M_a - \frac{1}{2} M_a \phi_a \Lambda_a \phi_a^T M_a$$

Finally, introducing the approximation $s = 2\Lambda$ in a similar fashion to the $m = I$ approximation of Chapter 4 gives:

$$M_{\text{error}} = \frac{1}{2} M_a \Phi \Phi^T M_a - \frac{1}{2} M_a \Phi_a \Phi_a^T M_a,$$

$$K_{\text{error}} = \frac{1}{2} M_a \Phi \Lambda^2 \Phi^T M_a - \frac{1}{2} M_a \Phi_a \Lambda_a^2 \Phi_a^T M_a,$$

$$D_{\text{error}} = \frac{1}{2} M_a \Phi \Lambda^{-1} \Phi^T M_a - \frac{1}{2} M_a \Phi_a \Lambda_a^{-1} \Phi_a^T M_a,$$

$$C_{\text{error}} = \frac{1}{2} M_a \Phi \Lambda \Phi^T M_a - \frac{1}{2} M_a \Phi_a \Lambda_a \Phi_a^T M_a.$$

5.8 Numerical Experiments

In order to investigate the potential of some of these error expressions, example 3 from Chapter 2 was utilised, which has non-proportional damping. That is, the first element has damping equal to 1% of that of the stiffness. For reasons discussed earlier (that is, the higher modes are analytical functions and would not be measurable in practice), only the first $n/2$ modes were used and compared with the correct form of the error matrix. The term 'correct' here means the form that the error matrix would take in the ideal situation where all the modes were known. Although this is unachievable in practice, it is included in order to examine the quality of results obtained using 1 to 5 modes (i.e. the likely practical situation).

Two examples are included here, where the 'incorrect' analytical model is set up as follows:

Test 1:

$C_a = 0$; $M_a = M$ (i.e. mass matrix correct, and adopting a correct normalisation); first element of $K_a = 0.5$ x first element of K , all other elements being correct.

Test 2:

$C_a = 0$; first element of $M_a = 0.5$ x first element of M (i.e.

massmatrix incorrect; normalisation errors exist); first element of $K_a = 0.5 \times$ first element of K , all other elements being correct.

The error expressions marked with an asterisk in Table 5.1 were calculated and the results for mass, damping and stiffness are presented for the two tests as Figures 5.1 to 5.6. Also, the elements of these three matrices for the two examples, with 5 or all modes used, are presented as Figures 5.7 to 5.12. The errors when using all the modes in the second test are those due to a normalisation using M_a .

5.9 Discussion of Error Expressions

In the preceding sections, proposals have been developed for the examination and comparison of an undamped analytical FE model with measured complex modes and complex eigenvalues, which represents the most likely practical situation. The damping has been taken as viscous, and no attempt has been made to eliminate it with efforts to convert complex modes to normal modes. Indeed, the discussion and examples of Chapter 2 illustrate that this is an extremely difficult, if not impossible, task for an incomplete system. The damping in the example is set up as $0.01 \times$ the terms in the stiffness matrix in the first element only, thereby introducing non-proportionality into the system.

The initial results, based upon the numerical experiment, are encouraging. As was expanded upon in Chapter 4, limitations on the expectations of error analysis do exist, but these apply equally to the damped case as to the undamped case. No serious additional problems emerge from the treatment of the damped problem.

Indeed, if damping exists in the system, some headway may be made towards establishing where the damping is concentrated by utilising the damping error expressions. Again, the same assertion that the region detected may only be as small as the wavelength of the highest mode applies.

As may be observed from the diagrams, the asymmetry of the mass matrix error expression is insignificant. It is brought about as a result of the non-proportionality, and it would not be observed if no damping or proportional damping existed (as simple tests have demonstrated). The normalisation does not affect the asymmetry, as may be observed in Figure 5.10 with all the modes included. Here, the only unsymmetrical terms are those coupled to the damping, and the (7x7) matrix in the lower right-hand corner is symmetric. So, in practice, many of the mass error expressions are extremely similar, since here non-proportionality has been imposed and yet asymmetry is small. Of major significance is the fact that in the second test, when an incorrect mass matrix was introduced, with the consequent effect on normalisation, the first five modes extracted nearly all the information concerning mass error that was available and the quality of damping error and stiffness error was affected very little.

An inevitable practical drawback is the fact that the error expressions are fairly involved and performing the normalisation may be difficult because of the use of complex arithmetic. However, this is nothing more than a reflection of the complexity of the real world, and must be accepted if an accurate model of the behaviour of the structure is to emerge. One note here is that the

inversion of s or t , which are complex matrices, should not present too many computational difficulties since they will only be as large as the number of modes used (say, at most (20×20)).

The tables show an enormous selection of error expressions to use. However, as was indicated for the undamped case, they should nearly all perform equally well, with the key issues remaining a good normalisation and quantity and quality of the measured information.

5.10 Hybrid Matrices

The use of hybrid matrices in the $(2n \times 2n)$ example is limited since they necessarily need to be derived in the $(2n \times 2n)$ environment and although the hybrid S and T matrices (S^H and T^H) will satisfy the necessary orthogonality and eigenvalue equations, the individual components of these matrices (e.g. M , C , K) cannot readily be extracted since other non-zero matrices will have been formed which affect the solution of the necessary constraints. In cases of light damping it may be possible to assume that these non-zero matrices are zero, and so approximations to the improved M , C and K will be extracted. As a result, these matrices will only approximately satisfy the necessary constraints. The nature or acceptability of these approximate solutions will depend largely upon the individual problem under investigation and the degree of damping that exists.

In parallel with the undamped case, the hybrid solutions for the S and T matrices are given by

$$\begin{aligned}
S_{S_a}^H &= P_{S_a}^T S P_{S_a} + (I - P_{S_a}^T) S_a (I - P_{S_a}) \\
&= S_a X_s^{-1} X^T S X_s^{-1} X^T S_a + (I - S_a X_s^{-1} X^T) S_a (I - X_s^{-1} X^T S_a) \\
&= 2 S_a X_s^{-1} \Lambda_s^{-1} X^T S_a + S_a - S_a X_s^{-1} X^T S_a
\end{aligned}$$

and

$$\begin{aligned}
T_{S_a}^H &= P_{S_a}^T T P_{S_a} + (I - P_{S_a}^T) T_a (I - P_{S_a}) \\
&= S_a X_s^{-1} X^T T X_s^{-1} X^T S_a + (I - S_a X_s^{-1} X^T) T_a (I - X_s^{-1} X^T S_a) \\
&= -2 S_a X_s^{-1} \Lambda_s^{-1} X^T T_a + T_a - S_a X_s^{-1} X^T T_a - T_a X_s^{-1} X^T S_a \\
&\quad + S_a X_s^{-1} X^T T_a X_s^{-1} X^T S_a
\end{aligned}$$

or, with respect to $[...]_{T_a}$

$$\begin{aligned}
S_{T_a}^H &= P_{T_a}^T S P_{T_a} + (I - P_{T_a}^T) S_a (I - P_{T_a}) \\
&= T_a X_t^{-1} X^T S X_t^{-1} X^T T_a + (I - T_a X_t^{-1} X^T) S_a (I - X_t^{-1} X^T T_a) \\
&= 2 T_a X_t^{-1} \Lambda_t^{-1} X^T S_a + S_a - T_a X_t^{-1} X^T S_a - S_a X_t^{-1} X^T T_a \\
&\quad + T_a X_t^{-1} X^T S_a X_t^{-1} X^T T_a
\end{aligned}$$

and

$$\begin{aligned}
T_{T_a}^H &= P_{T_a}^T T P_{T_a} + (I - P_{T_a}^T) T_a (I - P_{T_a}) \\
&= T_a X_t^{-1} X^T T X_t^{-1} X^T T_a + (I - T_a X_t^{-1} X^T) T_a (I - X_t^{-1} X^T T_a) \\
&= -2 T_a X_t^{-1} \Lambda_t^{-1} X^T T_a + T_a - T_a X_t^{-1} X^T T_a
\end{aligned}$$

These expressions then will satisfy the necessary constraints, but the system needs to remain as a $(2n \times 2n)$ problem for further analysis, which may itself be desirable since this in no way limits its use.

5.11 Origins of Transfer Function Expression

Analysing the problem in a $(2n \times 2n)$ normed space allows the derivation of the expression for the transfer function in a vector space environment. We have

$$S = \begin{bmatrix} C & M \\ M & O \end{bmatrix}; \quad T = \begin{bmatrix} K & 0 \\ 0 & -M \end{bmatrix} \text{ with } X = \begin{bmatrix} \Phi \\ \Phi\Lambda \end{bmatrix}$$

so that

$$SX\Lambda + TX = 0$$

with $X^T SX = 2A$ and $X^T TX = -2\Lambda^2$.

It is therefore possible to say that

$$X^T(\mu S + T)X = 2(\mu\Lambda - \Lambda^2).$$

If we have a complete set of modes $(X)^{-1}$ and $(X^T)^{-1}$ will exist so

$$(\mu S + T) = 2(X^T)^{-1}(\mu\Lambda - \Lambda^2)(X)^{-1}.$$

We have what is effectively a change of basis,

$$(\mu S + T)^{-1} = \frac{1}{2}X(\mu\Lambda - \Lambda^2)^{-1}X^T$$

$$\text{where } (\mu S + T) = \begin{bmatrix} \mu C + K & \mu M \\ \mu M & -M \end{bmatrix}$$

The inverse of $(\mu S + T)$ is given by

$$(\mu S + T)^{-1} = \begin{bmatrix} (\mu^2 M + \mu C + K)^{-1} & (\mu^2 M + \mu C + K)^{-1} \mu \\ (\mu^2 M + \mu C + K)^{-1} \mu & (\mu^2 M + \mu C + K)^{-1} \mu^2 - M^{-1} \end{bmatrix}$$

$$\text{since } \begin{bmatrix} (\mu^2 M + \mu C + K)^{-1} & (\mu^2 M + \mu C + K)^{-1} \mu \\ (\mu^2 M + \mu C + K)^{-1} \mu & (\mu^2 M + \mu C + K)^{-1} \mu^2 - M^{-1} \end{bmatrix} \begin{bmatrix} \mu C + K & \mu M \\ \mu M & -M \end{bmatrix} = \begin{bmatrix} I & 0 \\ 0 & I \end{bmatrix}$$

$$\text{and } \begin{bmatrix} \mu C + K & \mu M \\ \mu M & -M \end{bmatrix} \begin{bmatrix} (\mu^2 M + \mu C + K)^{-1} & (\mu^2 M + \mu C + K)^{-1} \mu \\ (\mu^2 M + \mu C + K)^{-1} \mu & (\mu^2 M + \mu C + K)^{-1} \mu^2 - M^{-1} \end{bmatrix} = \begin{bmatrix} 0 & 0 \\ 0 & I \end{bmatrix}$$

Therefore

$$\begin{aligned} & \begin{bmatrix} (\mu^2 M + \mu C + K)^{-1} & (\mu^2 M + \mu C + K)^{-1} \mu \\ (\mu^2 M + \mu C + K)^{-1} \mu & (\mu^2 M + \mu C + K)^{-1} \mu^2 - M^{-1} I \end{bmatrix} = \frac{1}{2} \begin{bmatrix} \Phi \\ \Phi \Lambda \end{bmatrix} [\mu \Lambda - A']^{-1} [\Phi^T \Lambda \Phi^T] \\ & = \begin{bmatrix} \frac{1}{2} \Phi (\mu \Lambda - \Lambda^2)^{-1} \Phi^T & \frac{1}{2} \Phi (\mu I - \Lambda)^{-1} \Phi^T \\ \frac{1}{2} \Phi (\mu I - \Lambda)^{-1} \Phi^T & \frac{1}{2} \Phi \Lambda (\mu I - \Lambda)^{-1} \Phi^T \end{bmatrix} \end{aligned}$$

giving three possible expressions for the transfer function of

$$H_1(\mu) = (\mu^2 M + \mu C + K)^{-1} = \frac{1}{2} \Phi (\mu \Lambda - \Lambda^2)^{-1} \Phi^T$$

$$H_2(\mu) = (\mu^2 M + \mu C + K)^{-1} = \frac{1}{2\mu} \Phi (\mu I - \Lambda)^{-1} \Phi^T$$

$$\begin{aligned} H_3(\mu) &= (\mu^2 M + \mu C + K)^{-1} = \frac{1}{2\mu^2} \Phi \Lambda (\mu I - \Lambda)^{-1} \Phi^T + \frac{1}{\mu^2} M^{-1} \\ &= \frac{1}{2\mu^2} \Phi \Lambda (\mu I - \Lambda)^{-1} \Phi^T + \frac{1}{2\mu^2} \Phi \Phi^T \end{aligned}$$

However, we know that for a complete system

$$\frac{1}{2} \Phi \Lambda^{-1} \Phi^T = 0$$

therefore

$$\frac{1}{2} \Phi (\mu \Lambda - \Lambda^2) \Phi^T = \frac{1}{2} \sum_{k=1}^{2n} x_k \left\{ \frac{1}{\lambda_k (\mu - \lambda_k)} \right\} x_k$$

and applying partial fractions gives

$$\begin{aligned} \frac{1}{2} \Phi (\mu \Lambda - \Lambda^2) \Phi^T &= \frac{1}{2\mu} \sum_{k=1}^{2n} x_k \left\{ \frac{1}{\lambda_k} + \frac{1}{(\mu - \lambda_k)} \right\} x_k^T \\ &= \frac{1}{2\mu} \left\{ \Phi \Lambda^{-1} \Phi^T + \Phi (\mu I - \Lambda)^{-1} \Phi^T \right\} \\ &= \frac{1}{2\mu} \Phi (\mu I - \Lambda)^{-1} \Phi^T \end{aligned}$$

Also, we may see that

$$\begin{aligned} \frac{1}{2\mu} \Phi (\mu I - \Lambda)^{-1} \Phi^T &= \frac{1}{2\mu} \sum_{k=1}^{2n} x_k \left\{ \frac{1}{(\mu - \lambda_k)} \right\} x_k^T \\ &= \frac{1}{2\mu} \sum_{k=1}^{2n} x_k \left\{ \frac{\lambda_k}{\mu(\mu - \lambda_k)} + \frac{(\mu - \lambda_k)}{\mu(\mu - \lambda_k)} \right\} x_k^T \end{aligned}$$

$$\begin{aligned}
&= \frac{1}{2u^2} \sum_{k=1}^{2n} x_k \left(\frac{\lambda_k}{(\mu - \lambda_k)} + 1 \right) x_k \\
&= \frac{1}{2u^2} \left\{ \Phi \Lambda (\mu - \Lambda)^{-1} \Phi^T + \Phi \Phi^T \right\}
\end{aligned}$$

so that all three expressions are effectively identical. $H_1(\mu)$ is the expression used for curvefitting since no multiplication or division of the variable μ appears. For low frequencies, the transfer function matrix of this expression approximates the flexibility matrix. Again, the frequency response function may be obtained by setting $\mu = i\Omega_j$ thus,

$$\begin{aligned}
H(i\Omega_j) &= \frac{1}{2} \Phi (i\Omega_j \Lambda - \Lambda^2)^{-1} \Phi^T \\
&= \frac{1}{2} \sum_{k=1}^{2n} x_k \frac{1}{\lambda_k (i\Omega_j - \lambda_k)} x_k^T
\end{aligned}$$

so we may see that the residue a_k is given by $x_k x_k^T / 2\lambda_k$, for this particular normalisation. If the normalisation $X^T S X = I$ were used, the residue would be simply $x_k x_k^T$. Therefore

$$\begin{aligned}
H(i\Omega_j) &= \sum_{k=1}^{2n} \frac{a_k}{(i\Omega_j - \lambda_k)} \\
&= \sum_{k=1}^n \frac{a_k}{i\Omega_j - \lambda_k} + \frac{\bar{a}_k}{i\Omega_j - \lambda_k} .
\end{aligned}$$

5.12 Overview

This chapter has set out to extend the analysis of the undamped problem of Chapter 4 to the viscously damped problem. This is in an effort to bring closer together the comparison between experiment and analysis. Curvefitting routines for experimental results usually fit an analytical function involving viscous damping (frequency response function), so it is logical to extend the

error analysis to incorporate this. The analysis has been directed towards the comparison of measured **complex** modes and frequencies with an undamped analytical FE model.

Possible ways of setting up the problem in the $(2n \times 2n)$ complex space and possible normalisations have been identified, and in each case the most convenient form has been selected for the analysis. A symmetric form for the problem was chosen so that the problem became self-dual, therefore allowing the extra **considerations** required by adopting a dual basis to be suppressed by making it identical to that of the primal. The normalisation chosen was that which made the problem identical to the undamped problem of Chapter 4 when **damping** is set to zero. That is, the phase shift of the modes tends to 0° or 180° .

Incomplete measured mass, damping and stiffness matrices were formulated, in order to allow an error analysis to be conducted, in the same fashion as that of the undamped case. In general, the numerical experiments demonstrated a strong similarity between the degree of success attained for the damped problem with that of the undamped problem. The asymmetry of the mass matrix error expressions was found to be produced by the non-proportionality of the system and, for the fairly typical example used, was observed as minimal. In general it was found that the move from the $(n \times n)$ undamped problem to the $(2n \times 2n)$ damped problem introduced relatively few additional difficulties, but allowed a more rigorous approach to error analysis using measured complex modes. The numerical experiments have indicated the possibility of detecting areas of concentrated damping using this technique and so offer the potential of rethinking the analysis in order to introduce a damping

matrix which reflects the observed measurements.

The possibility of **improving** mass, damping and stiffness matrices using a hybrid type of analysis was found to be limited to the $(2n \times 2n)$ problem and extracting the parts of matrices updated is not feasible if the necessary constraints are to be satisfied. Finally, a derivation of the frequency response function matrix used in curvefitting routines is described to demonstrate how the experiment and analysis are related when the problem is posed with the inclusion of viscous damping.

The way forward for a realistic comparison of likely types of measured and analytical information has been proposed. Indeed, an error matrix of zeros is of use here, since then one may assert that the mass and stiffness matrices derived for the undamped problem have been verified using measured information. This is a practical alternative, since it is unsound to compare undamped normal modes with measured complex ones for the purpose of model verification.

The effectiveness of the error analysis using *th*s and *pre*-ceding chapters hinges upon the fact that the measured modes need to be known at all the nodes of an FE model. In general, this is completely unachievable - since many of the nodes will be internal and therefore inaccessible to measurement. The complete mode needs to be determined by some sort of expansion process, and consideration of this problem is the theme of the next chapter.

| | | $\text{Proj}_{S_a}(\cdot) \mathcal{V}_{2m} - \text{Proj}_{S_a}(\cdot_a) \mathcal{V}_{2m}$ |
|----------|------------------------|---|
| S MATRIX | C_{error}^* | $M_a \phi \Lambda s^{-1} (2\Lambda - s) s^{-1} \Lambda \phi^T M_a$ |
| | M_{error}^1 | $M_a \phi \Lambda s^{-1} (2\Lambda - s) s^{-1} \phi^T M_a$ |
| | M_{error}^2 * | $M_a \phi s^{-1} (2\Lambda - s) s^{-1} \Lambda \phi^T M_a$ |
| | O_{error}^1 | $M_a \phi s^{-1} (2\Lambda - s) s^{-1} \phi^T M_a$ |
| T MATRIX | K_{error}^* | $M_a \phi \Lambda s^{-1} (2\Lambda^2 - t) s^{-1} \Lambda \phi^T M_a$ |
| | M_{error}^3 | $M_a \phi s^{-1} (2\Lambda^2 - t) s^{-1} \phi^T M_a$ |
| | O_{error}^2 | $M_a \phi \Lambda s^{-1} (2\Lambda^2 - t) s^{-1} \phi^T M_a$ |
| | O_{error}^3 | $M_a \phi s^{-1} (2\Lambda^2 - t) s^{-1} \Lambda \phi^T M_a$ |

TABLE 5.1: Error Matrices

| | | $\text{Proj}_s(\cdot) \mathcal{U}_{\gamma_m} - \text{Proj}_s(\cdot) \mathcal{U}_{\gamma_m}^A$ | |
|----------|----------------------|--|---|
| | | NO APPROXIMATION | APPROXIMATION $s = 2\Lambda$ |
| S MATRIX | C error | $M_a \phi \Lambda s^{-1} 2\Lambda s^{-1} \Lambda \phi^T M_a - \frac{1}{2} M_a \phi \Lambda \phi^T M_a$ | $\frac{1}{2} M_a \phi \Lambda \phi^T M_a - \frac{1}{2} M_a \phi \Lambda \phi^T M_a$ |
| | M ¹ error | $M_a \phi s^{-1} 2\Lambda s^{-1} \Lambda \phi^T M_a - \frac{1}{2} M_a \phi \phi^T M_a$ | $\frac{1}{2} M_a \phi \phi^T M_a - \frac{1}{2} M_a \phi \phi^T M_a$ |
| | M ² error | $M_a \phi \Lambda s^{-1} 2\Lambda s^{-1} \phi^T M_a - \frac{1}{2} M_a \phi \phi^T M_a$ | $\frac{1}{2} M_a \phi \phi^T M_a - \frac{1}{2} M_a \phi \phi^T M_a$ |
| | O ¹ error | $M_a \phi s^{-1} 2\Lambda s^{-1} \phi^T M_a - \frac{1}{2} M_a \phi \Lambda^{-1} \phi^T M_a$ | $\frac{1}{2} M_a \phi \Lambda^{-1} \phi^T M_a - \frac{1}{2} M_a \phi \Lambda^{-1} \phi^T M_a$ |
| T MATRIX | K error | $M_a \phi \Lambda s^{-1} 2\Lambda^2 s^{-1} \Lambda \phi^T M_a - \frac{1}{2} M_a \phi \Lambda \phi^T M_a$ | $\frac{1}{2} M_a \phi \Lambda^2 \phi^T M_a - \frac{1}{2} M_a \phi \Lambda^2 \phi^T M_a$ |
| | M ³ error | $M_a \phi s^{-1} 2\Lambda^2 s^{-1} \phi^T M_a - \frac{1}{2} M_a \phi \phi^T M_a$ | $\frac{1}{2} M_a \phi \phi^T M_a - \frac{1}{2} M_a \phi \phi^T M_a$ |
| | O ² error | $M_a \phi \Lambda s^{-1} 2\Lambda^2 s^{-1} \phi^T M_a - \frac{1}{2} M_a \phi \Lambda \phi^T M_a$ | $\frac{1}{2} M_a \phi \Lambda \phi^T M_a - \frac{1}{2} M_a \phi \Lambda \phi^T M_a$ |
| | O ³ error | $M_a \phi s^{-1} 2\Lambda^2 s^{-1} \Lambda \phi^T M_a - \frac{1}{2} M_a \phi \Lambda \phi^T M_a$ | $\frac{1}{2} M_a \phi \Lambda \phi^T M_a - \frac{1}{2} M_a \phi \Lambda \phi^T M_a$ |

TABLE 5.2: Error Matrices

| | | $\text{Proj}_{\Gamma_a}(\cdot)v_{2^m} - \text{Proj}_{\Gamma_a}(\cdot)v_{2^m}$ |
|----------|-------------|---|
| S MATRIX | C error | $K_a \phi t^{-1}(2\Lambda - s)t^{-1} \phi^T K_a$ |
| | M^1 error | $-K_a \phi t^{-1}(2\Lambda - s)t^{-1} \Lambda \phi^T M_a$ |
| | M^2 error | $M_a \phi \Lambda t^{-1}(2\Lambda - s)t^{-1} \phi^T K_a$ |
| | O^1 error | $M_a \phi \Lambda t^{-1}(2\Lambda - s)t^{-1} \Lambda \phi^T M_a$ |
| T MATRIX | K error | $K_a \phi t^{-1}(2\Lambda^2 - t)t^{-1} \phi^T K_a$ |
| | M^3 error | $M_a \phi \Lambda t^{-1}(2\Lambda^2 - t)t^{-1} \Lambda \phi^T M_a$ |
| | O^2 error | $M_a \phi \Lambda t^{-1}(2\Lambda^2 - t)t^{-1} \phi^T K_a$ |
| | O^3 error | $K_a \phi t^{-1}(2\Lambda^2 - t)t^{-1} \Lambda \phi^T M_a$ |

TABLE 5.3: Error Matrices

| | $\text{Proj}_{T_a}(\cdot) \mathcal{V}_{\tau_a}$ | $\text{Proj}_{T_a}(\cdot) \mathcal{V}_{\tau_a} - \text{Proj}_{T_a}(\cdot) \mathcal{V}_{\tau_a}$ |
|----------------------|---|---|
| | NO APPROXIMATION | APPROXIMATION $t = -2\Lambda^2$ |
| C error | $K_a \phi t^{-1} 2\Lambda t^{-1} \phi^T K_a - \frac{1}{2} K_a \phi \Lambda^{-3} \phi^T K_a$ | $\frac{1}{2} K_a \phi \Lambda^{-3} \phi^T K_a - \frac{1}{2} K_a \phi \Lambda^{-3} \phi^T K_a$ |
| M ¹ error | $K_a \phi t^{-1} 2\Lambda t^{-1} \Lambda \phi^T M_a - \frac{1}{2} K_a \phi \Lambda^{-2} \phi^T M_a$ | $\frac{1}{2} K_a \phi \Lambda^{-2} \phi^T M_a - \frac{1}{2} K_a \phi \Lambda^{-2} \phi^T M_a$ |
| M ² error | $M_a \phi \Lambda t^{-1} 2\Lambda t^{-1} \phi^T K_a - \frac{1}{2} M_a \phi \Lambda^{-2} \phi^T K_a$ | $\frac{1}{2} M_a \phi \Lambda^{-2} \phi^T K_a - \frac{1}{2} M_a \phi \Lambda^{-2} \phi^T K_a$ |
| O ¹ error | $M_a \phi \Lambda t^{-1} 2\Lambda t^{-1} \Lambda \phi^T M_a - \frac{1}{2} M_a \phi \Lambda^{-1} \phi^T M_a$ | $\frac{1}{2} M_a \phi \Lambda^{-1} \phi^T M_a - \frac{1}{2} M_a \phi \Lambda^{-1} \phi^T M_a$ |
| K error | $K_a \phi t^{-1} 2\Lambda^2 t^{-1} \phi^T K_a - \frac{1}{2} K_a \phi \Lambda^{-2} \phi^T K_a$ | $\frac{1}{2} K_a \phi \Lambda^{-2} \phi^T K_a - \frac{1}{2} K_a \phi \Lambda^{-2} \phi^T K_a$ |
| M ³ error | $M_a \phi \Lambda t^{-1} 2\Lambda^2 t^{-1} \Lambda \phi^T M_a - \frac{1}{2} M_a \phi \phi^T M_a$ | $\frac{1}{2} M_a \phi \phi^T M_a - \frac{1}{2} M_a \phi \phi^T M_a$ |
| O error | $M_a \phi \Lambda t^{-1} 2\Lambda^2 t^{-1} \phi^T K_a - \frac{1}{2} M_a \phi \Lambda^{-1} \phi^T K_a$ | $\frac{1}{2} M_a \phi \Lambda^{-1} \phi^T K_a - \frac{1}{2} M_a \phi \Lambda^{-1} \phi^T K_a$ |
| O ³ error | $K_a \phi t^{-1} 2\Lambda^2 t^{-1} \Lambda \phi^T M_a - \frac{1}{2} K_a \phi \Lambda^{-1} \phi^T M_a$ | $K_a \phi \Lambda^{-1} \phi^T M_a - \frac{1}{2} K_a \phi \Lambda^{-1} \phi^T M_a$ |

TABLE 5.4: E

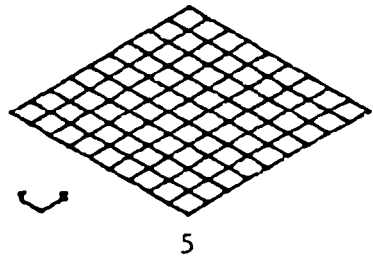
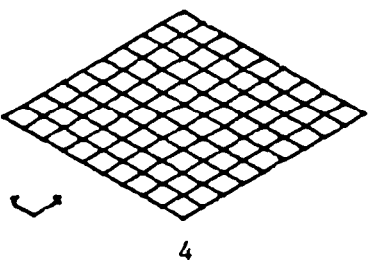
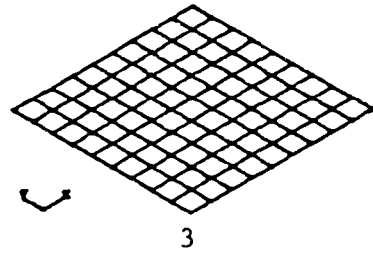
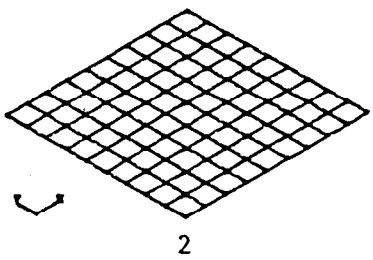
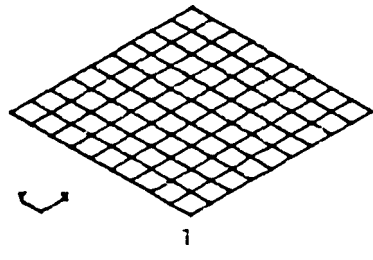
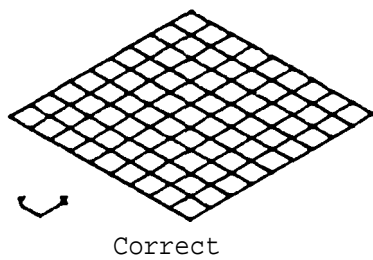


Figure 5.1: Mass Error Test 1 ($M=M_a$)

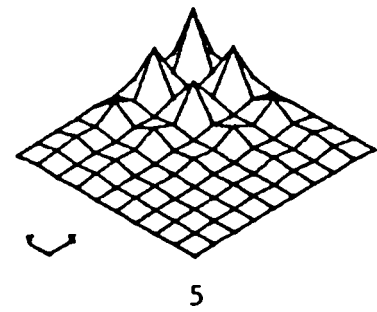
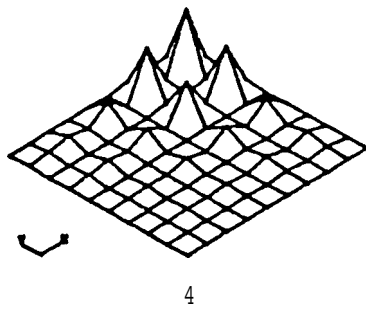
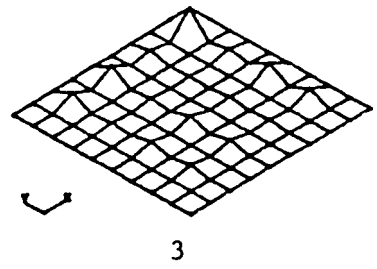
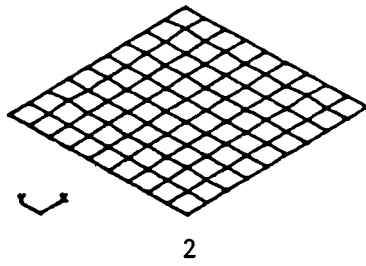
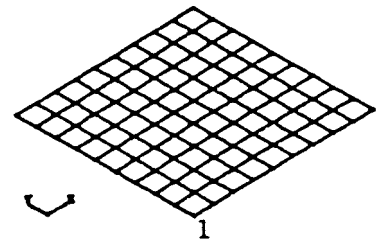
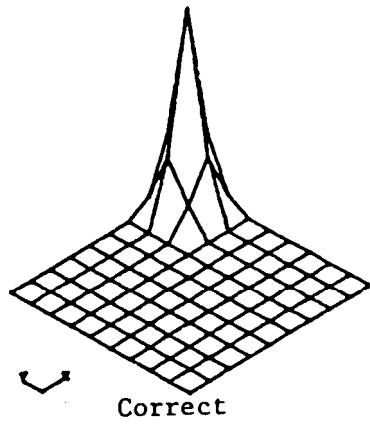
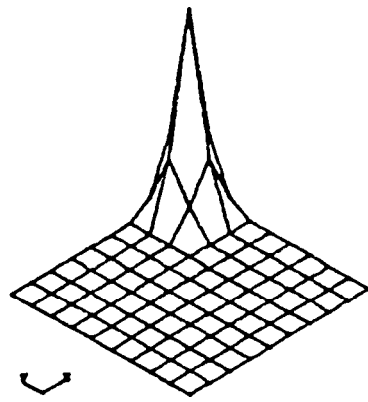
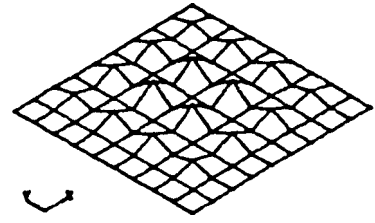


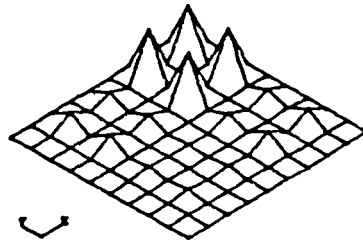
Figure 5.2: Damping Error Test 1 ($M=M_a$)



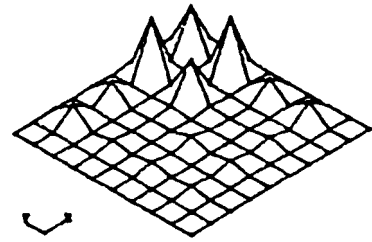
Correct



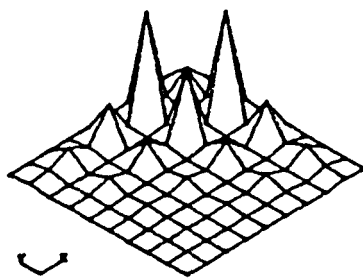
1



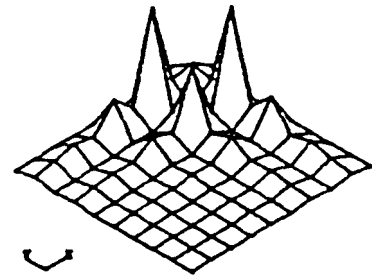
2



3

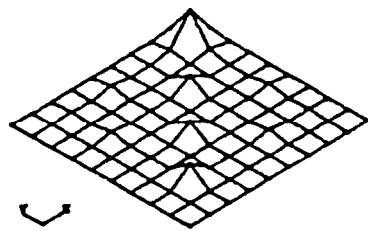


4

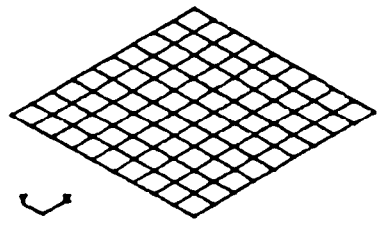


5

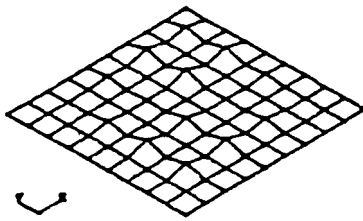
Figure 5.3: Stiffness Error Test 1 ($M=M_a$)



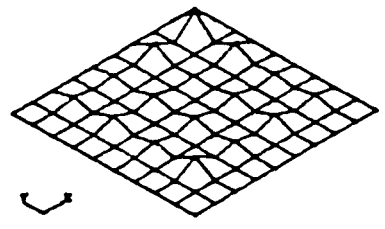
All 10 Modes



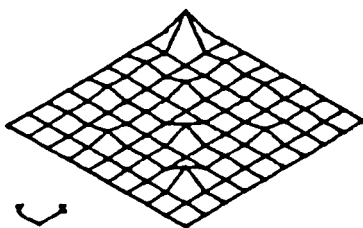
1



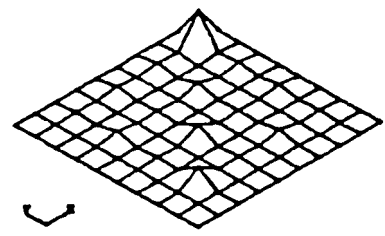
2



3

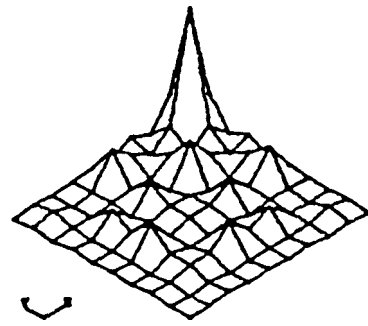


4

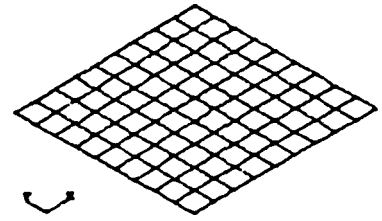


5

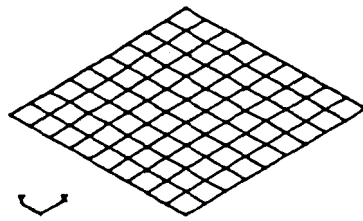
Figure 5.4: Mass Error Test 2 ($M \neq M_a$)



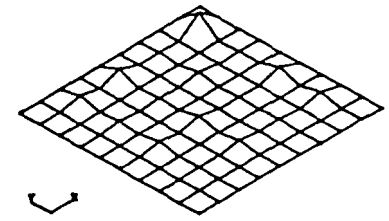
All 10 Modes



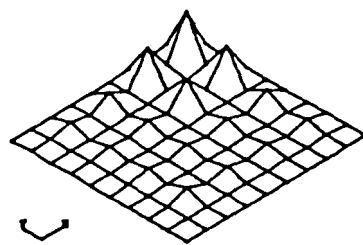
1



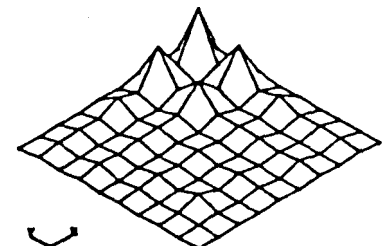
2



3

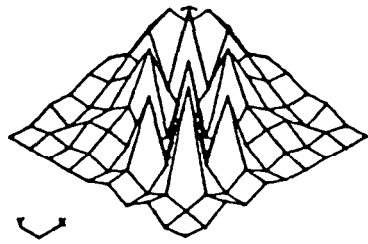


4

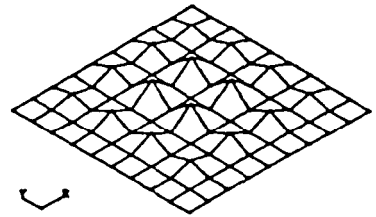


5

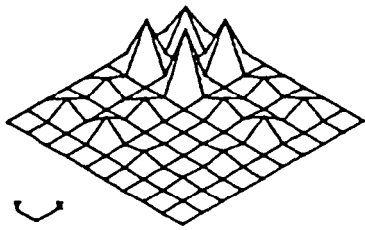
Figure 5.5: Damping Error Test 2 ($M+M_a$)



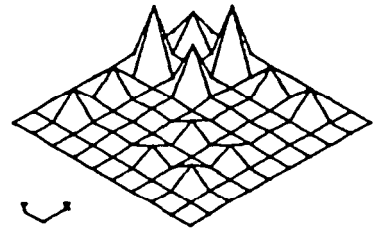
All 10 Modes



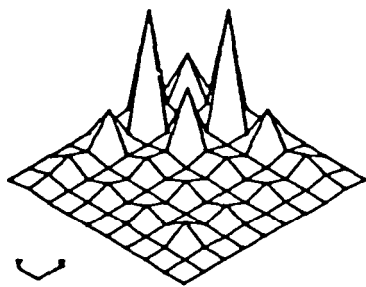
1



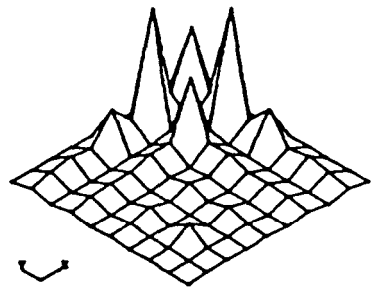
2



3



4



5

Figure 5.6: Stiffness Error Test 2 ($M+M_a$)

MASS ERROR MATRIX (10 MODES)

| | | | | | | | | | |
|-------|-------|-------|-------|-------|-------|-------|-------|-------|-------|
| 0.000 | 0.000 | 0.000 | 0.000 | 0.000 | 0.000 | 0.000 | 0.000 | 0.000 | 0.000 |
| 0.000 | 0.000 | 0.000 | 0.000 | 0.000 | 0.000 | 0.000 | 0.000 | 0.000 | 0.000 |
| 0.000 | 0.000 | 0.000 | 0.000 | 0.000 | 0.000 | 0.000 | 0.000 | 0.000 | 0.000 |
| 0.000 | 0.000 | 0.000 | 0.000 | 0.000 | 0.000 | 0.000 | 0.000 | 0.000 | 0.000 |
| 0.000 | 0.000 | 0.000 | 0.000 | 0.000 | 0.000 | 0.000 | 0.000 | 0.000 | 0.000 |
| 0.000 | 0.000 | 0.000 | 0.000 | 0.000 | 0.000 | 0.000 | 0.000 | 0.000 | 0.000 |
| 0.000 | 0.000 | 0.000 | 0.000 | 0.000 | 0.000 | 0.000 | 0.000 | 0.000 | 0.000 |
| 0.000 | 0.000 | 0.000 | 0.000 | 0.000 | 0.000 | 0.000 | 0.000 | 0.000 | 0.000 |
| 0.000 | 0.000 | 0.000 | 0.000 | 0.000 | 0.000 | 0.000 | 0.000 | 0.000 | 0.000 |
| 0.000 | 0.000 | 0.000 | 0.000 | 0.000 | 0.000 | 0.000 | 0.000 | 0.000 | 0.000 |

MASS ERROR MATRIX (5 MODES)

| | | | | | | | | | |
|--------|--------|--------|--------|--------|--------|--------|--------|--------|--------|
| 0.0000 | 0.0000 | 0.0000 | 0.0000 | 0.0000 | 0.0000 | 0.0000 | 0.0000 | 0.0000 | 0.0000 |
| 0.0000 | 0.0001 | 0.0001 | 0.0000 | 0.0000 | 0.0000 | 0.0000 | 0.0000 | 0.0000 | 0.0000 |
| 0.0000 | 0.0000 | 0.0000 | 0.0000 | 0.0000 | 0.0000 | 0.0000 | 0.0000 | 0.0000 | 0.0000 |
| 0.0000 | 0.0000 | 0.0000 | 0.0000 | 0.0000 | 0.0000 | 0.0000 | 0.0000 | 0.0000 | 0.0000 |
| 0.0000 | 0.0000 | 0.0000 | 0.0000 | 0.0000 | 0.0000 | 0.0000 | 0.0000 | 0.0000 | 0.0000 |
| 0.0000 | 0.0000 | 0.0000 | 0.0000 | 0.0000 | 0.0000 | 0.0000 | 0.0000 | 0.0000 | 0.0000 |
| 0.0000 | 0.0000 | 0.0000 | 0.0000 | 0.0000 | 0.0000 | 0.0000 | 0.0000 | 0.0000 | 0.0000 |
| 0.0000 | 0.0000 | 0.0000 | 0.0000 | 0.0000 | 0.0000 | 0.0000 | 0.0000 | 0.0000 | 0.0000 |
| 0.0000 | 0.0000 | 0.0000 | 0.0000 | 0.0000 | 0.0000 | 0.0000 | 0.0000 | 0.0000 | 0.0000 |
| 0.0000 | 0.0000 | 0.0000 | 0.0000 | 0.0000 | 0.0000 | 0.0000 | 0.0000 | 0.0000 | 0.0000 |

Figure 5.7: Mass Error (M=M₀)

DAMPING ERROR MATRIX (10 MODES)

| | | | | | | | | | |
|-------|-------|-------|-------|-------|-------|-------|-------|-------|-------|
| 0.083 | 0.151 | 0.031 | 0.000 | 0.000 | 0.000 | 0.000 | 0.000 | 0.000 | 0.000 |
| 0.151 | 0.483 | 0.151 | 0.000 | 0.000 | 0.000 | 0.000 | 0.000 | 0.000 | 0.000 |
| 0.031 | 0.151 | 0.083 | 0.000 | 0.000 | 0.000 | 0.000 | 0.000 | 0.000 | 0.000 |
| 0.000 | 0.000 | 0.000 | 0.000 | 0.000 | 0.000 | 0.000 | 0.000 | 0.000 | 0.000 |
| 0.000 | 0.000 | 0.000 | 0.000 | 0.000 | 0.000 | 0.000 | 0.000 | 0.000 | 0.000 |
| 0.000 | 0.000 | 0.000 | 0.000 | 0.000 | 0.000 | 0.000 | 0.000 | 0.000 | 0.000 |
| 0.000 | 0.000 | 0.000 | 0.000 | 0.000 | 0.000 | 0.000 | 0.000 | 0.000 | 0.000 |
| 0.000 | 0.000 | 0.000 | 0.000 | 0.000 | 0.000 | 0.000 | 0.000 | 0.000 | 0.000 |
| 0.000 | 0.000 | 0.000 | 0.000 | 0.000 | 0.000 | 0.000 | 0.000 | 0.000 | 0.000 |
| 0.000 | 0.000 | 0.000 | 0.000 | 0.000 | 0.000 | 0.000 | 0.000 | 0.000 | 0.000 |

DAMPING ERROR MATRIX (5 MODES)

| | | | | | | | | | |
|--------|--------|--------|--------|--------|--------|--------|--------|--------|--------|
| 0.0022 | 0.0182 | 0.0038 | 0.0140 | 0.0021 | 0.0055 | 0.0015 | 0.0023 | 0.0015 | 0.0007 |
| 0.0182 | 0.1508 | 0.0285 | 0.1141 | 0.0182 | 0.0435 | 0.0118 | 0.0188 | 0.0114 | 0.0057 |
| 0.0038 | 0.0285 | 0.0057 | 0.0221 | 0.0034 | 0.0088 | 0.0025 | 0.0038 | 0.0024 | 0.0012 |
| 0.0140 | 0.1141 | 0.0221 | 0.0872 | 0.0127 | 0.0337 | 0.0092 | 0.0145 | 0.0090 | 0.0045 |
| 0.0021 | 0.0182 | 0.0034 | 0.0127 | 0.0020 | 0.0052 | 0.0015 | 0.0022 | 0.0014 | 0.0007 |
| 0.0055 | 0.0435 | 0.0088 | 0.0337 | 0.0052 | 0.0135 | 0.0038 | 0.0058 | 0.0037 | 0.0018 |
| 0.0015 | 0.0118 | 0.0025 | 0.0092 | 0.0015 | 0.0038 | 0.0011 | 0.0018 | 0.0011 | 0.0005 |
| 0.0023 | 0.0188 | 0.0038 | 0.0145 | 0.0022 | 0.0058 | 0.0018 | 0.0025 | 0.0018 | 0.0008 |
| 0.0015 | 0.0114 | 0.0024 | 0.0090 | 0.0014 | 0.0037 | 0.0011 | 0.0018 | 0.0010 | 0.0005 |
| 0.0007 | 0.0057 | 0.0012 | 0.0045 | 0.0007 | 0.0018 | 0.0005 | 0.0008 | 0.0005 | 0.0002 |

Figure 58: Damping Error ($M=M_a$)

STIFFNESS ERROR MATRIX (10 MODES)

| | | | | | | | | | | |
|--------------|--------|-------|-------|-------|-------|-------|-------|-------|-------|--------------|
| 3.183 | 7.599 | 1.591 | 0.000 | 0.000 | 0.000 | 0.000 | 0.000 | 0.000 | 0.000 | 0.000 |
| 7.599 | 24.188 | 7.599 | 0.000 | 0.000 | 0.000 | 0.000 | 0.000 | 0.000 | 0.000 | 0.000 |
| 1.591 | 7.599 | 3.183 | 0.000 | 0.000 | 0.000 | 0.000 | 0.000 | 0.000 | 0.000 | 0.000 |
| 0.000 | 0.000 | 0.000 | 0.000 | 0.000 | 0.000 | 0.000 | 0.000 | 0.000 | 0.000 | 0.000 |
| 0.000 | 0.000 | 0.000 | 0.000 | 0.000 | 0.000 | 0.000 | 0.000 | 0.000 | 0.000 | 0.000 |
| 0.000 | 0.000 | 0.000 | 0.000 | 0.000 | 0.000 | 0.000 | 0.000 | 0.000 | 0.000 | 0.000 |
| 0.000 | 0.000 | 0.000 | 0.000 | 0.000 | 0.000 | 0.000 | 0.000 | 0.000 | 0.000 | 0.000 |
| 0.000 | 0.000 | 0.000 | 0.000 | 0.000 | 0.000 | 0.000 | 0.000 | 0.000 | 0.000 | 0.000 |
| 0.000 | 0.000 | 0.000 | 0.000 | 0.000 | 0.000 | 0.000 | 0.000 | 0.000 | 0.000 | 0.000 |
| 0.000 | 0.000 | 0.000 | 0.000 | 0.000 | 0.000 | 0.000 | 0.000 | 0.000 | 0.000 | 0.000 |

STIFFNESS ERROR MATRIX (5 MODES)

| | | | | | | | | | |
|-------|--------|-------|--------|-------|-------|-------|-------|-------|--------------|
| 0.052 | 1.225 | 0.018 | 0.166 | 0.047 | 0.052 | 0.022 | 0.022 | 0.019 | 0.009 |
| 1.225 | 3.027 | 2.472 | 12.491 | 1.845 | 4.270 | 1.166 | 1.811 | 1.123 | 0.558 |
| 0.018 | 2.472 | 0.150 | 1.248 | 0.240 | 0.402 | 0.132 | 0.168 | 0.118 | 0.057 |
| 0.166 | 12.491 | 1.248 | 7.967 | 1.526 | 2.370 | 0.815 | 0.964 | 0.717 | 0.347 |
| 0.047 | 1.845 | 0.240 | 1.526 | 0.276 | 0.490 | 0.154 | 0.203 | 0.139 | 0.068 |
| 0.052 | 4.270 | 0.402 | 2.370 | 0.490 | 0.680 | 0.254 | 0.269 | 0.215 | 0.103 |
| 0.022 | 1.166 | 0.132 | 0.815 | 0.154 | 0.254 | 0.083 | 0.103 | 0.072 | 0.035 |
| 0.022 | 1.811 | 0.168 | 0.964 | 0.203 | 0.269 | 0.103 | 0.105 | 0.086 | 0.041 |
| 0.019 | 1.123 | 0.118 | 0.717 | 0.139 | 0.215 | 0.072 | 0.086 | 0.062 | 0.030 |
| 0.009 | 0.558 | 0.057 | 0.347 | 0.068 | 0.103 | 0.035 | 0.041 | 0.030 | 0.014 |

Figure 5.9: Stiffness Error ($M=M_a$)

MASS ERROR MATRIX (10 MODES)

| | | | | | | | | | |
|---------------|---------------|---------------|---------------|---------------|---------------|---------------|--------|--------|--------|
| 0.0009 | 0.0060 | 0.0004 | 0.0007 | 0.0002 | 0.0003 | 0.0000 | 0.0001 | 0.0000 | 0.0000 |
| 0.0058 | 0.0787 | 0.0099 | 0.0003 | 0.0007 | 0.0089 | 0.0002 | 0.0035 | 0.0005 | 0.0000 |
| 0.0005 | 0.0103 | 0.0010 | 0.0004 | 0.0005 | 0.0008 | 0.0001 | 0.0004 | 0.0001 | 0.0000 |
| 0.0004 | 0.0011 | 0.0002 | 0.0298 | 0.0003 | 0.0032 | 0.0004 | 0.0087 | 0.0008 | 0.0005 |
| 0.0002 | 0.0008 | 0.0005 | 0.0003 | 0.0004 | 0.0008 | 0.0002 | 0.0004 | 0.0000 | 0.0000 |
| 0.0004 | 0.0087 | 0.0008 | 0.0032 | 0.0008 | 0.0299 | 0.0000 | 0.0003 | 0.0000 | 0.0005 |
| 0.0000 | 0.0000 | 0.0001 | 0.0004 | 0.0002 | 0.0000 | 0.0005 | 0.0010 | 0.0001 | 0.0000 |
| 0.0001 | 0.0038 | 0.0004 | 0.0087 | 0.0004 | 0.0003 | 0.0010 | 0.0388 | 0.0005 | 0.0005 |
| 0.0000 | 0.0007 | 0.0000 | 0.0008 | 0.0000 | 0.0000 | 0.0001 | 0.0005 | 0.0004 | 0.0002 |
| 0.0000 | 0.0000 | 0.0000 | 0.0005 | 0.0000 | 0.0005 | 0.0000 | 0.0005 | 0.0002 | 0.0002 |

MASS ERROR MATRIX (5 MODES)

| | | | | | | | | | |
|---------------|--------|--------|--------|--------|---------------|--------|--------|--------|---------------|
| 0.0000 | 0.0023 | 0.0001 | 0.0001 | 0.0000 | 0.0003 | 0.0000 | 0.0000 | 0.0000 | 0.0000 |
| 0.0023 | 0.0790 | 0.0035 | 0.0088 | 0.0024 | 0.0101 | 0.0008 | 0.0027 | 0.0008 | 0.0001 |
| 0.0001 | 0.0038 | 0.0002 | 0.0002 | 0.0000 | 0.0004 | 0.0000 | 0.0003 | 0.0000 | 0.0000 |
| 0.0001 | 0.0088 | 0.0002 | 0.0153 | 0.0018 | 0.0033 | 0.0022 | 0.0113 | 0.0011 | 0.0001 |
| 0.0000 | 0.0023 | 0.0000 | 0.0018 | 0.0000 | 0.0009 | 0.0000 | 0.0000 | 0.0000 | 0.0000 |
| 0.0002 | 0.0100 | 0.0004 | 0.0033 | 0.0009 | 0.0238 | 0.0003 | 0.0048 | 0.0013 | 0.0003 |
| 0.0000 | 0.0008 | 0.0000 | 0.0022 | 0.0000 | 0.0003 | 0.0001 | 0.0013 | 0.0000 | 0.0000 |
| 0.0000 | 0.0028 | 0.0003 | 0.0113 | 0.0000 | 0.0048 | 0.0013 | 0.0344 | 0.0003 | 0.0013 |
| 0.0000 | 0.0008 | 0.0000 | 0.0011 | 0.0000 | 0.0013 | 0.0000 | 0.0003 | 0.0001 | 0.0000 |
| 0.0000 | 0.0001 | 0.0000 | 0.0001 | 0.0000 | 0.0003 | 0.0000 | 0.0013 | 0.0000 | 0.0000 |

Figure 5.10: Mass Error (M_a)

DAMPING ERROR MATRIX (10 MODES)

| | | | | | | | | | |
|--------|--------|--------|--------|--------|--------|--------|--------|--------|---------------|
| 0.0284 | 0.0750 | 0.0058 | 0.0279 | 0.0059 | 0.0097 | 0.0053 | 0.0035 | 0.0085 | 0.0025 |
| 0.0750 | 0.3091 | 0.0524 | 0.0114 | 0.0411 | 0.0815 | 0.0073 | 0.0024 | 0.0208 | 0.0074 |
| 0.0058 | 0.0524 | 0.0170 | 0.0423 | 0.0082 | 0.0129 | 0.0110 | 0.0044 | 0.0087 | 0.0018 |
| 0.0279 | 0.0114 | 0.0423 | 0.0981 | 0.0085 | 0.0548 | 0.0007 | 0.0488 | 0.0011 | 0.0109 |
| 0.0059 | 0.0411 | 0.0082 | 0.0085 | 0.0218 | 0.0280 | 0.0171 | 0.0213 | 0.0038 | 0.0037 |
| 0.0097 | 0.0815 | 0.0129 | 0.0548 | 0.0280 | 0.0280 | 0.0113 | 0.0853 | 0.0028 | 0.0099 |
| 0.0053 | 0.0073 | 0.0110 | 0.0007 | 0.0171 | 0.0113 | 0.0090 | 0.0248 | 0.0017 | 0.0083 |
| 0.0035 | 0.0024 | 0.0044 | 0.0488 | 0.0213 | 0.0853 | 0.0248 | 0.0228 | 0.0099 | 0.0137 |
| 0.0085 | 0.0208 | 0.0087 | 0.0011 | 0.0038 | 0.0028 | 0.0017 | 0.0099 | 0.0000 | 0.0054 |
| 0.0025 | 0.0074 | 0.0018 | 0.0109 | 0.0037 | 0.0099 | 0.0083 | 0.0137 | 0.0054 | 0.0031 |

DAMPING ERROR MATRIX (5 MODES)

| | | | | | | | | | |
|--------|--------|--------|--------|--------|--------|--------|--------|--------|--------|
| 0.0007 | 0.0107 | 0.0020 | 0.0095 | 0.0011 | 0.0035 | 0.0007 | 0.0015 | 0.0008 | 0.0003 |
| 0.0107 | 0.1382 | 0.0279 | 0.1008 | 0.0180 | 0.0380 | 0.0131 | 0.0175 | 0.0124 | 0.0080 |
| 0.0020 | 0.0279 | 0.0054 | 0.0250 | 0.0031 | 0.0091 | 0.0020 | 0.0040 | 0.0019 | 0.0009 |
| 0.0095 | 0.1008 | 0.0250 | 0.0704 | 0.0198 | 0.0180 | 0.0184 | 0.0104 | 0.0182 | 0.0079 |
| 0.0011 | 0.0180 | 0.0031 | 0.0198 | 0.0014 | 0.0073 | 0.0008 | 0.0027 | 0.0005 | 0.0003 |
| 0.0035 | 0.0380 | 0.0091 | 0.0180 | 0.0073 | 0.0148 | 0.0071 | 0.0139 | 0.0088 | 0.0047 |
| 0.0007 | 0.0131 | 0.0020 | 0.0184 | 0.0008 | 0.0071 | 0.0001 | 0.0027 | 0.0001 | 0.0000 |
| 0.0015 | 0.0175 | 0.0040 | 0.0104 | 0.0027 | 0.0139 | 0.0027 | 0.0205 | 0.0048 | 0.0029 |
| 0.0008 | 0.0124 | 0.0019 | 0.0182 | 0.0005 | 0.0088 | 0.0001 | 0.0048 | 0.0004 | 0.0002 |
| 0.0003 | 0.0080 | 0.0009 | 0.0079 | 0.0003 | 0.0047 | 0.0000 | 0.0029 | 0.0002 | 0.0001 |

Figure 5.11: Damping Error (M_a)

STIFFNESS ERROR MATRIX (10 MODES)

| | | | | | | | | | |
|-------|-------|-------|--------|-------|--------|-------|--------|-------|-------|
| 3.280 | 3.902 | 3.803 | 1.923 | 2.663 | 2.153 | 1.142 | 1.310 | 0.085 | 0.187 |
| 3.902 | 5.148 | 7.196 | 6.036 | 4.493 | 2.540 | 0.973 | 0.047 | 0.735 | 0.114 |
| 3.803 | 7.198 | 6.923 | 0.543 | 4.011 | 4.720 | 2.066 | 2.072 | 0.284 | 0.391 |
| 1.923 | 6.036 | 0.543 | 11.329 | 3.102 | 9.434 | 3.887 | 2.432 | 0.994 | 0.272 |
| 2.683 | 4.493 | 4.011 | 3.102 | 0.934 | 0.208 | 0.581 | 1.944 | 0.090 | 0.445 |
| 2.153 | 2.540 | 4.720 | 9.434 | 0.208 | 10.892 | 0.493 | 9.230 | 1.808 | 1.451 |
| 1.142 | 0.973 | 2.068 | 3.887 | 0.581 | 0.493 | 1.380 | 2.323 | 0.214 | 0.220 |
| 1.310 | 0.047 | 2.072 | 2.432 | 1.944 | 9.230 | 2.323 | 13.133 | 1.451 | 2.066 |
| 0.085 | 0.735 | 0.284 | 0.994 | 0.090 | 1.808 | 0.214 | 1.451 | 0.853 | 0.229 |
| 0.187 | 0.114 | 0.391 | 0.272 | 0.445 | 1.451 | 0.220 | 2.066 | 0.229 | 0.537 |

STIFFNESS ERROR MATRIX (5 MODES)

| | | | | | | | | | |
|-------|--------|-------|--------|-------|-------|-------|-------|-------|-------|
| 0.036 | 0.863 | 0.073 | 0.029 | 0.010 | 0.031 | 0.022 | 0.008 | 0.025 | 0.012 |
| 0.863 | 8.958 | 2.554 | 14.099 | 1.872 | 4.667 | 1.222 | 1.736 | 1.227 | 0.622 |
| 0.073 | 2.554 | 0.097 | 0.681 | 0.088 | 0.117 | 0.000 | 0.051 | 0.011 | 0.008 |
| 0.029 | 14.099 | 0.681 | 8.503 | 1.897 | 1.906 | 1.079 | 1.141 | 0.975 | 0.465 |
| 0.010 | 1.872 | 0.088 | 1.897 | 0.208 | 0.488 | 0.058 | 0.148 | 0.050 | 0.025 |
| 0.031 | 4.667 | 0.117 | 1.906 | 0.488 | 1.113 | 0.301 | 1.035 | 0.399 | 0.223 |
| 0.022 | 1.222 | 0.000 | 1.079 | 0.058 | 0.301 | 0.036 | 0.080 | 0.044 | 0.021 |
| 0.008 | 1.736 | 0.051 | 1.141 | 0.148 | 1.035 | 0.060 | 1.743 | 0.203 | 0.151 |
| 0.025 | 1.227 | 0.011 | 0.975 | 0.050 | 0.399 | 0.044 | 0.203 | 0.088 | 0.037 |
| 0.012 | 0.622 | 0.008 | 0.465 | 0.025 | 0.223 | 0.021 | 0.151 | 0.037 | 0.022 |

Figure 5.12: Stiffness Error (M²/m³)

INTERPOLATION OF MEASURED MODES6.1 Preliminaries

In order to perform an analysis of the type described in the previous chapters, there needs to exist a compatibility between measurement and analysis, in terms of the dimension of the problem. It is usual for the number of measured modes, m , to be measured at n positions, which is often rather significantly smaller than the number of degrees-of-freedom of the mathematical model, N . To proceed, n needs to be set equal to N . This involves either a **reduction** of the mathematical model using an established technique or some sort of interpolation on the measured modes so that each mode has N elements instead of n . Reduction processes^(47, 77) condense the information with the result that the reduced matrices cannot readily be interpreted in terms of mass and stiffness distributions.

The more viable alternative is considered to be an expansion of the measured modes. Two approaches are considered in this chapter in order to achieve this goal: the first is the use of splines and the second is the use of the mathematical model once more in order to provide the information about the modes that has not been obtained experimentally. Needless to say, the more information that can be measured, the less the expansion process has to be relied upon. For simple structures such as beams, the number of unmeasured coordinates is not so significant as it is for large structures (such as dams) where the unmeasured coordinates would greatly outnumber those which have been measured. In general, measurement over as many channels as possible is desirable, although it is unlikely

that all the measurements can be made due to the difficulty of measuring rotational motion and internal degrees-of-freedom.

6.2 Interpolation Using Splines

Possible methods of interpolation of mode shapes in order to establish the full mode are many. They vary from literally drawing the smoothest curve possible through the measurement points to establish the intermediate values, to surface splines and other sophisticated techniques. The type of interpolation adopted depends largely on the type of the problem being considered. For the pinned beam investigated in this thesis, the use of the cubic spline was considered most appropriate for interpolating on the measured modes. The cubic spline is an interpolation between two points with the use of a polynomial of degree less than or equal to 3. The theory of cubic splines is well established^(2,17), but is included here to demonstrate its application to modal analysis. If we have a measured mode $x_i = \{\xi_0, \dots, \xi_n\}$ measured at positions $\{y_0, \dots, y_n\}$ and we wish to complete the mode by obtaining the missing gradients and displacements using the cubic spline, then we need to establish the vector $Q = \{Q_0, Q_1, \dots, Q_n\}$ such that on $[y_{i-1}, y_i]$ the second derivative of S , the cubic spline, is given by the linear function

$$S''(y) = Q_{i-1} \frac{(y_i - y)}{h_i} + Q_i \frac{(y - y_{i-1})}{h_i}$$

where $h_i = y_i - y_{i-1}$, $1 \leq i \leq n$. This implies, on integrating each segment twice with respect to y and determining the pairs of constants of integration to make $S(y_i) = \xi_i$, that on $[y_{i-1}, y_i]$

$$S(y) = \frac{Q_{i-1}}{6h_i} (y_i - y)^3 + \frac{Q_i}{6h_i} (y - y_{i-1})^3 + \left\{ \xi_i - \frac{Q_i h_i^2}{6} \right\} \frac{(y - y_{i-1})}{h_i} + \left\{ \xi_{i-1} - \frac{Q_{i-1} h_i^2}{6} \right\} \frac{(y_i - y)}{h_i}$$

For any choice of the values Q_i , this equation defines a piecewise cubic function of y which is continuous over the node and has a smooth second derivative. For S to be a spline function, however, we also require that $S'(y)$ be continuous. This is the case if, and only if, the derivatives of the cubics agree at the point y_i . Then, $S'(y)$ will exist for all y and it will follow that $S''(y)$ exists and is continuous. Therefore, differentiating we obtain for y in $[y_{i-1}, y_i]$

$$S'(y) = -\frac{Q_{i-1}}{2h_i} (y_i - y)^2 + \frac{Q_i}{2h_i} (y - y_{i-1})^2 + \frac{(\xi_i - \xi_{i-1})}{h_i} + (Q_{i-1} - Q_i) \frac{h_i}{6}.$$

We impose continuity on $S'(y)$ at y_i , $1 \leq i \leq n-1$. The derivative at y_i using the cubic over $[y_{i-1}, y_i]$ is

$$\frac{Q_i h_i}{3} + \frac{Q_{i-1} h_i}{6} + \frac{\xi_i - \xi_{i-1}}{h_i}$$

and the derivative at y_i using the cubic over $[y_i, y_{i+1}]$ is

$$\frac{Q_i h_{i+1}}{3} - \frac{Q_{i+1} h_{i+1}}{6} + \frac{\xi_{i+1} - \xi_i}{h_{i+1}}.$$

Upon equating these two expressions and simplifying, we obtain

$$a_i Q_{i-1} + 2Q_i + c_i Q_{i+1} = d_i \quad 1 \leq i \leq n-1$$

where $a_i = h_i / (h_i + h_{i+1})$ $c_i = 1 - a_i$

and $d_i = \frac{6[(\xi_{i+1} - \xi_i)/h_{i+1} - (\xi_i - \xi_{i-1})/h_i]}{h_i + h_{i+1}}$.

The remaining two equations for the Q_i are obtained by imposing arbitrary end conditions on Q_0 and Q_n . For convenience these are written as

$$2Q_0 + c_0Q_1 = d_0$$

$$\text{and } a_n Q_{n-1} + 2Q_n = d_n$$

where the choice of constants is at our disposal. These equations were then used to interpolate on the first three modes of the undamped pinned beam where the displacement at 6 nodes was taken as the measurement and the displacement and gradient at 11 nodes were required, so about one quarter of the required information was available

Each node was equally spaced along the beam, and every other node was considered as being measured (see Tables 6.1 to 6.6). As can be seen from the calculations, the quality of the first mode is good, but this quality decreases as the mode gets more complex, as would be expected.

Interpolation techniques clearly have their uses if the situation permits them, the beam example being one such case. However, difficulties arise because of the fact that the measurements are usually very sparse compared to the amount of information required, especially when the model has many degrees of freedom inaccessible to measurement. If this problem is severe, caution needs to be exercised upon applying interpolation techniques and inexplicable interpolated modes may emerge as a result of leaning too heavily on approximation methods where too much information is expected from too little supplied. A popular approach in such circumstances is the use of the FE mathematical model as the interpolating tool. This is discussed in the next section.

6.3 Interpolation Using an Analytical Model

The notion of using an analytical model to expand the measured

set of modes from that of $(n \times m)$ to $(N \times m)$ has been discussed in the literature. Here the problem is **analysed**, bearing in mind the likely scenario that will exist during an assessment-of the dynamic **properties** of a structure. For convenience, the envisaged situation involves three people referred to as the 'manufacturer' (or the person intending to construct the structure in question), the 'analytical engineer' (who is essentially a numerical analyst, well versed in the FE method), and the 'test engineer' (who is an **experimentalist** with experience in the analysis of data and the extraction of modal properties). The chain of events described here is a considered opinion, and is not an attempt to describe what happens in practice.

(a) The manufacturer has designed the new structure and expresses concern as to its likely dynamic performance.

(b) The analytical engineer is called in and performs the following tasks:

(i) Constructs an FE model of the structure, with the data available, in terms of mass and stiffness distributions. Analytical modes and frequencies are extracted.

(ii) Programs expressions for error analysis, to be used by the test engineer should the analytical modes and frequencies not be verified by experiment.

(iii) Sets up the mathematical model for ease of modification by the test engineer (in terms of $\bar{E}\bar{I}$, m parameters etc.).

(c) The manufacturer assesses the predicted dynamic performance and either redesigns or constructs a scale model or prototype.

(d) The test engineer is called in to take measurements on the

model and extract measured modes and frequencies. Problems arise because they disagree with the predicted ones. An error analysis is conducted to estimate the regions of the FE model-that have been incorrectly assessed. The software to do this is already available, as left by the analytical engineer. Areas of inaccurate modelling are identified, and the appropriate adjustments are made to improve the model (again, this facility has been made available by the analytical engineer). Agreement between test and analysis is reached.

(e) The manufacturer constructs the structure.

The purpose of this section is to consider interpolating on the measured modes in order to obtain full modes for use in the error analysis. This is essentially a job for the analytical engineer who, by the testing stage, has come and gone. The problem is therefore approached with a view to its assessment prior to the modal test being conducted.

In order to do this, the analytical engineer must know the points at which measurements are going to be made. This usually corresponds to the displacements of nodes at the surface of the structure, or those which are readily accessible to measurement. Two possible situations are examined: that where a preliminary test has been conducted and measured frequencies only are available, but not modes (assuming, for instance, that the scale model has already been constructed and the manufacturer has some simple test equipment with which to gain an initial assessment); and that where no information at all is available.

The FE mathematical model that is available is typically of the form

$$M\phi^a \Lambda^a = K\phi^a$$

$$\text{or } (\lambda_i^a M - K)x_i^a = \theta$$

where M and K are, of course, M_a and K_a of the previous chapters. Although the analysis here is, for convenience, carried through in terms of partitions, the analysis is, in fact, totally suitable for use in FE program equation solvers where banding is not disturbed by rearrangement. We have

$$\begin{bmatrix} \lambda_i M_{11} - K_{11} & | & \lambda_i M_{12} - K_{12} \\ \hline \lambda_i M_{21} - K_{21} & | & \lambda_i M_{22} - K_{22} \end{bmatrix} \begin{bmatrix} x_{1i} \\ x_{2i} \end{bmatrix} = \theta$$

where a subscript of 1 denotes a measurement position. This may be written as

$$\begin{bmatrix} L_{11}(\lambda_i) & | & L_{12}(\lambda_i) \\ \hline L_{21}(\lambda_i) & | & L_{22}(\lambda_i) \end{bmatrix} \begin{bmatrix} x_{1i} \\ x_{2i} \end{bmatrix} = \theta$$

We wish to determine the x_{2i} for each x_{1i} . The FE format of the equations is retained and the known x_{1i} coordinates are eliminated, essentially treating them in a standard way as boundary conditions thus

$$\begin{bmatrix} L_{11}(\lambda_i) & | & 0 \\ \hline 0 & | & L_{22}(\lambda_i) \end{bmatrix} \begin{bmatrix} x_{1i} \\ x_{2i} \end{bmatrix} = \begin{bmatrix} L_{11}(\lambda_i)x_{1i} \\ -L_{21}(\lambda_i)x_{1i} \end{bmatrix}$$

Therefore these equations can be solved using standard FE solution techniques. Since the x_{1i} are not known at the analysis stage, an indirect method needs to be adopted by finding x_{2i} for each of the 'basis unit measured modes'. x_{1i} can then be expressed at a later stage in terms of these basis vectors. Thus the x_{1i} vectors on the right-hand side are set to $(1,0,\dots,0)^T$, then $(0,1,\dots,0)^T$, and so on, so that the problem is solved n times which is merely an n-fold

repetition of a standard FE solver for the structure. This will produce n vectors for the x_{2i} given by $\zeta_i^{(r)}$, $r = 1, \dots, n$. These are interpolation vectors derived from a unit displacement at each of the measurement nodes in turn. Thus, the interpolated x_{2i} vector, when the measurements have been made, will be given by

$$x_{2i} = \sum_{r=1}^n \xi_r^i \zeta_i^{(r)} \text{ where } x_{1i} = (\xi_1^i, \dots, \xi_n^i)^T, i = 1, \dots, m$$

If the experimental frequencies are known, the $\zeta_i^{(r)}$ may be determined for each mode and all that is required of the test engineer is to insert the values of ξ_r^i once the measurements have been made.

If the eigenvalues are not known then this approach requires modification for a correction for λ_i once they become available. We make the assumption that the measured frequencies will not differ greatly from the analytical ones, and again we use an indirect analysis which will allow the incorporation of measurements at a later date. Essentially, the problem that has been solved is

$$L_{12}^T(\lambda_i)x_{1i} + L_{22}(\lambda_i)x_{2i} = \theta$$

or
$$x_{2i} = -L_{22}^{-1}(\lambda_i)L_{12}^T(\lambda_i)x_{1i}$$

where the x_{1i} and λ_i have been measured for each mode i ($i = 1, \dots, m$). If these are written as their analytical equivalents plus an error we have

$$x_{1i} = x_{1i}^a + \delta x_{1i} \text{ and } \lambda_i = \lambda_i^a + \delta \lambda_i.$$

Also, we write

$$x_{2i} = x_{2i}^a + \delta x_{2i}.$$

Therefore

$$L_{12}^T(\lambda_i^a + \delta\lambda_i)(x_{1i}^a + \delta x_{1i}) + \\ L_{22}(\lambda_i^a + \delta\lambda_i)(x_{2i}^a + \delta x_{2i}) = \theta$$

which, to a first order approximation, is equivalent to

$$L_{12}^T(\lambda_i^a)\delta x_{1i} + M_{12}^T(\delta\lambda_i)x_{1i}^a + L_{22}(\lambda_i^a)\delta x_{2i} + M_{22}(\delta\lambda_i)x_{2i}^a = \theta$$

so that

$$\delta x_{2i} = L_{22}^{-1}(\lambda_i^a)L_{12}^T(\lambda_i^a)\delta x_{1i} + L_{22}^{-1}(\lambda_i^a)(M_{12}^T x_{1i}^a + M_{22}x_{2i}^a)\delta\lambda_i$$

Also, we know that

$$x_{2i}^a = L_{22}^{-1}(\lambda_i^a)L_{12}^T(\lambda_i^a)x_{1i}^a$$

therefore

$$x_{2i} = x_{2i}^a + \delta x_{2i} \\ = L_{22}^{-1}(\lambda_i^a)L_{12}^T(\lambda_i^a)(x_{1i}^a + \delta x_{1i}) \\ + L_{22}^{-1}(\lambda_i^a)(M_{12}^T x_{1i}^a + M_{22}x_{2i}^a)\delta\lambda_i \\ = \sum_{r=1}^n \xi_r^i \zeta_i^a(r) + \hat{x}_{2i} \delta\lambda_i \quad i = 1, \dots, m$$

where $\hat{x}_{2i} = L_{22}^{-1}(\lambda_i^a)(M_{12}^T x_{1i}^a + M_{22}x_{2i}^a)$

Thus, calculations using analytical data can be corrected when measurements are available. There is only one correction vector \hat{x}_{2i} for each mode. This vector is found by solving

$$\begin{bmatrix} L_{11}(\lambda_i^a) & | & 0 \\ \hline 0 & | & L_{22}(\lambda_i^a) \end{bmatrix} \begin{bmatrix} \hat{x}_{1i} \\ \hat{x}_{2i} \end{bmatrix} = \begin{bmatrix} L_{11}(\lambda_i^a)\hat{x}_{1i} \\ \hline M_{12}^T x_{1i}^a + M_{22}x_{2i}^a \end{bmatrix}$$

with the \hat{x}_{1i} on the right-hand side being chosen arbitrarily. The ξ_r^i and λ_i are thus inserted by the test engineer at the measurement stage in order to obtain the full mode. This is essentially inter-

pulation using the functions of the mathematical model. Since the analytical model is invariably undamped, these expressions must be used to expand either real or **complex measured** modes;

To illustrate this technique, the pinned beam of example 2 was used. Both the correct mathematical model and the incorrect (or analytical) model were used for the interpolation of sine functions. The measurements were taken as the displacements and the slopes were determined by this method. These are compared with the correct discrete sine functions. The first five modes only were investigated.

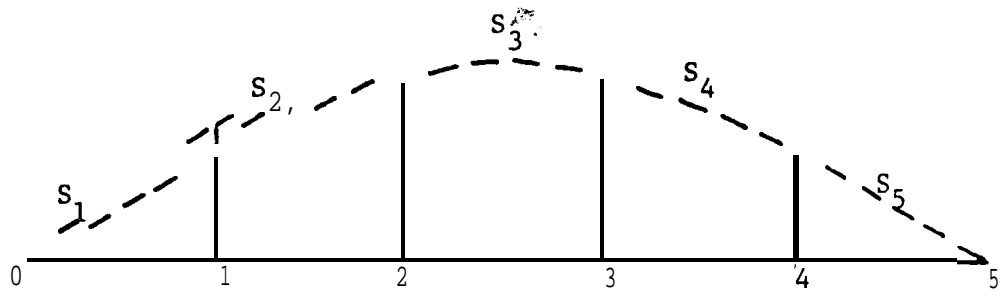
As can be seen from the tables (numbers 6.7 to 6.10), the good model interpolates effectively and very little error is produced, especially with the lower modes. The poor model (i.e. 'analytical') produces significant errors in the region of poor modelling with regard to interpolation. Therefore, as is to be expected, the quality of the model determines the quality of the full mode. The fifth mode has zero displacements at all the nodes and interpolation is found to be ineffective. However, this is not typical of a likely test situation.

6.4 Overview

Two interpolation techniques have been investigated. The first is the use of splines in order to determine the full mode. The type of spline used is largely problem-specific, and for the analysis of the pinned beam a cubic spline was adequate. In more general cases, surface splines may be used with the same overall conclusions applying. The second method is an interpolation technique which uses an existing analytical FE model. The method has

been presented so that the interpolation vectors can be set up at the analysis stage for subsequent use when the acquisition of measured modal information has been **achieved** and without having to resurrect the whole FE computational program. The compatibility of measured and analytical information is a necessary pre-requisite for the comparison of the two with a view to establishing an accurate finite degree-of-freedom representation of the structure under investigation.

Mode Number 1



----- chosen in advance

| i | y_i | ξ | i | a_i | c_i | d_i | Q_i |
|-----|-----------|-----------|-----|-------|------------|----------|---------|
| 0 | 0 | 0 | | 0.5 | 0 | 0 | 0.16317 |
| 1 | 0.6283185 | 0.5877852 | 0.5 | 0.5 | -1.1706108 | -0.65268 | |
| 2 | 1.256637 | 0.9510565 | 0.5 | 0.5 | -2.76053 | -0.97368 | |
| 3 | 1.884955 | 0.9510565 | 0.5 | 0.5 | -2.76053 | -0.97368 | |
| 4 | 2.513274 | 0.5877852 | 0.5 | 0.5 | -1.1706108 | -0.65268 | |
| 5 | 3.141593 | 0 | 0.5 | - | 0 | 0.16317 | |

Table 6.1

Mode Number 1

| d=disp. r=rot. | EXACT MODE | INTERPOLATED MODE |
|-------------------|------------|-------------------|
| d | 0 | <u>0</u> |
| r | 1 | 0.969663 |
| d | 0.3090169 | 0.30597077 |
| r | 0.9510565 | 0.95684812 |
| d | 0.5877852 | <u>0.5877852</u> |
| r | 0.8090169 | 0.815879 |
| d | 0.8090169 | 0.8095496 |
| r | 0.5877852 | 0.586568 |
| d | 0.9510565 | <u>0.9510565</u> |
| r | 0.3090169 | 0.3058887 |
| d | 1 | 0.9991 |
| r | 0 | 0 |
| d | 0.9510565 | <u>0.9510565</u> |
| r | -0.309017 | -0.30589056 |
| d | 0.8090169 | 0.809550249 |
| r | -0.5877852 | -0.58778566 |
| d | 0.5877852 | <u>0.5877852</u> |
| r | -0.8090169 | -0.816825125 |
| d | 0.3090169 | 0.30936624 |
| r | -0.9510565 | -0.955677 |
| d | 0 | <u>0</u> |
| r | -1 | -0.96965 |

_____ measured

Table 6.2

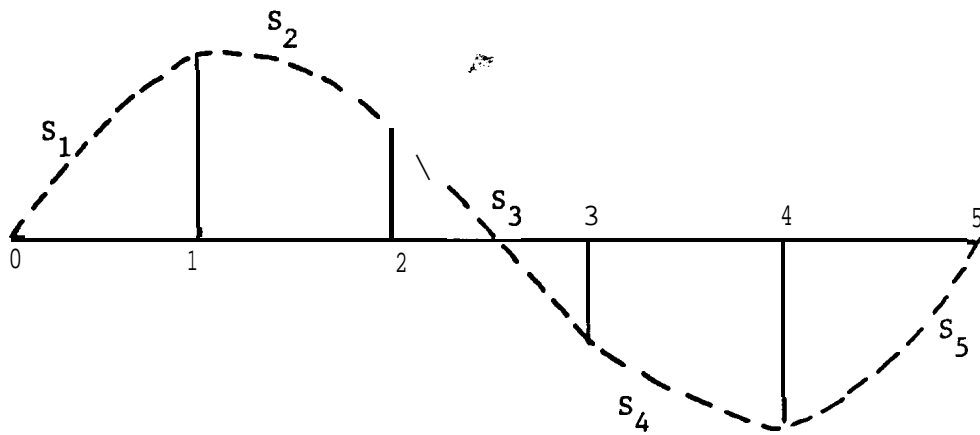
Mode Number 1

| d=disp. r=rot. | EXACT MODE | INTERPOLATED MODE |
|-------------------|------------|-------------------|
| d | 0 | <u>0</u> |
| r | 1 | 0.969663 |
| d | 0.3090169 | 0.30597077 |
| r | 0.9510565 | 0.95684812 |
| d | 0.5877852 | <u>0.5877852</u> |
| r | 0.8090169 | 0.815879 |
| d | 0.8090169 | 0.8095496 |
| r | 0.5877852 | 0.586568 |
| d | 0.9510565 | <u>0.9510565</u> |
| r | 0.3090169 | 0.3058887 |
| d | 1 | 0.9991 |
| r | 0 | 0 |
| d | 0.9510565 | <u>0.9510565</u> |
| r | -0.309017 | -0.30589056 |
| d | 0.8090169 | 0.809550249 |
| r | -0.5877852 | -0.58778566 |
| d | 0.5877852 | <u>0.5877852</u> |
| r | -0.8090169 | -0.816825125 |
| d | 0.3090169 | 0.30936624 |
| r | -0.9510565 | -0.955677 |
| d | 0 | <u>0</u> |
| r | -1 | -0.96965 |

_____ measured

Table 6.2

Mode Number 2



----- chosen in advance

| i | y_i | ξ_i | a_i | c_i | d_i | Q_i |
|-----|----------|------------|-------|-------|------------------|-----------------|
| 0 | 0 | 0 | | 0.5 | 0 | 1.16050 |
| 1 | 0.628318 | 0.9510516 | 0.5 | 0.5 | -9.9876936 | -4.64202 |
| 2 | 1.256637 | 0.58778.5 | 0.5 | 0.5 | -6.1727329 | --2.56782 |
| 3 | 1.884955 | 0.587785 | 0.5 | 0.5 | 6.1727329 | 2.56782* |
| 4 | 2.513274 | 1.95105635 | 0.5 | 0.5 | 9.9876936 | 4.64202 |
| 5 | 3.141593 | 0 | 0.5 | | 0 | -1.16050 |

Table 6.3

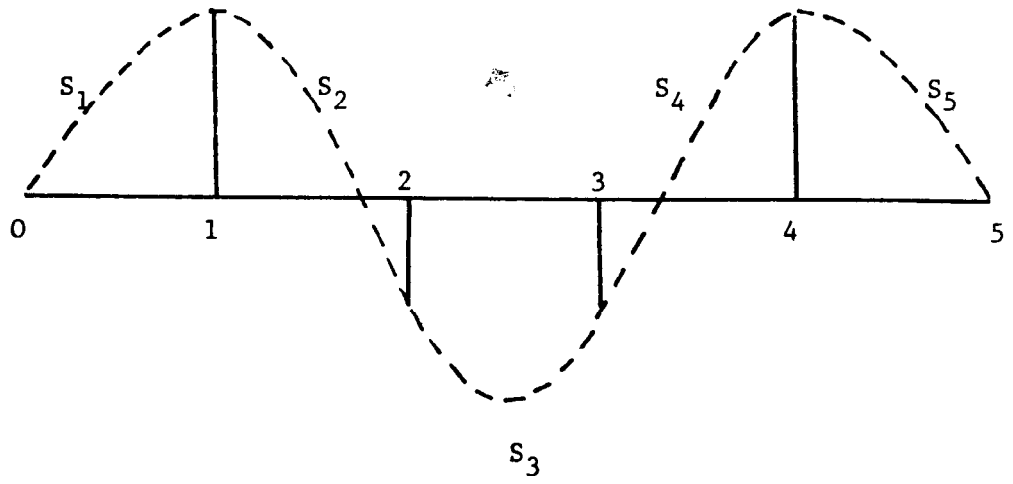
Mode Number

| d=disp. r=rot. | EXACT MODE | INTERPOLATED MODE |
|-------------------|------------|-------------------|
| d | 0 | <u>0</u> |
| r | 2 | 1.75671 |
| d | 0.5877852 | 0.5614313 |
| r | 1.6180339 | 1.6655630 |
| d | 0.9510565 | <u>0.9510565</u> |
| r | 0.618034 | 0.662958 |
| d | 0.9510565 | 0.947316 |
| r | -0.618034 | -0.632466 |
| d | 0.5877852 | <u>0.5877852</u> |
| r | -1.6180338 | -1.602073' |
| d | 0 | 0 |
| r | -2 | -2.005429 |
| d | -0.5877852 | <u>-0.5877852</u> |
| r | -1.6180338 | -1.602078 |
| d | -0.9510565 | -0.947317 |
| r | -0.618034 | -0.6324654 |
| d | -0.9510565 | <u>-0.9510565</u> |
| r | 0.618034 | 0.6629623 |
| d | -0.5877852 | -0.5614313 |
| r | 1.6180339 | 1.6655630 |
| d | 0 | <u>0</u> |
| r | 2 | 1.75671 |

_____ measured

Table 6.4

Mode Number 3



---- chosen in advance

| i | y_i | ξ_i | a_i | c_i | d_i | Q_i |
|-----|-----------|------------|-------|-------|-----------|-----------|
| 0 | 0 | 0 | - | 0.5 | 0 | 2.99433 |
| 1 | 0.6283185 | 0.9510565 | 0.5 | 0.5 | -18.92095 | -11.97730 |
| 2 | 1.256637 | -0.5877852 | 0.5 | 0.5 | 11.69379 | 7.07298 |
| 3 | 1.884955 | -0.5877852 | 0.5 | 0.5 | 11.69379 | 7.07298 |
| 4 | 2.5132741 | 0.9510565 | 0.5 | 0.5 | -18.97095 | -11.97730 |
| 5 | 3.1415926 | 0 | 0.5 | - | 0 | 2.99433 |

Table 6.5

Mode Number 3

| d=disp. r=rot. | EXACT MODE | INTERPOLATED MODE |
|-------------------|-------------|-------------------|
| d | 0 | <u>0</u> |
| r | 3 | 2.14078242 |
| d | 0.8090169 | 0.69717414 |
| r | 1.7633557 | 1.905609837 |
| d | 0.9510565 | <u>0.9510565</u> |
| r | -0.9270507 | -0.681300607 |
| d | 0.309017 | 0.30264503 |
| r | -2.85316951 | -2.9478778 |
| d | -0.5877852 | <u>-0.5877852</u> |
| r | -2.427051 | -2.22204127 |
| d | -1 | -0.93682217 |
| r | 0 | 0 |
| d | -0.5877852 | <u>-0.5877852</u> |
| r | 2.427051 | 2.2220384 |
| d | 0.309017 | 0.302645833 |
| r | 2.85316951 | 2.94787445 |
| d | 0.9510565 | <u>0.9510565</u> |
| r | 0.9270507 | 0.68129664 |
| d | 0.8090169 | 0.69817422 |
| r | -1.7633557 | -1.905609657 |
| d | 0 | <u>0</u> |
| r | -3 | -2.14078242 |

_____ measured

Table 6.6

| d=disp. r-rot. | MODE NUMBER 1 | | MODE NUMBER 2 | |
|-------------------|---------------|-------------------|---------------|-------------------|
| | EXACT MODE | INTERPOLATED MODE | EXACT MODE | INTERPOLATED MODE |
| d | 0 | <u>0</u> | 0 | <u>0</u> |
| r | 1 | 1.0021259 | 2 | 1.9989785 |
| d | 0.5877852 | <u>0.5877852</u> | 0.9510565 | <u>0.9510565</u> |
| r | 0.8090169 | 0.8094411 | 0.618034 | 0.6186028 |
| d | 0.9510565 | <u>0.9510565</u> | 0.5877852 | <u>0.5877852</u> |
| r | 0.309017 | 0.3075984 | -1.6180338 | -1.6185322 |
| d | 0.9510565 | <u>0.9510565</u> | -0.5877852 | <u>-0.5877852</u> |
| r | -0.309017 | -0.3075984 | -1.6180338 | -1.6185322 |
| d | 0.5877852 | <u>0.5877852</u> | -0.9510565 | <u>-0.9510565</u> |
| r | -0.8090169 | -0.8094411 | 0.618034 | 0.6186028 |
| d | 0 | <u>0</u> | 0 | <u>0</u> |
| r | -1 | -1.0021259 | 2 | -1.9989785 |

Table 6.7: Interpolation Using Good Model

| d=disp. r=rot. | MODE NUMBER 3 | | MODE NUMBER 4 | | MODE NUMBER 5 | |
|-------------------|---------------|-------------------|---------------|-------------------|---------------|----------|
| | EXACT MODE | INTERPOLATED MODE | EXACT MODE | INTERPOLATED MODE | EXACT | INT. |
| d | 0 | <u>0</u> | 0 | <u>0</u> | 0 | <u>0</u> |
| r | 3 | 2.9907334 | 4 | 3.828599 | 5 | 0 |
| d | 0.9510565 | <u>0.9510565</u> | 0.5877852 | <u>0.5877852</u> | 0 | <u>0</u> |
| r | -0.9270507 | -0.9241929 | -3.2360679 | -3.094314 | -5 | 0 |
| d | -0.8577852 | <u>-0.8577852</u> | -0.9510565 | <u>-0.9510565</u> | 0 | <u>0</u> |
| r | -2.427051 | -2.4200583 | 1.2360679 | 1.1816023 | 5 | 0 |
| d | -0.5877852 | <u>-0.5877852</u> | 0.9510565 | <u>0.9510565</u> | 0 | <u>0</u> |
| r | 2.427051 | 2.4200583 | 1.2360679 | 1.1816023 | -5 | 0 |
| d | 0.9510565 | <u>0.9510565</u> | -0.5877852 | <u>-0.5877852</u> | 0 | <u>0</u> |
| r | 0.9270507 | 0.9241929 | -3.2360679 | -3.094314 | 5 | 0 |
| d | 0 | <u>0</u> | 0 | <u>0</u> | 0 | <u>0</u> |
| r | -3 | -2.9907334 | 4 | -3.828599 | -5 | 0 |

Table 6.8 Interpolation Using Good Model

| d=disp. r=rot. | MODE NUMBER 1 | |
|-------------------|------------------|------------------|
| | EXACT MODE | INTERPOLATED M |
| d | 0 | <u>0</u> |
| r | 1 | 1.0201782 |
| d | 0.5877852 | <u>0.5877852</u> |
| r | 0.8090169 | 0.77177097 |
| d | 0.9510565 | <u>0.9510565</u> |
| r | 0.309017 | 0.31926434 |
| d | 0.9510565 | <u>0.9510565</u> |
| r | -0.309017 | -0.31183598 |
| d | 0.5877852 | <u>0.5877852</u> |
| r | -0.8090169 | -0.80890833 |
| d | 0 | <u>0</u> |
| r | -1 | -1.00001908 |

Table 6.9: In

| d=disp r=rot. | MODE NUMBER 3 | | MODE NUMBER 4 | | MODE NUMBER 5 | |
|------------------|---------------|-------------------|---------------|-------------------|---------------|----------|
| | EXACT MODE | INTERPOLATED MODE | EXACT MODE | INTERPOLATED MODE | EXACT | INT. |
| d | 0 | <u>0</u> | 0 | <u>0</u> | 0 | <u>0</u> |
| r | 3 | 3.310509 | 4 | 4.33066512 | 5 | 0 |
| d | 0.9510565 | <u>0.9510565</u> | 0.5877852 | <u>0.5877852</u> | 0 | <u>0</u> |
| r | -0.9270507 | -1.50802283 | -3.2360679 | -3.87611616 | -5 | 0 |
| d | -0.5877852 | <u>-0.5877852</u> | -0.9510565 | <u>-0.9510565</u> | 0 | <u>0</u> |
| r | -2.427051 | -2.24929326 | 1.2360679 | 1.4603033 | 5 | 0 |
| d | -0.5877852 | <u>-0.5877852</u> | 0.9510565 | <u>0.9510565</u> | 0 | <u>0</u> |
| r | 2.427051 | 2.3698065 | 1.2360679 | 1.08103498 | -5 | 0 |
| d | 0.9510565 | <u>0.9510565</u> | -0.5877852 | <u>-0.5877852</u> | 0 | <u>0</u> |
| r | 0.9270507 | 0.940022 | -3.2360679 | -3.054618129 | 5 | 0 |
| d | 0 | <u>0</u> | 0 | <u>0</u> | 0 | 0 |
| r | -3 | -2.999258 | 4 | 3.80348868 | -5 | 0 |

Table 6.10: Interpolation Using Poor Model

CHAPTER 7

CONCLUSIONS

Dynamic analysis, as it stands at present, is a two-pronged attack. The first approach is an application of the FE method in order to derive a mathematical model of the structure under investigation, and solve that model to extract analytical modes and frequencies of vibration. Thereby the dynamic characteristics of the structure are assessed and the likely subsequent performance predicted. For many years, with the possible exception of the aircraft industry, this was considered adequate - and if a satisfactory **performance** was predicted, no further work was considered necessary. The method is totally analytical. The predictions of an FE model have to be accepted whether right or wrong.

Not surprisingly, this was considered unsatisfactory. What was needed was a verification of the mathematical model with a test on the actual structure itself. From this was born the field of modal analysis, which is an experimental technique designed to do just that. The growth of digital computer technology has greatly enhanced the field of modal analysis. Test equipment and software are rapidly being developed which can analyse structures and extract measured modal parameters. In parallel with this, experimental engineers with a wealth of experience in dynamic testing grow in numbers. At present, very powerful and sometimes portable machines which contain the hardware and software capable of testing a structure, analysing the data and extracting the modal parameters are beginning to emerge. As the spread of knowledge increases, so will this type of machine - thus making available, at reasonable cost,

modal analysis test equipment to small construction companies.

However, what has also come to **light** is that a modal test will often disagree with the mathematical model previously formulated, in terms of modes and frequencies. One of the points that has been stressed in this thesis is that it is not possible to devise so-called measured mass and stiffness matrices that will have any physical significance in terms of the mass and stiffness distributions of the structure. This stems from the fact that the measurements made are of a flexibility-type nature, and do not satisfy the constraints necessary for a stiffness-type formulation, whereas the FE method is a displacement method which leads to a stiffness model. A flexibility model would arise from a stress FE method but, except in special cases, it is not feasible in practice to employ this approach. Thus, the FE displacement method is by far the most widely used - and could never be abandoned since, as far as a knowledge of mass and stiffness distributions goes, it is all we have. The only sensible course of action is to use the modal analysis measurements to improve the mathematical model so that it more closely resembles the actual structure. The objective of this thesis has been to explore this option.

Considering the case where damping is small and may be neglected, in the light of the work done in this thesis, the proposals summarised in Diagram 7.1 are made. This is a procedure for correcting and improving mathematical models using the information extracted from a modal test, It hinges upon an effective error analysis being able to detect regions of poor modelling within the model, thus emphasising some of the points made at earlier stages.

If damping is not insignificant, the problem becomes more difficult. It stems from the problems ~~that~~ arise because of the existence of real, normal analytical modes on the one hand (since usually no analytical damping matrix exists), to complex measured modes on the other. No direct comparison of the two is justifiable if significant imaginary parts of the complex mode exist. In this thesis a viscous damping model has been assumed, and the proposals for the course of action, if in this situation, are given in Diagram 7.2.

Here the procedure is less clear-cut, since some intuitive derivation of a viscous damping matrix is required, based only on the indications extracted from an error analysis.

Future Work

The next stage of this work is clearly an application to a full-size realistic problem. This thesis has dealt with simple examples only in order to point the way to the type of approach that needs to be adopted. A full-scale problem is, in itself, a long-term project with the structure being studied, analysed and tested in its entirety. Past work of this nature⁽¹⁰³⁾ has dealt with this successfully, but has stopped short once the modal tests and FE analysis had been completed - often with acknowledged discrepancies between the two.

The problem of damping is clearly an area that is, as yet, far from completely understood. Viscous damping has been studied in this thesis, because it is more convenient mathematically. However, observations often indicate that damping is independent of

frequency, and this is usually given the name hysteretic or structural damping. The use of a set of differential equations to **describe** this phenomenon runs into difficulties as frequency tends to zero and the equations have little physical justification. The use of integro-differential equations⁽⁶⁵⁾ allows the incorporation of structural damping, but the extension of the analysis to **multi-degree-of-freedom** systems, as in this thesis, will lead to considerably more complex analysis.

On the experimental front, the curvefitting routines are far from complete at present. Ideally, better data to analyse need to be made available. The curvefitter needs to be improved to account for modes outside the frequency range of **interest**, and adapted to analyse ambient data. The implementation of some sort of graphics facility to gain a visual insight into the modes of vibration would clearly be advantageous.

This thesis has assumed linearity throughout, and as this problem becomes understood the analysis could be extended to incorporate non-linearities. Some preliminary investigations into the way in which non-linearities affect modal analysis have been **conducted**⁽⁹²⁾, but much scope for further investigations exists.

As mentioned earlier, machines which test data to establish measured modal parameters are rapidly developing and becoming generally available. The original objective of this thesis was to write a computer package which would use modal analysis to improve and update existing mathematical models. However, a **survey** of the literature exposed a serious gap in the consideration of this problem. The problem had been neglected, perhaps because of the lack of a

mathematical tool with which to analyse it. The development of a computer package was soon seen as **being** over-ambitious. The complexity of the problem meant that the analysis needed to be more mathematical and **centred** upon the difficulties that were holding up this area of research. The proposed schemes built up from the experiences gained in this thesis **and summarised** in Diagram 7.1 and 7.2 are a result. The original optimism and simplicity expressed by early authors on this subject are exposed. What is left is a process to tackle the problems of the real world. The simple examples have shown that as long as the experimentalist is proficient, an error analysis can yield indications of areas of poor modelling, even if it is up to the experimentalist to decide **exactly** how the model is to be improved.

The next step is an application to an example of hundreds - possibly thousands - of degrees of freedom. With this will develop a feel for how best to interpret information from an error analysis. Ultimately, especially for the undamped case, the process is capable of being automated.

The situation envisaged is a dynamic analysis system consisting of two machines. One conducts the modal test and extracts modal parameters; the other stores the mathematical model. The data from the modal test is fed into the second machine. This then expands the measured data for compatibility with the model, conducts an error analysis to identify areas of poor modelling, decides how to change the analytical model, conducts a sensitivity analysis to see whether this has corrected or improved the model - and if not, repeats the error analysis in an iterative cycle until agreement has been reached and the updated model is consistent and reproduces

the measurements as closely as possible given the limitations of a finite degree-of-freedom **environment**. The computer's ability to assess and interpret the indications of an error analysis and decide the best changes in mass and stiffness parameters may well require some fourth-generation programming. Ultimately, the emergence of a 'mathematical model tuning machine' that uses experimental measurements and is fully automated could conceivably be standard equipment for dynamicists and vibration engineers in, say, 10 or 20 years from now.

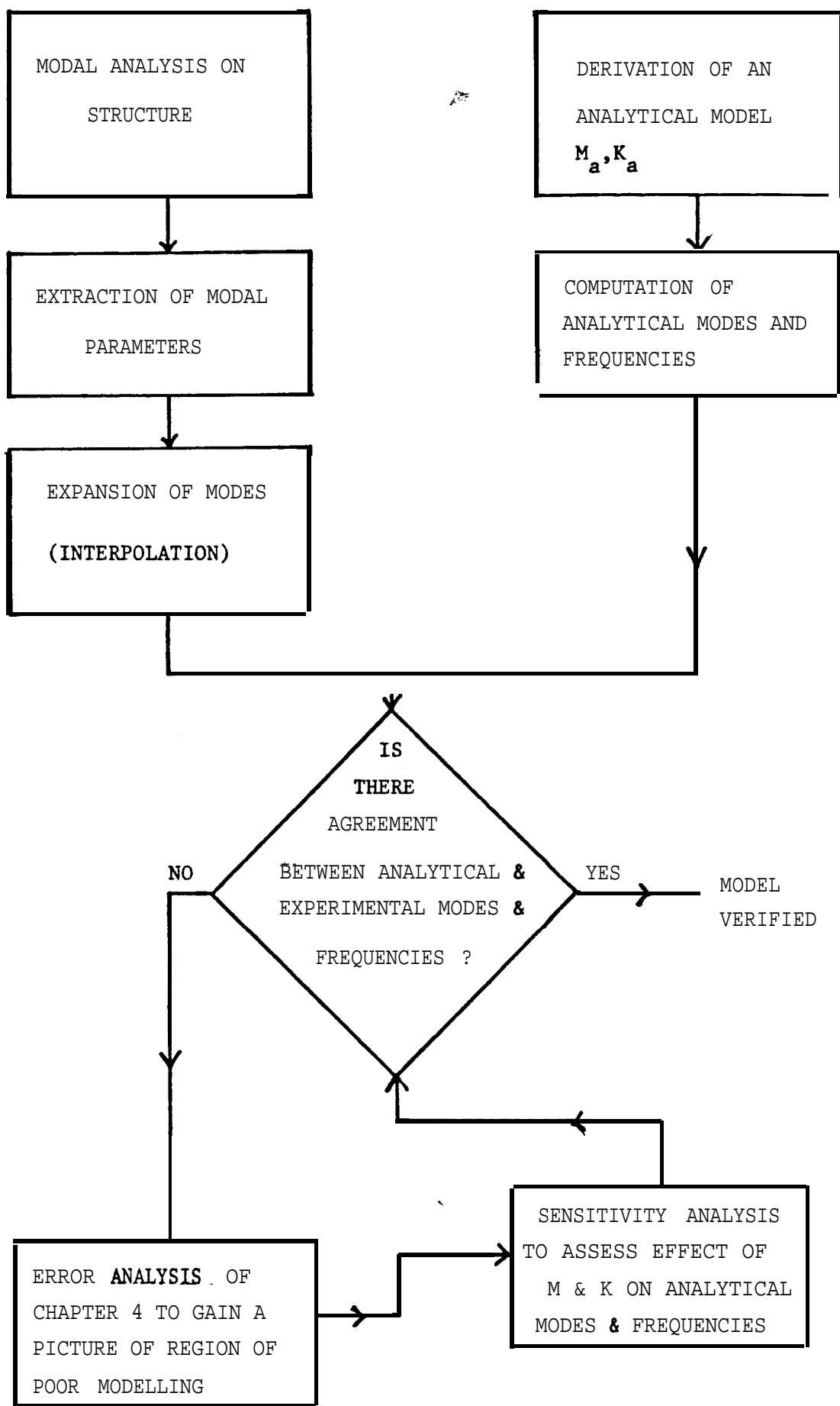


Diagram 7.1: Undamped Model Procedure

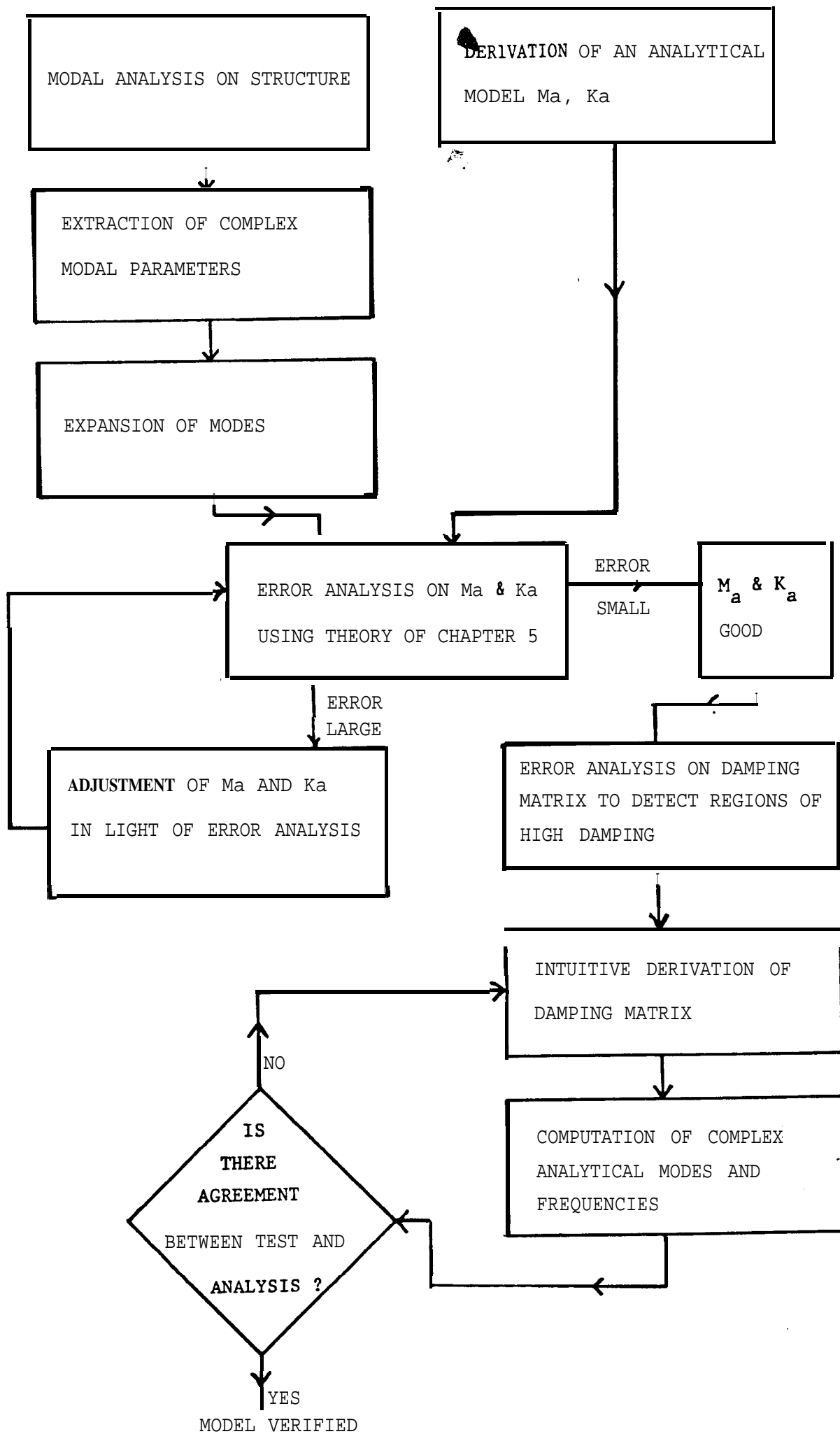


Diagram 7.2: Damped Model Procedure

REFERENCES

1. ADAMS, R.D, CAWLEY, P., PYE, C.J., STONE, B.J: 'A Vibration Technique for Non-Destructively Assessing the Integrity of Structures'. Journal of Mechanical Engineering Science, Vol.20, 1978, p.93.
2. AHLBERG, J.H., NILSON, E.N., WALSH, J.L: 'The Theory of Splines and Their Applications'. Academic Press, 1967.
3. ALLEMANG, R.J: 'Experimental Modal Analysis Bibliography'. Proc. IMAC I, 1982, p.714.
4. ALLEMANG, R.J., CROWLEY, S.M: 'Applications of the Poly-Reference Technique in Experimental Modal Analysis'. Proc. IMAC II, 1984, p.111.
5. BALSARA, J.P, NORMAN, C.D: 'Vibration Tests and Analysis of a Model Arch Dam'. Earthquake Eng. and Structural Dynamics, 1975, p.163.
6. BARLJCH, M., BAR ITZHACK, I.Y: 'Optimal Weighted Orthogonalisation of Measured Modes'. AIAA Journal, Vol.16, April 1978, p.346.
7. BARUCH, M: 'Optimisation Procedure to Correct Stiffness and Flexibility Matrices Using Vibration Tests'. AIAA Journal, Vol.16, November 1978, p.8.
8. BARUCH, M: 'Selective Optimal Orthogonalisation of Measured Modes'. AIAA Journal, Vol.17, January 1979, p.120.
9. BARUCH, M: 'Method of Reference Basis for Identification of Linear Dynamic Structures'. TAE No. 458, Israel Institute of Technology, September 1981.
10. BARUCH, M: 'Optimal Correction of Mass and Stiffness Matrices Using Measured Modes'. AIAA Journal, September 1982, p.1623.
11. BATHE, K-J: 'Finite-Element Procedures in Engineering Analysis'. Prentice Hall, 1982.
12. BERMAN, A., FLANELLY, W.G: 'Theory of Incomplete Models'. AIAA Journal, Vol.9, August 1971, p.1481.
13. BERMAN, A: 'Comment on 'Optimal Weighted Orthogonalisation of Measured Modes''. AIAA Journal, Vol.17, August 1979.
14. BERMAN, A: 'Mass Matrix Correction Using an Incomplete Set of Measured Modes'. AIAA Journal, Vol.17, October 1979, p.1147.
15. BERMAN, A., NAGY, E.J: 'Improvement of a Large Analytical Model Using Test Data'. AIAA Journal, Vol.21, August 1983, p.1168.

16. BERMAN, A: 'Limitations on the Identification of Discrete Structural Dynamic Models'. **Proc. 2nd International Conference on Recent Advances in Structural Dynamics**, 1984.
17. **BLUM, E-K**: 'Numerical Analysis and Computation: Theory and Practice'. Addison-Wesley, 1972.
18. BREBBIA, C.A., FERRANTE, A.J: 'Computational Methods for the Solution of Engineering Problems'. **Pentech Press**, 1978.
19. BROWN, D.L., ALLEMANG, R.J., ZIMMERMAN, R., MERGEAY, M: 'Parameter Estimation Techniques for Modal Analysis'. SAE Paper No. 790221, 1979.
20. BROWN, T.A., MILNE, R.D: 'Strategies for the Verification of a Finite Element Model'. **Proc. IMAC III**, 1985, **p.1031**.
21. CAWLEY, P., ADAMS, R.D: 'A Vibration Technique for Non-Destructive Testing of Fibre Composite Structures'. *J. Composite Materials*, Vol.13, April 1979, p.161.
22. CHEN, J-C., **GARBA, J.A**: 'Analytical Model Improvement using Model Test Results'. *AIAA Journal*, Vol.18, 1980, p.684.
23. **CHEN, J-C**: 'Analytical Model Accuracy Requirements for Structural Dynamic Systems'. *J. Spacecraft*, Vol.21, August 1984, p.366.
24. CHEN, S-Y, FUH, J-S: 'Application of the Generalised Inverse in Structural System Identification'. *AIAA Journal*, Vol.22, December 1984, p.1827.
25. CLOUGH, R.W., PENZIEN, J: 'Dynamics of Structures'. **McGraw-Hill**, 1975.
26. COLLINS, J.D., HART, G.C., HASSELMAN, **T.K.**, KENNEDY, B: 'Statistical Identification of Structures'. *AIAA Journal*, Vol.12, February 1974, p.185.
27. COOLEY, J.W., **TUKEY, J.W**: 'An Algorithm for the Machine Calculation of Complex Fourier Series'. *Mathematical Computation*, Vol.19, 1965.
28. CROWLEY, S.M., BROWN, D.L., ALLEMANG, R.J: 'The Extraction of Valid Residue Terms Using the Polyreference Technique'. **Proc. IMAC III**, 1985, **p.80**.
29. DAVIES, A.J: 'The Finite Element Method - A First Approach'. Clarendon Press, Oxford, 1980.
30. DEINUM, P.J., DUNGAR, R., ELLIS, B.R., **JEARY, A.P.**, REED, **G.A.L.**, SEVERN, R.T: 'Vibration Tests on Emosson Arch Dam, Switzerland'. *Earthquake Engineering and Structural Dynamics*, **Vol.10**, 1982, p.447.

31. DESAI, C.S., ABEL, J.F: 'Introduction to the Finite-Element Method'. Van Nostrand Reinhold Company, 1972.
32. DOBSON, B.J: 'Modification of Finite-Element Models Using Experimental Modal Analysis'. **Proc. IMAC II**, 1984, p.593.
33. DONE, G.T.S: 'Interpolation of Mode Shapes: A Matrix Scheme Using Two-Way Spline Curves'. Aeronautical Quarterly, Vol. 16, 1965, p.333.
34. DUMANOGLU, A.A., SEVERN, R.T: 'The Dynamic Foundation Interaction of Multistorey Frames'. Earthquake Eng. and Structural Dynamics, 1976, p.589.
35. EWINS, D.J: 'Modal Testing and the Average Structure'. **Euro-mech 168**, Manchester, June 1983.
36. EWINS, D.J: 'Keynote Address'. **Proc. IMAC III**, 1985, p.xiii.
37. EWINS, D.J: 'Modal Testing: Theory and Practice'. Research Studies Press, 1984.
38. FAWZY, I., BISHOP, R.E.D: 'On the Dynamics of Linear Non-Conservative Systems'. **Proc. Royal Society**, London, 1976, p.25.
39. FILLOD, R., PARANDA, J., BONNECASE, D: 'Taking Non-Linearities into Account in Modal Analysis by Curve Fitting of Transfer Functions'. **Proc. IMAC III**, 1985, p.88.
40. GAUKROGER, D.R., HAWKINS, F.J: 'Resonance Tests on a Motor Car Body'. RAE Technical Report 66022, January 1966.
41. GAUKROGER, D.R., SKINGLE, C.W., TAYLOR, G.A: 'Resonance Tests on a Model Dam'. RAE Technical Report 67083, March 1967.
42. GAUKROGER, D.R., COPLEY, J.C: 'Methods for Determining Undamped Normal Modes and Transfer Functions from Receptance Measurements'. RAE Technical Report 79071, June 1979.
43. GAUKROGER, D.R., COPLEY, J.C: 'Applications of Dynamic Response Analysis Techniques to Aircraft Shake Testing'. RAE Technical Report 81058, May 1981.
44. GIMENEZ, J.G., CARRASCOSA, L.I: 'On the Use of Constraint Equations in the Global Fitting Algorithms of Transfer Functions'. **Proc. IMAC II**, 1984, p.998.
45. GOYDER, H.G.D: 'Methods and Application of Structural Modelling from Measured Structural Frequency Response Data'. Journal of Sound and Vibration, **No.68**, 1980, p.209.
46. GRAVITZ, S.I: 'An Analytical Procedure for Orthogonalisation of Experimentally Measured Modes'. Journal of the Aerospace Sciences, Vol.25, November 1958, p.721.

47. GUYAN, R.J: 'Reduction of Stiffness and Mass Matrices'. AIAA Journal, Vol.3, February 1965, p.380.
48. HANSTEEN, O.E: 'Numerical Determination of Mode Shapes from Measurements on Offshore Structures'. Norwegian Geotechnical Institute, 1983.
49. HARDER, R.L., DESMARAIS, R.N: 'Interpolation Using Surface Splines'. Journal of Aircraft, Vol.9, February 1972, p.189.
50. HAUOI, A., VINH, T., SIMON, M., TOMLINSON, G.R: 'Some Applications of the Hilbert Transform to Non-Linear Systems'. Euromech 168, 1983.
51. HAWKINS, F.J: 'GRAMPA - An Automatic Technique for Exciting the Principal Modes of Vibration of Complex Structures'. RAE Technical Report No. 65142, July 1965.
52. HURTY, W.C., RUBENSTEIN, M.F: 'Dynamics of Structures'. Prentice-Hall, 1964.
53. IBRAHIM, S.R., PAPPA, R.S: 'Large Modal Survey Testing Using the Ibrahim Time Domain Identification Technique'. J. Spacecraft, Vol.19, No.5, 1982, p.459.
54. IBRAHIM, S.R: 'Computation of Normal Modes from Identified Complex Modes'. AIAA Journal, Vol.21, 1983, p.446.
55. IBRAHIM, S.R: 'Modal Identification Techniques - Assessment and Comparison'. Proc. IMAC III, 1985, p.831.
56. IRONS, B.M: 'Structural Eigenvalue Problems: Elimination of Unwanted Variables'. AIAA Journal, Vol.3, May 1965, p.961.
57. KENNEDY, C.C., PANCU, C.D.P: 'Use of Vectors in Vibration Measurement and Analysis'. Journal of the Aerospace Sciences, Vol.14, 1947, p.603.
58. LANCASTER, P: 'Lambda Matrices and Vibrating Systems'. Pergamon Press, 1966.
59. LEURIDAN, J., VOLD, H: 'A Time Domain Linear Model Estimation Technique for Global Modal Parameter Identification'. Proc. IMAC II, 1984, p.443.
60. LUENBERGER, D.G: 'Optimisation by Vector Space Methods'. John Wiley and Sons Inc., 1969.
61. MAGUIRE, J., SEVERN, R.T., TREVELYAN, J: 'Assessing the Dynamic Properties and Integrity of Structures of the Use of Transient Data'. Proc. 8th World Conference on Earthquake Engineering, San Francisco, July 1984.
62. MCGREW, J: 'Orthogonalisation of Measured Modes and Calculation of Influence Coefficients'. AIAA Journal, Vol.7, April 1969, p.774.

63. MEIROVITCH, L: 'Elements of Vibration Analysis'. McGraw Hill, 1975.
64. MILNE, R.D: 'An Oblique Matrix Pseudoinverse'. SIAM Journal of Applied Mathematics, Vol.16, September 1968, p.931.
65. MILNE, R.D: 'A Constructive Theory of Linear Damping'. Symposium on Structural Dynamics, Loughborough, 1970.
66. MILNE, R.D: 'Applied Functional Analysis - An Introductory Treatment'. Pitman, 1980.
67. MITCHELL, L.D., MITCHELL, L.D: 'Modal Analysis Bibliography - An Update 1980-1983'. Proc. IMAC II, 1984, p.1098.
68. MITCHELL, L.D., MITCHELL, L.D: 'Modal Analysis Bibliography - an Update 1980-1984'. Proc. IMAC III, 1985, p.1254.
69. NIEDBAL, N., KNORR, M: 'An Analytical Method to Determine Normal Mode Parameters out of Measured Complex Responses'. Euromech 168, Manchester, 1983.
70. NOBLE, B: 'Methods for Computing the Moore Penrose Inverse and Related Matters', in Generalised Inverses and Applications, Academic Press, 1973, p.245.
71. NORRIE, D.H., DeVRIES, G: 'An Introduction to Finite Element Analysis'. Academic Press, 1978.
72. O'CALLAHAN, J.C., AVITABILE, P., LEUNG, R.K: 'Development of Mass and Stiffness Matrices for an Analytical Model Using Experimental Modal Data'. Proc. IMAC II, 1984, p.585.
73. O'CALLAHAN, J.C., LEUNG, R.K: 'Optimisation of Mass and Stiffness Matrices Using a Generalised Inverse Technique on the Measured Modes'. Proc. IMAC III, 1985, p.75.
74. O'CALLAHAN, J.C., LIEU, I-W., CHOU, C-M: 'Determination of Rotational Degrees of Freedom for Moment Transfer in Structural Modifications'. Proc. IMAC III, 1985, p.465.
75. PENROSE, R: 'A Generalised Inverse for Matrices'. Proc. Cambridge Philos. Soc., 1955, p.406.
76. PAZ, M: 'Practical Reduction of Structural Eigenproblems'. Journal of Structural Engineering, ASCE, Vol.109, November 1983, p.2591.
77. PAZ, M: 'Dynamic Condensation'. AIAA Journal, Vol.22, May 1984, p.724.
78. PAZ, M: 'Modal Analysis Using Dynamic Condensation Method'. Proc. IMAC III, 1985, p.242.
79. RAMSEY, K.A: 'Effective Measurements for Structural Dynamics Testing'. Sound and Vibration, November 1975 and April 1976.

80. RICHARDSON, M., POTTER, R: 'Identification of the Modal Properties of an Elastic Structure from Measured Transfer Function Data'. **Hewlett-Packard**, 1974.
81. RICHARDSON, M., POTTER, R: 'Evaluation of Mass, Stiffness and Damping Parameters from Measured Modal Data'. ISA Conf. New York City, 1974.
82. RICHARDSON, M: 'Modal Analysis Using Digital Test Systems'. Hewlett-Packard, 1975.
83. RICHARDSON, M., FORMENTI, D.L: 'Parameter Estimation from Frequency Response Measurements Using Rational Fraction Polynomials'. **Proc. IMAC I**, 1982, p.167.
84. RICHARDSON, M., POTTER, R: 'Global Curve Fitting of Frequency Response Measurements Using the Rational Fraction Polynomial Method'. **Proc. IMAC III**, 1985, **p.390**.
85. ROCKEY, K.C., EVANS, H.R., GRIFFITHS, D.W., NETHERCOT, D.A: 'The Finite Element Method'. Granada Publishing Limited, 1975.
86. RODDEN, W.P: 'A Method for Deriving Structural Influence Coefficients from Ground Vibration Tests'. AIAA Journal, Vol.5, May 1967, **p.991**.
87. RODDEN, W.P., MCGREW, J.A., KALMAN, T.P: 'Comment on 'Interpolation Using Surface Splines''. Journal of Aircraft, Vol.9, December 1972, p.869.
88. RODDEN, W.P: 'Comment on Orthogonality Check and Correction of Measured Modes'. AIAA Journal, Vol.15, July 1977, **p.1054**.
89. ROSS, R.G: 'Synthesis of Stiffness and Mass Matrices from Experimental Vibration Modes'. SAE Paper No. 710787, 1971.
90. SCHUMAKER, L.L: 'Spline Functions: Basic Theory'. John Wiley and Sons. 1981.
91. SIDHU, J., EWINS, D.J: 'Correlation of Finite Element and Modal Test Studies of a Practical Structure'. **Proc. IMAC II**, 1984, p.756.
92. SIDHU, J: Ph.D. Thesis, Imperial College, London, 1984.
93. SIMON, M., TOMLINSON, G.R: 'Modal Analysis of Linear and Non-Linear Structures Employing the Hilbert Transform'. Journal of Sound and Vibration, Vol.96, 1984.
94. STARKEY, J.M: 'Inverse Modal Transformations for Structural Dynamics Modification'. **Proc. IMAC III**, 1985, p.949.
95. STEIN, P.K: 'Dynamic Measurements on and with Non-Linear Systems: Problems and Approaches'. **Proc. IMAC I**, 1982, p.358.

96. STEIN, P.K: 'Experimental Error? No! Experimenters Errors! A Measurements Engineer's View of Experimental Modal Analysis'. **Proc. IMAC III**, 1985, p.824.
97. TARGOFF, W.P: 'Orthogonality Check and Correction of Measured Modes'. **AIAA Journal**, Vol.14, February 1976, p.164.
98. TARGOFF, W.P: 'Reply by Author to W.P. **Rodden**'. **AIAA Journal**, Vol.15, July 1977, p.1054.
99. TAYLOR, C.A: 'Development of the Bristol Seismic Shaking Table and its Use in Embankment Dam Research'. Ph.D. Thesis, Bristol University, 1984.
100. TAYLOR, C.A., DUMANOGLU, A.A., TREVELYAN, J., MAGUIRE, J.R., SEVERN, R.T., ALLEN, A.C: 'Seismic Analysis of the Upper and Lower Glendevon Dams'. **Earthquake Engineering in Britain**, 1985, p.271.
101. TAYLOR, G.A., GAUKROGER, D.R., SKINGLE, C.W: 'MAMA - A Semi-Automatic Technique for Exciting the Principal Modes of Vibration of Complex Structures'. **RAE Technical Report 67211**, August 1967.
102. TOMLINSON, G.R: 'Using the Hilbert Transform with Linear and Non-Linear Multi-Mode Systems'. **Proc. IMAC III**, 1985, p.255.
103. TREVELYAN, J: 'The Assessment of the Dynamic Properties of Concrete Arch Dams Using Transfer Function Techniques'. Ph.D. Thesis, 'Bristol University, 1984.
104. VINH, T., HAOUI, A., CHEVALIER, Y: 'Extension of Modal Analysis to Non-Linear Structures by Using Hilbert Transform'. **Proc. IMAC II**, 1984, p.852.
105. VOLD, H., ROCKLIN, G.T: 'The Numerical Implementation of a Multi-Input Modal Estimation Method for Mini-Computers'. **Proc. IMAC I**, 1982, p.542.
106. WADA, H., WARBURTON, G.B: 'Errors in Response Calculations for Beams'. **Earthquake Eng. and Structural Dynamics**, June 1985, p.293.
107. WEI, F-S: 'Stiffness Matrix Correction from Incomplete Test Data'. **AIAA Journal**, Vol.18, October 1980, p.1274.
108. ZHANG, Q., LALLEMENT, G: 'New Method of Determining the Eigensolutions of the Associated Conservative Structure from the Identified Eigensolutions'. **Proc. IMAC III**, 1985, p.322.
109. ZHANG, Q., LALLEMENT, G: 'Experimental Determination of Eigensolutions of Non-Self-Adjoint Mechanical Structures'. **Proc. IMAC III**, 1985, p.768.
110. ZIENKIEWICZ, O.C: 'The Finite-Element Method'. 3rd Edition, McGraw-Hill, 1977.

111. User Manuals, Modal Analysis Package, Signal Processing and Applications Group, Cranfield Institute of Technology, 1981.
112. Numerical Algorithms Group **Fortran** Library Manual Mark **11**, 1984.

APPENDIX 1

PERTURBATION ANALYSIS FOR A BEAM

The viscous damping model has a constitutive equation of the form

$$\sigma = E\epsilon + d\dot{\epsilon}$$

where $\epsilon = \eta \frac{d^2 y}{dx^2}$. (Engineer's theory of bending beam)

This gives the terms

$$EI \frac{\partial^4 y}{\partial x^4} + dI \frac{\partial^5 y}{\partial x^4 \partial t}$$

so the variational equation of motion is

$$\int m \frac{\partial^2 y}{\partial t^2} z + \int dI \frac{\partial^3 y}{\partial x^2 \partial t} \frac{\partial^2 z}{\partial x^2} + \int EI \frac{\partial^2 y}{\partial x^2} \frac{\partial^2 z}{\partial x^2} = 0.$$

If we assume that y is $a e^{\lambda t}$ we have

$$\lambda^2 \int m y z + \lambda \int dI \frac{\partial^2 y}{\partial x^2} \frac{\partial^2 z}{\partial x^2} + \int EI \frac{\partial^2 y}{\partial x^2} \frac{\partial^2 z}{\partial x^2} = 0$$

i.e. $M\lambda^2 + D\lambda + K = 0$

where $d_{ij} = \int dI y_i'' y_j''$.

If we consider a uniform, simply-supported beam of unit mass then the perturbation problem may be written as

$$(\lambda_i + \delta\lambda_i)^2 (x_i + \delta x_i) + (\lambda_i + \delta\lambda_i) \delta dx_i + k(x_i + \delta x_i) = 0$$

which is, to first order,

$$(\lambda_i^2 + k)x_i + 2\lambda_i \delta\lambda_i x_i + \lambda_i^2 \delta x_i + \lambda_i \delta dx_i + k \delta x_i = 0$$

so, taking the inner product with x_j ,

$$2\lambda_i \delta\lambda_i \langle x_i, x_j \rangle + \lambda_i^2 \langle \delta x_i, x_j \rangle + \lambda_i \langle \delta dx_i, x_j \rangle + k \langle \delta x_i, x_j \rangle = 0.$$

We assume that

$$\delta x_i = \sum_{k=1}^n \alpha_{ik} x_k$$

hence

$$2\lambda_i \delta\lambda_i \delta_{ij} + \lambda_i^2 \sum_{k=1}^n \alpha_{ik} \delta_{kj} + \lambda_i \langle \delta dx_i, x_j \rangle - \sum_{k=1}^n \alpha_{ik} \lambda_k^2 \delta_{kj} = 0$$

$$2\lambda_i \delta\lambda_i \delta_{ij} + \lambda_i \langle \delta dx_i, x_j \rangle + \lambda_i^2 \alpha_{ij} - \lambda_j^2 \alpha_{ij} = 0$$

so if $i = j$ then we have

$$2\lambda_i \delta\lambda_i + \lambda_i \langle \delta dx_i, x_i \rangle = 0$$

and if $i \neq j$ then

$$a_{ij} = - \frac{\lambda_i \langle \delta dx_i, x_j \rangle}{\lambda_i^2 - \lambda_j^2}, \quad a_{ii} = 0$$

so $\delta\lambda_i = - \frac{\delta d_{ii}}{2}$ and $a_{ij} = \frac{-\lambda_i \delta d_{ij}}{\lambda_i^2 - \lambda_j^2}$.

The perturbed eigenvalues are therefore given by

$$\lambda_i + \delta\lambda_i = \lambda_i - \frac{\delta d_{ii}}{2} \left(= \lambda_i - k^4 \frac{\phi_{kk}}{\pi} d_e \right)$$

The first five may be calculated as:

1. $1 - 0.00024i$
2. $4 - 0.01226i$
3. $9 - 0.09363i$
4. $16 - 0.30444i$
5. $25 - 0.62500i$

and the perturbed first mode, for displacement, is given by

$$0.46908 - 0.0002883i$$

$$0.7590 - 0.000013i$$

$$0.7590 + 0.000202i$$

$$0.46908 + 0.000109i$$

These figures are in good agreement with those predicted by the FE model (Figure 2.7), and serve as a good check of the analysis.

MAMA-2
USERS
GUIDE

CONTENTS

1. INTRODUCTION
2. LAYOUT
 - (a) Complete System
 - (b) MAMA Microprocessor
 - (c) Keypad
 - (d) Excitor Apparatus
3. OPERATION
 - (a) Manual
 - (i) Setting Force
 - (ii) Changing Frequency
 - (iii) Changing Frequency and Frequency Step
 - (iv) Frequency Sweeps
 - (v) Plotter
 - (vi) **CRO** Connections
 - (b) Automatic Frequency Control
4. ACKNOWLEDGEMENTS

1. INTRODUCTION

The solution of vibration **problems** frequently requires a knowledge of the principal modes of vibration of a structure. Where the modes are obtained experimentally, in a resonance test, the main difficulty lies in exciting the undamped modes of a structure.

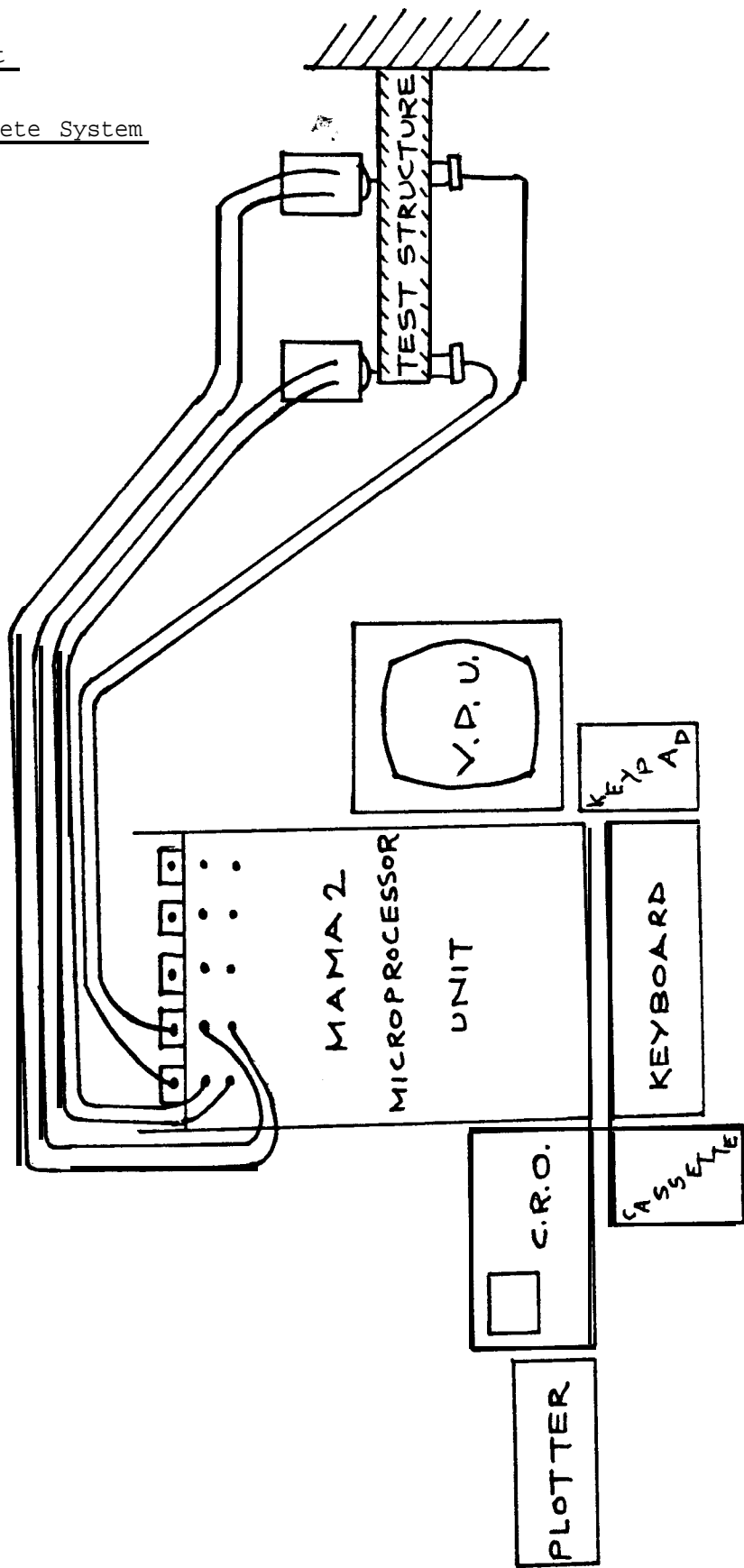
The development of the MAMA (Manual-Automatic Multipoint Apparatus) control system was initiated when the limitations of its predecessor, **GRAMPA** (Ground Resonance Automatic Multipoint Apparatus), came to light. It had been **recognised** that the frequency range over which **GRAMPA** operated was too restricted for use with many structures, particularly model structures where mode frequencies of interest might be as high as one KiloHertz. The MAMA system sought to overcome this restriction, and also adopt a manual adjustment of the force control when it became apparent that automatic setting of force levels, as utilised in **GRAMPA**, was often unnecessary and time-consuming.

Subsequently, due to recent developments in microprocessor technology, a replacement for the MAMA system - in favour of a microprocessor-controlled system - became desirable. **MAMA-2** has the major advantage of cheapness, and also utilises the facility of each unit (i.e. **VDU**, cassette, plotter) communicating with the microprocessor only, thus the system behaviour and characteristics are a function of the microcomputer program.

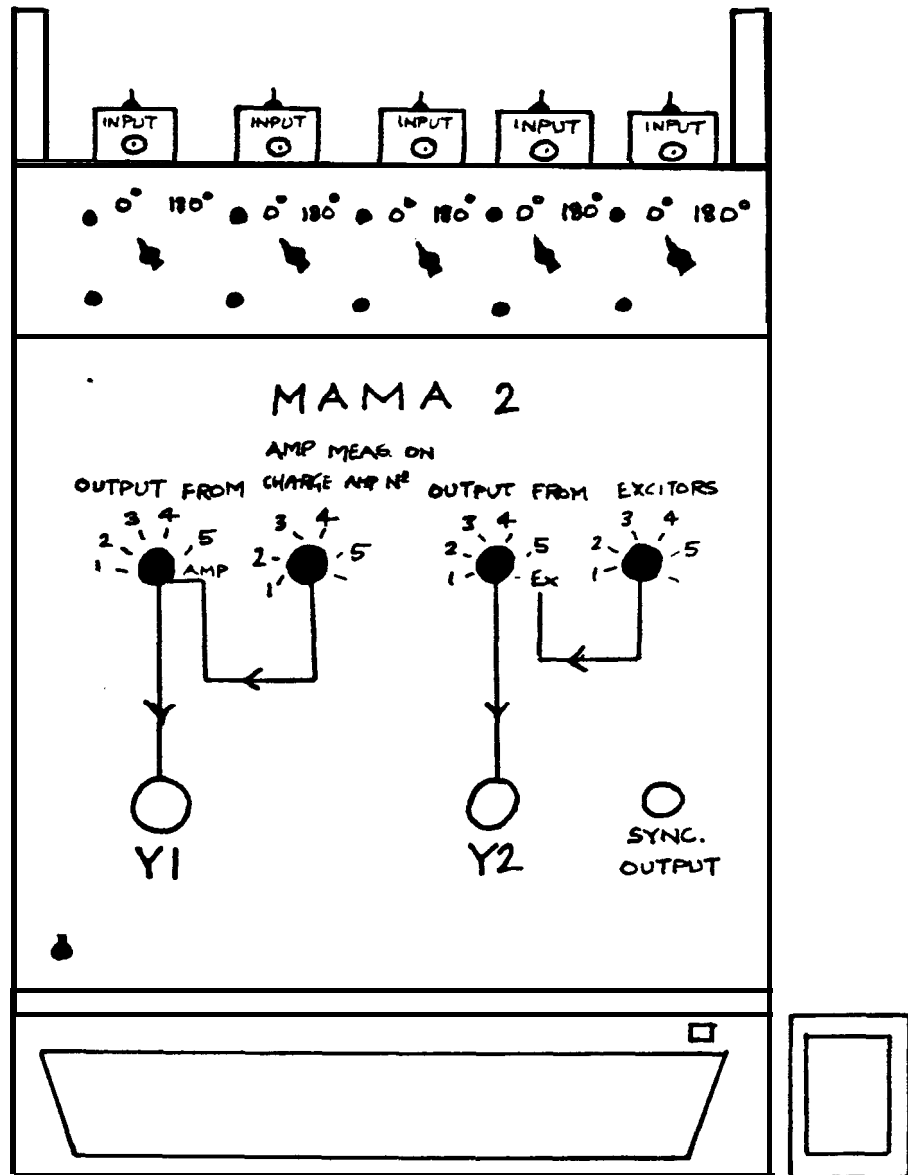
The operational details of the **MAMA-2** system are described within this manual, and are designed as a guide to its use.

2. Layout

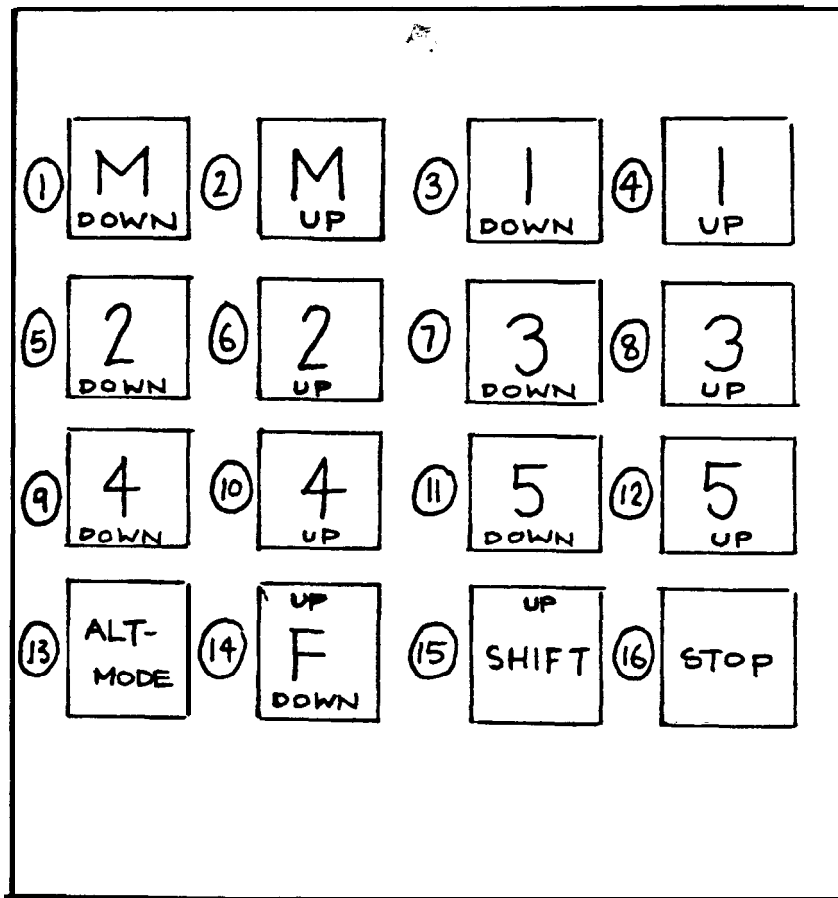
(a) Complete System



(b) MAMA Microprocessor



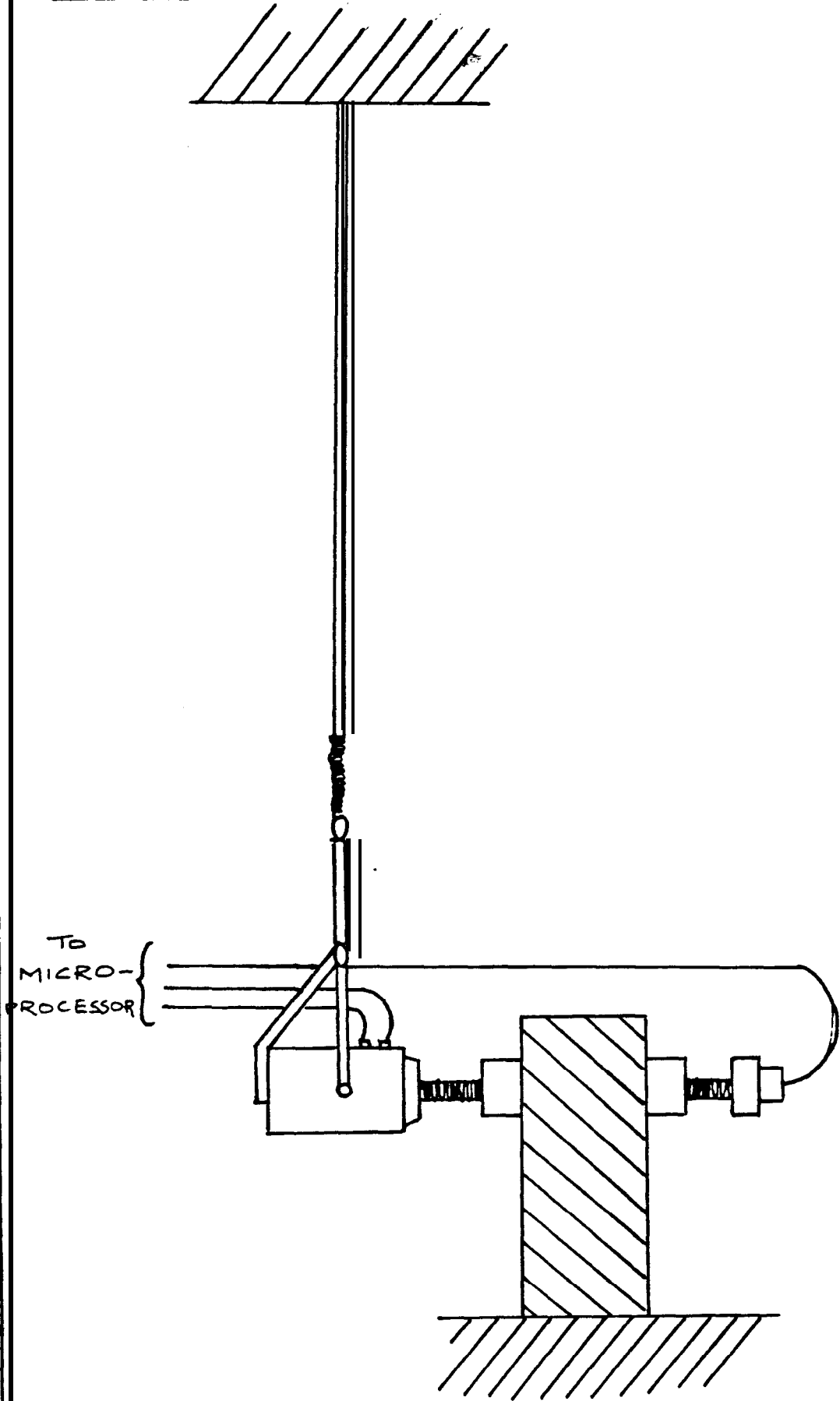
(c) Keypad



KEYPAD FUNCTIONS

- | | | | |
|-----|----------------------------|-----------|----------------------------|
| (1) | Master force level down | (9) | Channel 4 force level down |
| (2) | Master force level up | (10) | Channel 4 force level up |
| (3) | Channel 1 force level down | (11) | Channel 5 force level down |
| (4) | Channel 1 force level up | (12) | Channel 5 force level up |
| (5) | Channel 2 force level down | (13) | Frequency sweep |
| (6) | Channel 2 force level up | (14) | Frequency down by delta f |
| (7) | Channel 3 force level down | (14)+(15) | Frequency up by delta f |
| (8) | Channel 3 force level up | (16) | Switch to A.F.C. |
| | | (15)+(16) | Change frequency |

(d) Excitor Apparatus



3. OPERATION

(a) Manual Control

(i) Setting of Force

The exciters are connected to the test structure and to the corresponding excitor outputs on the MAMA-2 unit. The exciters need to be suspended freely so that their mass does not affect the natural frequency of the test structure (see Diagram D). The principal excitor should be located at the most important point, i.e. where the maximum amplitude is anticipated. This is then connected to the channel 1 output (extreme left). This is the channel which should be set first, and subsequently controls the frequency automatically. The remaining exciters may be set in some order so as to avoid confusion as to which excitor is operating through which channel. The accelerometers are then set up with the accelerometer measuring response at excitor 1 connected to charge-amp 1, and so on.

MAMA-2 is then switched on and the software is run. The channels being used, the frequency and the frequency step are set initially. Operation is then transferred to the keypad, the controls of which are shown in Diagram C. Operation of keypad function should be used in conjunction with a CRO monitoring the output and input of the system. The first operation is to set the master force level at a fairly low level. Channel 1 force level is then adjusted using the full force level range (0-255) until the best sinusoidal response is observed on the oscilloscope. It may be necessary to adjust other force channels to obtain a good wave. At low forces, the sensitivity of the charge-amp may be increased by switching from $\times 1$ to $\times 10$, should this be found to be

necessary. However, the corresponding noise content is also increased and this should be **avoided if possible**.

When a good sine wave has been obtained the frequency may be altered up or down until a quadrature input/output phase shift is obtained on channel 1 (either 90° or 270°). The quality of the sine wave needs to be constantly monitored.

(ii) Changing Frequency

A jump in the frequency being considered may be achieved by pressing **SHIFT** and **STOP** simultaneously. The new frequency will be observed, and this is input via the keyboard. Operations will continue at the new frequency.

(iii) Frequency Resetting

Complete resetting of the frequency and frequency step may be obtained by pressing **SHIFT** and **ALT-MODE**.

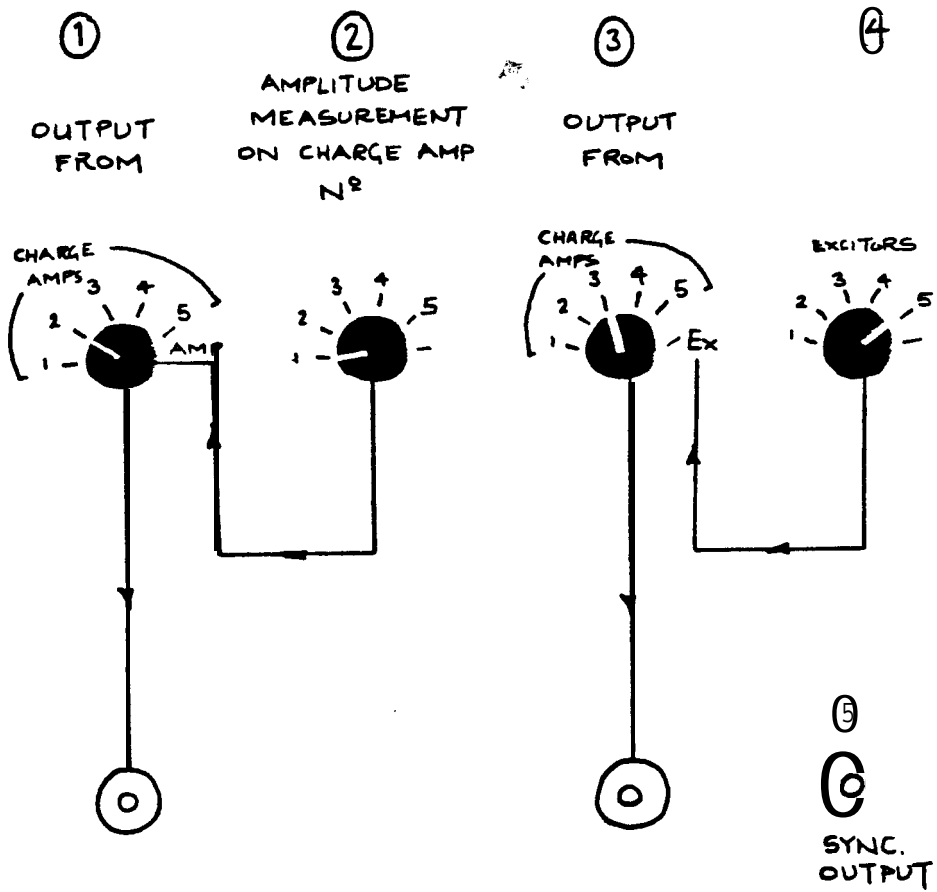
(iv) Frequency Sweeps

A frequency sweep is obtained by pressing **ALT-MODE**. The upper and lower values for the sweep will be required and also the frequency step. At any time the sweep may be terminated by pressing the **ALT-MODE** key to return the system to normal operation at the frequency the system was at at interruption.

(v) The Plotter

A plotting routine also exists for use with the frequency sweep. This shows the phase change as a result of steadily increasing frequency, giving a cross of the y-axis at resonance.

(vi) C.R.O. Connections



- ① Output from Charge Amps
- ② Output from Charge Amps (measured from amplitude board)
- ③ Output from Charge Amps
- ④ Input to Excitors
- ⑤ Sync. Output (used as external trigger)

(b) Transfer to Automatic Frequency Control

At this stage, if the **STOP** button is depressed the system will offer the option of transferring to automatic frequency control (via channel 1).

If using accelerometers, the required phase angle will normally be 90° or 270° (resonance). The frequency step (i.e. steps used under automatic control) and control accuracy (i.e. the error which decides whether or not an adjustment in frequency is required) are set according to the time available and accuracy requirement of the user.

The other channels are then adjusted (either in phase (0°) or antiphase (180°)) carefully, constantly monitoring the quality of the response signals, until all channels are as near to the resonance phase measurement as is considered possible. Should the adjustment of the other channels result in resonance on channel 1 being lost, the system will return to the manual mode after a while.

During automatic frequency control the frequency step or control accuracy may be altered using the keypad controls (see list of alternative keypad controls used under automatic frequency control).

Hence, when all the responses are in quadrature an undamped mode is being excited.

Keypad Functions Under Automatic Frequency Control

| | |
|--------------------|--|
| 13 | |
| 13 + 15 | Break from automatic frequency control |
| 14 + 15 | ↑ Change frequency step |
| 16 | End program |
| 15 + 16 | Change control accuracy |

4. ACKNOWLEDGEMENTS

Acknowledgements go to the following people for their contribution in the making of this machine:

Dr. Duncan Grant (Lecturer in Electrical Engineering)

Mr. Graham Ogden (Electrical Engineering postgraduate - now departed)

Mr. Roy Sampon (Civil Engineering Electrical Technician)

Mr. John Maguire (Civil Engineering postgraduate)

Mr. Tim Brown (Engineering Mathematics postgraduate)

SDOF
AND
MDOF
USERS
GUIDE

CONTENTS

1. THEORY
2. PRELIMINARY ANALYSIS
3. IMPLEMENTATION OF SDOF
4. IMPLEMENTATION OF MDOF
5. DATA COLLATION

1. THEORY

Programs SDOF and MDOF are **single-degree-of-freedom** and multi-degree-of-freedom curvefitting routines which fit an analytical mathematical function to experimentally measured frequency response function data in order to extract the modal parameters of the structure under test. The programs use a non-linear least squares NAG routine, employing single precision arithmetic, based on the theory of Reference (1). In order to formulate a mathematical expression for the frequency response function we first consider the one-degree-of-freedom equation of motion given by

$$m\ddot{x} + c\dot{x} + kx = f$$

where m , c and k are the mass, damping and stiffness respectively and f and x represent the input and the output. It is usual to divide through by the mass and so rewrite the equation as

$$\ddot{x} + \frac{c}{m}\dot{x} + \frac{k}{m}x = \frac{f}{m}$$

or
$$\ddot{x} + 2\mu\omega\dot{x} + \omega^2x = z$$

where $\frac{c}{m} = 2\mu\omega$; $\frac{k}{m} = \omega^2$ and $z = \frac{f}{m}$.

If we let the input be of the form $z = ze^{-\lambda t}$, then we may assume an output of the form $x = xe^{-\lambda t}$. λ is complex and can take any values, i.e. $\lambda = \xi + i\Omega$. We have

$$\lambda^2 e^{-\lambda t} x + 2\mu\omega\lambda e^{-\lambda t} x + \omega^2 e^{-\lambda t} x = e^{-\lambda t} z$$

or
$$(\lambda^2 + 2\mu\omega\lambda + \omega^2)x = z.$$

The transfer function is the output divided by the input, thus

$$H(X) = \frac{x}{z} = \frac{1}{\lambda^2 + 2\mu\omega\lambda + \omega^2}.$$

If the equation $\lambda^2 + 2\mu\omega\lambda + \omega^2 = 0$ is solved we get $\lambda = -\mu\omega \pm i\omega(1 - \mu^2)^{1/2}$. The expression for the transfer function may then be

expanded as

$$H(h) = \frac{1}{\lambda^2 + 2\mu\omega\lambda + \omega^2}$$

$$= \frac{1}{(\lambda + \mu\omega - i\omega(1 - \mu^2)^{\frac{1}{2}})(\lambda + \mu\omega + i\omega(1 - \mu^2)^{\frac{1}{2}})}$$

or
$$H(X) = \frac{a' + ia''}{(\lambda + \mu\omega - i\omega(1 - \mu^2)^{\frac{1}{2}})} + \frac{a' - ia''}{(\lambda + \mu\omega + i\omega(1 - \mu^2)^{\frac{1}{2}})}$$

$$H(\lambda) = \frac{a_1}{\lambda - \lambda_1} + \frac{a_1^*}{\lambda - \lambda_1^*}$$

This analysis may be expanded to n degrees of freedom to give an expression for the transfer function as

$$H(\lambda) = \sum_{k=1}^n \frac{a_k}{\lambda - \lambda_k} + \frac{a_k^*}{\lambda - \lambda_k^*}$$

The frequency response function is simply the transfer function evaluated along the frequency axis and so ξ is set equal to zero, giving $\lambda = i\Omega$, thus

$$H(i\Omega) = \sum_{k=1}^n \frac{a_k}{i\Omega - \lambda_k} + \frac{a_k^*}{i\Omega - \lambda_k^*}$$

where a_k = complex residue of kth mode

$$\lambda_k = -\mu_k \omega_k + i\omega_k(1 - \mu_k^2)^{\frac{1}{2}}$$

ω_k = undamped natural frequency

(100×) μ_k = percentage critical damping

$-\mu_k \omega_k$ = damping factor

$\omega_k(1 - \mu_k^2)^{\frac{1}{2}}$ = damped natural frequency.

If discrete values of Ω are taken (corresponding to measurement frequencies) from $j = 1$ to M , then the measured frequency response function data will be given by

$$H_{\text{MEASURED}}(i\Omega_j) \quad j = 1, \dots, M \quad M = \text{no. of data points}$$

and the analytical function is given by

$$H_{\text{ANALYTICAL}}(i\Omega_j) = \sum_{k=1}^n \frac{a_k}{i\Omega_j - \lambda_k} + \frac{a_k^*}{i\Omega_j - \lambda_k^*}$$

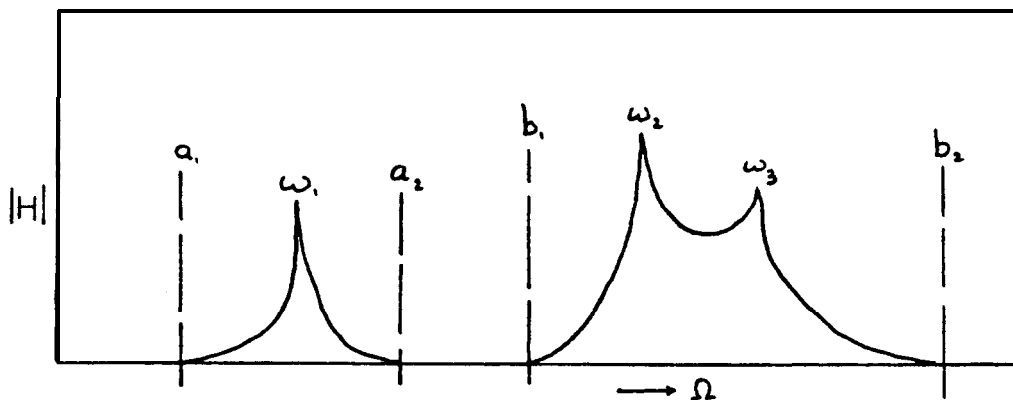
where the a_k 's and the λ_k 's are to be fixed. These need to be chosen so as to minimise the error function

$$\epsilon = \sum_{j=1}^M H_{\text{MEASURED}}(i\Omega_j) - H_{\text{ANALYTICAL}}(i\Omega_j)$$

So, with SDOF and MDOF $\|\epsilon\|^2 = \epsilon\bar{\epsilon}$ is minimised by allowing a variation of the a_k 's and λ_k 's to obtain the closest analytical expression to the measured information.

2. PRELIMINARY ANALYSIS

Prior to the implementation of SDOF and MDOF, a preliminary analysis of the data under investigation is recommended. Initial estimates may be extracted by analysing the magnitude of the frequency response function data for each channel. An illustrative example is given below:



ω_1 is a well-separated peak, and it is assumed that the effect of other frequencies over the range a_1 to a_2 will be negligible. SDOF

may be used to **curvefit** this peak. The peak will serve as an initial estimate for the frequency of this mode and the frequency range **a₁** to **a₂** needs to be noted. **ω₂** and **ω₃** are noted and used as initial estimates for the frequencies of these two modes and the frequency range **b₁** to **b₂** is also noted. Again, the effect of modes outside this frequency range is assumed to be negligible. This type of preliminary data is required for all modes to be analysed, for all channels available. Although some preliminary concept of the values of damping and residues (for MDOF only) are advantageous, they are not essential for an accurate curvefit, but will speed up the process. A suitable estimate of damping of between 1 and 3% will usually suffice and if no residue information is available they may be set to 1. Other values may be tried if success is not achieved in the first instance.

3. IMPLEMENTATION OF SDOF

Data for SDOF needs to be frequency response function data in real and imaginary form. The data needs to be in DSP format⁽³⁾.

That is:

```

$$$$                : flag indicating DSP format
Title               : 72 characters maximum
Data Type           : (always = 2 (complex data))
Number of Channels  : (always = 1)
Number of Data Points
Sampling Interval   : in Hz
Frequency of First Data Point : in Hz
Frequency of Last Data Point : in Hz

Data
:
:
End

```

SDOF curvefits for one-degree-of-freedom and requires an initial estimates of the damping and **frequency** only. Residue initial estimates are obtained by solving the linear least squares problem using the damping and frequency initial estimates and the NAG routine **FO4ARF**. To run SDOF the following command in **inputed**:
RUN SDOF.

The channel that is to be analysed is then fed in when prompted. The channel usually has the suffix **'.DAT'**. An initial estimate for the frequency and damping are then fed in, followed by the frequency range over which the fit is to take place. The program informs the user when information from the relevant channel is being read in and when the curve-fit is in progress, along with the number of data points involved. The NAG routine used is called **EO4FDF** and is a non-linear least squares curvefitting algorithm.

On a successful fit the following results are outputted:

| | | |
|----------------------------|---|--|
| damping factor | : | $-\mu_k \omega_k$ |
| % critical damping | : | $\mu_k * 100$ |
| damped natural frequency | : | $\omega_k (1 - \mu_k^2)^{\frac{1}{2}}$ |
| undamped natural frequency | : | ω_k |
| real part of residue | : | $\text{Re}(a_k)$ |
| imaginary part of residue | : | $\text{Im}(a_k)$ |
| error message | : | Integer |

The error messages are as those given in the **EO4FDF** documentation. 0 indicates a successful curvefit, whereas errors 5 to 8 indicate that there is some doubt about the quality of fit. Error =5 indicates that the **curvefit** is most probably accurate, whereas error =8 (see NAG literature) indicates that it is very unlikely that the **curvefit** has been successful. The program may be rerun, starting

at the last values of the previous run.

4. IMPLEMENTATION OF MDOF

MDOF is used in an identical fashion to SDOF, with the following exceptions:

- (a) The number of modes involved in the **curvefit** needs to be known.
- (b) Residue initial estimates, as well as damping and natural frequency for each mode, need to be available, although these estimates need not be necessarily good - except in the case of frequency.
- (c) The data is **outputted** with the relevant parameters for each mode.

5. DATA COLLATION

Once each channel has been analysed (assuming there are n channels), n different estimates for the damping factors and natural frequencies of the m modes will exist. If the structure is truly linear, these will all coincide. However, in practice some variation may exist, especially with damping due to the effect of **non-linearities**. Some averaging process will be required in order to provide one estimate of damping and one of frequency for each mode, as the theory requires. For each channel the residues will contain modal information, with one element of each of the m modes being provided by each of the n channels. These will be complex in nature. The modes may be normalised so that the largest element of **each**^{is} **equal** to unity. If the other elements of the modes then have negligible imaginary parts the damping may be assumed to be proportional and the imaginary parts neglected. If this is not the

case, the **curvefit** will have produced complex modes, and further analysis will have to account for this. The end result will be a knowledge of each of the modes investigated in terms of natural frequency, % of critical damping and either complex or real mode shapes. An error analysis of a corresponding mathematical model may then be conducted as described in Reference (2).

REFERENCES

1. GILL, P.E. AND MURRAY, W: Algorithms for the Solution of Non-Linear Least Squares Problems. SIAM Journal on Numerical Analysis, 15, 1978, pp.977-992.
2. BROWN, T.A: Ph.D. Thesis, Bristol University, 1985.
3. TAYLOR, C.A: BEEDAPS DSP Reference Manual, Bristol University, 1983.

C
C
C
C

*****READ DATA FROM FILE*****

REWIND 1
READ(1,401) AST
READ(1,402) TITLE
READ(1,*) ITYYE
READ(1,*) NCHN
READ(1,*) L2
READ(1,*) T4
~~READ(1,*) T5~~
READ(1,*) T6
DO 30 I= 1,L2
 BUF(I)=(T4*I)+T5
L3=L2/4

30

C
C
C
C

*****DETERMINE UPPER AND LOWER*****
*****FREQUENCY FOR CURVEFIT*****

WRITE (5,35)
READ (5,*) ZZ1
WRITE (5,36)
READ (5,*) ZZ2
ID1=0
ID2=0
DO 39 I=1,L2
 IF (BUF(I).LT,ZZ1) ID1=I
 IF (BUF(I).LT,ZZ2) ID2=I
CONTINUE
ID1=ID1+1
ID3=(ID2+1)-ID1
IF (ID3.GT.300) GOTO 9999

39

C
C
C
C

*****READMORE DATA & SET ARRAYS*****

DO 45 I=ID1, ID2
 FR((I-(ID1+1)))=BUF(I)
WRITE(5,8)
WRITE(5,72)
WRITE(5,8)
DO 46 I=1,L3
 READ (1,*) R1,R2,R3,R4,R5,R6,R7,R8
 BUF(((4*I)-3))=R1
 BUF(((4*I)-2))=R3
 BUF(((4*I)-1))=R5
 BUF((4*I))=R7
DO 47 I=ID1, ID2
 REH((I-(ID1+1)))=BUF(I)

45

46

47

C

*****LINEAR LEAST SQUARES ESTIMATE*****
*****OF RESIDUE FROM POLES*****

DO 48 I=1,2
V1(I)=0
V2(I)=0
V3(I)=0
DO 48 J=1,2
VV1(I,J)=0
DO 50 I=1,ID3
Z=FR(I)
Y=REH(I)
X1=A1(2)
X2=A1(1)
X3=Z+X1
X4=Z-X1
X5=(X2*X2)+(X3*X3)
X6=(X2*X2)+(X4*X4)
V4(1)=((-X2/X5)+(-X2/X6))
V4(2)=((-X3/X5)+(X4/X6))
DO 50 J=1,192
V1(J)=V1(J)+(Y*V4(J))
DO 50 K=1,2
VV1(J,K)=VV1(J,K)+(V4(J)*V4(K))

IA=2
IFAIL=0
N=2

*****CALL OF NAG ROUTINE TO SOLVE AX=B*****

CALL F04ARF(VV1,IA,V1,N,V2,V3,IFAIL)

LIW=10
LW=2048
IFAIL=1
DO 60 I=1,2
X((I+2))=V2(I)
X(I)=A1(I)
WRITE(5,61) ID3
WRITE(5,8)
WRITE(5,62)
WRITE(5,8)

*****CURVEFIT USING NAG SUBROUTINE*****
CALL E04FDF(ID3,4,X,FSUMSQ,IW,LIW,BUF,LW,IFAIL)

*****UIF=UNDAMPED NATURAL FREQUENCY*****
*****PCC=% CRITICAL DAMPING*****

UIF=SQRT((X(1)*X(1))+(X(2)*X(2)))
PCC=-(X(1)/UIF)*100

*****OUTPUT RESULTS*****

WRITE (5,105)
WRITE (5,110)X(1)
WRITE (5,115) PCC
WRITE (5,120)X(2)
WRITE (5,125)UDF
WRITE (5,130)X(3)
WRITE (5,140)X(4)
WRITE (5,145) IFAIL
WRITE (5,105)

*****FORMATS*****

6 FORMAT(' SDOF CURVEFIT PROGRAM MARK 4: PDP11 FORTRAN')
7 FORMAT(' *****')
8 FORMAT(' ')
9 FORMAT(' INPUT INITIAL NATURAL FREQUENCY ESTIMATE >','\$')
10 FORMAT(' INPUT INITIAL %CRITICAL DAMPING ESTIMATE >','\$')
35 FORMAT(' INPUT LOWER FREQUENCY LIMIT FOR SDOF FIT >','\$')
36 FORMAT(' INPUT UPPER FREQUENCY LIMIT FOR SDOF FIT >','\$')
61 FORMAT(' NUMBER OF CURVEFIT POINTS =','I4')
62 FORMAT(' *****CURVEFIT NOW' IN PROGRESS*****')
72 FORMAT(' *****DATA NOW BEING READ FROM FILE*****')
102 FORMAT(' INPUT FILENAME >','\$')
105 FORMAT(' *****')
110 FORMAT(' DAMPING VALUE:','F12.4')
115 FORMAT(' PERCENTAGE CRITICAL DAMPING:','F12.4')
120 FORMAT(' DAMPED NATURAL FREQUENCY:','F12.4')
125 FORMAT(' UNDAMPED NATURAL FREQUENCY:','F12.4')
130 FORMAT(' ~~REAL RESIDUE:','F12.4~~)
140 FORMAT(' IMAGINARY RESIDUE:','F12.4')
145 FORMAT(' ERROR MESSAGE:','I12')
250 FORMAT('***VERSION 4.2 -UP SINCE JAN 1985***')
251 FORMAT(' CURRENT MAX LENGTH OF FILE=2048 COMPLEX DATA POINTS ')
252 FORMAT(' -TRANSFER FUNCTION DATA REAL AND IMAGINARY PARTS ')
253 FORMAT(' CURRENT MAX NUMBER OF CURVEFIT POINTS =300')
301 FORMAT(64A1)
401 FORMAT(4A1)
402 FORMAT(64A1)
9999 STOP
END

=====
=====SUBROUTINE TO ADD A ZERO TO FILENAME=====

SUBROUTINE CHKNUL(FILNAM,NBYTE)
BYTE FILNAM(1)
J=NBYTE+1
DO 100 I=1,NBYTE
J=J-1
IF(FILNAM(J).NE.'40')GOTO 101 !'40 = SPACE
CONTINUE
J=J+1
100
101

C
C
C
C

=====LSFUN1=====

```
SUBROUTINE LSFUN1(M,N,XC,FVECC)
COMMON /DSPACE/FR,REH,ID3
DIMENSION FVECC(M),XC(N),FR(300),REH(300)
REAL*4 FVECC, XC, FR,REH
REAL*4 HH, X1, X2, U, W, A, B, VZ1, VZ2
REAL*4 VZ3, VZ4, VZ5, VZ6, VZ7, VZ8
INTEGER I, J, ID3, M, N
DO 200 I=1, ID3
  HH=0.0
  X1=FR(I)
  X2=REH(I)
  N2=N/4
  DO 190 J=1, N2
    U=XC(J)
    W=XC((J+N2))
    A=XC((J+(2*N2)))
    B=XC((J+(3*N2)))
    VZ1=X1+W
    VZ2=X1-W
    VZ3=(U*U)+(VZ1*VZ1)
    VZ4=(U*U)+(VZ2*VZ2)
    VZ5=(U*U)-(VZ1*VZ1)
    VZ6=(U*U)-(VZ2*VZ2)
    VZ7=((A*U)-(B*VZ2))/VZ4
    VZ8=((A*U)+(B*VZ1))/VZ3
190    HH=(X2/N2)+VZ7+VZ8+HH
200  FVECC(I) = HH
  CONTINUE
  RETURN
END
```

190
200

C
C
C
C
C

=====NAG NAME PRINT=====

C
105
99999

```
SUBROUTINE FRNAME(NAME)
REAL*8 NAME
WRITE (5,105,ERR=99999) NAME
FORMAT (1X,A8)
RETURN
END
```

MDOF LISTING

PROGRAM MDOF

*****MULTI-DEGREE OF FREEDOM CURVEFIT PROGRAM*****

4444444444444444PARAMETER DECLARATION4444444444444444

```

IMPLICIT REAL44 (A-H,O-Z)
COMMON /DSFACE/FR,REH,ID3
DIMENSION FR(300),REH(300),X(20),UDF(5),BUF(2048),FCC(5)
INTEGER IW(20),FILLEN
BYTE FILE(64),AST(4),TITLE(64)
DATA FILLEN/64/
LOGICAL TRUE,FALSE
TRUE = .TRUE.
FALSE = .FALSE.
CALL ERRSET(73, TRUE, FALSE, FALSE, FALSE, 200)

```

4444444444444444OUTPUT TITLES4444444444444444

```

WRITE (5,1)
WRITE (5,2)
WRITE (5,3)
WRITE (5,1)
WRITE (5,250)
WRITE (5,251)
WRITE (5,252)
WRITE (5,253)
WRITE (5,1)

```

4444444444444444SELECT FILE FOR CURVEFIT*****

```

WRITE (5,102)
READ (5,301) FILE
CALL CHKNUL (FILE,FILLEN)
OPEN (UNIT=1,TYPE='OLD',NAME=FILE)

```

4444444444444444INPUT INITIAL ESTIMATES4444444444444444

```

WRITE (5,7)
READ (5,*) L1
LL1=4*L1
DO 25 I=1,L1
  WRITE (5,1)
  WRITE (5,10) I
  READ (5,*) X((I+L1))
  WRITE (5,11)
  READ (5,*) FC
  X(I)= -(FC/100)*X((I+L1))
  WRITE (5,12)
  READ (5,*) X((I+(2*L1)))
  WRITE (5,13)
  READ (5,*) X((I+(3*L1)))
CONTINUE

```

C
C
C
C
*****READ DATA FROM FILE*****

REWIND 1
READ (1,401) AST
READ (1,402) TITLE
READ (1,*) ITYPE
READ (1,*) NCHN
READ (1,*) L2
READ (1,*) T4
READ (1,*) T5
READ (1,*) T6
DO 30 I=1,L2
 BUF(I)=(T4*I)-T5
L3=L2/4

C
C
C
C
*****DETERMINE UPPER AND LOWER*****
*****FREQUENCY FOR CURVEFIT*****

WRITE (5,1)
WRITE (5,35)
READ (5,*) ZZ1
WRITE (5,36)
READ (5,*) ZZ2
ID1=0
ID2=0
DO 38 I=1,L2
 IF (BUF(I).LT.ZZ1) ID1=I
 IF (BUF(I).LT.ZZ2) ID2=I
CONTINUE
ID1=ID1+1
LIW=10
LW=2048
IFAIL=1
ID3=(ID2+1)-ID1
IF(ID3.GT.300) GOTO 9999

C
C
C
C
*****READ MORE DATA AND SET ARRAYS*****

DO 45 I=ID1,ID2
 FR((I-(ID1+1)))=BUF(I)
WRITE(5,1)
 FR(5,72)
 FR(5,1)
 DO 46 I=1,L3
 READ (1,*) R1,R2,R3,R4,R5,R6,R7,R8
 BUF(((4*I)-3))=R1
 BUF(((4*I)-2))=R3
 BUF(((4*I)-1))=R5
 BUF((4*I))=R7
DO 47 I=ID1,ID2
 REH((I-(ID1+1)))=BUF(I)
WRITE(5,61) ID3
WRITE (5,1)
WRITE (5,39)
WRITE (5,1)

C
C
C
C
*****CALL NAG CURVEFITTING ROUTINE*****
CALL E04FDF (ID3,LL1,X,FSUMSQ,IW,LIW,BUF,LW,IFAIL)

C
C
C
C
65
C
C
C
C
70
C
C
C
C
1
2
3
7
10
11
12
13
35
36
39
61
72
99
100
102
110
120
130
140
150
160
170
250
251
252
253
301
401
402
9999

*****UDF=UNDAMPED NATURAL FREQUENCY*****
*****PCC=% CRITICAL DAMPING*****

```
DO 65 I=1,L1
  UDF(I)=SQRT((X(I)*X(I))+X((I+L1))*X((I+L1)))
  PCC(I)=-X(I)/UDF(I)*100
```

*****OUTPUT RESULTS*****

```
DO 70 I=1,L1
  WRITE (5,99)
  WRITE (5,100) I
  WRITE (5,1)
  WRITE (5,110) X(I)
  WRITE (5,120) PCC(I)
  WRITE (5,130) X((I+L1))
  WRITE (5,140) UDF(I)
  WRITE (5,150) X((I+(2*L1)))
  WRITE (5,160) X((I+(3*L1)))
  WRITE (5,170) IFAIL
WRITE (5,99)
```

*****FORMATS*****

```
FORMAT(' ')
FORMAT(' MDOF CURVEFIT PROGRAM MARK4: PDF11 FORTRAN')
FORMAT(' *****')
FORMAT(' INPUT THE NUMBER OF MODES RECOGNIZED >',$)
FORMAT(' INPUT NATURAL FREQUENCY ',I2,'>',$)
FORMAT(' INPUT XCRITICAL DAMPING ESTIMATE >',$)
FORMAT(' INPUT REAL RESIDUE ESTIMATE >',$)
FORMAT(' INPUT IMAGINARY RESIDUE ESTIMATE >',$)
FORMAT(' INPUT LOWER FREQUENCY LIMIT FOR MDOF FIT >',$)
FORMAT(' INPUT UPPER FREQUENCY LIMIT FOR MDOF FIT >',$)
FORMAT(' *****CURVEFIT NOW IN PROGRESS*****')
FORMAT(' N U M B E R O F C U R V E F I T P O I N T S = ',I4)
FORMAT(' *****DATA NOW BEING READ FROM FILE*****')
FORMAT(' *****')
FORMAT(' MODE NUMBER ',I2)
FORMAT(' INPUT FILENAME >',$)
FORMAT('          DAMPING FACTOR:',F12.4)
FORMAT('          PERCENT CRITICAL DAMPING:',F12.4)
FORMAT('          DAMPED NATURAL FREQUENCY:',F12.4)
FORMAT('          UNDAMPED NATURAL FREQUENCY:',F12.4)
FORMAT('          REAL RESIDUE:',F12.4)
FORMAT('          IMAGINARY RESIDUE:',F12.4)
FORMAT('          ERROR MESSAGE:',I12)
FORMAT(' ****VERSION 4.2 -Up SINCE JAN 1985****')
FORMAT(' CURRENT MAX LENGTH OF FILE=2048 COMPLEX DATA POINTS ')
FORMAT(' -TRANSFER FUNCTION DATA REAL AND IMAGINARY PARTS')
FORMAT(' CURRENT MAX NUMBER OF CURVEFIT POINTS =300')
FORMAT(64A1)
FORMAT(4A1)
FORMAT(64A1)
STOP
END
```

=====**SUBROUTINE TO ADD A ZERO TO FILENAME**=====

SUBROUTINE CHKNUL(FILNAM,NBYTE)
BYTE FILNAM(1)
J=NBYTE+1
DO 100 I=1,NBYTE
J=J-1
IF (FILNAM(J).NE.'40')GOTO 101 !'40 = SPACE
CONTINUE
J=J+1
FILNAM(J)=0
RETURN
END

=====**LSFUN1**=====

SUBROUTINE LSFUN1(M,N,XC,FVECC)
COMMON /DSFACE/FR,REH,ID3
DIMENSION FVECC(M), XC(N), FR(300), REH(300)
REAL*4 FVECC,XC,FR, R E H
REAL*4 HH, X1, X2, U, W, A t B, VZ1, VZ2
REAL*4 VZ3, VZ4, VZ5, VZ6, VZ7, V Z 8
INTEGER It J, ID3, M, N
DO 200 I=1, ID3
HH=0.0
X1=FR(I)
X2=REH(I)
N2=N/4
DO 190 J=1, N2
U=XC(J)
W=XC((J+N2))
A=XC((J+(2*N2)))
B=XC((J+(3*N2)))
VZ1=X1+W
VZ2=X1-W
VZ3=(U*U)+(VZ1*VZ1)
VZ4=(U*U)+(VZ2*VZ2)
VZ5=(U*U)-(VZ1*VZ1)
VZ6=(U*U)-(VZ2*VZ2)
VZ7=((A*U)-(B*VZ2))/VZ4
VZ8=((A*U)+(B*VZ1))/VZ3
HH=(X2/N2)+VZ7+VZ8+HH
190 FVECC(I)=HH
CONTINUE
RETURN
END

=====**NAG NAME PRINT**=====

SUBROUTINE FRNAME(NAME)
REAL*8 NAME
WRITE (5,105,ERR=99999) NAME
FORMAT (1X,A8)
RETURN
END